University of Reading

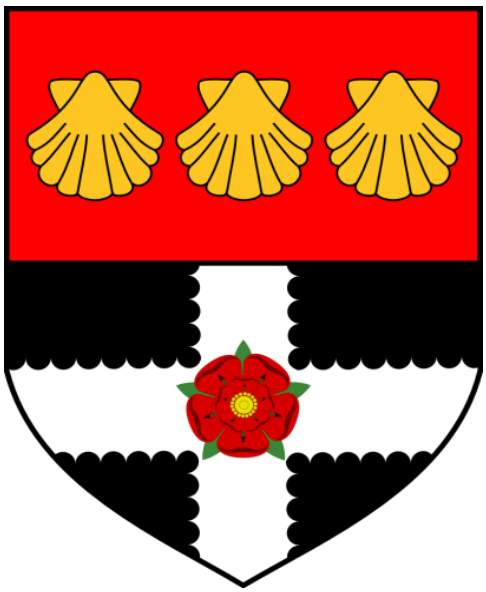

The kinetics and regulators of integrin clustering and activation: implications for platelet function in haemostasis and haematological disorders.

A thesis submitted for the degree of Doctor of Philosophy

By

Mohammad Suhaim Abo Hassan

Institute for Cardiovascular and Metabolic Research

School of Biological Sciences

October 2019

Declaration

I confirm that this is my own work and the use of all material from other sources has been properly and fully acknowledged.

Signed: Mohammad Abo Hassan

Date: October 2019

Abstract

Introduction: Platelets are small a-nucleate blood cells that stop bleeding at vascular injury. Platelets form a haemostatic plug by sticking to exposed extracellular matrix proteins and aggregating at the site of injured vessel. Integrins are transmembrane receptors linked to actin cytoskeleton. Integrin $\alpha_{IIb}\beta_3$ activation and clustering is a vital part of platelet activation and is mediated in part through the association of kindlin-3 with integrin β_3. Recent studies also revealed the interaction between kindlin-3 and β_3 is necessary to regulate and support integrin activation in platelet at the site of injury. ILK is a known effector molecule which recruits kindlin-3 to bind to the cytoplasmic tail of β_3. However, the temporal interaction between kindlin-3 - β_3 and the mechanisms of $\alpha_{IIb}\beta_3$ clustering are not fully understood. The objective of this study was to develop a Stochastic Optical Reconstruction Microscopy (STORM) method for measuring β_3-β_3 clustering in human platelets and use this to investigate the time course of integrin β_3 clustering, its association with kindlin-3 and the role of ILK in this process.

Results: The localization of integrin β_3 and kindlin-3 were analysed using the ImageJ plugin ThunderSTORM and a novel cluster analysis method was developed for defining clustering in R. The density of β_3 molecules surrounding each β_3 molecule (a measure of clustering) showed a biphasic pattern increasing from a low in resting platelets to peak at 60 seconds, falling at 90 seconds, then increasing again by 180 seconds before again declining by 300 seconds. β_3-β_3 FRET signals were observed in a biphasic fashion and confirmed our initial data presented on $\beta_3\beta_3$ clustering. The density of β_3 molecules surrounding each kindlin-3 molecule showed the opposite trend of β_3 clustering for the first 30 seconds (decreasing from a high in resting platelets) and then followed the same pattern as β_3 clustering. The kindlin-3 - β_3 co-cluster and β_3-β_3 cluster were positively

associated after 30 seconds stimulation but not in the first 15 seconds. (N-Methyl-3-(1-(4-(piperazin-1-yl) phenyl)-5-(4′-(trifluoromethyl) [1, 1′-biphenyl]-4-yl)-1H-pyrazol-3-yl) propanamide (22), Cpd-22, a selective ILK inhibitor, was characterised and found to inhibit different platelet functions such as platelet aggregation, fibrinogen binding and alpha granule secretion. Cpd-22 impaired thrombin mediated kindlin-3 - β_3 co-clustering over time (in resting and after stimulation). Cpd-22 treated platelets displayed reduction in the percentage of β_3 clustering in response to thrombin or CRP-XL. Therefore, real time of rate fibrinogen binding was measured and found to be inhibited and not totally dependent β_3-β_3 clustering. Cpd-22 impaired thrombin or CRP-XL stimulated integrin β_3, Src, and Syk downstream signalling at late time points, corresponding with the second peak of β_3 clustering.

Conclusion: A STORM microscopy method was developed and used to quantify the temporal changes in the co-clustering of kindlin-3 with integrin β_3, and the biphasic clustering of integrin β_3 in human platelets following thrombin or CRP-XL stimulation. This was used to show that ILK has a role in platelet activation. Inhibition of ILK reduces kindlin-3 - β_3 association. Thus, reduction of kindlin-3 - β_3 leads to inhibition of β_3-β_3 clustering, and inhibition of β_3 downstream signalling in late time points, corresponding with the second peak of β_3 clustering.

Acknowledgments

I would like to thank Dr. Chris Jones for his great supervision and giving me great opportunity to study interesting project over four years. I am really grateful for his help and advices. I would also express my gratitude to Professor Jonathan Gibbins for his support and guidance on this project. I appreciate his help and encouragement. Thank you for Dr. Sara Jones and Dr. Alice pollitt for being my PhD committee. I am thankful for King Khalid University for scholarship and helped me to achieve my dream.

Thank you for all lab members and staff for their support and help. Thanks to Dr. Sarah Al-Oudah for her great support and help. Thanks to Dr. Khaled Sahli for his support. Thanks to Dr. Alex Bye, Dr. Alex Stainer, Dr. Jo, Sophie, Dr. Neline, Tanya and Dr. Amanda for their advices. I am thankful to Mrs. Helen Yeshayahoo for her support and encouragement. Thanks to all blood donors.

Importantly, a huge thank you to mum and dad for supporting me throughout the years spent in the research. Without them I would have nothing in my life. Thanks to my brothers and sisters for their support and encouragement. I am really thankful to my wife, Taraf, Aljazi and Whard for their patience and cheering me up throughout the study. I also grateful for their celebrating the wonderful moments.

Presentations

1) **Poster presentation: Analysis of integrin β_3 clustering and kindlin association using a novel STORM microscopy method.** International Society on Thrombosis and Haemostasis (ISTH) Congress, Berlin, Germany, 2017.
2) **Poster presentation: ILK role on kindlin regulation and integrin β_3 clustering in platelet function.** 4th EUPLAN (European platelet network) conference, Bruges, Belgium from September, 2018.

List of Abbreviations

3D	Three dimension
ACD	Acid citrate dextrose
ADP	Adenosine diphosphate
ANOVA	Analysis of variance
ATP	Adenosine triphosphate
BFU-MK	Burst-forming unit-MK
BSS	Bernard-Soulier Syndrome
CalDAG-GEFI	Calcium- and diacylglycerol-regulated guanine nucleotide
cAMP	Cyclic adenosine monophosphate
cGMP	Cyclic guanosine monophosphate
CH	Calponin homology
CHO	Chinese hamster ovary
CRP-XL	Crosslinked collagen-related peptide
Csk	C- terminal Src kinase
C-terminal	Carboxyl-terminal
DAG	Diacylglycerol
DTS	Dense tubular system
ECM	Extracellular matrix
EGTA	Ethylene glycol-bis (β-aminoethylether)-N, N, N', N'-tetraacetic acid
EM	Electron microscopy
FA	Focal adhesion

FcRγ	Fc receptor γ-chain
FII	Factor II
FITC	Fluorescein isothiocyanate
FIX	Factor IX
FRET	Fluorescence resonance energy transfer
FVII	Factor VII
GC	Guanylyl cyclase
GDP	Guanosine diphosphate
GEF	Guanine nucleotide exchange factor
GP	Glycoprotein
GPCR	G-protein-coupled receptor
GPO	G-Glycine, P-Proline, O-Hydroxyproline
GPRP	Peptide Gly-Pro-Arg-Pro
GTP	Guanosine triphosphate
HEPES	4-(2-hydroxyethyl)-1-piperazineethanesulfonic acid
HSC	Haematopoietic stem cell
IC50	Half maximal inhibitory concentration
Ig	Immunoglobulin
ILK	Integrin linked kinase
IP	Prostacyclin receptor
IP3	Inositol 1, 4, 5-trisphosphate
IPP	ILK–PINCH–Parvin

ITAM	Immunoreceptor tyrosine-based activation motif LAT Linker for activation of T cells
ITIM	Immunoreceptor tyrosine-based inhibition motif
LADIII	Leukocyte adhesion deficiency type III
LTA	Light transmission assay
mAbs	Monoclonal antibodies
MK	Megakaryocyte
MLC	Myosin light chain
ms	millisecond
NO	Nitric oxide
NOS	Nitric oxide synthases
N-terminal	Amino-terminal
OCS	Open canalicular system
PAGE	Polyacrylamide gel electrophoresis
PAR	Protease-activated receptors
PBS	Phosphate-buffered saline
Pe	Phycoerythrin
PECAM-1	Platelet–endothelial cell adhesion molecule 1
PGH2	Prostaglandin endoperoxide H2
PGI2	Prostaglandin
PH	Pleckstrin homology
PI3K	Phosphoinositide 3-kinase
Pinch	Particularly interesting new cysteine–histidine protein

PIP_2	Phosphatidylinositol 4, 5-bisphosphate
PIP3	Phosphatidylinositol (3, 4, 5)-trisphosphate
PKA	Protein kinase A
PKC	Protein kinase C
PKD	Pseudokinase domain
PKG	Protein kinase G
PLC	Phospholipase C
PM	Plasma membrane
PRP	Platelet-rich plasma
PS	Phosphatidylserine
PSF	point spread function
PSGL-1	P-selectin glycoprotein ligand
PTB	Phosphotyrosine-binding
PVDF	Polyvinylidene difluoride
RASA3	Ras GTPase-activating protein 3
RIAM	Rap1b-interacting adaptor molecule
ROI	Region of interest
SDS	Sodium dodecyl sulphate
SFK	Src family tyrosine kinase
SH	Src homology
SH2	Src homology 2
SH3	Src homology 3
SLP-76	Src homology 2 domain-containing leukocyte protein of 76 kDa

SNARE	Soluble NSF attachment protein receptor
SOCE	Store-operated calcium entry
STIM1	Stromal interaction molecule 1
STORM	Stochastic optical reconstruction microscopy
TBST	Tris-buffered saline-TWEEN® 20
TF	Tissue factor
TP	Thromboxane A2 receptor
TPO	Thrombopoietin
TRPC	Transient receptor potential channel
tSNARE	Target soluble NSF attachment protein receptor
TxA2	Thromboxane A2
TxS	Thromboxane synthase
VASP	Vasodilator-stimulated phosphoprotein
v-SNARE	Vesicle-soluble N-ethylmaleimide–sensitive fusion protein receptor
VWF	Von Willebrand factor

List of Figures

Figure 1.1 Thrombus formation at the site of injury. 7

Figure 1.2 Glycoprotein VI signalling pathway.....13

Figure 1.3 G-protein-coupled receptors signalling pathway. 20

Figure 1.4 Schematic diagram $\alpha_{IIb}\beta_3$ activation (inside-out signalling) by thrombin receptors.....25

Figure 1.5 RAP1 is critical for integrin inside-out activation and the formation of a hemostatic plug.....28

Figure 1.6 Talin and Kindlin structure. 32

Figure 1.7 Src activation following β_3 clustering.....38

Figure 3.1 Three dimension images β_3 molecules in platelets.....57

Figure 3.2 Three dimension images of β_3 clustering in platelets. 58

Figure 3.3 Diagram of β_3 integrin clustering analysis using ImageJ plugin ThunderSTORM. 61

Figure 3.4 Percentage β_3 clusters within 50 nm. 62

Figure 3.5 Percentage of nearest $\beta_3\beta_3$ cluster in each individual.....63

Figure 3.6 Defining β_3 clustering in platelets. 66

Figure 3.7 Temporal changes in integrin ($\beta_3\beta_32$) clustering in response to thrombin stimulation. 67

Figure 3.8 Number of β_3 molecules. 68

Figure 3.9 Optimisation of Alexa fluor 647- and PE- fluorescent dyes labelling. ..70

Figure 3.10 Membrane localization of integrin β_3-β_3 association on thrombin stimulated platelet surface.....72

Figure 3.11 Three dimension images of kindlin molecules in platelets. 76

Figure 3.12 Three dimension of kindlin-β_3 association in platelets. 78

Figure 3.13 Defining kindlin-β_3 co-clusters within 50 nm in human platelets. 79

Figure 3.14 Temporal changes in kindlin-β_3 co-clustering. 80

Figure 4.1 The time course of integrin β_3 clustering and co-localisation with kindlin in response to thrombin. 91

Figure 4.2 Level of β_3 molecules within $\beta_3\beta_3$2 clustering in response to thrombin.92

Figure 4.3 The time course of integrin β_3 clustering and co-localisation with kindlin in response to CRP-XL. 95

Figure 4.4 CRP-XL mediates level of β_3 molecules within $\beta_3\beta_3$2 clustering.....96

Figure 4.5 Thrombin induces kindlin molecules within k$\beta_3$2 co-cluster. 98

Figure 4.6 Level of kindlin molecules within k$\beta_3$2 co-cluster induced by CRP-XL. 99

Figure 4.7 Correlation between β_3-β_3 density and kindlin-β_3 from 0 to 300 seconds. 101

Figure 4.8 Human platelet aggregation in response to 300 seconds stimulation with thrombin and CRP-XL. 103

Figure 4.9 Real time flow cytometry of fibrinogen binding induced by thrombin or CRP-XL.....105

Figure 4.10 Phosphorylation patterns of β_3, Src and Syk in thrombin aggregated platelets.....108

Figure 4.11 Phosphorylation patterns of β_3, Src and Syk in CRP-XL aggregated platelets.....109

Figure 5.1 Fibrinogen binding mediated by CRP-XL is inhibited by Cpd-22.....118

Figure 5.2 Cpd-22 inhibits fibrinogen binding induced by thrombin. 121

Figure 5.3 Cpd-22 inhibits fibrinogen binding in response to CRP-XL.....123

Figure 5.4 Cpd-22 down regulates P-selectin exposure in response to thrombin. 127

Figure 5.5 Cpd-22 inhibits P-selectin exposure evoked by CRP-XL. 129

Figure 5.6 Cpd-22 inhibits Platelet Aggregation induced by thrombin 131

Figure 5.7 Cpd-22 attenuates CRP-XL mediated aggregation 133

Figure 5.8 Cpd-22 does not impair receptor levels in human platelets. 136

Figure 5.9 Cpd-22 selectively reduces the function of ILK. 138

Figure 6.1 Cpd-22 reduces integrin β_3 clustering and co-localisation with kindlin in response to thrombin 146

Figure 6.2 Cpd-22 inhibits integrin β_3 clustering and co-localisation with kindlin evoked by CRP-XL. 148

Figure 6.3 Kindlin-β_3 association is inhibited by Cpd-22 in response to thrombin or CRP-XL.....150

Figure 6.4 Cpd-22 down regulates thrombin or CRP-XL induced β_3-β_3. 153

Figure 6.5 Cpd-22 inhibits real time fibrinogen binding in response to thrombin or CRP-XL.....155

Figure 6.6 The impact of ILK inhibition of signal downstream of β_3 in response to thrombin.....159

Figure 6.7 Effect of Cpd-22 on tyrosine phosphorylation of β_3 and downstream signalling induced by CRP-XL. 161

Table of Contents

Declaration……...I

Abstract…….…II

Acknowledgements……...IV

Presentations……..V

Abbreviations……VI

1 Introduction 1

1.1 Platelet overview.....2

1.2 Platelets structure.....2

1.3 Platelet formation.....4

1.4 Role of platelet in haemostasis 4

1.4.1 Tethering and adhesion.....5

1.4.2 Integrin activation and secretion 5

1.4.3 Thrombus formation.....5

1.5 Platelets receptors and signalling pathway 8

1.5.1 Tyrosine kinases receptors 8

1.5.2 G protein–coupled receptors.....15

1.6 Platelet Degranulation.....18

1.7 Platelets inhibition 21

1.7.1 Platelet regulation by Nitric oxide (NO) 21

1.7.2 Platelet regulation by Prostaglandin I_2 (PGI_2).....22

1.7.3 Platelet regulation by PECAM-1.....22

1.8 Integrin $\alpha_{IIb}\beta_3$, inside-out signalling activation....23

1.8.1 Rap1b and Rap1-GTP-interacting adaptor molecule (RIAM) are effectors of inside-out pathway....26

1.8.2 Talin is a key regulator of $\alpha_{IIb}\beta_3$ activation....29

1.8.3 Kindlin is a co-activator of integrin....30

1.8.4 Integrin-linked kinase regulates integrin activation (ILK)....33

1.9 $\alpha_{IIb}\beta_3$ clustering and outside-in signalling....35

1.10 Aims....39

2 Materials and methods....40

2.1 Materials....41

2.1.1 Reagents....41

2.1.2 Primary Antibodies....41

2.1.3 Secondary antibodies....42

2.2 Buffer compositions....42

2.2.1 HEPES-buffer....42

2.2.2 Imaging blinking buffer....43

2.3 Methods....43

2.3.1 Cell Preparation....43

2.3.2 Permeabilised platelet stochastic optical reconstruction microscopy (STORM) method....44

2.4 Light Transmission Aggregometry (LTA)....45

2.5 Flow cytometry....46

2.5.1 Fluorescence Resonance Energy Transfer (FRET) assay. 46

2.5.2 Fibrinogen Binding and α-granule Secretion 47

2.5.3 Platelet Receptor Expression.....48

2.6 Protein biochemistry.....48

2.6.1 Platelets Signalling Studies 48

2.6.2 SDS-polyacrylamide Gel Electrophoresis.....49

2.6.3 Immunoblotting.....50

2.7 Statistical analysis.....50

3 Analyzing integrin β_3 clustering and kindlin-3 - β_3 association in human platelets using a novel super resolution STORM microscopy method.....51

3.1 Introduction.....52

3.2 Stochastic Optical Reconstruction Microscopy (STORM) imaging of β_3 clustering and kindlin-3 - β_3 association in platelets 54

3.3 Analysis of β_3 molecules clustering.....59

3.4 FRET flow cytometric analysis further confirmed β_3-β_3 clustering observed in STORM analysis.....69

3.5 Defining kindlin-3 - β_3 co-clusters within 50 nm in human platelets.....73

3.6 General Discussion 81

4 Time scales of integrin β_3 clustering and kindlin-3 - β_3 co-clustering in human platelets using STORM 84

4.1 Introduction.....85

4.2 Temporal changes in time course of integrin β_3 clustering and co-clustering with kindlin-3.....88

4.2.1 Temporal changes in time course of integrin β_3 clustering evoked by thrombin. 88

4.2.2 Temporal changes in time course of integrin β_3 clustering in response to CRP-XL.....93

4.2.3 Temporal changes in time course of kindlin-3 co-clustering with integrin β_3 mediated by thrombin or CRP-XL.....97

4.2.4 Association of β_3-β_3 clustering and kindlin-3 - β_3 co-clustering in human platelet……100

4.3 Platelets aggregation induced by thrombin or CRP-XL 102

4.4 Quantifying the rate of fibrinogen binding by flow cytometric real time assay in response to thrombin or CRP-XL 104

4.5 β_3, Src and Syk phosphorylation in thrombin and CRP-XL aggregated platelets 106

4.6 Discussion.....110

5 Screening the optimal condition of Cpd-22 and its effect on platelet function 113

5.1 Introduction.....114

5.2 Defining the optimal concentration and incubation time for which platelets need to be treated with Cpd-22 in fibrinogen binding and alpha granules secretion tests…. 117

5.3 Role of Cpd-22 in platelet aggregation.....130

5.3.1 Cpd-22 inhibits Platelet Aggregation induced by thrombin.....130

5.3.2 Cpd-22 attenuates CRP-XL mediated aggregation 132

5.4 Cpd-22 does not affect different receptors 135

5.5 Cpd-22 selectively reduces the function of ILK.....137

5.6 Discussion.....139

5.6.1 Effect of Cpd-22 on platelet functions 139

5.6.2 Cpd-22 does not affect human platelet receptor levels and selectively inhibits ILK platelets.....140

6 Evaluation of ILK and its effect on β_3-β_3 and kindlin-3 - β_3 co clustering in human platelets.....142

6.1 Introduction.....143

6.2 Cpd-22 downregulated thrombin or CRP-XL induced kindlin-3 - β_3 co-clustering.....144

6.3 Cpd-22 downregulated thrombin or CRP-XL induced β_3 - β_3 clustering.....151

6.4 Cpd-22 inhibits fibrinogen binding to integrin in real time flow cytometry .154

6.5 Cpd-22 negatively impacted β_3, Src and Syk phosphorylation in thrombin and CRP-XL aggregated platelets 156

6.6 Discussion.....162

6.6.1 Down regulation of kindlin-β_3 co-clustering and β_3-β_3 by Cpd-22.....162

6.6.2 Cpd-22 inhibits thrombin or CRP-XL mediated rate of fibrinogen binding.....163

6.6.3 Cpd-22 negatively impacted β_3, Src and Syk phosphorylation in thrombin and CRP-XL aggregated platelets 163

7 General Discussion 165

7.1 Introduction 166

7.1.1 Role of ILK in integrin β_3 clustering and co-localisation with kindlin in human platelets using a novel super resolution STORM microscopy method 167

7.1.2 Effect of Cpd-22 in platelet function 170

7.1.3 Impact of ILK inhibition on β_3 downstream signalling events 171

7.1.4 Conclusion and future work 172

7.1.5 Concluding remarks 173

8 References 174

9 Appendix: Novel cluster analysis for β_3 clustering using R 199

9.1 Appendix 1: Processing raw data for thunderstorm 199

9.2 Appendix 2: Extracting data from thunderstorm. 200

9.3 Appendix 3: Mean number of β_3 molecules surrounded each β_3 molecules in all individuals 201

9.4 Appendix 4: Percentage of β_3 molecules within cluster. 202

1 Introduction

1.1 Platelet overview

Platelets play an essential role in haemostasis and arterial thrombosis. Platelet activation at places of vascular injury is a multiple process involving the exposure of platelets to sub-endothelium extracellular matrix (ECM) mediating firm aggregation of adjacent platelets to the injured vessel wall and forming a haemostatic plug. However, the pathology of platelets can also be caused by inappropriate stimulation such as vessel rupture and thrombotic disorders resulting in stroke, atherosclerosis and heart attack (Ruggeri, 2002; Gibbins, 2004; Coller, 2012).

1.2 Platelets structure

Platelets are the smallest of the blood cells with disc-like shape and lack a nucleus. Their diameter ranges from 2-4 μm with an average volume of 6-7 fimtoliters (fl) and their count in blood in circulation ranges from 150 - 400 x 10^9/L (Zucker-Franklin, 1997; Yuan et al., 2012; Al Ghumlas, 2013). Lifespan of platelets in blood circulation ranges from 8-14 days (Eyre and Gamlin, 2010).

Heemskerk et al. (2002) demonstrated that platelets are composed of plasma membrane (phospholipid bilayer) in which glycoproteins, glycolipids and cholesterol are embedded. Plasma membrane (PM) is responsible for multiple functions in the body such as molecule interactions, receptor activation, and binding in the haemostatic process. Moreover, the plasma membrane contains specialised microdomains known as lipid rafts which are important in signalling and trafficking of elements in platelets. Lipid rafts contain protein markers in quiescent state such as CD36, CD63 and GPIIb/IIIa. Other proteins such as GPVI, Fc receptor γ-chain, GPIb/IX/V and c-Src are present in in lipid rafts of activated platelets which contribute in platelets interaction, receptor clustering

and activation (Blair and Flaumenhaft, 2009).

As well as the plasma membrane platelets contain an open canalicular system (OCS) which is developed via an invagination of the membrane and dense tubular system (DTS) (Behnke, 1970; White, 1972). As described by Michelson (1992), the OCS is composed of an internal membrane which may form filopodia after platelet activation, leading to increase surface area of the PM. In addition, the OCS may serve as a pool for plasma membrane glycoproteins. For instance, following platelet activation, GPIb/IX becomes attach to OCS and hence sequestered. OCS perform multiple functions in platelets; as the entry of external molecules into the platelets as well as release of granules from platelets upon platelets activation. DTS is a sequestered channel network of endoplasmic reticulum, which is largely thought to store Ca^{2+} (White, 1972). The calcium is important for regulating a number of downstream messenger molecules after platelet activation (Gerrard et al., 1978; Varga-Szabo et al., 2009).

Platelets comprises the cytoskeleton, which is important to support plasma membrane of resting platelets. Discoid shape of quiescent platelets is maintained by the cytoskeleton, which contains the actin cytoskeleton, spectrin-based membrane skeleton and microtubules (Hartwig and DeSisto, 1991; Thon and Italiano, 2012).

The platelet cytoplasm hosts a number of intracellular organelles such as, α-granules and dense granules and lysosomes. α- granules are the most abundant granules (~40-80 per platelet), which constitute numerous proteins responsible for platelets aggregation and thrombus formation (fibrinogen, Von Willbrand Factor (VWF), $\alpha_{IIb}\beta_3$, P-selectin) (Maynard et al., 2007). P-selectin (CD62P) translocates to the membrane after activation (Merten et al., 2000). Also, neutrophils are recruited to platelet via membrane receptor P-selectin glycoprotein ligand (PSGL-1) (Frenette et al., 2000). Dense granules have a

number of elements, like adenosine diphosphate (ADP), adenosine triphosphate (ATP), Ca^{2+} and serotonin, Mg^{2+}, which are released after platelet activation (Thon and Italiano, 2012; Golebiewska and Poole, 2015).

1.3 Platelet formation

Megakaryocytes (MK), one of largest cells in the bone marrow, give rise to platelets. The diameter of a megakaryocyte is 50-100 µm (Nakeff and Maat, 1974). The MK nucleus replicates via a process called endomitosis without cell division producing polyploidy cells. This event is not yet completely understood; however, the process involves repeated cycles of DNA replication (Richardson et al., 2005).

Haematopoietic stem cells (HSC) differentiate to original MK progenitor cells which is called burst-forming unit-MK (BFU-MK) which is further divided to megakaryocyte and erythrocytes. This is followed by the generation of promegakaryoblasts and megakaryoblasts and lastly megakaryocytes. Cytoplasmic projections of megakaryocyte gives rise to proplatelets and eventually release of platelets into the circulation (Briddell et al., 1989; Richardson et al., 2005). Regulation of platelets is controlled by thrombopoietin (TPO), which is released by the liver, and plays a vital role in the stimulation of platelets and megakaryocyte formation (Kaushansky, 1995; Kaushansky, 2009). Each MK is capable of producing 2000–3000 platelets in the circulation (Watson and Harrison, 2010).

1.4 Role of platelet in haemostasis

Platelets play a central role in haemostasis. During normal physiological haemostatic conditions process, a series of processes and signalling pathways occur during platelet accumulation. The biological function of platelets starts with adhesion to the site of

damage, then aggregation to the forming thrombus causing a haemostatic plug **(Figure 1.1)** (Semple et al., 2011; Brass et al., 2011; Wang et al., 2014).

1.4.1 Tethering and adhesion

In normal physiological conditions, platelets exist in a resting state. However, following vascular injury, platelets encounter sub-endothelium matrix proteins where platelets get tethered and rolled over. Tethering is mediated by GPIb-IX-V, a complex receptor in platelets which bind collagen-immobilised VWF (ligand for GPIb) (Jurk and Kehrel, 2005; Angiolillo et al., 2010). GPIb-IX-V binding to collagen-bound VWF is unstable resulting in rolling of platelets and exposure of GPVI (collagen receptors on the platelet surface) to collagen (Kumar et al., 2003). GPVI maintains firmer adhesion along with cascade of activatory signals inside platelets (Savage et al., 1998).

1.4.2 Integrin activation and secretion

Following platelets adhesion, activated platelets change shape, release their granule contents, secret secondary mediators (ADP, Thromboxane A2 (TxA_2) and thrombin) and change the conformation of integrin $\alpha_2\beta_1$ and $\alpha_{IIb}\beta_3$ (Kulkarni et al., 2000; Nieswandt and Watson, 2003; Makris, 2009). These changes switch integrins from low affinity to high affinity. Activated integrin $\alpha_2\beta_1$ binds collagen and hence maintain firmer and stable platelet adhesion to collagen, allowing platelet aggregation and subsequent thrombus formation (Rivera et al., 2009). Interaction of integrin $\alpha_{IIb}\beta_3$ to its ligands (fibrinogen and VWF), facilitate platelet aggregation and formation of thrombus at the site of injury (Coller et al., 1991; Bennett, 2005; Cimmino and Golino, 2013).

1.4.3 Thrombus formation

Tissue factor (TF) is a transmembrane protein present in endothelial cells. This factor plays an important effect on blood coagulation factors such as FVII. TF is exposed on

damaged endothelial cells and binds to VIIa, initiating the activation of the coagulation pathway and thrombin generation. Thrombin is a potent agonist that converts fibrinogen to fibrin monomer. It also activates platelets by cleaving protease activated receptors (PARs) (PAR1-PAR4) in the human platelet membrane. The fibrin mesh then adds to the strength of the platelet plug resulting in a stabilised thrombus (Coughlin, 1998; Ossovskaya and Bunnett, 2004). The thrombus is further stabilised via process of clot retraction which is triggered by contractile forces of the actin cytoskeleton via ligand engaged GPIIb/IIIa (Shattil and Newman, 2004).

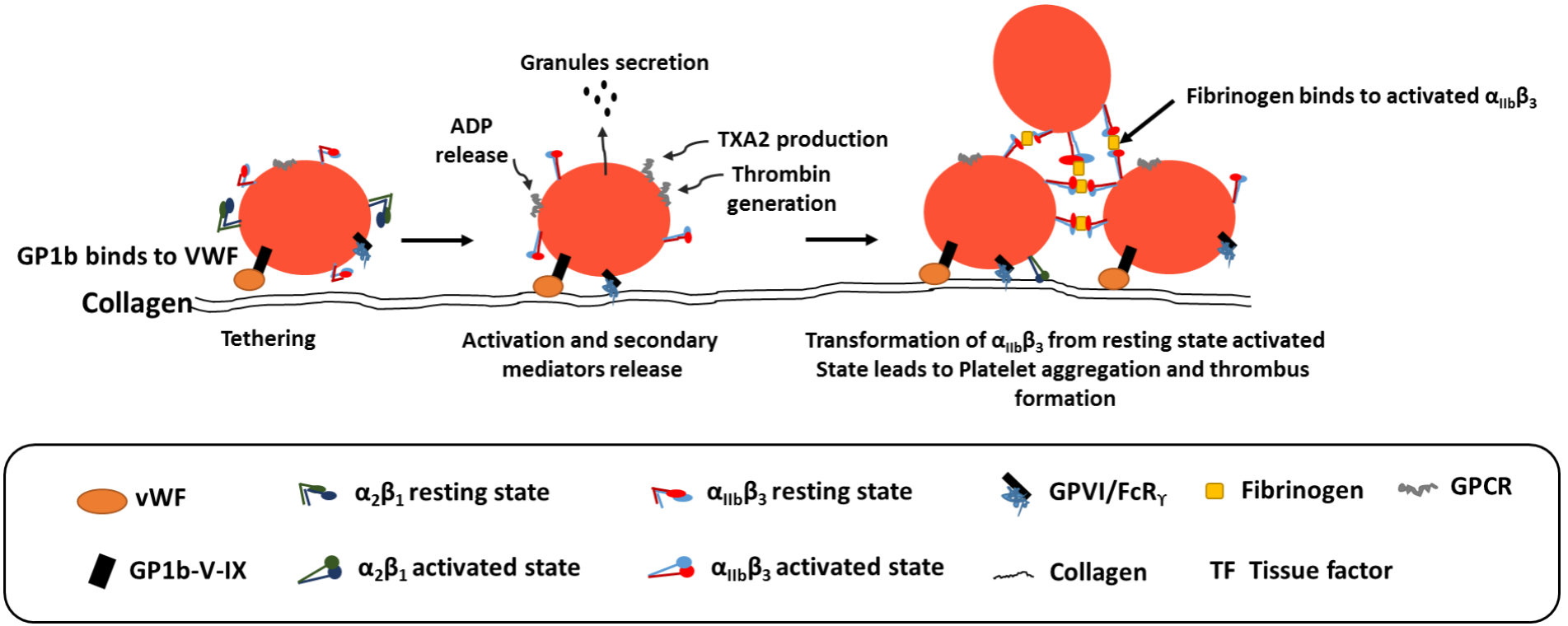

Figure 1.1 Thrombus formation at the site of injury.

Binding between GPIbα, a component of (GPIb-IX-V), to collagen bound VWF allowed platelet rolling on collagen. This rolling enables the interaction of platelets to collagen via its receptor (GPVI). Activatory signalling events take place down-stream of GPVI resulting in integrin activation. Integrin $\alpha_2\beta_1$ maintains firmer platelets-collagen adhesion. Integrin $\alpha_{IIb}\beta_3$ allows platelet crosslinking and aggregate formation. Also, activated platelets undergo shape changes, secretion of granules contents and release of potent platelet agonist (TxA_2, ADP and thrombin).

1.5 Platelets receptors and signalling pathway

Agonists binding to its receptor on the surface of the platelet during vascular damage triggers the activation of signalling waves downstream of engaged receptors. Signalling pathways include tyrosine kinases-dependent phosphorylation involving collagen or G protein-coupled receptors (GPCRs) involving thrombin, ADP, and TxA_2 (Offermanns, 2006; Li et al., 2010). Platelet receptors will be discussed below in detail.

1.5.1 Tyrosine kinases receptors

1.5.1.1 Platelet Collagen receptors GPVI and $\alpha_2\beta_1$

Subendothelial fibrillar collagen is a very potent thrombogenic substrate. Platelets binding to collagen induces powerful activation and supports their adhesion and aggregate formation (Wilner et al., 1968; Clemetson and Clemetson, 2001; Varga-Szabo et al., 2009). Fibrillar collagen types I, III and IV are the major components of the ECM of vascular walls. Collagens consist of repeated GXY motifs where G is glycine and X and Y are proline and hydroxy proline amino acids (Morton et al., 1995).

There are two types of collagen receptors on platelet surface: the immunoreceptor GPVI and the integrin $\alpha_2\beta_1$ (Nieswandt and Watson, 2003). GPVI and $\alpha_2\beta_1$ recognise different regions of collagen where GPVI binds to the GPO repeat, while integrin $\alpha_2\beta_1$ binds to the GFOGER sequence. GPVI primarily induces platelet activation through rapid activatory signals, whereas integrin $\alpha_2\beta_1$ maintains firm adhesion (Holtkotter et al., 2002; Massberg et al., 2003). However, integrin $\alpha_2\beta_1$ has been reported to participate in platelets activation (Inoue et al., 2003).

Integrin $\alpha_2\beta_1$ (also known as GPIa/IIa) was the first collagen binding receptor identified

on platelets and acts mainly as an adhesion receptor. It binds with high affinity to collagen types I and V (Holtkotter et al., 2002; Nieswandt and Watson, 2003). It is expressed on resting platelet surface at approximately 2,000-4,000 copies (Clemetson and Clemetson, 2001; Best et al., 2003). Integrin $\alpha_2\beta_1$ is normally present in a 'low-affinity' state on the surface of quiescent platelets. However, such resting confirmation is readily converted to a 'high-affinity' state in response to agonist- mediated 'inside-out' signaling (Briddon and Watson, 1999; Jung and Moroi, 2000; Lecut et al., 2004). As mentioned earlier, in addition to maintaining firm platelet adhesion, binding of $\alpha_2\beta_1$ to collagen contributes to platelet activation. This contribution is via a series of intracellular signalling events (outside-in signalling) **(Figure 1.2)** or indirectly by reinforcing GPVI-collagen binding (Jung and Moroi, 2000; Nieswandt and Watson, 2003).

Integrin $\alpha_2\beta_1$ signalling pathway shares similar signalling molecules as the GPVI signalling pathway, including Src, Syk, Src homology 2 domain-containing leukocyte protein of 76 kDa (SLP-76), and phospholipase Cγ (PLCγ2). However, generated signalling is much weaker than GPVI and less likely to play major role in thrombus formation (Jung and Moroi, 2000; Inoue et al., 2003).

1.5.1.2 GPVI/ FcRγ-chain complex

GPVI (62 kDa) is a type I transmembrane receptor that non-covalently binds with the FcRγ subunit (Tsuji et al., 1997; Watson and Gibbins, 1998). It is exclusively expressed in megakaryocytes and platelets and contains two Ig- like extracellular domains, a mucin-like stalk, a transmembrane region, and a short 51-aa cytoplasmic tail (Clemetson et al., 1999; Wei et al., 2009). Quiescent human platelets express 2,000-4,500 copies of GPVI on their surface, which does not change upon platelet stimulation (Best et al., 2003).

However, to regulate its signalling, GPVI is shed from the surface of stimulated platelets (Bergmeier et al., 2004; Gardiner et al., 2007).

Positively charged arginine amino acids residing within the transmembrane region of GPVI mediates a constitutive noncovalent association with the FcRγ-chain (Watson et al., 2005). Such association is essential for expression and signalling of GPVI (Gibbins et al., 1996; Poole et al., 1997). GPVI recognises and binds collagen and laminin (Inoue et al., 2006). Also, synthetic collagen- related peptide (CRP) serves as non-physiological GPVI-specific ligand and is widely used for research purposes (Asselin et al., 1997). Moreover, GPVI binds snake toxin convulxin which is also a ligand for GPIb-IX-V (Kanaji et al., 2003).

Phosphorylation of the conserved immunoreceptor tyrosine-based activation motif (ITAM) (YXX[L/I]X_{6-12}YXX[L/I]) in the FcRγ-chain marks the trigger of GPVI signalling in platelets (Gibbins et al., 1996; Poole et al., 1997). This phosphorylation is mediated by Fyn and Lyn, constitutively associated kinases with a proline-rich region in the cytoplasmic tail of GPVI **(Figure 1.2)** (Ezumi et al., 1998; Briddon and Watson, 1999). Studies on Fyn and Lyn single and double-ablated mice showed positive regulation of Fyn on GPVI signalling. On the other hand, Lyn regulates GPVI signalling in a positive and negative manner. Also, other SFKs may compensate for the absence of Fyn and Lyn (Quek et al., 2000).

The tyrosine kinase Syk then binds to the phosphorylated FcRγ-chain ITAM via its tandem Src-homology 2 domains (SH2) and undergoes autophosphorylation and Src family kinase (SFKs) mediated phosphorylation **(Figure 1.2)**. Consequently, activatory signals accumulate a number of signalling proteins including the transmembrane adapter linker for activated T cell (LAT), SLP-76,Vav of GTPases, Tec family kinases and

effector proteins such as phosphoinositide 3-kinase (PI3K) and PLCγ2 **(Figure 1.2)** (Watson et al., 2005; Offermanns, 2006).

Activated PLCγ2 mediates the generation of two messengers including Inositol 1, 4, 5-trisphosphate (IP3) and 1, 2-diacylglycerol (DAG). IP3 mediates mobilization of Ca^{2+} and DAG is required for the activation of protein kinase C (PKC). Increasing concentration of Ca^{2+} in the cytosol and PKC activation lead to integrin activation, platelets aggregation and subsequently thrombus formation **(Figure 1.2)** (Grosse et al., 2007; Shattil et al., 2010).

The pivotal role of GPVI receptor in collagen-induced platelet activation, thrombosis and haemostasis is shown in FcRγ-chain–deficient, GPVI- depleted or GPVI-deficient mice which show markedly reduced platelet attachment and thrombus formation at sites of arterial injury (Konishi et al., 2002; Massberg et al., 2003; Lockyer et al., 2006).

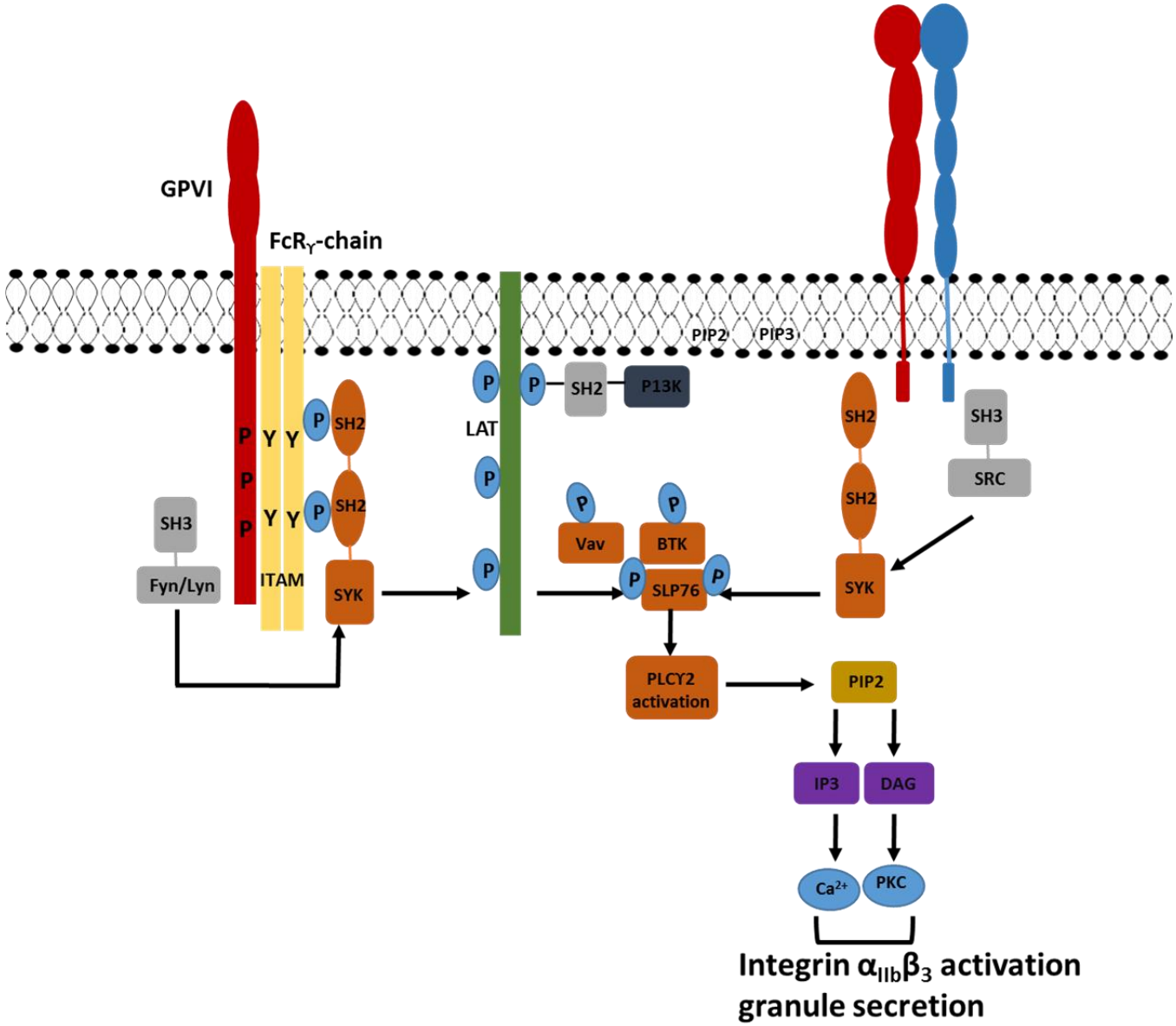
GPVI
FcRγ-chain
P P P
Y Y
Y Y
ITAM
SH3
Fyn/Lyn
P
SH2
SYK
LAT
P
SH2
P13K
Vav
BTK
SLP76
PLCY2 activation
PIP2
PIP3
SH2
SH2
SYK
SH3
SRC
PIP2
IP3
DAG
Ca2+
PKC
Integrin αIIbβ3 activation
granule secretion

Figure 1.2 Glycoprotein VI signalling pathway.

Following GPVI- collagen interaction, Src Family Kinase SFKs (Fyn and Lyn) bind GPVI via Src-homology 3 (SH3) domain. Autophosophorylation of SFK via collagen induced GPVI clustering causing tyrosine phosphorylation of FcRγ-chain. Phosphorylated residues act as docking sites for Syk, which involves SH2 domains. Syk phosphorylates downstream signalling molecules including linker for activation of T cells (LAT) and assembly of the LAT signalosome. The LAT signalosome includes Src homology 2 domain-containing leukocyte protein of 76 kDa (SLP-76), Vav and Gads. It is important for phosphoinositide 3- kinase (PI3K) recruitment, which mediates the conversion of phosphatidylinositol 4, 5-bisphosphate (PIP2) to phosphatidylinositol 3, 4, 5-trisphosphate (PIP3). Interaction of Bruton tyrosine kinase (BTK) and activates phospholipase Cγ2 (PLCγ2), generating diacylglycerol (DAG) and inositol 1, 4, 5-trisphosphate (IP3). IP3 mobilises intracellular Ca^{2+} and DAG promotes activation of protein kinas C (PKC). These events lead to degranulation, promotes the affinity of integrin $\alpha_{IIb}\beta_3$ and hence the signalling pathway enhances platelet aggregation.

1.5.1.3 VWF receptor; GPIb-IX receptor

GPIb-V-IX is a highly abundant receptor (25,000 copies per platelet) with a structurally unique receptor complex that is exclusively expressed in platelets and megakaryocytes (Nurden and Caen, 1975). The α- and β-subunits of GPIb, GPIX, and GPV of this complex all belong to the leucine-rich repeat protein superfamily and are characterized by the presence of 1 or more leucine- rich repeats (Berndt et al., 2001; Luo et al., 2007).

At the high shear rates in small arteries and arterioles, platelets are recruited to the injured vessel via GPIb-V-IX. The interaction between GPIb and the A1 domain of VWf immobilised on collagen or on the surface of stimulated platelets is crucial for the initial tethering of circulating platelets. This tethering enables the interaction of other receptors on the platelet surface with exposed collagen (Savage et al., 1998).

Besides its adhesion function, increasing reports suggest that GPIb-V-IX also acts as signal transducer with the capacity to induce integrin $\alpha_{IIb}\beta_3$ activation and thereby maintaining firm adhesion of the platelets independently of other principal activatory receptors, such as GPCRs or GPVI (Arthur et al., 2005). Moreover, GPIb-V-IX has been proposed to contribute to ITAM signalling. This proposal was based on the observed recruitment of this complex to lipid rafts, where it may interact with GPVI and hence, mediates phosphorylation of the FcRγ-chain associated ITAM (Wu et al., 2001; Shrimpton et al., 2002; Arthur et al., 2005).

Lack or impairment of GPIb-V-IX has been associated with the Bernard-Soulier Syndrome (BSS), a congenital bleeding disorder characterized by mild thrombocytopenia, giant platelets formation along with failure to form platelet aggregates (Lopez et al., 1998).

1.5.2 G protein–coupled receptors

Stimulated platelets generate and secrete a large amount of thrombin, TxA_2 and ADP. Binding of these mediators augments platelet activation and stabilises the formed thrombus. Platelets express an array of G protein coupled receptors **(Figure 1.3)**. For instance, thrombin receptors (PAR1 and PAR4); ADP receptors ($P2Y_1$ and $P2Y_{12}$) and TxA_2 (TP receptor) (Offermanns, 2006).

1.5.2.1 Thrombin: PARs

Exposure of phosphatidylserine on the surface of stimulated platelets enables assembly and accumulation of the prothrombinase complex and the generation of thrombin. This soluble plasma serine protease is generated via a series of enzymatic reactions in a multistep coagulation cascade that takes place on the surface of stimulated platelets (Opal et al., 2002). Inactive zymogen prothrombin is converted to active thrombin, which in turn catalyses the cleavage of soluble fibrinogen into insoluble fibrin polymers. Fibrin provides a mesh like structure that further stabilizes the formed thrombus (Weisel and Litvinov, 2017).

As shown in **Figure 1.3**, human platelets express PAR-1 and PAR-4 whilst PAR-3 and PAR-4 are expressed on murine platelets. Thrombin mediates platelet activation by cleaving PAR-1 and PAR-4 exposing a short activatory peptide sequence that acts as tethered ligand (Coughlin, 2000; Ofosu, 2003). Both PAR-1 and-4 receptors are coupled to heterotrimeric G proteins (G_q, $G_{12}/_{13}$ and G_i Gα-subunits). The G_q pathway is the main PAR-1 and PAR-4 activation pathway leading to activation of PLCβ and consequent generation of IP3 and DAG mediators which in turn activate Ca^{2+} mobilization and PKC, respectively. The $G_{12}/_{13}$ pathway contributes to activation of Rho kinase and cytoskeletal reorganization (Coughlin, 2000).

1.5.2.2 ADP receptors: $P2Y_1$ and $P2Y_{12}$

Dense granules contain high levels of ADP that get released upon platelet stimulation. ADP binds $P2Y_1$ and $P2Y_{12}$ mediating platelet activation through positive feedback mechanism (Murugappa and Kunapuli, 2006; Gachet et al., 2006). $P2Y_1$ couples to G_q, whereas $P2Y_{12}$ associates with G_i **(Figure 1.3)** (Savi et al., 1998; Hechler et al., 1998; Jantzen et al., 2001).

$P2Y_1$ mediates Ca^{2+} mobilization, morphological changes of platelets along with weak aggregation (Hechler et al., 1998). Nevertheless, $P2Y_{12}$ causes the inhibition of adenylyl cyclase, and thereby reducing intracellular Cyclic Adenosine Monophosphate (cAMP) levels, activates of Phosphoinositide 3-kinase (PI3K) and Rap1b level **(Figure 1.3)** (Lova et al., 2003; Gachet et al., 2006; Joo, 2012). Mice lacking the ADP receptors showed reduced platelet aggregation (Offermanns, 2006).

1.5.2.3 Thromboxane A_2 receptor: TP

TxA_2 is a short-lived lipid mediator. Release of TxA_2 by activated platelets improves activation signals and aids in recruiting more platelets to the developing thrombus (FitzGerald, 1991). Also, this mediator acts as potent vasoconstrictor (Huang et al., 2004). TxA_2 is produced from arachidonic acid through conversion by cyclooxygenase-1 and thromboxane synthase. The lipid soluble nature of this mediator enables rapid diffusion across the plasma membrane and binding to the TxA_2 receptor on the surface of either the same or other platelets in an auto- and paracrine fashion, respectively (Suzuki-Inoue et al., 2002; Davi and Patrono, 2007).

Like thrombin receptors PAR-1 and PAR-4, and the $P2Y_1$ ADP receptor, the activated TP receptor in platelets are mainly coupled to the G_q and $G_{12}/_{13}$ α-subunits **(Figure 1.3)**

(Djellas et al., 1999). Patients lacking TxA_2 display a minor bleeding disorder reflecting the vital role of TxA_2 as a positive feedback agonist (Mumford et al., 2010; Dawood et al., 2012). Also, TP knockout mouse showed an extended bleeding time (Thomas et al., 1998). Aspirin is an anti-platelet drug which inhibits platelet activation through irreversible inhibition of cyclooxygenase-1 causing blockage TxA_2 production (Patrono et al., 2005).

1.5.2.4 Calcium Signalling in Platelet

Ca^{2+} is a crucial second messenger in virtually all cells, controlling a wide range of vital cellular processes (Berridge et al., 2003). In platelets, Ca^{2+} elevation contributes to several steps of cellular activation, such as cytoskeletal reorganization of actin necessary for shape change, degranulation or inside-out activation of integrin $\alpha_{IIb}\beta_3$ (indispensable for platelet aggregation) **(Figure 1.3)** (Hathaway and Adelstein, 1979; Shattil and Brass, 1987; Li et al., 2010). Cytosolic elevation in Ca^{2+} comes from two major sources: IP3 mediated release of compartmentalized Ca^{2+} and the entry of extracellular Ca^{2+} through the PM into platelet cytosol in process referred as store operated calcium entry (SOCE) (Parekh and Putney, 2005; Varga-Szabo et al., 2009).

Depletion of calcium from DTS induces instant influx of calcium across the plasma membrane through stromal interaction molecule 1 (STIM1) and calcium-release activated modulator 1 (Orai1) that is expressed in the cell membrane (Liou et al., 2005; Grosse et al., 2007). Besides these players, canonical transient receptor potential channel (TRPC) contributes to Ca^{2+} entry through the PM (Rosado et al., 2000; Vemana et al., 2015).

Platelet stimulation evokes activation of several PLC isoforms, which in turn hydrolyse PIP2 to IP3 and DAG. IP3 caused the elevation of Ca^{2+} in cytosol resulting in TxA_2 generation, granule secretion and integrin activation (Crittenden et al., 2004).

1.6 Platelet Degranulation

Several adhesion proteins such as fibrinogen, VWF, coagulation and fibrinolytic factors, cytokines, growth factors, and adhesion receptors are stored in platelet α-granules. Also, dense granules host nucleotides such as (ADP, ATP, GTP; serotonin; histamine; pyrophosphates; and divalent cations). Lastly, proteolytic enzymes are kept in platelet lysozomes (Ren et al., 2008). Granule secretion serves in the amplification of platelet activation, the recruitment of platelets into aggregate sites and stabilisation of the thrombus (Reed et al., 2000). Also, released granule contents play important roles in inflammatory disorder, atherosclerosis, and wound healing (Blair and Flaumenhaft, 2009).

Soluble NSF attachment protein receptors (SNAREs) facilitates the process of granule release (Polgar et al., 2002; Ren et al., 2010). Fusion between plasma membrane (target)–SNARE (t-SNAR) and vesicle-soluble N-ethylmaleimide–sensitive fusion protein attachment receptor (v-SNARE) proteins allows release of granule contents (Ren et al., 2008). In addition to SNARE complexes, other signalling events and pathways are also involved in granule secretion such as calcium signalling, PKC-dependent phosphorylation, integrin outside-in signalling and TxA_2 generation (Akbar et al., 2007; Huang et al., 2007; Konopatskaya et al., 2009).

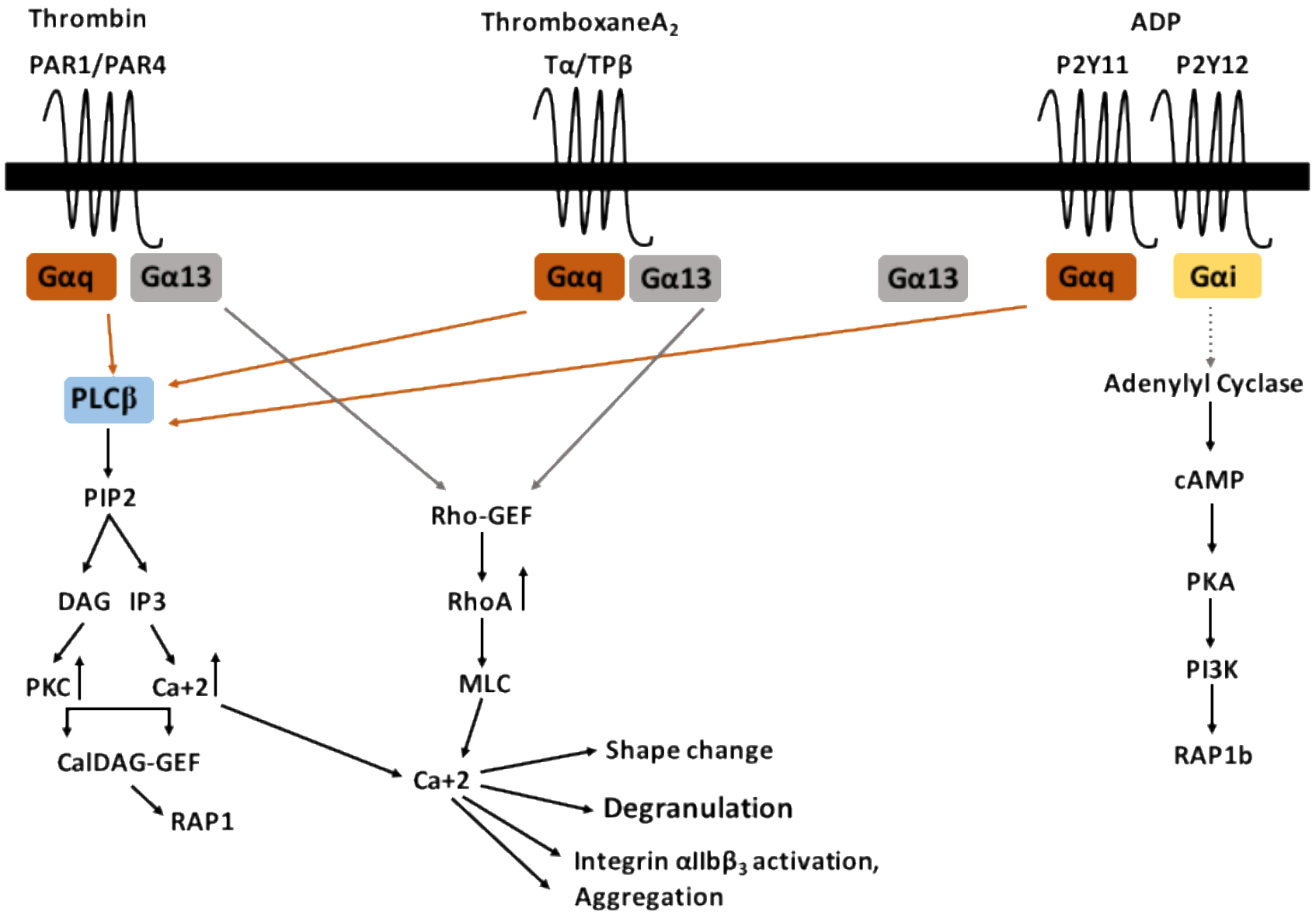
Thrombin
PAR1/PAR4
ThromboxaneA2
Tα/TPβ
ADP
P2Y11
P2Y12
Gαq
Gα13
Gαq
Gα13
Gα13
Gαq
Gαi
PLCβ
PIP2
DAG
IP3
PKC
Ca+2
CalDAG-GEF
RAP1
Rho-GEF
RhoA
MLC
Ca+2
Shape change
Degranulation
Integrin αIIbβ3 activation,
Aggregation
Adenylyl Cyclase
cAMP
PKA
PI3K
RAP1b

Figure 1.3 G-protein-coupled receptors signalling pathway.

Platelet activation leads to the release and synthesis of soluble mediators such as adenosine diphosphate (ADP), the thromboxane A2 (TxA_2) and thrombin acting via GPCRs. The ADP receptors ($P2Y_1$, $P2Y_{12}$), TxA_2 receptor and receptors for thrombin (PAR-1 and PAR-4). These receptors work through binding $G_{\alpha q}$, generating PLCβ and hence mediating the dissociation of Phosphatidylinositol 3,4- bisphosphate (PIP2) and consequent generation of inositol 1,4,5-trisphosphate (IP3) and diacylglycerol (DAG). As result, platelet- shape changes in addition to granules secretion and Ca^{2+} release. Calcium elevation increases the affinity of integrin $\alpha_{IIb}\beta_3$ to bind its ligand fibrinogen. PAR-1, PAR-4 and TP can also mediate signalling through $G_{\alpha 13}$. Phosphorylation of Rho kinase induces the activation of myosin light chain (MLC) resulting in degranulation, cytoskeletal reorganisation and conformational changes in platelets. The ADP receptor $P2Y_{12}$, which is coupled to $G_{\alpha i}$ and decreases the level of cyclic adenosine monophosphate (cAMP) induced by adenylyl cyclase resulting in RAP1b and PI3K activation. Together, these pathways inhibit the activation of protein kinase A (PKA) and mediate platelet activation. Also, the $G_{\beta/\gamma}$ dimer pathways play through phosphoinositide 3-kinase (PI3K) activation, which in turn results in protein kinase B (PKB) activation.

1.7 Platelet inhibition

Platelets normally circulate in the body in a quiescent state. Three mechanism can maintain platelets in a resting state and play an important role in an inhibitory mechanisms in platelets activation. Key inhibitors are nitric oxide (NO), PGI_2 and immunoreceptor tyrosine-based inhibition motif (ITIM)-containing receptors platelet endothelial cell adhesion molecule-1 (PECAM-1). These three mechanisms will be described in the next section.

1.7.1 Platelet regulation by Nitric oxide (NO)

Nitric oxide is synthesized by the catalytic action of Nitric oxide synthases (NOS), enzyme from the semi-essential amino acid L-arginine and molecular oxygen. NOS are classified into three isoforms, NOSI, NOSII and NOSIII (Ghosh and Salerno, 2003). NOSI is found predominantly in nerves and NOSII mainly in inflammatory cells, whereas NOSIII is found in endothelial cells. NOSI and NOSIII are constitutively expressed and calcium is required for their activation. Calcium binds to calmodulin, which then interacts with NOSI or NOSIII as part of the enzyme activation (Pollock et al., 1991).

NO acts as an inhibitor for platelets aggregation, adhesion and fibrinogen binding to its receptors (Schafer et al., 1980; Lieberman et al., 1991; Moncada and Higgs, 2006). NO binds guanylyl cyclase (GC) via passing through cell membrane, causing the hydrolysis of GTP and hence increasing the level of cyclic guanosine monophosphate (cGMP). Elevation of cGMP leads to the activation of protein kinase G (PKG) resulting in the reduction of calcium mobilisation, integrin activation and platelet reactivity and aggregation (Hanafy et al., 2001; Roberts et al., 2004; Walter and Gambaryan, 2009).

1.7.2 Platelet regulation by Prostaglandin I_2 (PGI_2)

PGI_2 is a powerful vasodilator with short half-life (minutes) (Vane and Botting, 1995; Dorris and Peebles, 2012). PGI_2 is synthesized in endothelial cells from Prostaglandin endoperoxide H2 (PGH2) by the action of prostacyclin synthase and released into the circulation (Mitchell et al., 2008). PGI_2 binds seven transmembrane G-protein-coupled receptors known as IP receptor (Offermanns, 2006; Stitham et al., 2007). IP is coupled to G_S protein that stimulates adenylyl cyclase activity leading to increased levels of intracellular cyclic AMP (cAMP). Consequently, increased cAMP causes the activation of protein kinase A (PKA). Several key proteins such as vasodilator- stimulated phosphoprotein (VASP) which interact with many cytoskeletal proteins at focal adhesions retaining platelet in resting morphology (Niebuhr et al., 1997; Soberman and Christmas, 2006; El-Haroun et al., 2008; Mohite et al., 2011).

1.7.3 Platelet regulation by PECAM-1

Platelet endothelial cell adhesion molecule-1 (PECAM-1), also known as CD31, is a 130-kDa immunoreceptor tyrosine-based inhibition motif (ITIM)-containing receptors. PECAM-1 is expressed on the platelet surface at approximately 10,000 copies (Albelda et al., 1991). The inhibitory action of PECAM-1 targets collagen ITAM containing receptor GPVI-FcRγ-chain, GPIb-IX-V (VWF receptor) and PAR4 (G protein-coupled thrombin receptor) (Newman and Newman, 2003). PECAM-1 acts as a potent inhibitor for platelet activation and thrombus formation at the site of injured vessels(Falati et al., 2006; Dhanjal et al., 2007). Studies have confirmed PECAM-1 mediated negative regulation of signalling events downstream of collagen receptors along with attenuated platelet aggregation and thrombus formation in vitro (Jones et al., 2001; Cicmil et al., 2002; Jones et al., 2009). PECAM-1 ablated mouse platelets

demonstrate hyper-responsiveness to collagen stimulation and increased thrombus formation (Patil et al., 2001; Falati et al., 2006).

1.8 Integrin $\alpha_{IIb}\beta_3$, inside-out signalling activation

Integrin $\alpha_{IIb}\beta_3$ is a heterodimeric glycoprotein, which is composed of non-covalently bond of α and β subunits. It is absolutely necessary for platelet aggregation in response to injury (Hynes, 2002; Nieswandt et al., 2009). Integrin $\alpha_{IIb}\beta_3$ is the most abundant glycoprotein on the platelet surface with 60,000 to 80,000 copies per cell and an additional intracellular store that is exposed on the surface on activation (Wagner et al., 1996; Hynes, 1987; Emambokus and Frampton, 2003; Shattil and Newman, 2004; Coller and Shattil, 2008). The affinity of this integrin for its ligands (fibrinogen) is upregulated on platelet activation. Hence, it mediates platelet adhesion, aggregation and spreading over the injured vessel wall and thrombus formation (Shattil et al., 1998; Ruggeri, 2002).

Integrin $\alpha_{IIb}\beta_3$ is also stored in platelet α-granules, therefore following platelet activation, integrins are translocated to the platelet surface, resulting in the increase of their surface expression by 30-50 %. The β_3 subunit is expressed in various cell types where it binds with other α subunits whereas the α_{IIb} subunit is exclusively expressed by the megakaryocyte/platelet lineage (Shattil et al., 1998; Shattil and Newman, 2004).

In resting platelets, the affinity of integrin $\alpha_{IIb}\beta_3$ for fibrinogen is normally in low state. Integrin $\alpha_{IIb}\beta_3$ undergoes conformational changes resulting in the increase in ligand affinity. This requires transmission of activatory signals from within the cell to the extracellular domain of integrin $\alpha_{IIb}\beta_3$, a process referred to as inside-out signalling (Shattil et al., 2010; Li et al., 2010). In this process, activated platelets generate IP3 and DAG. IP_3 increases Ca^{2+} concentration in cytosol and then activates calcium- and

diacylglycerol-regulated guanine nucleotide exchange factor I (CalDAG-GEFI) (Cifuni et al., 2008). DAG and Ca^{2+} activate PKC and CALDAG-GEFI, leading to activation of RAP-1 from RAP-1-GDP to RAP-1-GTP. RAP-1-GTP binds to Rap1-GTP-interacting adaptor molecule (RIAM), which results in recruitment and activation of talin to bind cytoplasmic tail of β_3 which causes integrin activation **(Figure 1.4)** (This is discussed in more details below) (Shattil et al., 2010; Anthis and Campbell, 2011).

Platelets that fail to aggregate via $\alpha_{IIb}\beta_3$ cause a bleeding disorder which is called Glanzmann's thrombasthenia. Deficiency in $\alpha_{IIb}\beta_3$ completely inhibits the ability of platelets to aggregate and adhere to sites of injury (Hodivala-Dilke et al., 1999; Ni et al., 2000; Nurden, 2006). β_3-deficient mice platelets showed prolonged tail bleeding times and failed to form thrombi (Ni et al., 2000). Targeting integrin $\alpha_{IIb}\beta_3$ with inhibitors provides protection from thrombotic complications, however, risk of bleeding complications is inevitable (Stolla et al., 2011).

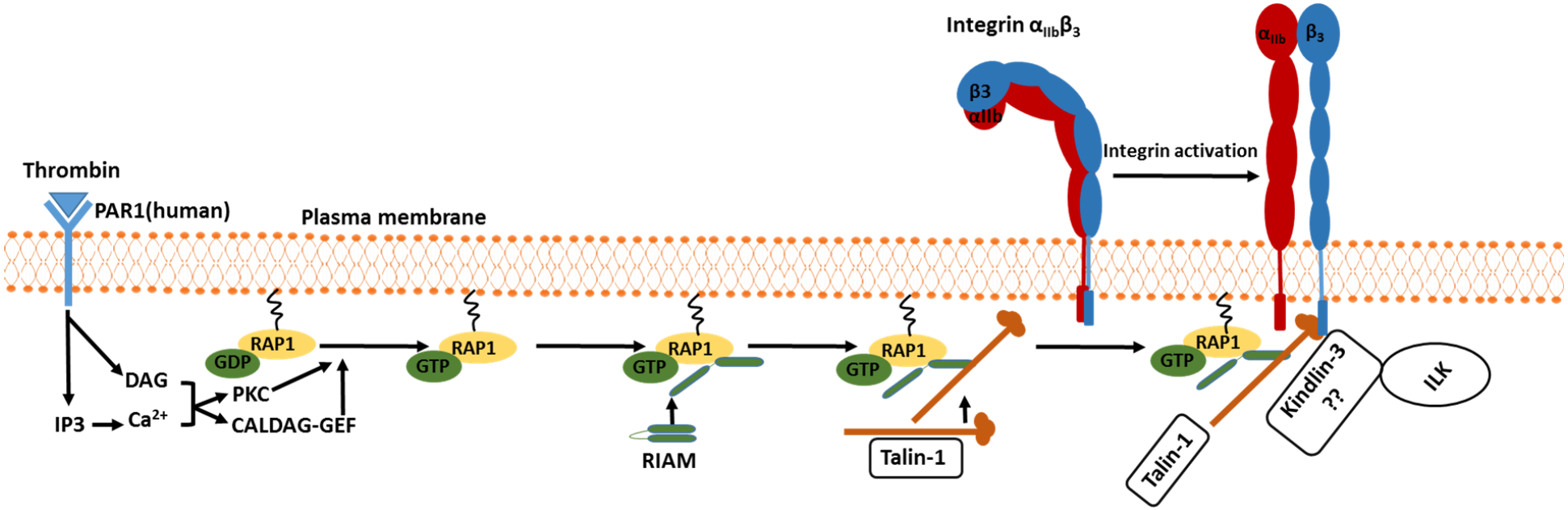

Figure 1.4 Schematic diagram $\alpha_{IIb}\beta_3$ activation (inside-out signalling) by thrombin receptors.

Thrombin mediates the hydrolysis of membrane phospholipids into inositol 1, 4, 5-triphosphate (IP3) and diacylglycerol (DAG). IP3 increases the level of cytoplasmic Ca^{2+}, leading to activation. CALDAG-GEFI. DAG and Ca^{2+} activates PKC and CALDAG-GEFI, leading to transformation of RAP-1-GDP (inactive) to RAP-1-GTP (active). RAP-1-GTP binds to RIAM, which causes recruitment and activation of talin to binds cytoplasmic tail of β_3 integrin and talin mediated $\alpha_{IIb}\beta_3$ activation. Kindlin-3 play a significant role in integrin $\alpha_{IIb}\beta_3$ activation.

1.8.1 Rap1b and RIAM are effectors of inside-out pathway

Rap1b is a small GTP binding protein of the Ras family. This mediator plays pivotal role in inside-out integrin β_3 activation. Also, Rap GTPases are recognized for their role in the regulation of cell-cell interactions and the control of exocytosis (D'Silva et al., 1998; Raaijmakers and Bos, 2009; Frische and Zwartkruis, 2010). In mammals, the Rap family consists of 2 Rap1 genes and 3 Rap2 genes. Platelets express low levels of Rap1a and Rap2a (Klinz et al., 1992). Significant levels of Rap1b and Rap2b were detected in platelets. Rap1b is the most abundant GTPase, accounting for 90% of the total Rap protein (Torti and Lapetina, 1994; Banno and Ginsberg, 2008; Guidetti and Torti, 2012).

Rap1b activation is tightly monitored to ensure platelet activation when appropriate. As mentioned earlier, following platelet stimulation activated CalDAG-GEFI causes the activation of Rap1b. This CalDAG-GEFI mediated activation is counteracted by the inhibitory action of Ras GTPase-activating protein 3 (RASA3) and therefore limiting platelet reactivity **(Figure 1.5)** (Stefanini et al., 2009; Stefanini and Bergmeier, 2018). Inhibition of CalDAG-GEFI (or any other molecules that are involved in the early events of integrin $\alpha_{IIb}\beta_3$ activation) has been employed as a new strategy for antiplatelet agents (Stolla et al., 2011). Lack of Rap1b inhibits integrin $\alpha_{IIb}\beta_3$ activation and affects platelet spreading on fibrinogen. Moreover, Rap1b deficient murine platelets showed decreased platelet aggregation, integrin $\alpha_{IIb}\beta_3$ activation and provided protection from arterial thrombosis (Chrzanowska-Wodnicka et al., 2005).

RIAM is an effector molecule of Rap1b, which belongs to the MRL family of adaptor molecules. MRL associates with talin-1 and Rap1-GTP through short amino-terminal sequences **(Figure 1.5)**. Therefore, this binding facilitates Rap1-mediated adhesion of integrins β_3 by forming a scaffold to bind with Ras GTPase membrane targeting

sequences to talin-1 (Lee et al., 2009). Overexpression of RIAM resulted in slight enhancement of integrin activation. On the other hand, RIAM ablation attenuated integrin activation (Han et al., 2006; Lee et al., 2009). RIAM inhibition hinders recruitment of talin-1 to integrin $\alpha_{IIb}\beta_3$ leading to inhibition of platelet aggregation (Watanabe et al., 2008; Banno and Ginsberg, 2008; Lagarrigue et al., 2016).

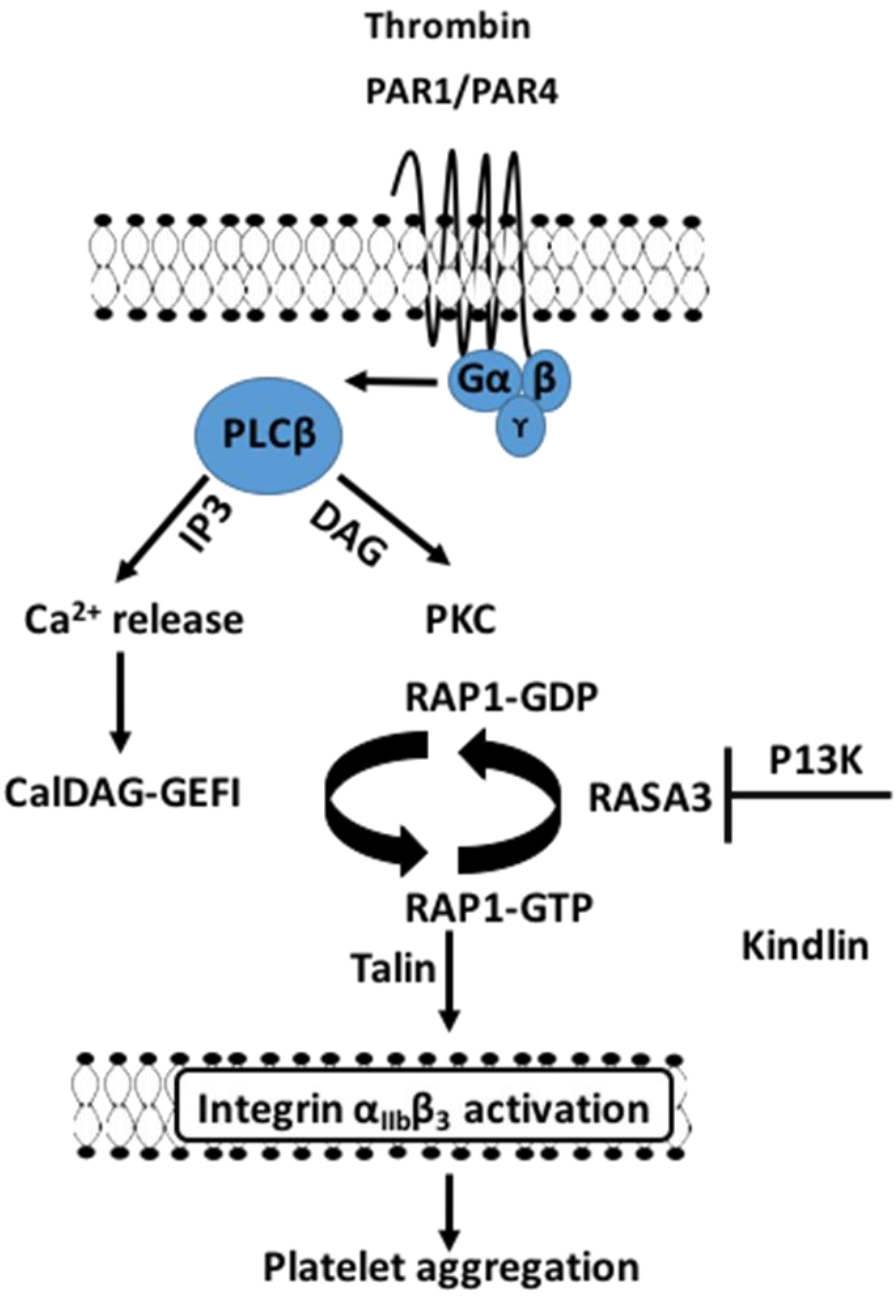

Figure 1.5 RAP1 is critical for integrin inside-out activation and the formation of a hemostatic plug

Thrombin triggers the hydrolysis of membrane phospholipids into inositol 1, 4, 5-triphosphate (IP3) and diacylglycerol (DAG). IP3 enhances the level of cytoplasmic Ca^{2+}, leading to activation of CALDAG-GEFI. DAG and Ca^{2+} promotes PKC and CALDAG-GEFI, which triggers transformation of RAP-1-GDP to RAP-1-GTP. RAP-1-GTP binds to RIAM, which contributes to the recruitment of talin-dependent $\alpha_{IIb}\beta_3$ activation. Kindlin-3 is required to mediate integrin $\alpha_{IIb}\beta_3$ activation and ultimately platelet aggregation. RASA3 stabilises CALDAG-GEFI/RAP1 activation to maintain platelet in quiescent state.

1.8.2 Talin is a key regulator of $\alpha_{IIb}\beta_3$ activation

Talin-1 is 270 kDa protein, consisting of a N-terminal head domain (~50kDa) and C-terminal rod domain (~220 kDa) (Calderwood, 2004). The talin head domain has been proposed to bind to the cytoplasmic tail of β_3. It is composed of a FERM (4.1, ezrin, radixin, moesin) domain with three sub-domains (F1, F2, and F3). Phosphotyrosine-binding (PTB) region in the β_3 integrin cytoplasmic tail contains a membrane proximal NPXY motif, where the F3 talin subdomain binds **(Figure 1.6)** (Calderwood et al., 2002; Anthis et al., 2010). Structural and biochemical studies revealed that the association of F3 subdomain with NPXY motif is crucial for talin mediated integrin activation via intracellular events (Tadokoro et al., 2003; Petrich, 2009).

Furthermore, two integrin binding sites on talin-1 have been revealed which are known IBS-1 and IBS-2 (Gingras et al., 2009). In resting platelets, structural studies revealed that talin-1 is distributed randomly, exist in an autoinhibited state from association with integrin (Bertagnolli and Beckerle, 1993; Goksoy et al., 2008; Song et al., 2012). As described earlier, talin recruitment and activation by RIAM results in integrin activation (Calderwood et al., 2013). The mechanisms of how the effectors recruit talin remain unresolved (Das et al., 2014). Talin-1-deficient platelets failed to activate integrin $\alpha_{IIb}\beta_3$ and aggregate in response to several agonists. Furthermore, platelets spreading on immobilized fibrinogen was hindered, suggesting that talin-1 is essential component for $\alpha_{IIb}\beta_3$-dependent outside-in signalling and inside-out signalling. Likewise, in vivo thrombus formation was similarly impacted (Nieswandt et al., 2007; Joo, 2012).

1.8.3 Kindlin is a co-activator of integrin

Kindlin is an intracellular protein that triggers integrin activation (Malinin et al., 2010; Ye et al., 2014). The three members of the kindlin family are the 75 kDa kindlin-1 (known as fermitin family homolog 1(FERM1)), kindlin-2 (FERM2), and kindlin-3 (URP2) which is restricted to platelets. The kindlins structure is divided into three subdomains F1, F2, F3 (Ussar et al., 2006; Bottcher et al., 2009). F2 subdomain is interrupted by a pleckstrin homology (PH) domain which is crucial for recruiting kindlins to the membrane via an association with phosphoinositides especially with PIP3 and PIP2 **(Figure 1.6)** (Lemmon, 2004; Kloeker et al., 2004; Shi and Wu, 2008; Legate et al., 2012). Kindlins are capable of binding to the cytoplasmic tail of the integrin β subunit via their F3 subdomain (Larjava et al., 2008). Researchers found that F3 is involved in integrin activation by binding to the cytoplasmic tail of β_3 integrin (Shi et al., 2007). The pathway and function of kindlins in these positions are not clear (Rognoni et al., 2016).

Kindlin-3 is widely expressed in haemopoetic cells and is important for integrin activation (Siegel et al., 2003; Ussar et al., 2006; Karakose et al., 2010). Although the important role of kindlin in supporting integrin activation, their mechanisms of action are unclear (Rognoni et al., 2016). Kindlin-3 is suggested to bind directly to the cytoplasmic tail of integrin β_3 via their F3 subdomain with the same affinity as talin-1 (Larjava et al., 2008). Such notion had been supported by Moser et al. (2009) who reported that kindlin-3 binds with high affinity to the NXXY motif of integrin β_3 cytoplasmic tail. Recent findings demonstrated that kindlin plays a vital role as co-activator of $\alpha_{IIb}\beta_3$ (Meves et al., 2009). However, kindlin alone is not sufficient to activate β_3 integrin. It requires to cooperate with the talin head domain to stimulate $\alpha_{IIb}\beta_3$ in Chinese hamster ovary (CHO) cells (Ma et al., 2008; Harburger et al., 2009). Kindlins

can also bind other proteins such as Integrin Linked Kinase (ILK) which is important for the integrin bidirectional signalling (Honda et al., 2009).

Previous studies in human have shown that deficiency of kindlin-3 leads to leukocyte adhesion deficiency type III (LAD-III), which is described by preventing integrin $\alpha_{IIb}\beta_3$-mediated platelet aggregation. Therefore, haemorrhage in these patients might be attributed to the attenuated platelet aggregation capacity. In patients with LAD-III disorder are characterised by deficiency in β_1, β_2 and β_3 integrin activation in platelets and white blood cells, leading to haemorrhage and recurrent infection (Moser et al., 2008; Moser et al., 2009; Fagerholm et al., 2014).

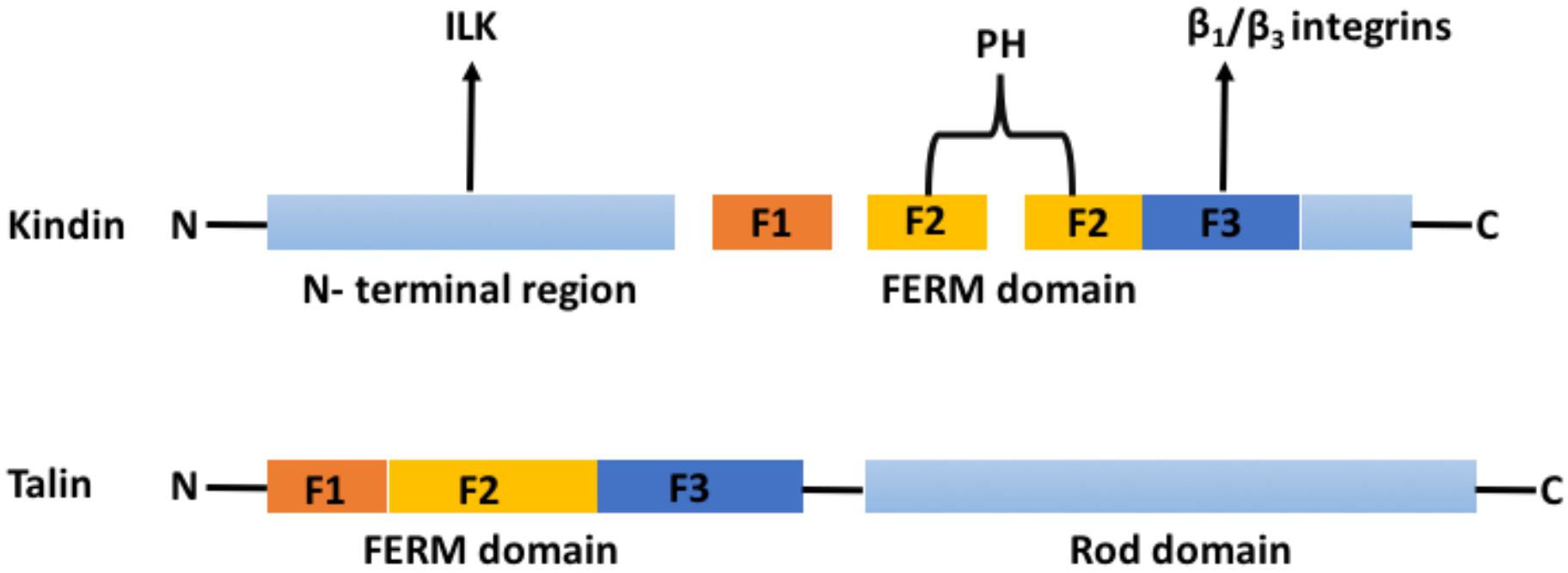

Figure 1.6 Talin and Kindlin structure.

An important feature of talin, is composed of F1, F2 and F3 which is located on N-terminal head. Kindlins also contain F1, F2 and F3 domains, which are situated at the carboxyl terminus. A PH domain which split the F2 region. Arrows indicate that kindlins associate with β_1, β_3 integrin and ILK.

1.8.4 Integrin-linked kinase regulates integrin activation (ILK)

Integrin-linked kinase (ILK), was first identified in a yeast two-hybrid screen based on its ability to interact with the cytoplasmic domain of β_1 integrin (Hannigan et al., 1996). ILK is ubiquitously expressed in various mammalian tissues such as, heart, placenta, kidney, liver and platelets (Hannigan et al., 1996; Stevens et al., 2004). Structure of this 59-KDa ILK involves three distinct domains. The N-terminus contains 4 ankyrin repeats followed by a pleckstrin homology (PH)-like domain and a C-terminal pseudokinase domain (pKD) (Chiswell et al., 2008). The ankyrin repeats mediate the binding with PINCH, a family of LIM domain only containing proteins (Zhang et al., 2002; Braun et al., 2003). The PH domain of ILK has been shown to interact with PIP3 (Delcommenne et al., 1998; Pasquali et al., 2007). Lastly, the C-terminal kinase-like domain interacts with several adaptor proteins including the parvins via its calponin homology (CH) domains (Nikolopoulos and Turner, 2001; Tu et al., 2001; Chu et al., 2006). Moreover, the ILK C-terminus binds β_1 and β_3 integrin cytoplasmic domains along with the effector protein kindlin. These interactions result in the assembly of complex structure known as IPP, ILK-PINCH-parvin. Such assembly is presumed to take place in the cytoplasm and is then recruited to the integrins (Zhang et al., 2002). IPP complex supports integrin clustering and development of focal adhesion linking extracellular matrix with cytoskeleton (Hannigan et al., 1996; Legate et al., 2006).

Also, kindlins lack designated actin-binding sites; therefore, linkage to actin is facilitated through their binding to the ILK-PINCH-Parvin (IPP) complex (Tu et al., 2001; Wickstrom et al., 2010). Previous reports revealed that IPP complex has an important role in regulating integrin signalling and focal adhesion (Legate et al., 2006). ILK-deficient mice platelets showed a reduced level of both proteins PINCH and Parvins. This indicate that ILK is an essential molecule that controls the expression of

these proteins (Tucker et al., 2008). Recent studies suggested that ILK - kindlin binding supports its localization to focal adhesions (FA) and kindlin-induced integrin activation, however, the underlying mechanisms remain unclear. It has been proposed that binding of ILK to kindlin in nematode triggered a conformational change of kindlin that induces its binding to integrin cytoplasmic tails (Qadota et al., 2012). However, such a mechanism has not been observed with mammalian kindlin (Huet-Calderwood et al., 2014; Fukuda et al., 2014).

ILK was previously implicated to play a key role in the activation of integrin $\alpha_{IIb}\beta_3$ and trigger outside-in signalling (Legate et al., 2006; Tucker et al., 2008; Fukuda et al., 2014). Moreover, a large body of experimental data suggests that the ILK-kindlin interaction is crucial for integrin mediated signalling. The interaction between Kindlin-2 and ILK has been found to involve the F2 subdomain of kindlin2 and PKD of ILK. This association is essential for mediating integrin bidirectional signalling (Fukuda et al., 2014; Guan et al., 2018).

The importance of ILK was examined on knockdown HeLa cells and showed defect in cell spreading and focal adhesion formation (Kadry et al., 2018). Researchers reported that gene deletion of ILK displayed a defect in outside-in signalling with no effect in the inside-out pathway (Bottcher et al., 2009; Honda et al., 2013). Moreover, the number of active β_1 integrin was reduced on the surface of ILK-ablated endothelial cells (Friedrich et al., 2004). ILK deficient mouse cells showed altered actin cytoskeleton arrangement, defected cell-ECM adhesion and spreading along with reduced cell spreading and focal adhesion formation (Sakai et al., 2003; Grashoff et al., 2003; Kadry et al., 2018). It has also been reported that kindlin-binding-defective ILK mutants in mammalian cells leads to defects in focal adhesion localization and are unable to fully support defects seen in

ILK knockdown HeLa cells. Depletion of ILK is lethal at the embryonic stage in mice, and absence of ILK in mammalian cells and in C. elegans muscle cells in vivo causes reduction of cell spreading and focal adhesion formation (Fukuda et al., 2014; Kadry et al., 2018). In platelets, In vivo studies reported a reduced level of fibrinogen binding to integrin $\alpha_{IIb}\beta_3$, inhibited platelets aggregation and diminished α-granule secretion in the absence of ILK (Tucker et al., 2008; Jones et al., 2014).

1.9 $\alpha_{IIb}\beta_3$ clustering and outside-in signalling

Following integrin $\alpha_{IIb}\beta_3$ activation, integrin clustering initiates outside-in signals including platelet spreading, granule secretion, firm adhesion and clot retraction (Shattil and Newman, 2004; Lam et al., 2011). Ligand binding induces integrin clustering and conformational changes to the cytoplasmic region (Shattil and Newman, 2004). The β_3 cytoplasmic tail involves arginine-glycine-aspartic acid (RGD) sequence that serves as a binding site for SFKs (Fyn and Src) (Woodside et al., 2001). C- terminal Src kinase (Csk) is also associated with cytoplasmic tail of β_3 (Obergfell et al., 2002). Upon fibrinogen binding to activated $\alpha_{IIb}\beta_3$ and clustering, Csk dissociate from $\alpha_{IIb}\beta_3$ leading to SFKs activation (Arias-Salgado et al., 2005). Syk also has been demonstrated to bind the tail of β_3 through the association of the integrin and the Syk N-terminal SH2 domain (Obergfell et al., 2002; Coller and Shattil, 2008).

One of the earliest detectable events taking place during integrin outside-in signalling is the tyrosine phosphorylation of specific protein substrates. Early studies of integrin $\alpha_{IIb}\beta_3$-mediated outside-in signalling followed the observation that platelet aggregation or fibrinogen-binding triggered tyrosine phosphorylation events of several proteins (Golden et al., 1990; Huang et al., 1993). Src activation is a key element in integrin $\alpha_{IIb}\beta_3$ mediated signalling (Jackson et al., 1996; Shattil et al., 1998; Phillips et al., 2001).

As shown in **Figure 1.7**, Src was originally suggested to be constitutively associated with the C-terminal tail of β_3 integrin in resting platelets via its SH3 domain in an inactive conformation. This is maintained by Csk-mediated phosphorylation on Tyr-529 located on β_3 integrin. Following ligand binding and integrin clustering, protein phosphatases, such as PTP-1B, relieve the inhibitory action of Src phosphorylation, with dissociation of Csk from β_3, allowing Src activation. However, recent work shows that c-Src associates with β_3 integrin predominantly in activated platelets (Obergfell et al., 2002; Arias-Salgado et al., 2005; Goggs and Poole, 2012; Wu et al., 2015). $\alpha_{IIb}\beta_3$ clustering is important for full Src activation, permitting trans-autophosphorylation of the Tyr-418 residue in the Src activation loop (Fong et al., 2016).

Integrin-mediated SFK activation results in the phosphorylation and activation of the tyrosine kinase Syk (Obergfell et al., 2002). Syk can interact directly via an SH2 domain-mediated interaction with the cytoplasmic tail of integrin β_3. Also, Syk associates with FcγRIIa following integrin $\alpha_{IIb}\beta_3$ activation-dependent phosphorylation of the tyrosine residues within its ITAM (Boylan et al., 2008). Syk deficient platelets spread poorly on fibrinogen coated surfaces (Gao et al., 1997).

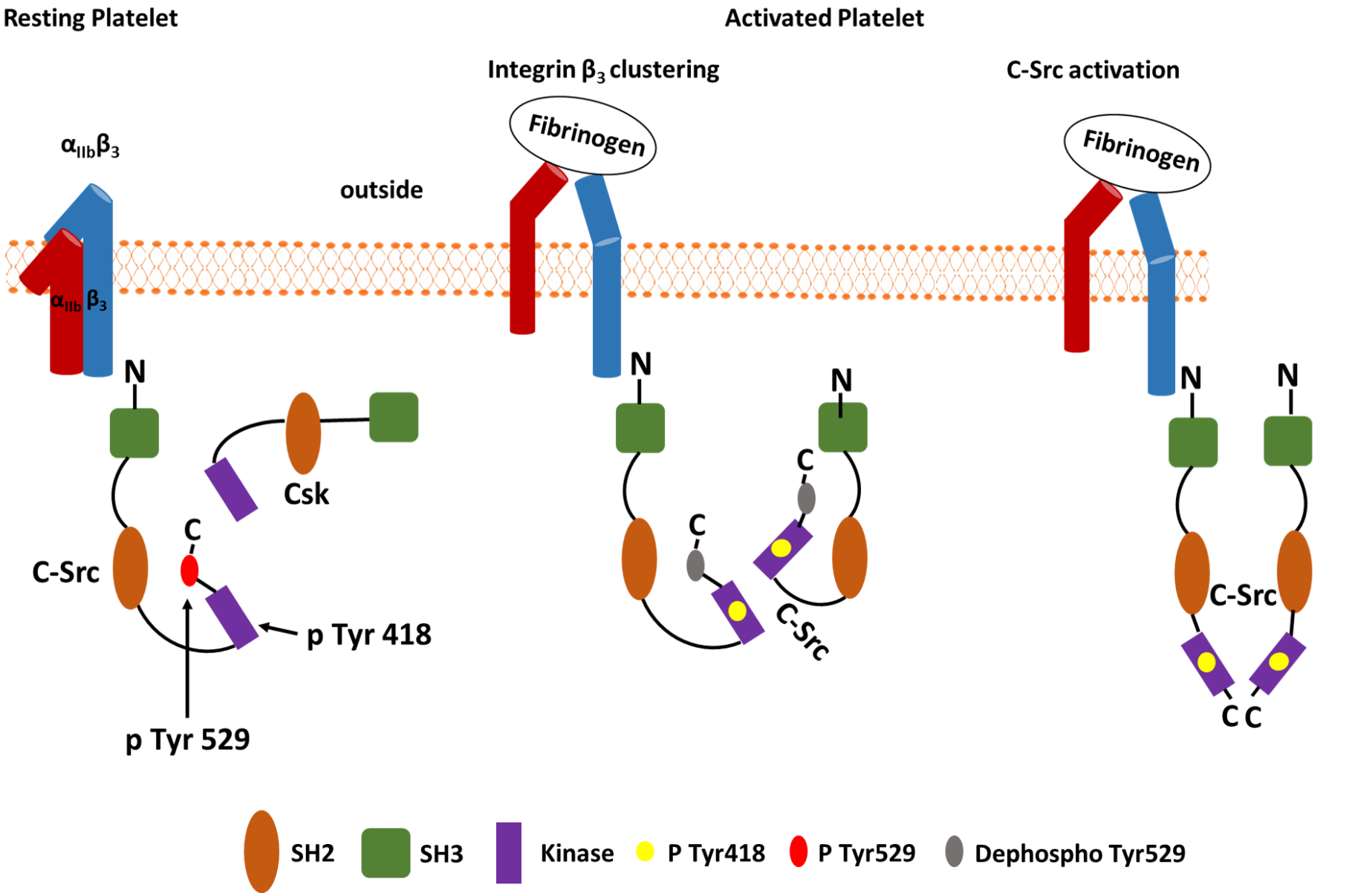
Resting Platelet
Activated Platelet
Integrin β3 clustering
C-Src activation
αIIbβ3
outside
αIIb β3
Fibrinogen
Fibrinogen
N
N
N
N
N
Csk
C
C-Src
p Tyr 418
p Tyr 529
C
C
C-Src
C-Src
C C
SH2
SH3
Kinase
P Tyr418
P Tyr529
Dephospho Tyr529

Figure 1.7 Src activation following β_3 clustering

In resting platelets, an intramolecular association maintains the bulk of c-Src in an inactive state. c-Src can associate with the RGT motif of the β_3-integrin C-terminal tail via its SH3 domain. C-Src activation is limited by phosphorylation of Tyr-529 via integrin-associated Csk. Following inside-out signalling, the integrin adopts a conformation that enables it to bind ligands such as fibrinogen with high affinity. Dephosphorylation of Tyr-529 is also promoted by tyrosine phosphatases and dissociation of Csk from β_3 contributing to stabilization of the activated state. Clustering of β_3 by ligands (fibrinogen) mediates homo-oligomerization of integrin subunits, increases local c-Src concentration resulting in the trans-autophosphorylation of Tyr-418 and eventually, the ‘‘switching’’ of c-Src to an activated state.

1.10 Aims

The initial step in the formation of haemostatic plug is the accumulation of platelets at the site of vascular injury, which helps in preventing blood loss. Cardiovascular system integrity relies on β_3 integrin. Also, activation of integrin $\alpha_{IIb}\beta_3$ is essential for physiologic and pathologic thrombosis (Bennett and Vilaire, 1979; Hynes, 2002). Kindlin is one of the main intracellular proteins that controls integrin activation and potentially β_3 clustering. ILK is a well-known effector kinase that is required for the functioning of kindlin via kindlin-β_3 interaction. In the present study, we hypothesise the following; ILK mediates kindlins role in the regulation β_3 activation and clustering and its presence is required for β_3-β_3 kinetics and clustering. Also, subsequent integrin β_3 downstream signalling.

The goals are: **1)** to investigate the time course of integrin β_3 clustering and kindlin colocalisation with β_3 and their role in platelets activation and function. **2)** To explore the role of kindlin in β_3 integrin activation and β_3 clustering. **3)** To identify the role of ILK in the regulation of platelet function, integrin activation, thrombus formation and how the kindlin molecule is regulated by ILK and its impact on platelet function and signalling using Cpd-22 (ILK inhibitor).

2 Materials and methods

2.1 Materials

2.1.1 Reagents

BD^{TM} phosflow Perm Buffer III (Cat. No. 557870) was purchased from BD Biosciences (Franklin Lakes, New Jersey, USA). Thrombin and Gly-Pro-Arg-Pro (GPRP) were purchased from Sigma–Aldrich (Poole, UK). Collagen-Related Peptide (CRP-XL) was bought from Prof Richard Farndale (University of Cambridge. UK) Poly-L-lysine-coated slides were obtained from VWR (Leicestershire, UK). Mini-PROTEAN® TGXTM precast polyacrylamide gels (4-20 % and 10 % gradient), dual-stained molecular weight markers and polyvinylidene difluoride (PVDF) membranes were purchased from Bio-Rad (Hemel Hempstead, UK). 96-well flat bottom plates were purchased from Greiner Bio-One (Frickenhausen, Germany). Ibidi-Slides 8 well with glass bottom were purchased from Thistlescientific (Glasgow, UK) (Cat. No: 80827). N-Methyl-3-(1-(4-(piperazin-1-yl) phenyl)-5-(4′-(trifluoromethyl)-[1, 1′-biphenyl]-4-yl)-1H-pyrazol-3-yl) propanamide (22) Cpd-22 (Cat. No. 407331) was purchased from Merck Millipore (Watford, UK). ILK-specific inhibitor QLT0267 (QLT, Vancouver, BC, Canada) and obtained from Dr. Chris Jones (University of Reading, UK). R software was used (www.r-project.org).

2.1.2 Primary Antibodies

Mouse monoclonal Anti-integrin β_3 IgG antibody was purchased from Santa Cruz, Biotechnology (Calne, UK) (Cat. No. sc-52685). Rabbit polyclonal anti-kindlin-3 antibody (Cat. No. ab68040) was purchased from Abcam (Cambridge, UK). Rabbit polyclonal anti-human fibrinogen fluorescein isothiocyanate (FITC) labelled was purchased from Dako (Glostrup, Denmark) (Cat. No. F0111). Anti-human CD62P mouse monoclonal antibody-PE-CY^{TM}5 antibody was purchased from BD Biosciences

(Franklin Lakes, New Jersey, USA) (Cat. No. 551142). Mouse anti- integrin $\alpha_2\beta_1$ (Cat. No. sc-59955), rabbit anti-GPVI (cat No. sc-20149) and mouse anti-GPIb (Cat. No. sc-80728) were purchased from Santa Cruz technology (Calne, UK). Mouse Anti-Integrin $\alpha_{IIb}\beta_3$ (Cat. No. Ab11027) was from Abcam (Cambridge, UK). Rabbit anti-phospho-Syk (Y525/526) (Cat. No. ab58575) and mouse anti-phospho β_3 (Y773) (Cat. No. ab38460) antibody were purchased from Abcam (Cambridge, UK). Polyclonal anti- phospho-Src (Tyr418) antibody (Cat. No. OPA1-03091) was purchased from Thermo Fisher Scientific (Waltham, MA). Mouse monoclonal anti-14-3-3 ζ (Cat. No. sc-293415) was bought from Santa Cruz, Biotechnology (Calne, UK).

2.1.3 Secondary antibodies

Alexa Fluor® 488-conjugated donkey anti-mouse IgG (Cat. No. A-21202), Alexa Fluor® 555-conjugated donkey anti-mouse IgG (Cat. No. A-31570) and Alexa Fluor® 647-conjugated donkey anti-rabbit IgG (Cat. No. A-31573) were purchased from Life Technologies (Paisley, UK). Zenon™ Alexa Fluor 647 mouse IgG1 labelling Kit and Zenon™ R-Phycoerythrin Mouse IgG1 labelling Kit were purchased from Thermo Fisher Scientific (Waltham, MA). FITC-labelled mouse IgG isotype control antibodies were obtained from BD Technologies (Franklin Lakes, NJ).

2.2 Buffer compositions

2.2.1 HEPES-buffer

150 mM of NaCl, 5 mM of KCl, 1 mM of $MgSO_4.7H_2O$, 10 mM 4-(2-hydroxyethyl)-1-piperazineethanesulfonic acid (HEPES) (free salt), 500 ml diH_2O (pH 7.4).

2.2.2 Imaging blinking buffer

Stock A: 0.90 g/ml of catalase (Cat. No. C1345-1G), 0.182 mM of Tris (2-carboxyelthyl) phosphine hydrochloride (TCEP) (Cat. No. C4706-2G), 2.27 % (v/v) of glycerine, 0.045 mg/mL of glucose oxidase (Cat. No G2133-50KU) were purchased from Sigma-Aldrich (Poole, UK). 1.14 mM of KCl, 0.91 mM of Tris-HCl at pH 7.5 (Cat. No. C4706-2G) was purchased from Sigma-Aldrich (Poole, UK) and 5 ml of diH2O. **Stock B:** 36 mg/ml of glucose, 3.6 % (v/v) of glycerin and 36 ml of H_2O. **Stock C:** 77 mg of MEA-HCl purchased from Sigma-Aldrich (Poole, UK) and 1 ml 0.25 NHCL. Blinking buffer: 50 µl of stock A, 400 µl of stock B and 100 µl of stock C were mixed with 550 µl of phosphate-buffered saline (PBS)

2.3 Methods

2.3.1 Cell Preparation

2.3.1.1 Preparation of Platelets Rich Plasma (PRP)

Whole blood from healthy and drug-free donors that had given informed consent and using procedures approved by the University of Reading Research Ethics Committee Whole blood was collected in a (4.5 ml) vacutainers containing 3.2 % sodium citrate to prepare PRP. PRP was then obtained by centrifugation at 100 g for 20 minutes at room temperature and was removed gently and rested for 30 minutes prior to the experimentation.

2.3.1.2 Preparation of washed human platelets

Blood from healthy donors was collected into (50 ml) syringes containing 4 % (w/v) sodium citrate. Acid citrate dextrose (ACD 7.5 ml; 85 mM sodium citrate, 71 mM citric

acid and 110 mM glucose was added to the samples and were centrifuged at 100 g for 20 minutes. Washed platelets were prepared by centrifugation of PRP at 350 g for 10 minutes after the addition of PGI_2 (10 µl; prepared at 125 µg/ml in ethanol). Platelets were resuspended in Tyrodes-HEPES buffer containing (25 ml; 134 mM NaCl, 2.9 mM KCl, 0.34 mM Na_2HPO_4, 12 mM $NaHCO_3$, 20 mM HEPES, 1 mM $MgCl_2$ and 5 mM glucose; pH 7.3) with ACD (3 ml) and PGI_2 (10 µl; 125 µg/ml). Platelet counts were determined using a model Z2^{TM} COULTER COUNTER® (Beckman Coulter, High Wycombe, UK). The platelets were then pelleted by centrifugation at 1,413 g for 10 minutes, resuspended in modified Tyrode's-HEPES buffer (1 ml) and adjusted to the desired concentration with modified Tyrode's-HEPES buffer. Prior to the use of washed platelets, they were incubated at 37 °C for 30 minutes.

2.3.2 Permeabilised platelet stochastic optical reconstruction microscopy (STORM) method

Human PRP was prepared from whole blood as shown in section 2.3.1.1. PRP was diluted in HEPES and was incubated with Cpd-22 at 37 °C for 30 minutes. Samples were then stimulated with 1 U/ml thrombin in the presence (25 mg/ml of GPRP to prevent fibrin polymerization) or (3 µg/ml) CRP-XL for 0, 30, 60, 90, 150 and 300 seconds. Platelets were fixed with 2 % (v/v) formyl saline, followed by centrifugation at 500 g for 15 minutes. After centrifugation, the supernatant was discarded, pellets containing platelets were resuspended in Perm Buffer III (100 µl) (BD Biosciences, Oxford, UK) in ice for 30 minutes. Platelets were washed with HEPES buffer (2 ml) two times and at 550 g for 20 minutes. After removal the supernatant, pellets were resuspended in HEPES buffer (50 µl). Kindlin and integrin β_3 were identified with primary antibodies (mouse monoclonal IgG for integrin β_3 and rabbit polyclonal antibody for kindlin, diluted in

1:50) prior to incubation at 37 °C for 30 minutes. Supernatant was removed and washed two times with HEPES buffer (2 ml) followed by centrifugation at 550 g for 20 minutes. Antibody bound platelets were then detected using Alexa Fluor® 647-labelled donkey anti-rabbit to detect kindlin and Alexa Fluor®555 labelled goat anti-mouse to detect β_3. Labelled platelets were washed with HEPES buffer (2 ml) and centrifuged at 550g for 20minutes. Pellets were resuspended in HEPES buffer (100 μl) and adhered to poly-L-lysine coated ibidi slides. Slides were incubated overnight at 4 °C. The following day, unattached platelets were discarded and blinking buffer was added before 3 dimension STORM imaging as described in next section 2.3.2.1. STORM microscopy was used to image platelets under 100x oil immersion lens.

2.3.2.1 STORM imaging and post-processing.

Samples were visualised and imaged in blinking buffer. For each STORM image reconstruction, 30,000 imaging frames with an exposure time of 10 ms were recorded. Single-molecule localizations were extracted, captured and reconstructed from the movies with the software NIKON-NIS-Elements. STORM was collected with 100x oil TIRF objective lens and Andor DU897 EMCCD camera. For colour imaging, pair of laser was set (488-561) to identify β_3 while pair of laser (405-647) for kindlin. Then, the region of interest (ROI) was set and analysed. The obtained localization files were loaded into ImageJ software using ImageJ Plugin ThnunderStorm.

2.4 Light Transmission Aggregometry (LTA)

LTA was studied on PRP using an aggregometer (Chrono-Log, Havertpwn, PA, USA). PRP was incubated with range of concentrations (1, 3 or 10 μM) of ILK inhibitor Cpd-22 for 30 minutes or (0.1 % v/v) DMSO vehicle control. Under stirring condition (1,200 rpm at 37 °C), platelets were then stimulated with CRP-XL (3 μg/ml) or thrombin (1

U/mL). In the presence of thrombin, 25 mg/mL of GPRP was added to prevent fibrin polymerisation. The aggregation traces were recorded over 5 minutes.

2.5 Flow cytometry

2.5.1 Fluorescence Resonance Energy Transfer (FRET) assay.

Alexa Fluor 647-and PE-fluorescent labels pair was chosen to measure FRET signals of β_3-β_3 association as the emission of the former dye would sufficiently causes the excitation of PE fluorophore. Zenon® mouse IgG Labeling Kits were used to label anti-β_3 monoclonal antibodies, with Alexa Fluor® 647 and Phycoerythrin (PE). Initial optimization of the staining protocol was carried out using precisely titrated Alexa Fluor® 647-and PE-fluorescent conjugated anti-β_3 monoclonal antibodies in the range of 0, 0.01, 0.03, 0.06, 0.1, 0.3, 0.6, 1, 3, 6 and 10 μg/ml. Stained platelets along with appropriate isotype controls were then fixed using 0.2 % (v/v) formyl saline. BD Accuri^{TM}C6 flowcytometry was used to analyse antibody binding. 1 μg/ml β_3 antibody bound to Alexa Fluor® 647-and PE-fluorescent labels were compared to isotype control.

Following obtaining the optimal concentration of the β_3 labelling antibodies with Alexa Fluor® 647-and PE-fluorescent, FRET analysis of β_3-β_3 association was performed. PRP was stained with 1μg/ml of Alexa Fluor® 647-labelled anti-β_3 monoclonal antibodies with 1μg/ml of isotype control, PE-fluorescent labelled anti-β_3 monoclonal antibodies with 1μg/ml of isotype control or 1μg/ml of both 647 and PE labelled anti-β_3 monoclonal antibodies. Samples were then stimulated with (1 U/ml) thrombin for 0, 15, 30, 60, 90, 120, 180 and 300 seconds in presence of (25 mg/ml) GPRP. 0.2 % (v/v) formyl saline was then used to fix the samples prior to flow cytometric analysis. A right shift in fluorescent intensity at 647 double stained platelets indicates FRET. A decrease in the fluorescent intensity at PE double stained platelets indicates FRET.

2.5.2 Fibrinogen Binding and α-granule Secretion

Fibrinogen binding to the platelet surface and P-selectin exposure were measured using flow cytometry, which measures activation of integrin $\alpha_{IIb}\beta_3$ receptors and α-granule secretion, respectively. Fluorescein isothiocyanate (FITC)-labelled rabbit anti-human fibrinogen antibody (Dako, Ely, UK) was used to detect fibrinogen binding. PE-Cy^{TM}5-labelled mouse anti-human CD62P antibody (BD Biosciences, Oxford, UK) was used to analyse P-selectin exposure.

Total volume assay (50 µl), containing (5 µl) human PRP, (38 µl) of HEPES buffer, (5 µl) of Cpd-22 or (0.1 % v/v) DMSO vehicle control and (2 µl) of each antibody were incubated at 37 °C for 0, 5, 10, 15, 30 and 60 minutes. Platelets were stimulated with 1µg/mL of CRP-XL for 20 minutes and fixed with 0.2 % (v/v) formyl saline for 20 minutes. Negative controls for antibodies were set by using appropriate isotype controls; Ethylene glycol-bis (β-aminoethylether)-N, N, N', N'-tetraacetic acid (EGTA) (final concentration, 1 mM) was used for fibrinogen binding or isotype controls for P-selectin exposure were used as negative controls for the antibody response. Samples were analysed by BD Accuri^{TM}C6 flow cytometry (BD Biosciences, Oxford, UK). Median fluorescence of 10,000 gated platelets was analysed.

For real time flow cytometry experiments, human PRP was treated with (3 µM) Cpd-22 at 37 °C for 30 minutes. Fibrinogen binding or P-selectin exposure level to vehicle control (0.1 %) DMSO or (3 µM) Cpd-22 platelets from human platelets were measured by diluting PRP in HEPES, followed by FITC labelled anti-fibrinogen antibody or PE-Cy^{TM}5-labelled mouse anti-human CD62P antibody. Negative controls for antibodies were used for fibrinogen binding (EGTA final concentration 1 mM) or isotype controls for P-selectin exposure were used as for the antibody response. Samples were transferred

to a 96-well plate with gentle mixing and analysed by BD Accuri C6™ flow cytometry at 37 °C. During data acquisition, (1 U/ml) thrombin in the presence of GPRP 25 mg/ml and (3 μg/ml) CRP-XL were added for 300 seconds. Median fluorescence of 10,000 events gated were analysed.

2.5.3 Platelet Receptor Expression

The expression level of GPVI, integrin $\alpha_2\beta_1$, integrin $\alpha_{IIb}\beta_3$ and GPIb were studied. PRP was pre-treated with Cpd-22 (3 μM) or DMSO (0.1 % v/v) at 37 °C for 30 minutes. Then, samples were incubated with antibodies against receptors; integrin $\alpha_2\beta_1$, GPIb, GPVI and integrin $\alpha_{IIb}\beta_3$ for 20 minutes followed by stimulation with (1 U/ml) thrombin in the presence of GPRP 25 mg/ml. Samples were fixed with 0.2 % (v/v) formyl saline (250 μl). 10,000 events were analysed on a BD Accuri C6™ flow cytometry (BD Biosciences, Oxford, UK).

For selectivity experiment of Cpd-22, PRP was obtained from healthy donors, drug free as described in section 2.3.1.1 and incubated with FITC-labelled anti-human Fibrinogen antibody followed by treatment with QLT0267 (1 μM) or Cpd-22 (3 μM) or and combined them at 37 °C for 30 minutes. PRP was then stimulated with (1 U/ml) thrombin for 20 minutes with gentle mixing in presence of GPRP (25 mg/ml). 0.2 % (v/v) formyl saline was used to fix samples. 10,000 events were analysed by BD Accuri C6™ flow cytometry.

2.6 Protein biochemistry

2.6.1 Platelets Signalling Studies

Human washed platelets were obtained as described in section 2. 3.1. 2. Human washed platelets (4×10^8 cells/ml) were used to study platelets signalling. Washed platelets were

pre-treated with (3 μM) Cpd-22 or vehicle control at 37 °C for 30 minutes. Samples were then stimulated with HEPES buffer (resting), (1 U/mL) thrombin and (3 μg/mL) CRP-XL under stirring conditions (1,200 rpm at 37 °C) using an aggregometer (Chrono-Log, Havertpwn, PA, USA) for 30, 60, 90, 150, 300 seconds. Samples were then lysed with 6× Laemmli reducing buffer; (4 % (w/v) sodium dodecyl sulphate (SDS), 20 % (v/v) glycerol, 0.5 M Tris, 0.001 % (w/v) Brilliant Blue R and 10 % (v/v) 2-mercaptoethanol). The samples were heated at 95 °C for 5 minutes prior to store at -20 °C for future experiments.

2.6.2 SDS-polyacrylamide Gel Electrophoresis

After heating platelet lysates at 95 °C for 10 minutes, proteins from platelet lysates were separated on SDS-PAGE gels. Samples and molecular weight markers were loaded on 4-20 % acrylamide gradient gels (Bio-Rad precast gels; Bio-Rad, Watford, UK). Gels were run at voltage (100 mA) for 90 minutes in a Mini-PROTEAN® II apparatus (Bio-Rad, Watford, UK) with Tris-glycine buffer (2 mM Tris, 192 nM glycine and 0.1 % [w/v] SDS; pH 8.3) in the running container. Proteins were transferred from SDS-PAGE gels to polyvinylidene diflouride membranes (PVDF) (Bio-Rad, Watford, UK) by semi-dry transfer. PVDF membranes were soaked in methanol and placed under gels. 3-mm filter papers were soaked in anode buffer (300 mM Tris base and 20 % [v/v] methanol; pH 10.4) prior to place below the membranes and 3-mm filter papers were soaked in cathode buffer (25 mM Tris base and 40 mM 6-amino-n- hexanoic acid; pH 9.4) before place above the gels. Proteins were then transferred from gels to membrane at voltage (150 mA) for 2 hours.

2.6.3 Immunoblotting

PVDF membranes were blocked with 5 % (w/v) BSA dissolved in 1 % (v/v) Tris-buffered saline–TWEEN® 20 (TBST; 20 mM Tris, 137 mM NaCl and 0.1 % [v/v] TWEEN® 20; pH 7.6) for 1hour at room temperature. Membranes were incubated with primary antibodies were diluted to (1;1000) in 1 % (v/v) TBST with 2 % (w/v) BSA overnight at 4 °C. Following the next day, unbound antibodies were washed with TBST three times and each wash for 5 minutes. Conjugated secondary antibodies were diluted to (1;500) in 1 % (v/v) TBST containing 2 % (w/v) BSA and subsequently incubated with membranes at room temperature for 1 hour in dark room. Membranes were then washed with TBST three times for 5 minutes prior to visualisation on a Typhoon FLA 9500 fluroimager (Amersham Biosciences, Buckinghamshire, UK). Fluorescence Intensities of bands were acquired and quantified using Image Quant software version 8.1 (GE healthcare). To control for protein loading, blots were probed with 14-3-3-ζ antibody.

2.7 Statistical analysis

Prism software was used to perform statistical analysis (version 7.00, GraphPad, San Diego, CA). More than two groups was analysed by One-way ANOVA, post hoc test Dunnett's multiple comparisons test. To determine the statistical significance difference between two groups a student's t-test was used. Two-way ANOVA with Sidak's multiple comparisons was used. Mean ± standard deviation or standard error of the mean are considered. P value ≤ 0.05 was used for data analysis indicated statistically significant. Statistical data analyses were performed using R software (https://www.R-project.org).

3 Analyzing integrin β_3 clustering and kindlin-3 - β_3 association in human platelets using a novel super resolution STORM microscopy method

3.1 Introduction

Fluorescence microscopy is a technique that is used for examining cell biology and detecting dynamic process of cells (Leung and Chou, 2011). However, because the diffraction limit of resolution is ~ 250 nm that leaves many biological structures too small to be visualised (Bates et al., 2013). Super-resolution microscopy such as Stochastic Optical Reconstruction Microscopy (STORM) has been developed to determine the localisation of single individual molecule with nanometre resolution (Rust et al., 2006a).

STORM microscopy is a valuable tool that facilitates studying molecules co- localisation in cells (Moerner, 2012). Images can be reconstructed by detecting the centre position of fluorescent molecule because the light that is emitted from a single fluorescent molecule spreads out in what is known as a point spread function (PSF). The centre of the PSF can be determined mathematically (Bates et al., 2013). Therefore, if all fluorescent molecules with in an image can be illuminated without overlapping then the precise localisation of each molecule can be calculated and the image reconstructed with a greater resolution than allowed by the diffraction limit of light (Rust et al., 2006b). To achieve single illumination of fluorescent molecules fluorophores are rapidly switched between fluorescent and non-fluorescent states. Repeating this cycle tens of thousands of times allows a sufficient number of molecules to be localised to build an image of cellular structures with nanometer scale accuracy (Huang et al., 2008; Bates et al., 2013)

To better understand the kinetics and regulation integrin β_3 activation and clustering in response to platelet stimulation, the present chapter investigated kindlin-3 - β_3 association and integrin β_3 clustering using STORM microscopy. To enable this, we developed a novel clustering analysis method designed to execute analysis of imaged clustering. That

produced a simple, biologically relevant method of describing and quantifying clustered molecules.

3.2 Stochastic Optical Reconstruction Microscopy (STORM) imaging of β_3 clustering and kindlin-3 - β_3 association in platelets

Upon stimulation of platelets with agonist, integrin $\alpha_{IIb}\beta_3$ shift from a low affinity to a high ligand affinity conformation, known as integrin $\alpha_{IIb}\beta_3$ activation. Ligand binding and platelet activation induces β_3 clustering. However, the mechanism underlying β_3 clustering is still unclear (Shattil and Newman, 2004; Wu et al., 2015; Rognoni et al., 2016).

$\alpha_{IIb}\beta_3$ activation is controlled by intracellular proteins including kindlin-3 in platelets. Kindlin-3 has been identified as a regulator for integrin $\alpha_{IIb}\beta_3$ activation, through the binding to β_3 cytoplasmic tail (Meves et al., 2009). So far, although kindlin-3 contributes to integrin $\alpha_{IIb}\beta_3$ activation, the underlying mechanism remains unclear (Rognoni et al., 2016). To further delineate the molecular aspects underlying β_3 activation, we sought to visualise molecular changes in β_3 integrin and other contributing proteins such as kindlins. For this purpose, we developed a STORM method for measuring clustering and investigate the time course of integrin β_3 clustering.

Platelet-rich-plasma (PRP) was activated with (1 U/ml) thrombin in the presence of GPRP (25 mg/ml) for 0 and 300 seconds, fixed with 2 % (v/v) formyl saline and permeabilised with BD Phos Flow Perm Buffer III. Integrin β_3 were identified with primary and Alexa Fluor® 555 labelled secondary antibodies. Labelled platelets were washed then adhered overnight to poly-D-lysine coated ibidi slides before 3D STORM imaging and images were reconstructed using Nikon-NIS-Elements.

As shown in **Figure 3.1,** three dimension (3D) STORM images were acquired and reconstructed using Nikon-NIS-Elements. In resting platelet, 3D images of platelets

showed circular and uniform morphology. However, upon activation by 1 U/ml thrombin, the platelets changed shape, leading to the extension of numerous long pseudopodia. β_3 integrin was observed on the surface of resting platelets (green color). However, during platelet activation, β_3 distribution was changed **(Figure 3.1).** The molecular distribution of β_3 molecules was also examined at the clustering level and stimulated platelets showed clusters when compared to resting. Also, β_3 was not evenly distributed but appeared to form clusters **(Figure 3.2)**.

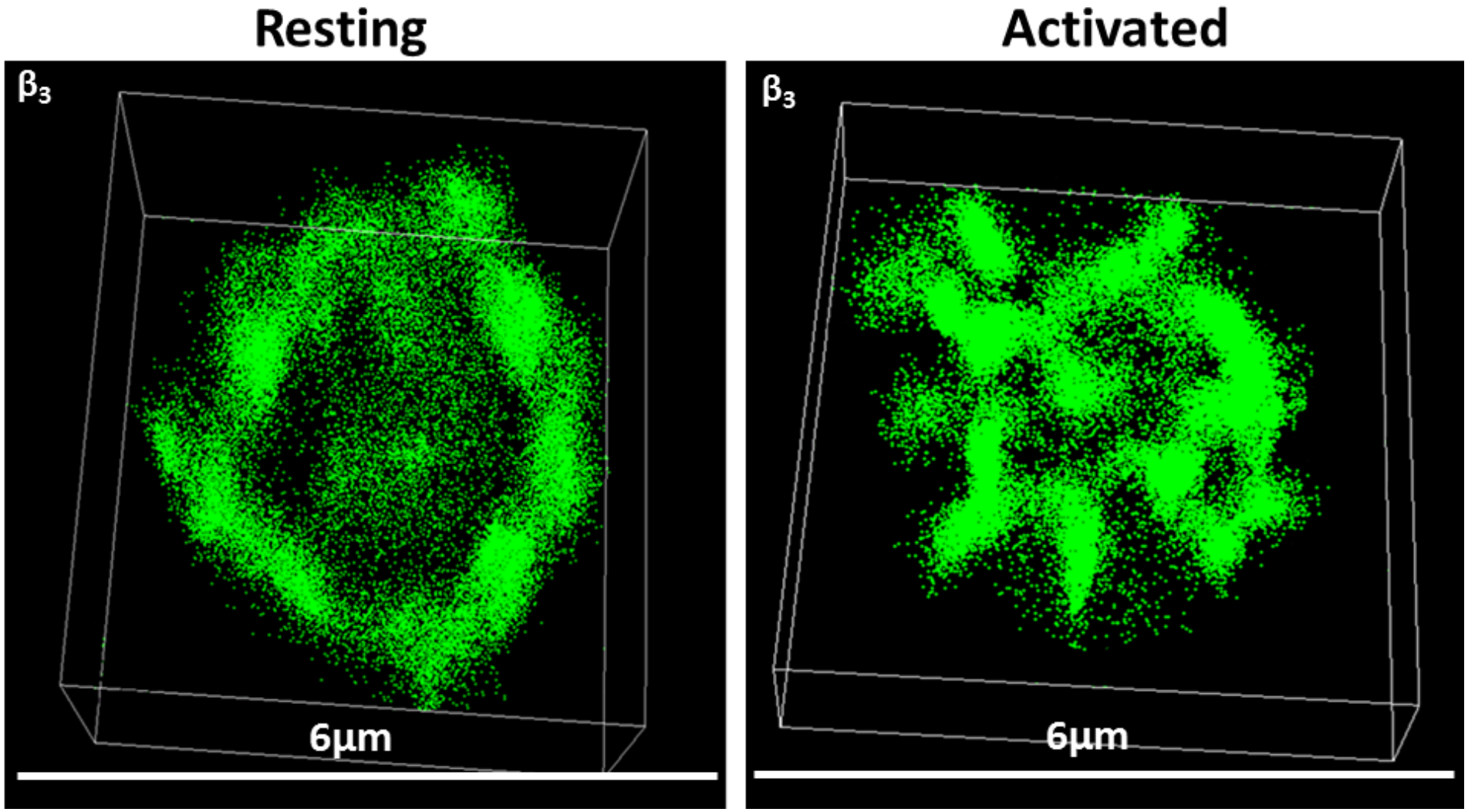
Resting
β3
6µm
Activated
β3
6µm

Figure 3.1 Three dimension images β_3 molecules in platelets.

Platelet-rich-plasma (PRP) was activated with thrombin (1 U/ml) in the presence of GPRP (25 mg/ml) for 0 and 300 seconds, fixed with 2 % (v/v) formyl saline and permeablised with BD Phos Flow Perm Buffer III. Integrin β_3 was identified with primary and Alexa Fluor® 555 labelled secondary antibodies. Labelled platelets were washed then adhered overnight to poly-D-lysine coated ibidi slides before 3D STORM imaging. Images were reconstructed using Nikon-NIS-Elements.

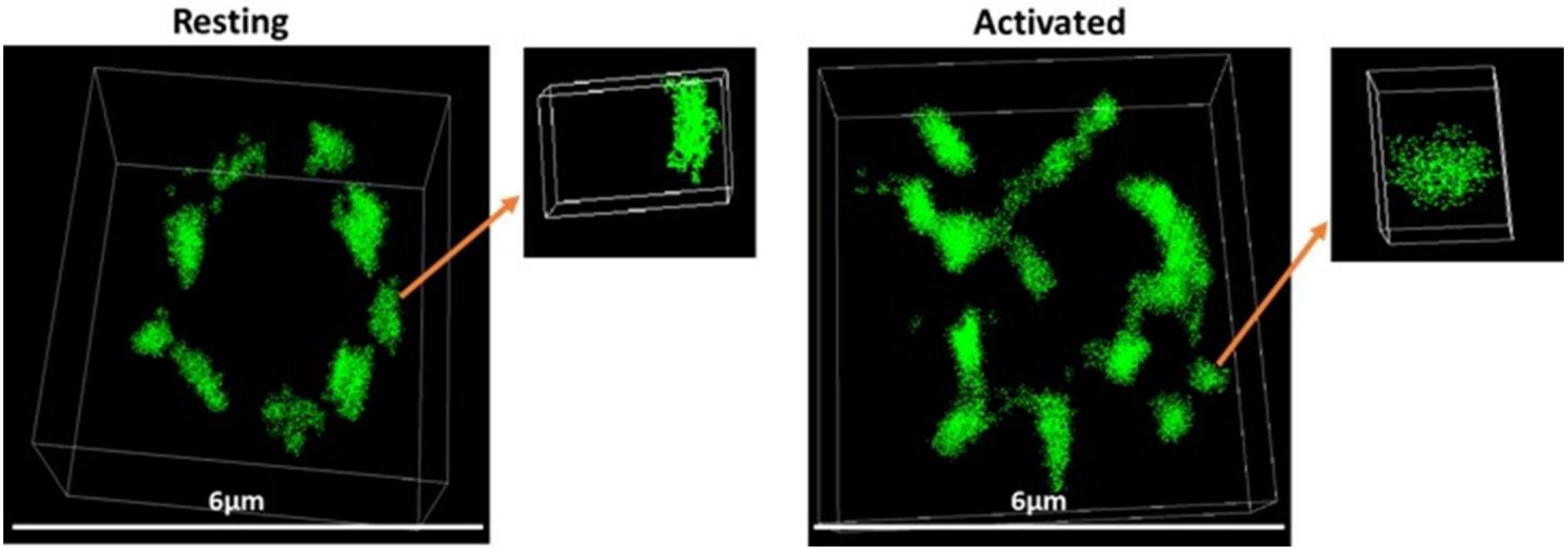

Figure 3.2 Three dimension images of β_3 clustering in platelets.

3D STORM images of β_3 clustering were acquired and reconstructed using NIKON-NIS-Elements . Resting platelet showed low β_3 clustering in comparison with thrombin-mediated platelet.

3.3 Analysis of β_3 molecules clustering

STORM imaging revealed the differential distribution and clustering of β_3 integrin molecules on resting and activated platelets, therefore, we sought to quantify and analyse this distribution.

Human PRP was rested for 1 hour prior to experiments. PRP resting or activated with (1 U/ml of thrombin in the presence of 25 mg/ml GPRP) for 300 seconds, platelets were fixed in 2 % (v/v) formyl saline then permeabilised with BD Phos Flow Perm Buffer III. Anti-Kindlin-3 and anti-integrin β_3 were added and labelled with Alexa Fluor® 647 and Alexa Fluor® 555 secondary antibodies, respectively. Labelled platelets were washed and then adhered on poly-L-lysine coated ibidi slides overnight at 4 °C. Platelets were examined under x100 oil immersion using STORM microscopy.

Imaged STORM was then constructed using NIKON-NIS-Elements followed by ImageJ plugin ThunderSTORM to examine β_3-β_3 clustering. It is a valuable computational tool to investigate data from acquired images. As described in **Figure 3.3**, obtained raw data from STORM image of β_3 molecules clustering which gave the x, y, z coordinate of each molecule in each platelet analysed was imported into ThunderSTORM **(Appendix 1)**.

Then, number of β_3 molecules that surrounded each β_3 molecules within 50 nm was analysed. To define clusters, as shown in **Figure 3.4**, we calculated the percentage of β_3 molecule that were surrounded by 1-5 β_3 molecules, 5-10 β_3 molecules and >10 β_3 molecules over different time-points of stimulation **(Appendix 2)**. Whilst there appeared to be some variation in clustering overtime. High variability in the level of β_3 molecules between individuals was noted which could be attributed to the differences in the numbers of β_3 molecules in platelets among tested donors **(Figure 3.5)**. Furthermore,

size of platelets along with platelets-antibody labelling may account for the observed variation. Therefore, other analytical methods were considered. We decided to develop a new approach to define β_3 clustering using R in which we could normalise clustering between individuals.

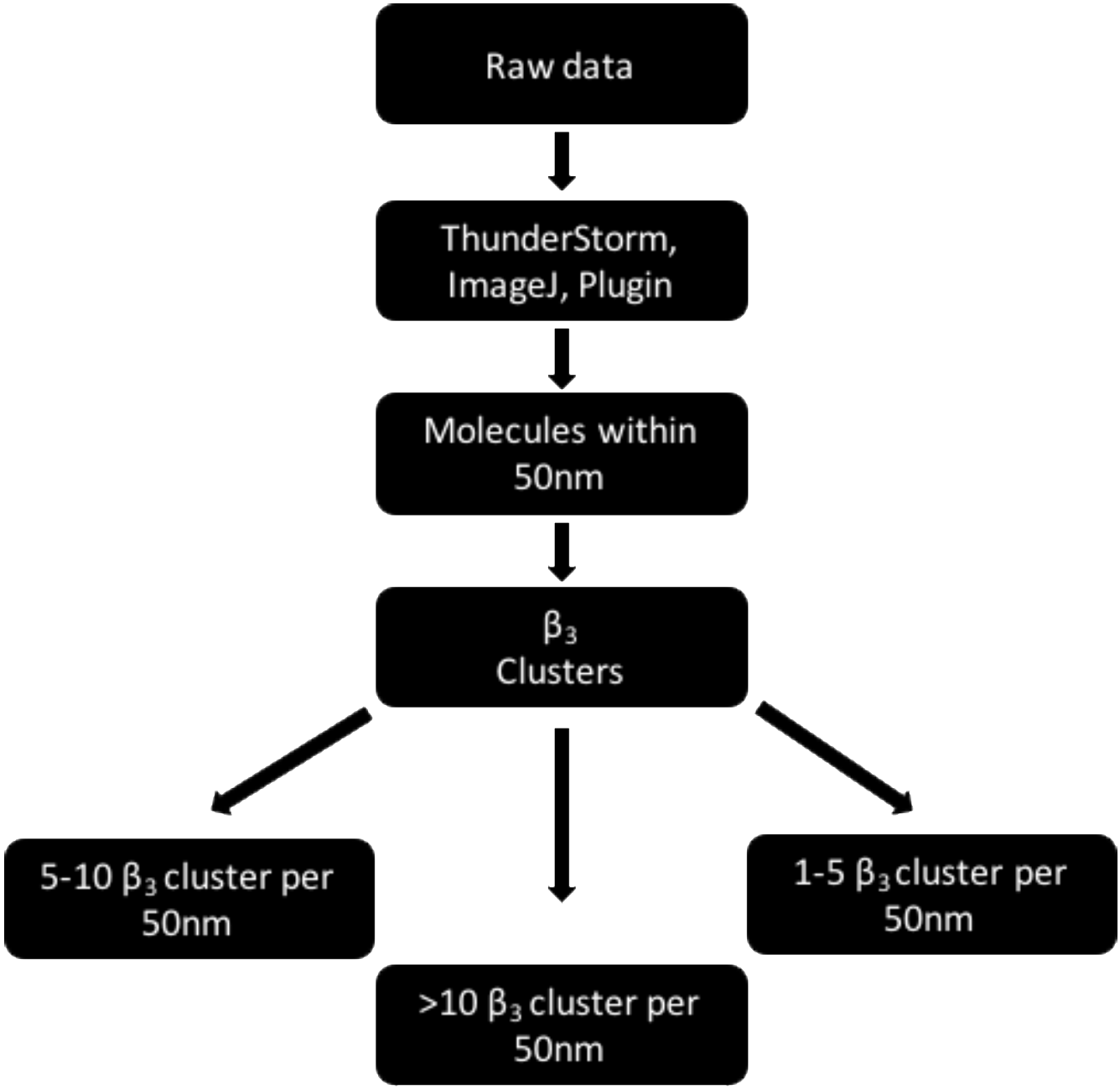

Figure 3.3 Diagram of β_3 integrin clustering analysis using ImageJ plugin ThunderSTORM.

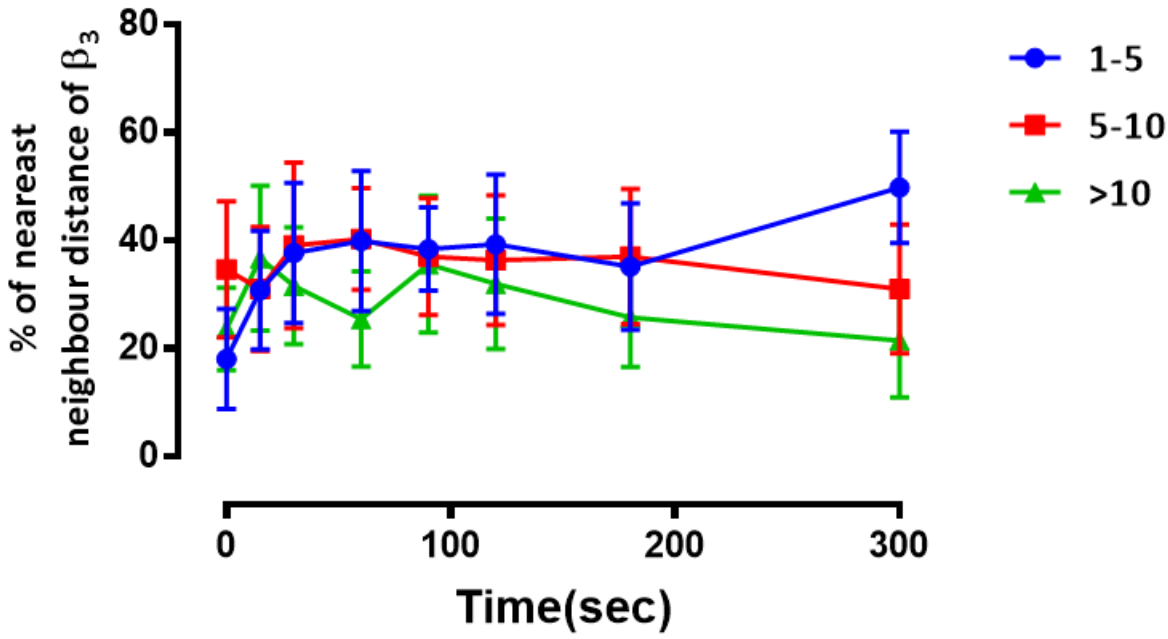

Figure 3.4 Percentage β_3 clusters within 50 nm.

$\beta_3\beta_3$ per 50 nm was analysed using ImageJ ThunderSTORM. Raw data of β_3 molecule surrounding each β_3 within 50 nm was selected between (1-5, 5-10 and >10). Percentage of $\beta_3\beta_3$ molecules were calculated over different time points of stimulation with (1 U/ml) thrombin. Data represents mean ± SEM ($n \geq 3$).

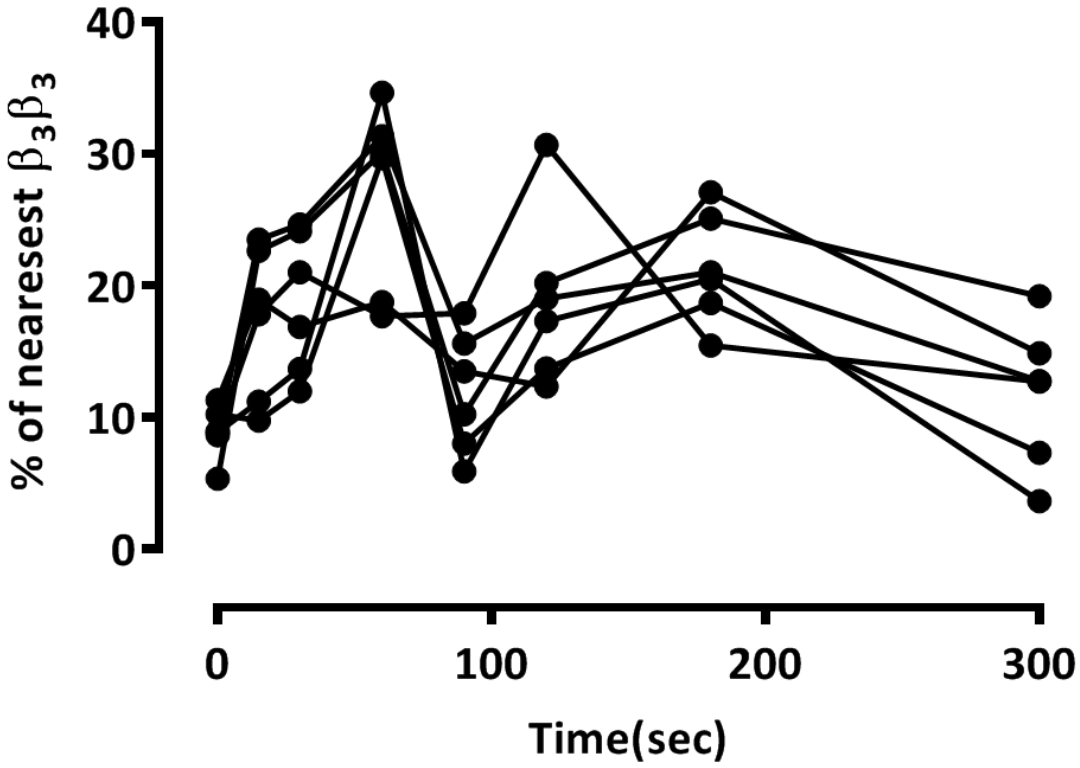

Figure 3.5 Percentage of nearest $\beta_3\beta_3$ cluster in each individual.

Percentage of $\beta_3\beta_3$ clustering over 300 seconds in 6 donors was analysed within 50 nm. Variation was noted between different donors following platelet stimulation, (n = 6).

The first step was to analyse the mean number of β_3 molecules within 50 nm of each β_3 molecule for all resting platelets from each individual **(Appendix 3)**. Diameter of 50 nm was selected, as it is approximately the limit of resolution of this system. This mean value was the "mean density" of β_3 molecules surrounding each β_3 molecule. Clusters can then be described as β_3 molecules that are surrounded by greater than the mean density of β_3 molecules. The simplicity of this approach means that the degree of clustering can be easily altered and the consequences of this easily assessed. The percentage of β_3 molecules that fall into clusters can then be assessed and used as a mark of clustering **(Appendix 4)**.

To understand the impact of different cluster definitions on the time course of β_3 clustering , β_3 clusters were selected as having two times ($\beta_3\beta_3$2), four times ($\beta_3\beta_3$4) or ten times ($\beta_3\beta_3$10) the density of β_3 **(Figure 3.6)**. This will define any clustering observation and whether they follow the same or different clustering pattern overtime.

No changes were seen in the pattern of $\beta_3\beta_3$ clusters among different mean densities overtime suggesting that β_3 clusters are dynamic and contain molecules at a range of densities **(Figure 3.6)**. As a result, clusters as 2 times mean density ($\beta_3\beta_3$2) **(Figure 3.7)** was then selected for the rest of the clustering and co-clustering analysis in the present project **(Described in details in chapter 4).** Taking a similar approach to that used in existing clustering by Levet et al. (2015). As the change in the percentage of β_3 molecules with more than 2 times mean density of β_3 within 50 nm (i.e. the percentage of β_3 in clusters)

The density of β_3 molecules surrounding each β_3 molecule (a measure of clustering) showed a biphasic pattern. The percentage of β_3 clustering that have 2 times the mean density of β_3 molecules in 50 nm increasing from a low in resting platelet to peak at 60

seconds, decreasing at 90 seconds. Then, the percentage of β_3 clustering that have 2 times the mean density of β_3 molecules in 50 nm increasing again by 180 seconds before again falling by 300 seconds **(Figure 3.7).** Moreover, the pattern of $\beta_3\beta_3$ clustering also show temporal variation between individuals over different time-points **(Figure 3.7)**. It is noteworthy to mention that Levet et al. (2015) used same mean density number in the quantification of localization-based super-resolution microscopy data in a method refereed as SR-Tesseler method.

Differences in the number of β_3 integrin clusters in resting and stimulated platelets were observed. We quantified the number of β_3 integrin clusters and it showed changes over time (**Figure 3.8**). Interestingly, the increase in cluster number (**Figure 3.8**) followed a similar pattern to the $\beta_3\beta_3$ clustering observed in **Figure 3.7**. In conclusion, we have developed a STORM microscopy method and used it to quantify β_3-β_3 clustering in platelets. Changing the density of β_3 molecules used to define a cluster and did not affect the pattern of movement of molecules overtime.

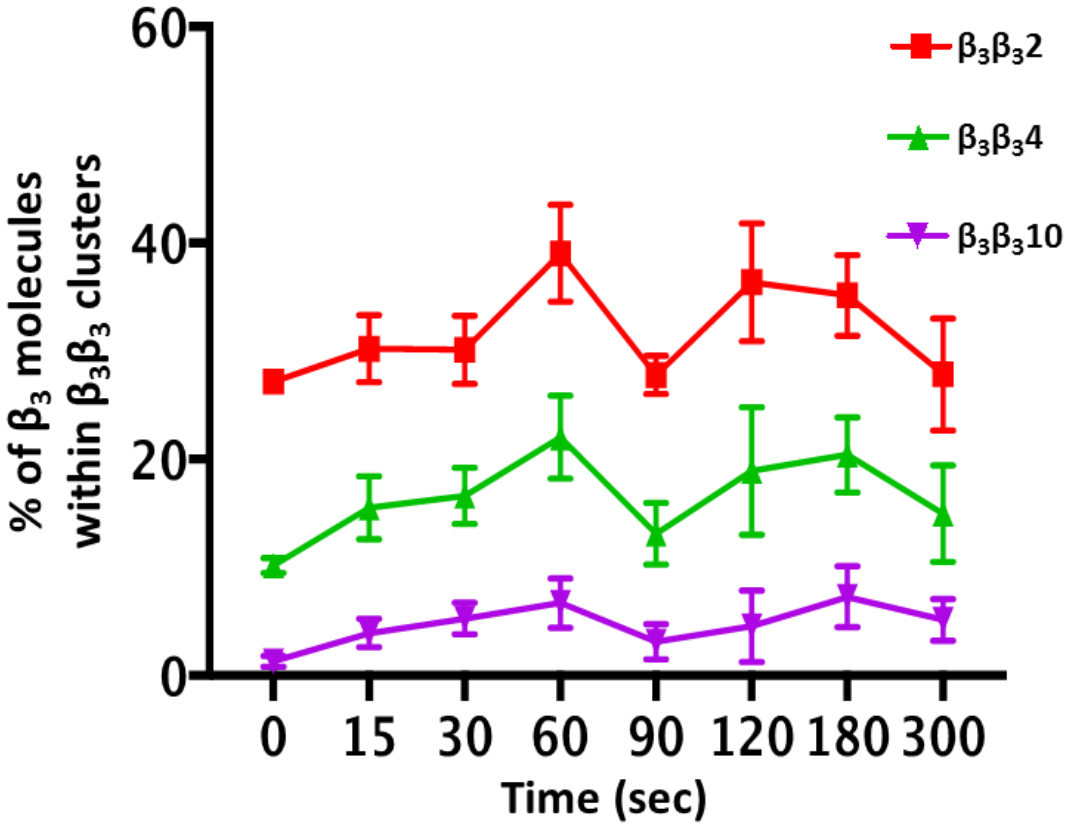

Figure 3.6 Defining β_3 clustering in platelets.

The change in the percentage of integrin β_3 molecules defined as being within $\beta_3\beta_3$ clusters over time. The mean number of β_3 molecules within 50 nm of each β_3 molecule for all resting platelets from each individual. This mean value was the "average density" of β_3 molecules surrounding each β_3 molecules in resting platelets. We define clusters as having 2 times ($\beta_3\beta_32$), 4 times ($\beta_3\beta_34$) or 10 times ($\beta_3\beta_310$) the mean density of β_3 clusters. Clustering was analysed using ImageJ plugin ThunderSTORM and the presently developed R based novel clustering analysis method. Data represents mean ± SEM ($n \geq 3$).

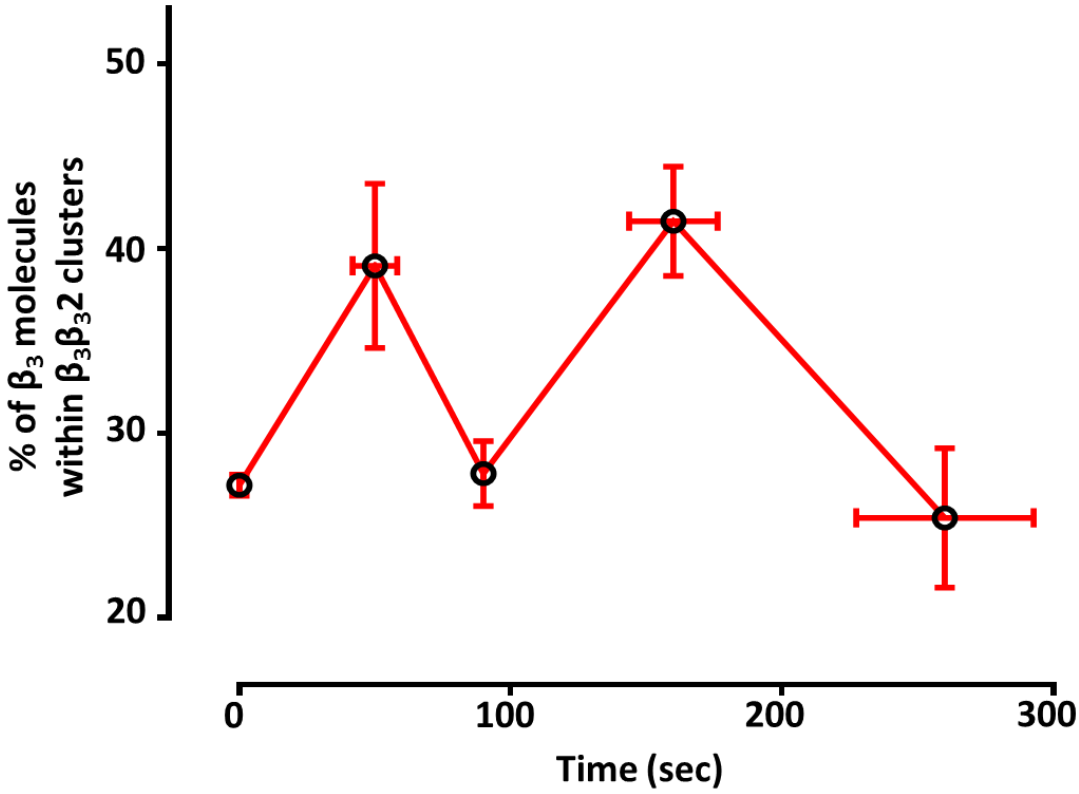

Figure 3.7 Temporal changes in integrin ($\beta_3\beta_3$2) clustering in response to thrombin stimulation.

The mean number of β_3 molecules within 50 nm of each β_3 molecule ($\beta_3\beta_3$2) over 300 seconds (1 U/ml) thrombin stimulated platelets were analysed using ImageJ plugin ThunderSTORM and the presently developed R based novel clustering analysis method. Data represents mean ± SEM ($n \geq 3$), *$P \leq 0.05$ was calculated by one-way ANOVA, (One-way ANOVA P = 0.026).

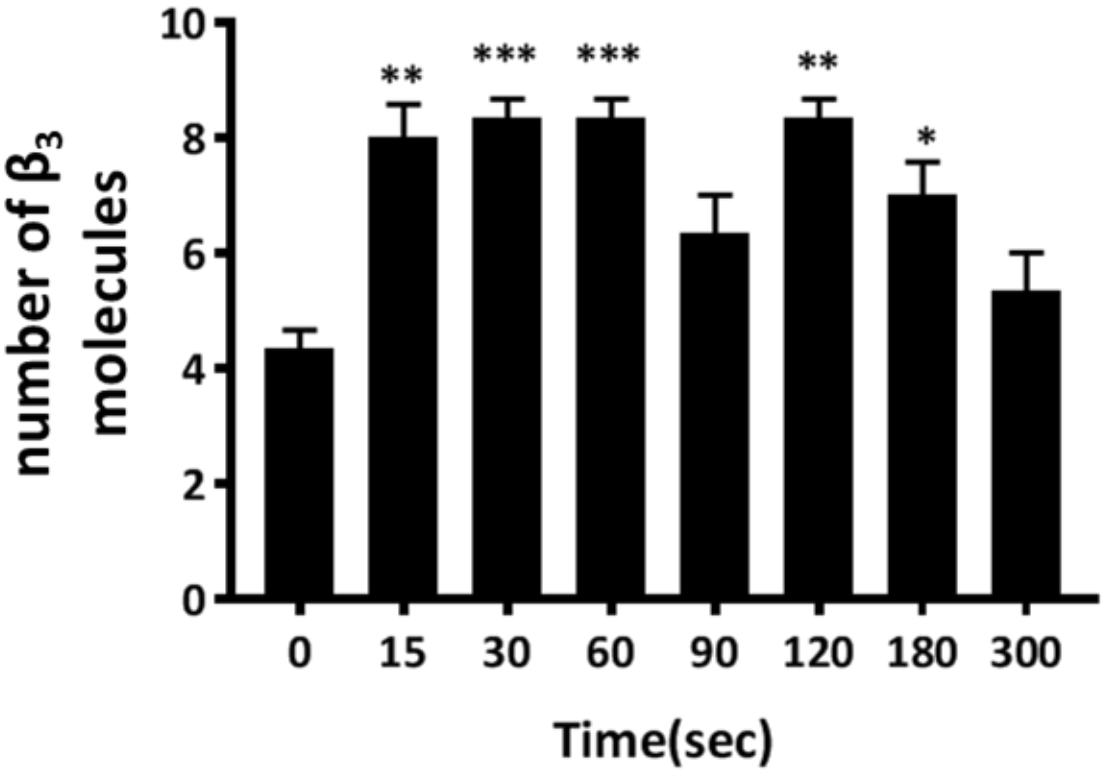

Figure 3.8 Number of β_3 molecules.

β_3 clusters were calculated overs different time-points of platelets stimulation with 1U/ml thrombin. Data represents mean ± SEM ($n \geq 3$), *$P \leq 0.05$ **$P \leq 0.01$ ***$P \leq 0.001$ were calculated by one-way ANOVA.

3.4 FRET flow cytometric analysis further confirmed β_3-β_3 clustering observed in STORM analysis

Temporal changes of integrin β_3 clustering observed in STORM images were analysed in the newly developed R based clustering method. However, as a novel method with no preceding reporting in the literature, confirmation of generated findings was prudent. Fluorescence resonance energy transfer (FRET)-based method is highly sensitive tool to determine proteins proximity at the cell surface level and inside the cells too (Szollosi et al., 1998; Szollosi et al., 2002).Therefore, such application makes FRET an excellent choice to confirm aforementioned findings. Using a pair of monoclonal antibodies (mAbs) labelled with fluorescence donor, such as Phycoerythrin (PE), and fluorescence acceptor dye, such as Alexa Fluor 647, it is possible to detect protein-protein interaction in the tested cell.

PE- fluorescent- and Alexa Fluor® 647 labels pair was chosen to measure FRET signals of β_3-β_3 association as the emission of the PE dye would sufficiently causes the excitation of 647 fluorophore. Zenon® Mouse IgG Labeling Kits were used to label anti-β_3 mAbs, with Alexa Fluor® 647 and PE. Initial optimization of the staining protocol was carried out using precisely titrated Alexa Fuor® 647- and PE- fluorescent conjugated anti-β_3 mAbs in the range of 0, 0.01, 0.03, 0.06, 0.1, 0.3, 0.6, 1, 3, 6 and 10 µg/ml. Stained platelets along with appropriate isotype controls were then fixed using 0.2 % formyl saline and detected for antibody binding using flow cytometry. When compared to isotype control, significant β_3 antibody binding was observed following the increase of Alexa Fluor® 647- and PE- fluorescent labels concentration to 1 µg/ml **(Figure 3.9 a and b)**. This is the lowest concentration that gave a signal and was used in order to maximise the signal to noise ratio.

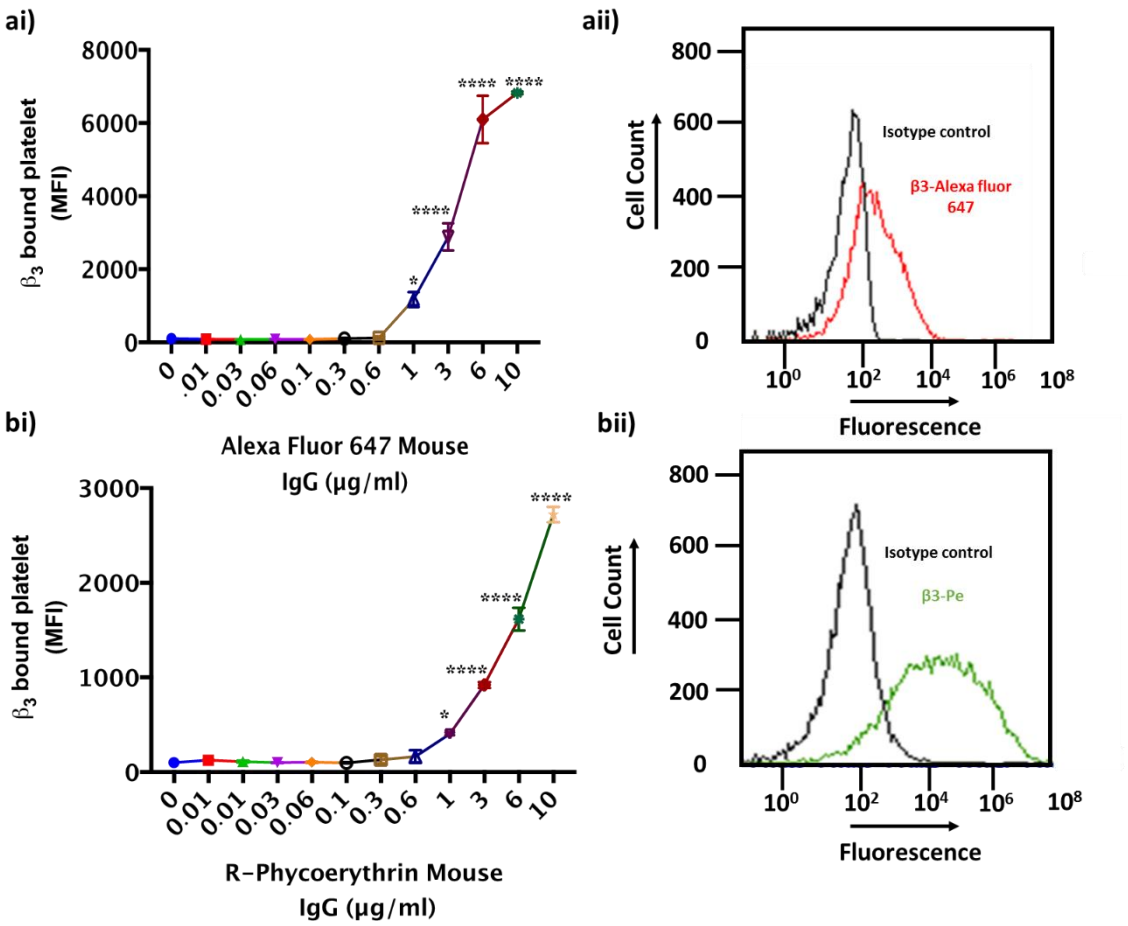

Figure 3.9 Optimisation of Alexa fluor 647- and PE- fluorescent dyes labelling.

Anti- β_3 mouse mAbs were incubated with different concentrations of Alexa Fluor® 647 and PE labelled for 5 minutes at room temperature, followed by 5 minutes blocking step. Labelled antibodies were then added to PRP and after 10 minutes, 0.2 % formyl saline added to fix the samples. Alexa Fuor® 647- and PE- fluorescent labelled β_3 mouse mAbs bound platelets were then detected using flow cytometry appropriate filters. **ai)** MFI of Alexa Fluor 647 labelled antibody bound platelets. **aii)** Representative histograms of isotype control and β_3 bound platelets using 1µg/ml of Alexa Fluor® 647 labelling reagent. **bi)** MFI of PE labelled antibody bound platelets. **bii)** Representative histograms of isotype control and β_3 bound platelets using 1 µg/ml of PE labelling reagent. Data represents mean ± SEM ($n \geq 3$), *$P \leq 0.05$ and ****$P \leq 0.0001$ was calculated by one-way ANOVA.

Having established the concentration of the staining antibodies (1 µg/ml), FRET analysis of β_3-β_3 association was performed. PRP was stained with 1µg/ml of Alexa Fluor® 647-labelled anti-β_3 monoclonal antibodies with 1 µg/ml of isotype control or PE-fluorescent labelled anti-β_3 monoclonal antibodies 1 µg/ml of isotype control or 1 µg/ml of both 647 and PE labelled anti-β_3 monoclonal antibodies and samples were then stimulated with (1 U/ml) thrombin for 0, 15, 30, 60, 90, 120, 180 and 300 seconds in presence of (25 mg/ml) GPRP. 0.2 % formyl saline was then used to fix the samples prior to flow cytometric analysis. A right shift in fluorescent intensity at 647 double stained platelet indicates FRET (increase in fluorescence from the Alexa Fluor® 647 labelled anti-β_3). Likewise, a decrease in intensity of double stained platelets indicates FRET (decrease in fluorescence from the PE-conjugated anti-β_3 mAbs as it is quenched by Alexa Fluor 647 **(Figure 3.10).**

Interestingly, β_3-β_3 FRET signals were observed and elevated in a biphasic fashion, at 60 and 180 seconds **(Figure 3.10)**, similar to the findings in $\beta_3\beta_3$ clustering mode analysed with presently developed R based method **(Figure 3.6)**. This finding validates the STORM method developed in this chapter, and supports our initial finding that β_3 clusters is in biphasic manner upon platelet activation.

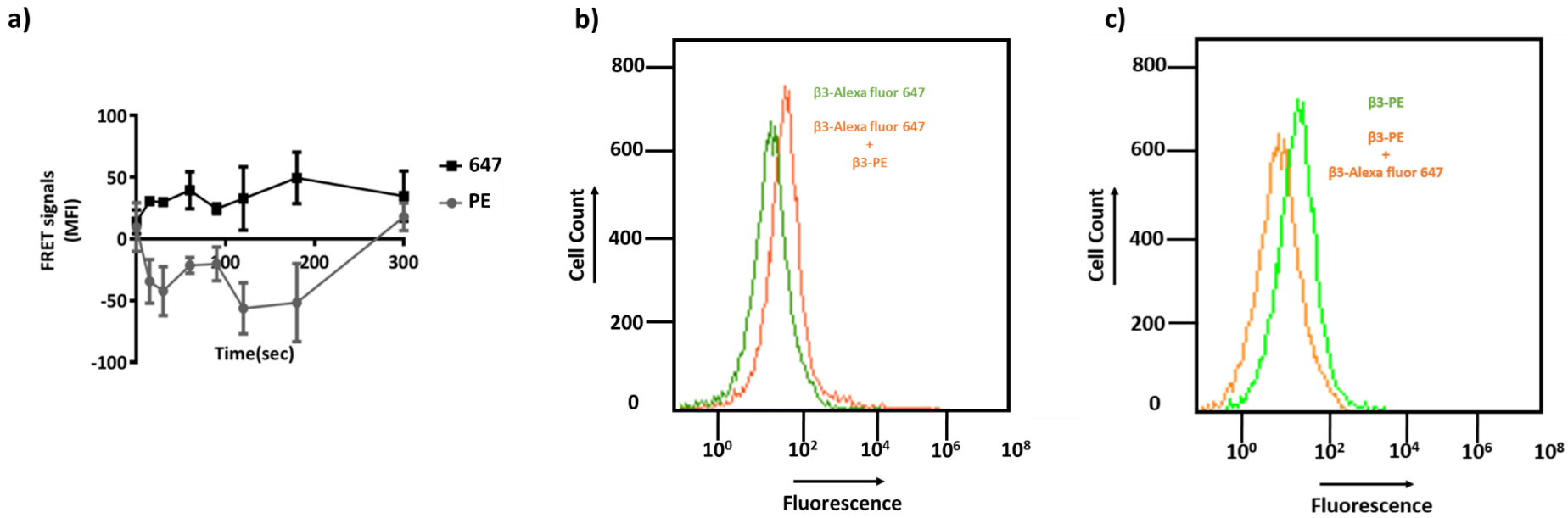

Figure 3.10 Membrane localization of integrin β_3-β_3 association on thrombin stimulated platelet surface.

Alexa Fluor 647- conjugated anti-β_3 mAb and PE-conjugated anti-β_3 mAb stained PRP was stimulated with (1 U/ml) thrombin for 0,15, 30, 60, 90, 120, 180 and 300 seconds in presence of (25 mg/ml) GPRP. Reactions were stopped with 0.2 % formyl saline and FRET analysis of platelet stained with Alexa Fluor 647- conjugated anti-β_3 mAb and PE-conjugated anti- β_3 mAb along with appropriate isotype controls was measured using flow cytometry. Alexa Fluor 647 was excited at 650 nm, and PE were emitted at more than 578 nm. **a)** MFI of FRET signals over different time points. **b)** Representative histogram showing right shift FRET signal at 30 seconds stimulation. **c)** Representative histogram showing left shift FRET signal following 30 seconds stimulation. Data represents mean ± SEM ($n \geq 3$), *$P \leq 0.05$ and ****$P \leq 0.0001$ was calculated by one-way ANOVA. One-way ANOVA (Alexa Fluor 647- conjugated anti-β_3, $P = 0.03$) (PE-conjugated anti- β_3, $P = 0.01$).

3.5 Defining kindlin-3 - β_3 co-clusters within 50 nm in human platelets

As shown in **Figure 3.11,** kindlin-3 was shown to be located inside resting platelets (red color) with peripheral mobilisation following platelet activation. This mobilisation was also noted where platelet was stained for kindlin-3 and β_3 (**Figure 3.12**).

Having established a method of analysing clusters as 2 times mean density ($\beta_3\beta_3 2$) in thrombin stimulated platelets, investigation was extended to examine whether the association of kindlin-3 - β_3 could be defined similarly. We called this co-cluster of $k\beta_3$ analysis. Using the same approach shown in **appendix 1, 2, 3 and 4.** The "mean density" of β_3 molecules surrounding each kindlin was analysed using R software. The mean number of β_3 molecules within 50 nm of each kindlin molecule for all resting platelets from each individual was analysed. This mean value gave us the "mean density" of β_3 molecules surrounding each kindlin. We define co-clusters as having two times ($k\beta_3 2$), four times ($k\beta_3 4$) or ten times ($k\beta_3 10$) the mean density of β_3 to define varies co-cluster overtime **(Figure 3.13)**.

Consistent with the mean density patterns observed in ($\beta_3\beta_3$) clustering, no notable changes were seen in the pattern of kindlin-β_3 co-clustering between 2, 4 and 10 times mean density values of β_3 molecule **(Figure 3.13)** and therefore, 2 times mean density ($k\beta_3 2$) was chosen to define ($k\beta_3 2$) co-cluster. As shown in **Figure 3.14**, upon stimulation, the percentage of kindlin molecules within $k\beta_3 2$ co-clusters initially showed the opposite trend of β_3 clustering for the first 30 seconds (decreasing from a high in resting platelets), after which $k\beta_3 2$ peak at 60 seconds, declining at 90 seconds, increasing again before falling at 300 seconds). There were again temporal changes in this pattern

between individuals. This pattern corresponds with the pattern of β_3-β_3 clusters following 30 seconds agonist stimulation **(Figure 3.7).** Therefore**,** a STORM microscopy method was developed to quantify the temporal changes in the co-clustering of kindlin and integrin β_3, and the clustering of integrin β_3 in human platelets.

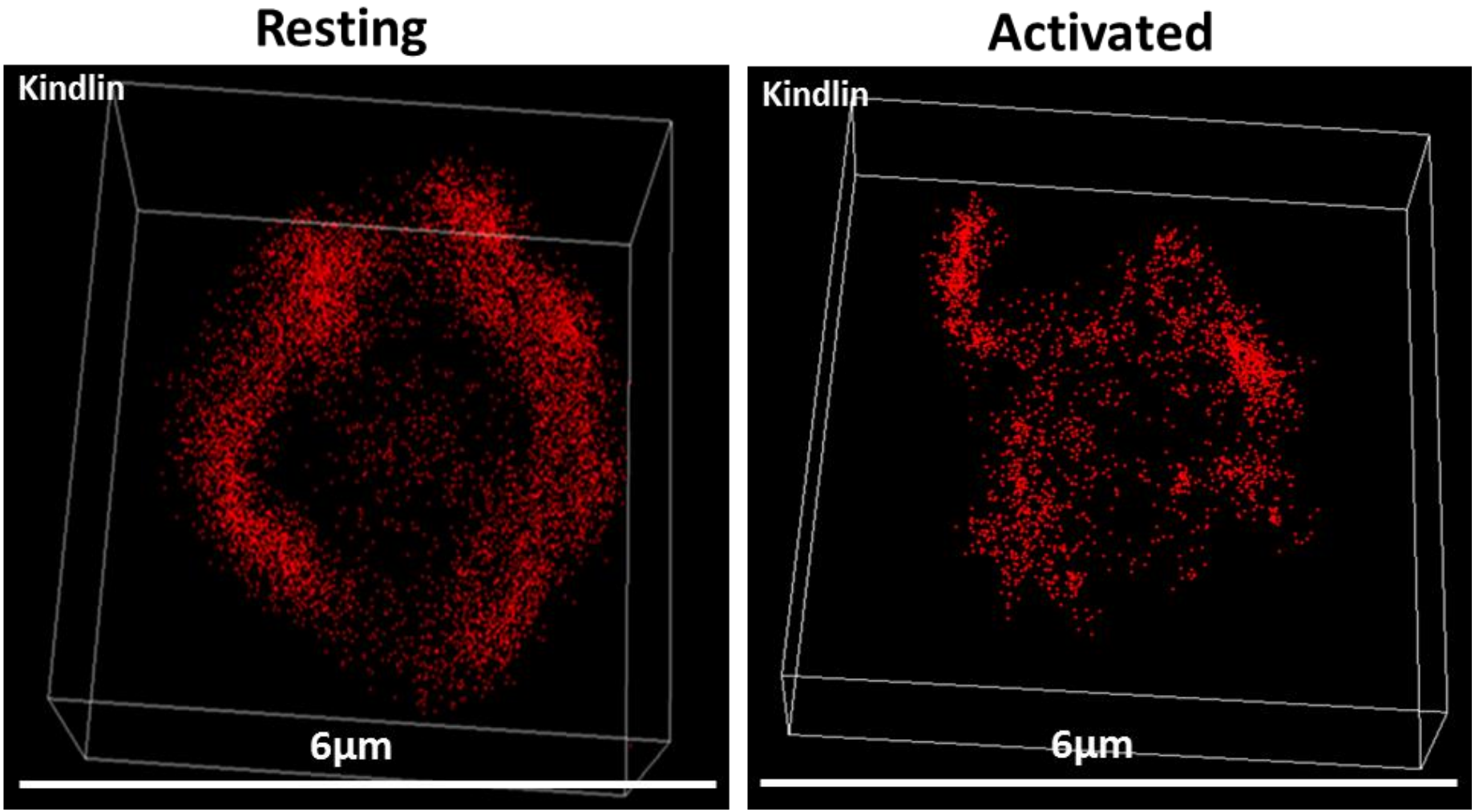
Resting
Kindlin
6µm
Activated
Kindlin
6µm

Figure 3.11 Three dimension images of kindlin molecules in platelets.

Platelet-rich-plasma (PRP) was activated with thrombin (1 U/mL) in the presence of GPRP (25 mg/ml) for 0 and 300 seconds, fixed with 2 % (v/v) formyl saline and permeablised with BD Phos Flow Perm Buffer III. Kindlin was identified with primary and Alexa Fuor® 647-labelled secondary antibodies. Labelled platelets were washed then adhered overnight to poly-D-lysine coated ibidi slides before 3D STORM imaging. Kindlin was analysed using the ImageJ plugin ThunderSTORM.

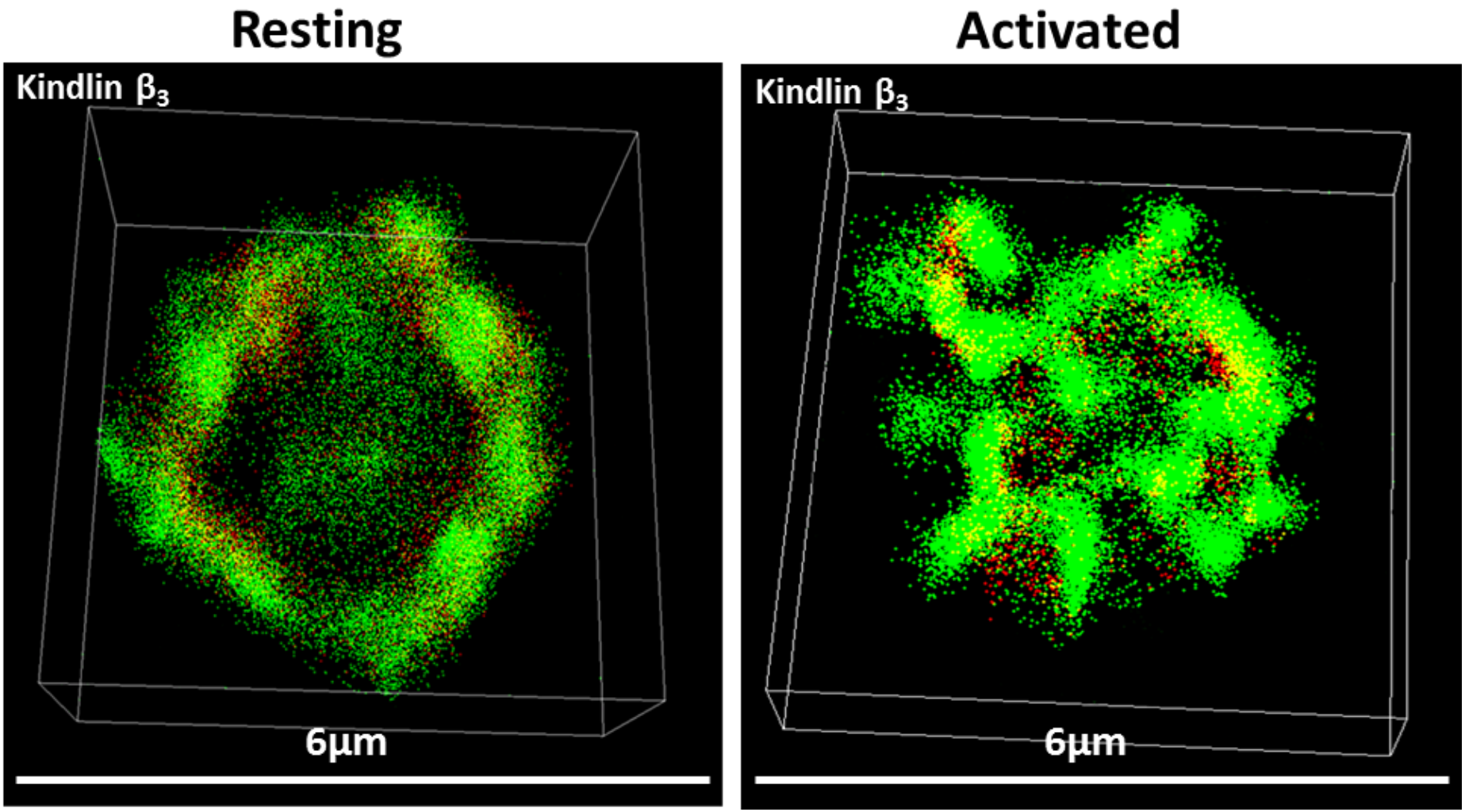
Resting
Kindlin β3
6µm
Activated
Kindlin β3
6µm

Figure 3.12 Three dimension of kindlin-β_3 association in platelets.

Platelet-rich-plasma (PRP) was incubated with vehicle; resting and activated platelets with thrombin (1 U/ml) for 300 seconds were fixed with 2 % (v/v) formyl saline and permeablised with BD Phos Flow Perm Buffer III. Secondary antibodies were used to recognize Kindlin and integrin β_3 antibodies, respectively. Labelled platelets were washed then adhered overnight to poly-D-lysine coated ibidi slides. Images were reconstructed using Nikon-NIS-Elements.

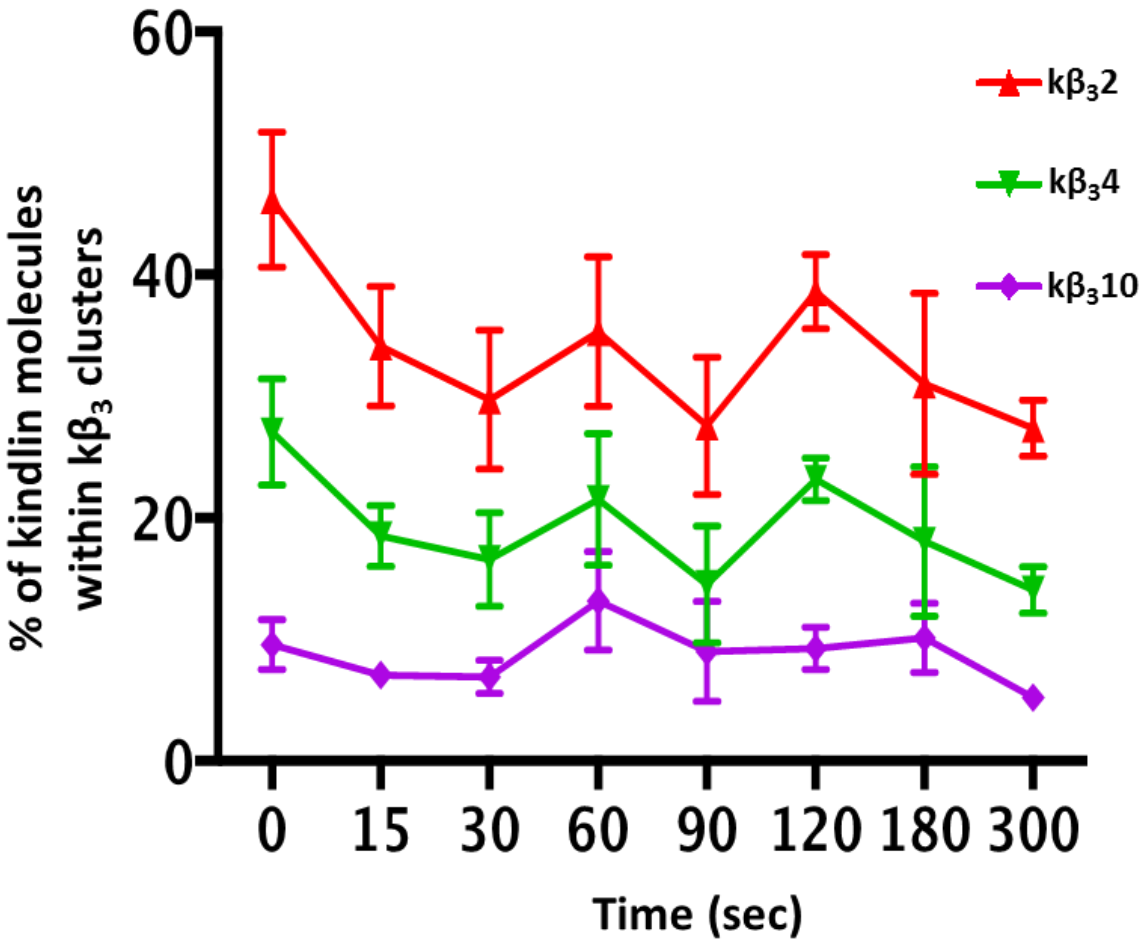

Figure 3.13 Defining kindlin-β_3 co-clusters within 50 nm in human platelets.

The change in the percentage of kindlin molecules defined as being within kβ_3 co-clusters over time. The mean number of β_3 molecules within 50 nm of each kindlin molecule for all resting platelets from each individual was analysed. This mean value gave us the "average density" of β_3 molecules surrounding each kindlin. We define co-clusters as having 2 times (k$\beta_3$2), 4 times (k$\beta_3$4) or 10 times (k$\beta_3$10) the mean density of β_3. Co-clustering was analysed using ImageJ plugin ThunderSTORM and the presently developed R based novel clustering analysis method. Data represents mean ± SEM ($n \geq 3$).

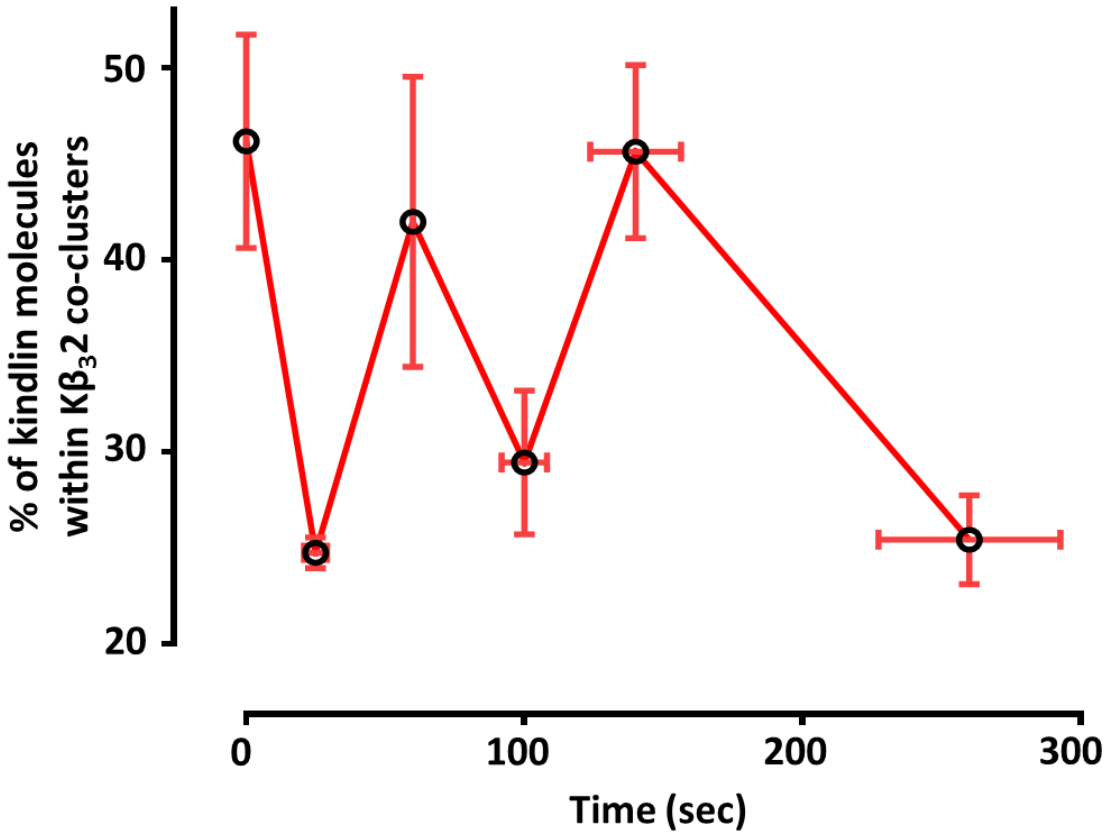

Figure 3.14 Temporal changes in kindlin-β_3 co-clustering.

Upon stimulation with (1U/ml) thrombin for 0, 30, 60, 90, 150 and 280 seconds, the percentage of kindlin molecules within k$\beta_3$2 co-clusters (k$\beta_3$2) was analysed using ImageJ plugin ThunderSTORM and the presently developed R based novel clustering analysis method. Data represents mean ± SEM ($n \geq 3$), **$P \leq 0.01$ was calculated by one-way ANOVA, (one-way ANOVA P = 0.008).

3.6 General Discussion

STORM microscopy offers an opportunity to detect single fluorophores with nanometere resolution (Heilemann et al., 2008; Moerner, 2012) STORM images were reconstructed by blinking the fluorescent molecule in dark and fluorescent state. Repeating this cycle allow molecules to be measured individually from which individual molecules could be colocalised and images reconstructed (Rust et al., 2006a; Henriques et al., 2010). This advantage makes STORM a suitable candidate tool meeting the purposes of the present study in regards to imaging small sized platelets along with examination of delicate intracellular details at molecular, nano-scale levels.

Several methods have been established to quantify the temporal changes in the co-clustering of two proteins imaged by super-resolution microscopy such as co-clustering methods and K-Ripley (Ripley, 1977; Owen et al., 2010; Malkusch et al., 2012; Rossy et al., 2014). However, these methods are restricted to distinguish between different shapes of clusters. For instance, SR-Tesseler method provides precise and automatic quantification of protein organization at different scales, from the cellular level down to clusters of a few fluorescent markers. Although robust, this method cannot be applied in 3D setting. Clustering quantification is defined mathematically not biologically (Levet et al., 2015). Furthermore, Density-based spatial clustering analysis with noise (DBSCAN) has been used extensively but the definition and quantification of clusters is complicated and not biologically intuitive (Nan et al., 2013). Therefore, it was necessary to develop new approach to analyse integrin β_3 clustering and kindlin colocalisation with β_3.

Here, we developed a novel STORM microscopy analysis method and used it to quantify the temporal changes in the co-clustering of kindlin-3 and integrin β_3, and the clustering

of integrin β_3 in human platelets following thrombin stimulation. Our method provides a biological measure to identify kindlin-3 colocalisaion and integrin β_3 clustering in a STORM setting.

Integrin $\alpha_{IIb}\beta_3$ activation has been studied extensively because it involves both inside-out and outside-in signalling pathway which may offer novel anti-thrombotic drug targets for platelet activation (Nieswandt et al., 2009). Previous researches have studied $\alpha_{IIb}\beta_3$ and confirmed the presence of β_3 integrin on the platelet surface (Grüner et al., 2003). Kindlin has been studied and confirmed to be an intercellular protein that leads to the activation of $\alpha_{IIb}\beta_3$ integrin (Campbell and Humphries, 2011).

As the main goal of the present project is to study the kinetic and mechanisms underlying integrin β_3 clustering and activation along with its association with other cytosolic proteins, at microscopical level using STORM, much of the initial work was invested in achieving applicable method of studying and analysing such phenomenon in human platelets, an aspect that has not been fully understood yet. We developed an effective clustering and co-clustering analytical tool that helped us in analyzing different pattern of β_3 clustering and kβ_3 co-clustering that were obtained by STORM images. β_3 clustering findings revealed a characteristic biphasic pattern with β_3 clustering going through two peaks starting early within 30 seconds during platelet stimulation with thrombin. Paszek et al. (2009) reported similar behavior of integrin clustering triggered within tens of seconds of stimulation. Moreover, observed drops and peaks of β_3 clustering pattern could be attributed to the nature of integrin clustering that is known to undergo repeated bondage and breakage during the process of clustering (Paszek et al., 2009) and hence, it explains aforementioned biphasic pattern of β_3 integrin in platelets. Lastly, FRET

findings of β_3-β_3 association are in alignment with the STORM based method generated findings and therefore, the method was validated and confirmed effective.

In summary, this chapter demonstrated the analysis of clustering and co-clustering using a newly developed and validated method. In the next chapter, other aspects involving integrin β_3 activation and subsequent platelet aggregation along with β_3 clustering and co-clustering with kindlin-3 at molecular level using STORM would be demonstrated in a similar setting of platelet stimulation time.

4 Time scales of integrin β_3 clustering and kindlin-3 - β_3 co-clustering in human platelets using STORM

4.1 Introduction

Integrins are heterodimeric surface receptors that facilitate cell adhesion and interaction with extra cellular matrix (Hynes, 2002). Beside their adhesive function, integrins take part in signal transduction and consequently regulate vital cellular aspects such as cell division, differentiation, survival and motility (Miranti and Brugge, 2002; Berrier and Yamada, 2007). Such role is thought to be facilitated by the assembly and clustering of integrin molecules in response to ligand binding and thereby, enabling recruitment of several signalling proteins downstream of clustered integrins. Additionally, clustered integrins serve as a linker of the cellular cytoskeleton to the ECM, allowing transmission of mechanical traction required for cell motility and cytoskeletal reorganization and shape change (Beningo et al., 2001; Tan et al., 2003).

In platelets, several agonists induce platelet activation via initiation of signalling process, known as "inside-out" signalling, resulting in conformational changes within integrin $\alpha_{IIb}\beta_3$. Such changes allow upregulation of integrin affinity for its primary ligand, fibrinogen. Bound fibrinogen forms a bridge between adjacent platelets and thereby their interaction. Moreover, fibrinogen binding to $\alpha_{IIb}\beta_3$ triggers a further outside-in signalling cascade causing the amplification of platelet interaction and aggregate formation (Parise, 1999; Li et al., 2010).

Activated PLCγ2 mediates the generation of IP3 and DAG. IP3 mediates mobilization of Ca^{2+} and DAG is required for the activation of PKC. Increasing concentration of Ca^{2+} in the cytosol and PKC activation (Grosse et al., 2007; Shattil et al., 2010). DAG and Ca^{2+} generate CALDAG-GEFI, leading to activate RAP-1-GTP. RAP-1-GTP binds to RIAM, which results in recruitment and activation of talin to bind the cytoplasmic tail of β_3 causing integrin activation. Studies have revealed the interaction between kindlin

and β_3 is necessary to regulate and support integrin activation in platelets at the site of injury (Huang et al., 2019). ILK is a known effector molecule which recruits kindlin to bind the cytoplasmic tail of β_3 (inside-out signalling) (Qadota et al., 2012; Honda et al., 2013). However, the temporal interaction between kindlin-β_3, the mechanisms of $\alpha_{IIb}\beta_3$ clustering and the role of ILK in this process are not fully understood (Anthis and Campbell, 2011).

According to Huang et al. (1993), outside-in signalling triggered tyrosine phosphorylation events of several proteins. Src activation is a key element in integrin $\alpha_{IIb}\beta_3$ mediated outside in signalling (Phillips et al., 2001). Src is associated with the C-terminal tail of β_3 integrin in resting platelets via its SH3 domain in an inactive conformation. This is maintained by Csk-mediated phosphorylation on Tyr-529 located on β_3 integrin. Csk detaches from β_3, allowing Src activation. However, recent work shows that c-Src associates with β_3 integrin predominantly in activated platelets (Obergfell et al., 2002; Goggs and Poole, 2012; Wu et al., 2015). $\alpha_{IIb}\beta_3$ clustering is important for full Src activation, permitting trans-auto phosphorylation of the Tyr-418 residue in the Src activation loop. Moreover, Syk can interact directly via SH2 domain-mediated interaction with the cytoplasmic tail of integrin β_3 (Fong et al., 2016).

Following our established methods for analysing integrin β_3 clustering and colocalisation of kindlin-3 - β_3 in human platelets using STORM microscopy, work carried out in this chapter to investigate the time course of β_3 clustering, kindlin-3 - β_3 co-clustering. Moreover, to identify whether a link between the observed patterns of β_3 clustering and temporal changes of kindlin-3 - β_3 association along with fibrinogen binding, platelet aggregation and ultimately signalling events following β_3 activation. The purpose of this

was to identify if β_3 clustering is dependent on fibrinogen binding and essential for the regulation of β_3 and downstream signalling.

4.2 Temporal changes in integrin β_3 clustering and co-clustering with kindlin-3

4.2.1 Temporal changes in time course of integrin β_3 clustering evoked by thrombin

Having established a novel cluster analysis of integrin β_3 clustering, integrin β_3 clustering overtime in response to thrombin (GPCR agonist) was assessed.

Human PRP was rested for 1 hour prior to experiments. PRP resting or activated with (1 U/ml) of thrombin for 30, 60, 90, 150 and 300 seconds **(Figure 3.7) (as selected based on the previous chapter 3)** (in the presence of 25 mg/ml GPRP), were fixed in 2 % (v/v) formyl saline then permeabilised with BD Phos Flow Perm Buffer III. Primary antibodies anti-Kindlin-3 and anti-integrin β_3 were added and probed then with and Alexa Fluor® 647 and Alexa Fluor® 555 secondary antibodies, respectively.

The location of kindlin-3 was found inside the platelet (red colour) whereas β_3 integrin was detected on the surface of platelet (green colour) **(Figure 4.1)**. In unstimulated platelet, platelet showed circular and uniform morphology. However, following activation of platelet with 1 U/ml of thrombin **(Figure 4.1)**, platelet changed its shape, leading to mobilise kindlin-3 close to membrane and extension of numerous long pseudopodia. Also, changes were observed in β_3 clustering over 5 minutes.

As shown in **Figure 4.2**, upon stimulation with thrombin, it was observed the percentage of β_3 molecules within $\beta_3\beta_3 2$ cluster increased from low in resting state, peaking at 30 seconds, and then falling before peaking at 150 seconds, and decreasing again at 300 seconds. Moreover, the level of integrin β_3 clustering was significantly high at 30, 90,

150 and 300 seconds in comparison with 0 seconds. This finding supports the initial data shown in **chapter 3**.

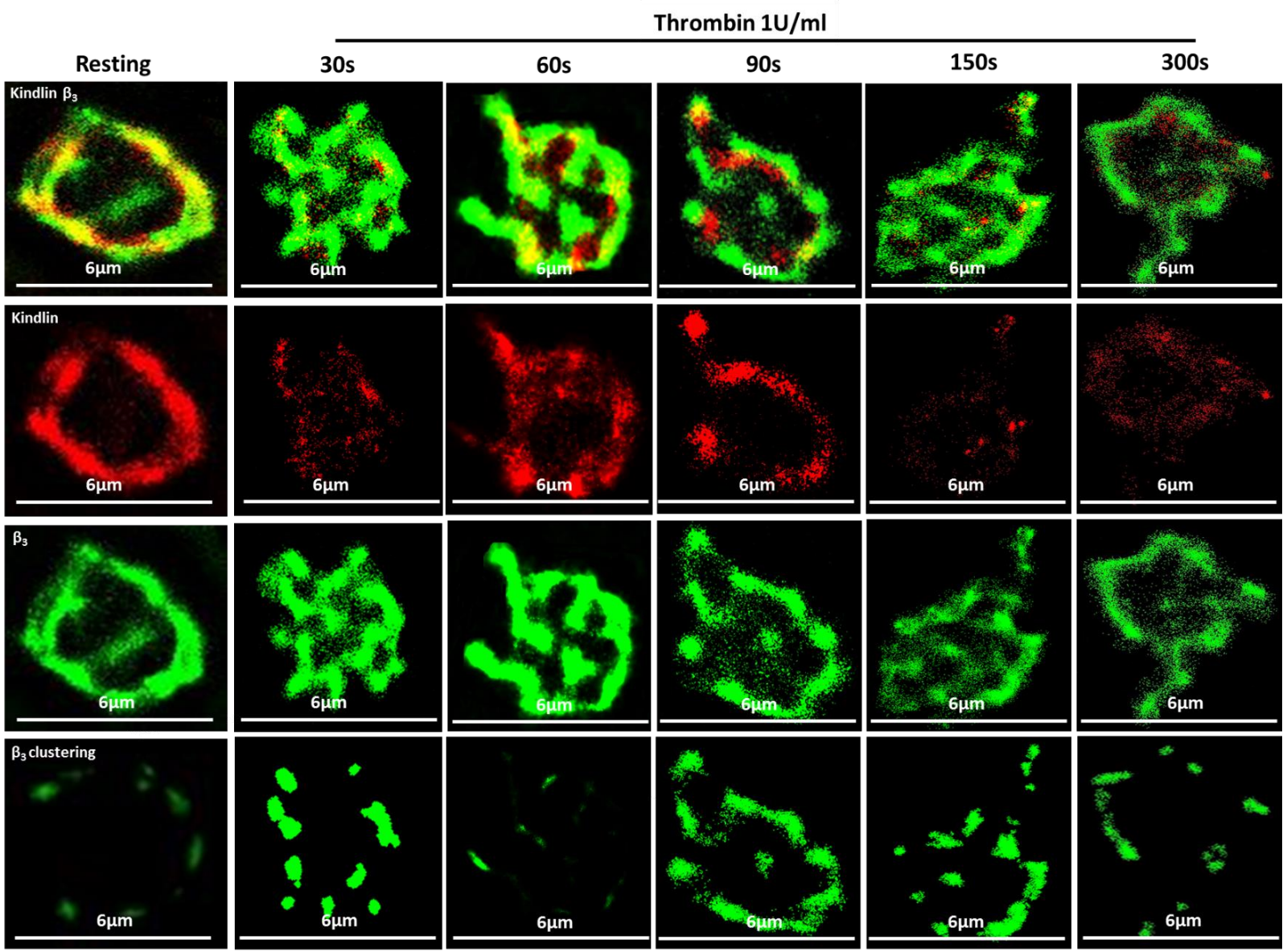
Thrombin 1U/ml
Resting
30s
60s
90s
150s
300s
Kindlin β3
Kindlin
β3
β3 clustering
6µm

Figure 4.1 The time course of integrin β_3 clustering and co-localisation with kindlin in response to thrombin.

3D images of β_3 and kindlin-3 were reconstructed using NIKON-NIS-Elements. 0, 30, 60, 90, 150 and 300 seconds thrombin (1 U/ml) stimulated platelets in the presence of GPRP (25 mg/ml) were fixed and permeabilised with 2 % (v/v) formyl saline and BD Phos Flow Perm Buffer III, respectively. Anti-Kindlin and anti-integrin β_3 were incubated with platelets at 37 °C for 30 minutes. Antibody bound platelets were then detected using Alexa Fluor-647 (kindlin) and -555 (β_3) labelled secondary antibodies. Labelled platelets were washed and allowed to adhere on poly-D-lysine coated ibidi slides before 3D STORM imaging. The results are representative of ≥ 3 individual experiments.

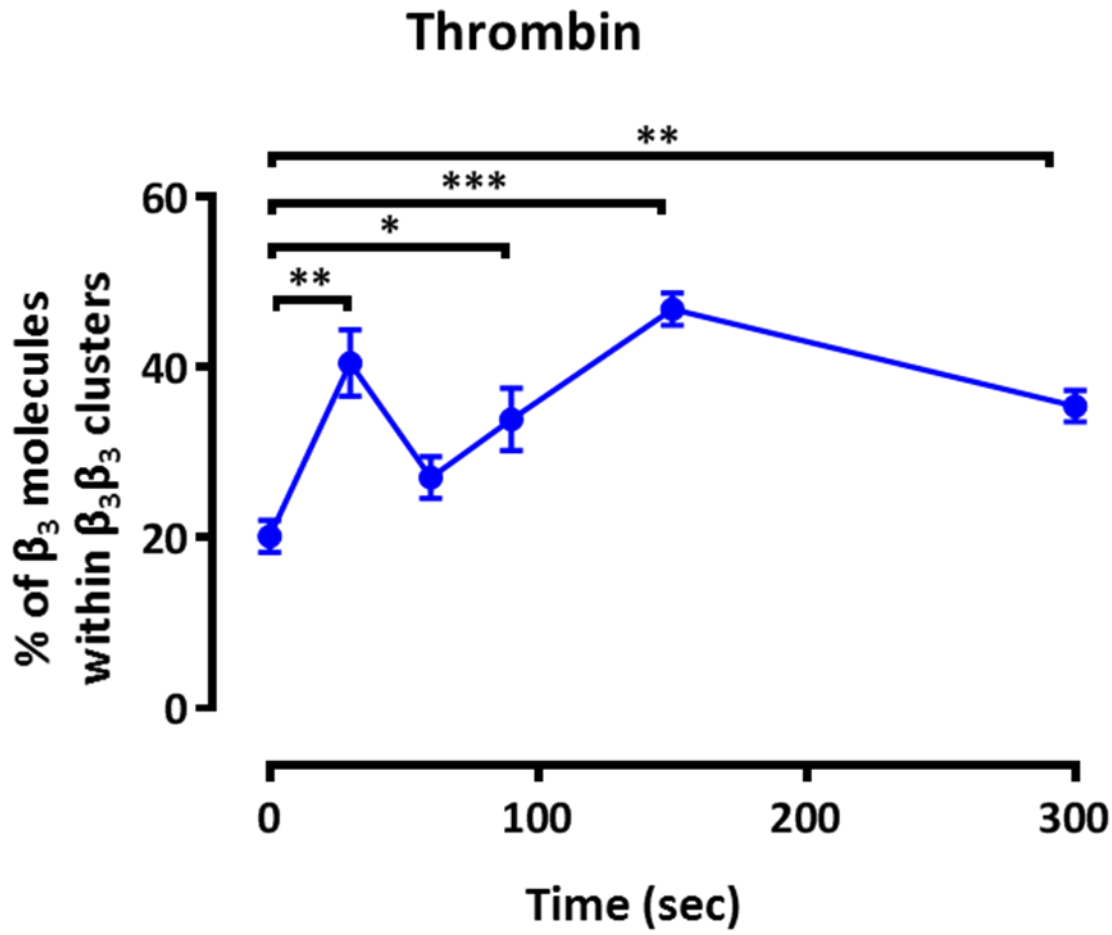

Figure 4.2 Level of β_3 molecules within $\beta_3\beta_3$2 clustering in response to thrombin.

The mean number of β_3 molecules within 50 nm of each β_3 molecule ($\beta_3\beta_3$2) in 0, 30, 60, 90, 150 and 300 seconds (1 U/ml) thrombin stimulated platelets were analysed using ImageJplugin ThunderSTORM and developed R based novel clustering analysis method. Results are mean ±SEM ($n \geq 3$), *$P \leq 0.05$, **$P \leq 0.01$, *** ≤ 0.001 was calculated by one-way ANOVA.

4.2.2 Temporal changes in time course of integrin β_3 clustering in response to CRP-XL

Having confirmed the biphasic β_3 clustering occurs in platelets stimulated with thrombin. Work was carried out to investigate whether a similar pattern occurred with CRP-XL (GPVI agonist).

PRP resting or stimulated with (3 µg/ml) of CRP-XL for 30, 60, 90, 150 and 300 seconds, then fixed in 2 % (v/v) formyl saline and followed by permeabilised BD Phos Flow Perm Buffer III. Primary antibodies anti-kindlin-3 and anti-integrin β_3 were added and labelled with Alexa Fluor® 647 and Alexa Fluor® 555 secondary antibodies, respectively. Labelled platelets were washed and then allowed to adhere on poly-D-lysine coated ibidi slides prior to overnight incubation. 3D STORM Images were reconstructed using Nikon-NIS-Elements.

The location of kindlin-3 was observed inside the platelet (red colour) whereas β_3 integrin was found on the surface of platelet (green colour) **(Figure 4.3)**. In resting platelet, platelet showed circular and uniform morphology. However, following stimulation of the platelet using 3 µg/ml of CRP-XL **(Figure 4.3)**, platelet shape has changed, leading to mobilise kindlin-3 close to membrane and extension of numerous long pseudopodia. β_3 clustering changed over 300 seconds.

β_3 clustering CRP-XL treated in platelets followed the same pattern starting from low in unstimulated platelet, then peaking at 30 seconds, then decreasing at 60 seconds and again peaking at 90 seconds before decreasing at 300 seconds. CRP-XL facilitated substantial activation in the percentage of β_3 molecules within β_3 clustering at 30, 90, 150, and 300 seconds compared to the resting platelet **(Figure 4.4).**

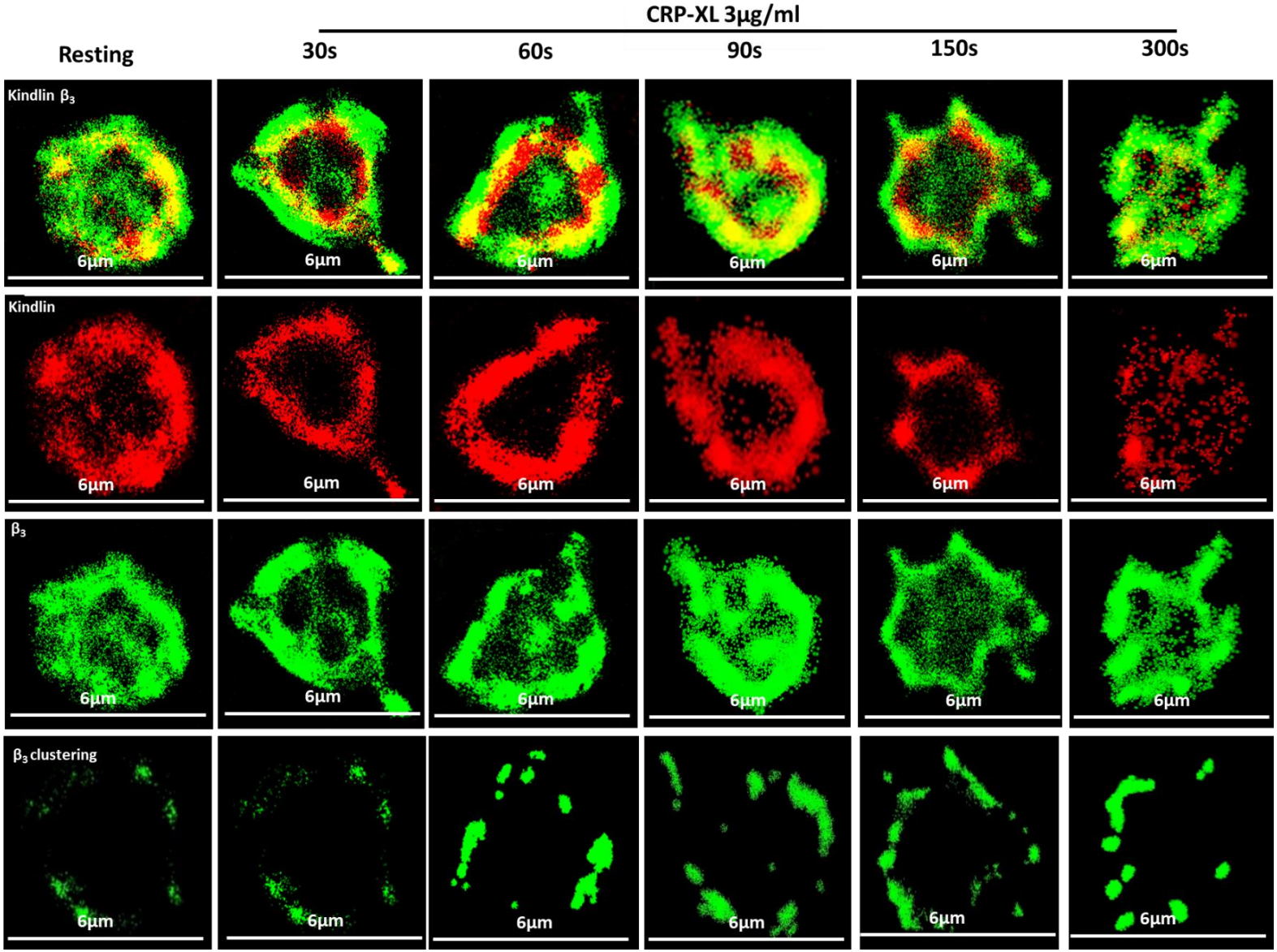
CRP-XL 3µg/ml
Resting
30s
60s
90s
150s
300s
Kindlin β3
Kindlin
β3
β3 clustering
6µm

Figure 4.3 The time course of integrin β_3 clustering and co-localisation with kindlin in response to CRP-XL.

Platelets were stimulated for 0, 30, 60, 90, 150 and 300 seconds with CRP-XL (3 µg/ml) followed by fixation with 2 % (v/v) formyl saline. Fixed samples were then permeabilised with BD Phos Flow Perm Buffer III, kindlin-3 and integrin β_3 antibodies were added. After 30 minutes, unbound antibodies were removed and kindlin-3 and β_3 probed platelets were detected using Alexa Fluor -647 and -555, respectively. Following multiple washing cycles, platelets were allowed to adhere on poly-D-lysine coated ibidi slides overnight. Samples were then imaged using STORM Nikon-NIS-Elements. Data are representative of ≥ 3 separate experiments.

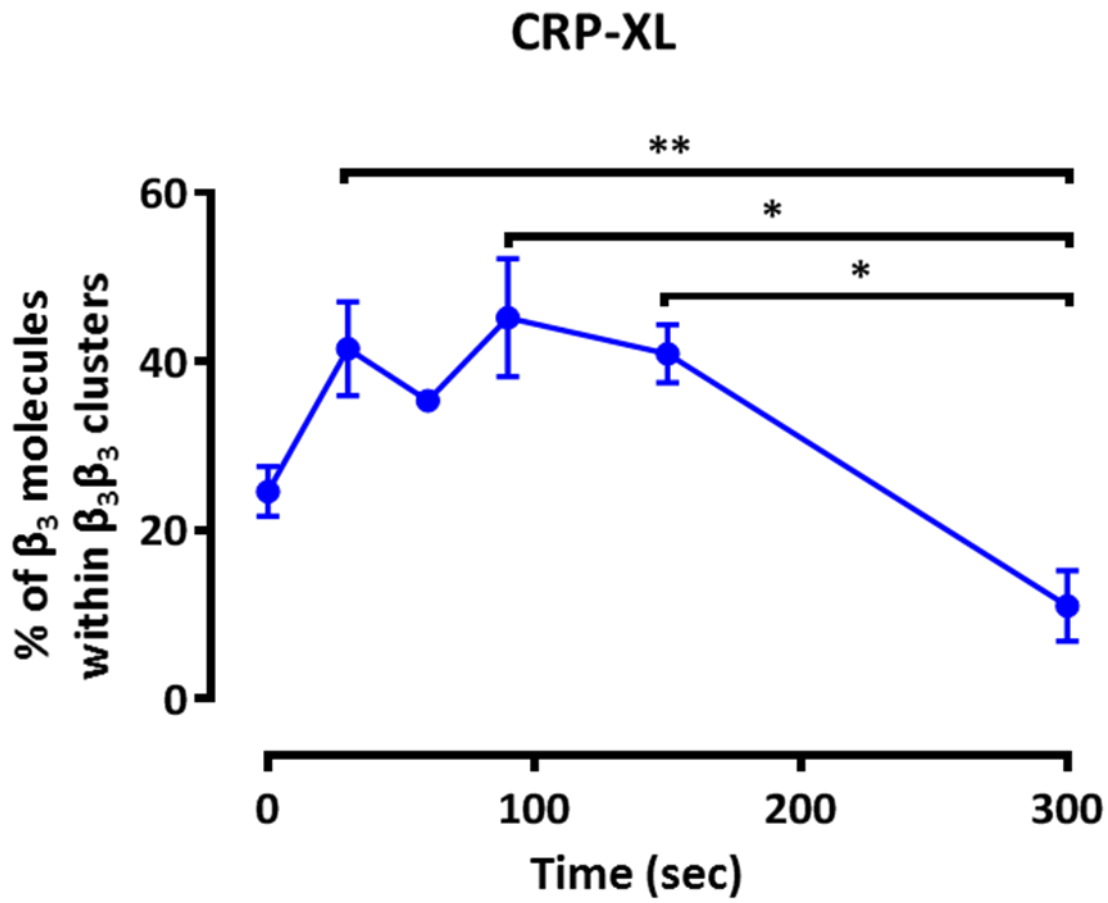

Figure 4.4 CRP-XL mediates level of β_3 molecules within $\beta_3\beta_3$2 clustering.

The mean number of β_3 molecules within 50 nm surrounding each ($\beta_3\beta_3$2) in 0, 30, 60, 90, 150 and 300 seconds (3 µg/ml) CRP-XL mediated platelets were analysed using ImageJ plugin ThunderSTORM and developed R based novel clustering analysis method. Results are mean ±SEM ($n \geq 3$), *$P \leq 0.05$ and **$P \leq 0.01$ was calculated by one-way ANOVA.

4.2.3 Temporal changes in time course of kindlin-3 co-clustering with integrin β_3 mediated by thrombin or CRP-XL

Using the established novel cluster analysis of integrin β_3 clustering, integrin β_3 co-clustering with kindlin-3 mediated by (1 U/ml) thrombin or (3 μg/ml) was carried out.

As shown in **Figure 4.5**, the density of kindlin-3 molecules surrounding each β_3 molecule in response to thrombin showed a relatively high association with integrin β_3 in resting platelets. Following stimulation with thrombin, the percentage of kindlin-3 molecules within kindlin-3 - β_3 co-clusters initially fell showing the opposite trend to β_3-β_3 clusters. This followed by a peak in association at 90 seconds and decreasing at 150 seconds before increasing at 300 seconds.

A similar trend was seen in CRP-XL treated platelets. It showed high levels of kindlin-3 - β_3 co-clustering before 30 seconds, followed by a decrease upon stimulation at 30 seconds, then peaking at 60 second and again decline later time points **(Figure 4.6).**

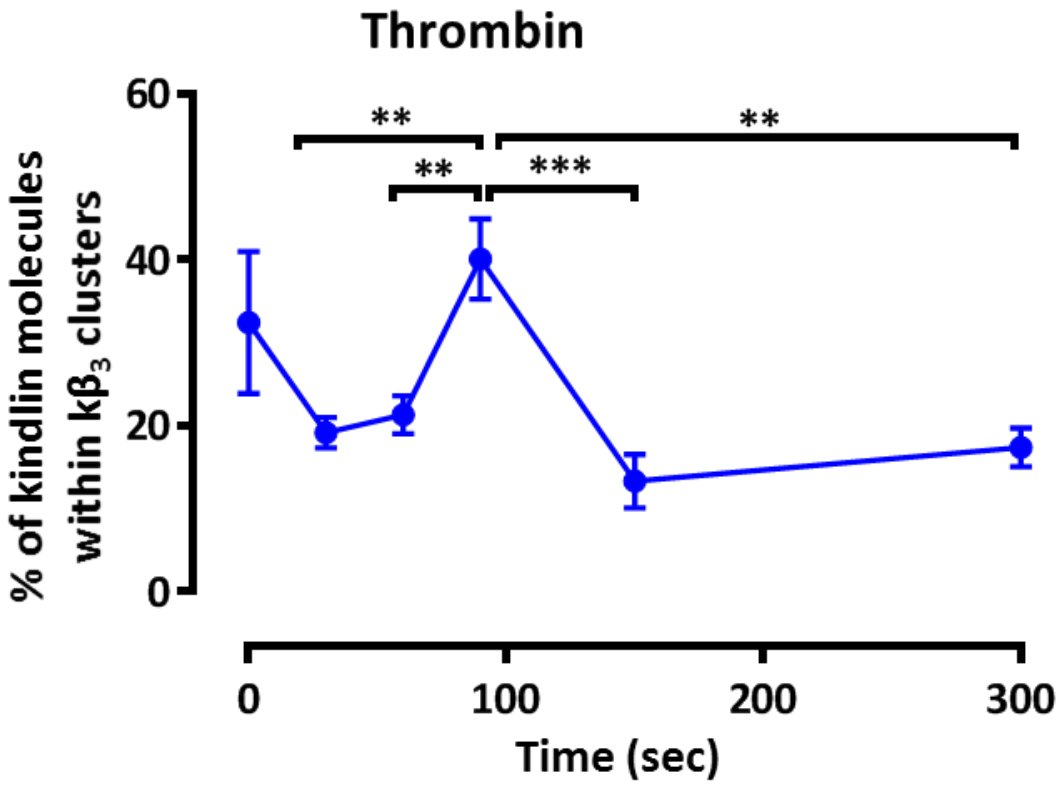

Figure 4.5 Thrombin induces kindlin molecules within kβ$_3$2 co-cluster.

The mean number of β_3 molecules within 50 nm of each kindlin molecule in 0, 30, 60, 90, 150 and 300 seconds (1 U/ml) thrombin mediated platelets were analysed. This mean value was the "average density" of β_3 molecules surrounding each kindlin molecules using ThunderSTORM and cluster analysis in R. The statistical differences in the mean ± SEM ($n \geq 3$) were assessed by One-way ANOVA. *$P \leq 0.05$, **$P \leq 0.01$ and ***$P \leq 0.001$.

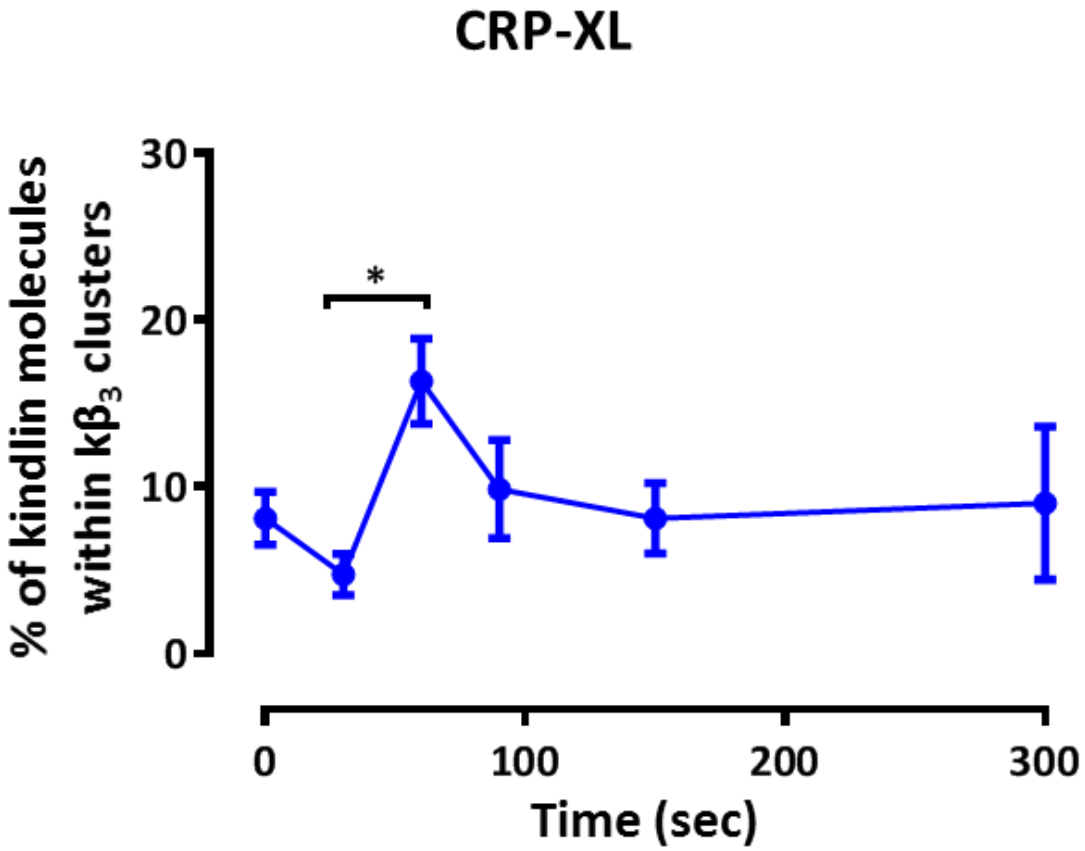

Figure 4.6 Level of kindlin molecules within kβ3 2 co-cluster induced by CRP-XL.

The mean number of β_3 molecules within 50 nm of each kindlin molecule in 0, 30, 60, 90, 150 and 300 seconds CRP-XL (3 µg/ml) stimulated platelets were analysed. This mean value was the "average density" of β_3 molecules surrounding each kindlin molecules using ThunderSTORM and cluster analysis in R. The statistical differences in the mean ± SEM ($n \geq 3$) were assessed by One-way ANOVA. *$P \leq 0.05$.

4.2.4 Association of β_3-β_3 clustering and kindlin-3 - β_3 co-clustering in human platelet

After determining temporal changes in integrin β_3-β_3 clustering and kindlin-3 - β_3 association overtime, the correlation between the level of β_3-β_3 and kindlin-3 - β_3 association from 0-300 seconds in response to 1 U/ml was analysed. As seen in **Figure 4.7**, the association between integrin β_3 clustering and kindlin-3 - β_3 co-clustering from 0-15 and 30-300 seconds was analysed. In first 15 seconds, the association between the level of integrin β_3 clustering and kindlin-3 - β_3 co-clustering was not observed. However, the level of integrin β_3 clustering and kindlin-3 -β_3 co-clustering following 30 seconds stimulation was positively associated.

Taken together, in resting conditions, kindlin-3 - β_3 association did not affect β_3 clustering while after stimulation, kindlin-3 - β_3 co-clustering may affect β_3 clustering and followed the same pattern and this effect was investigated in **chapter 6.**

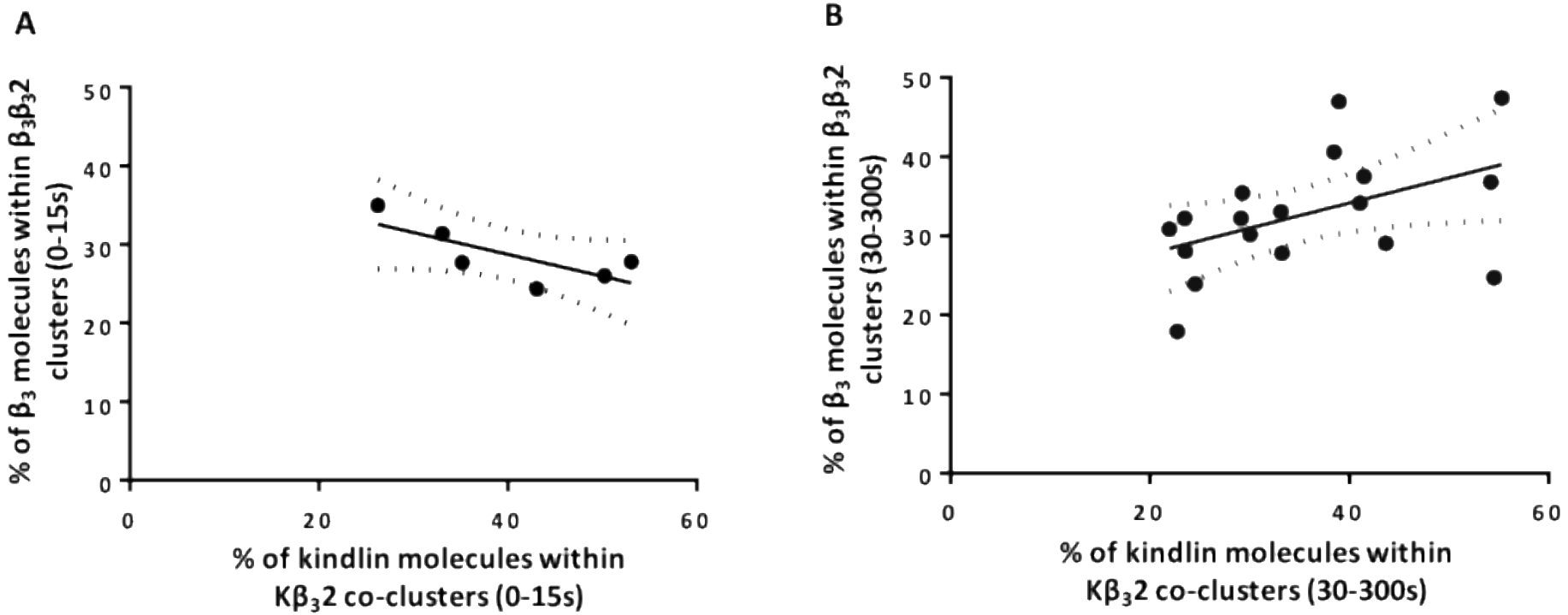

Figure 4.7 Correlation between β_3-β_3 density and kindlin-β_3 from 0 to 300 seconds.

A) In first 15 seconds, the level of β_3-β_3 and kindlin-3 - β_3 association were not associated (Slope = -0.28, $r^2 = 0.57$, P = 0.08). **B)** The percentage of β_3-β_3 and kindlin-3 - β_3 association was positively associated after 30 second activation with 1 U/ml thrombin (Slope = 0.32, $r^2 = 0.22$, P = 0.047). Mean ± SEM (n = 3), *P ≤ 0.05, ***P≤0.001 and ****P ≤ 0.0001 was calculated by one-way ANOVA.

4.3 Platelets aggregation induced by thrombin or CRP-XL

Platelet aggregation is a critical process at the site of vascular injury. This process is mediated by fibrinogen which cross links between adjacent platelets via $\alpha_{IIb}\beta_3$ receptor (Ruggeri, 2002). The purpose of this experiment was to test whether the observed changes of integrin β_3 clustering overtime affect platelets aggregation in response to thrombin or CRP-XL.

To assess the effect of thrombin (1 U/ml) or CRP-XL (3 μg/ml) on platelet aggregation, PRP was stimulated with thrombin or CRP-XL. Aggregation responses (changes in light transmission) were recorded using an optical aggregometer with stirring (1,200 rpm) for 5 minutes at 37 °C.

As shown in **Figure 4.8**, vehicle treated platelets responded to 300 seconds stimulation with CRP-XL and thrombin. It was observed that aggregation is continuous and smooth overtime. In conclusion, platelets aggregation is not attributable to the pattern of β_3-β_3 clustering **(Figure 4.2 and Figure 4.4).**

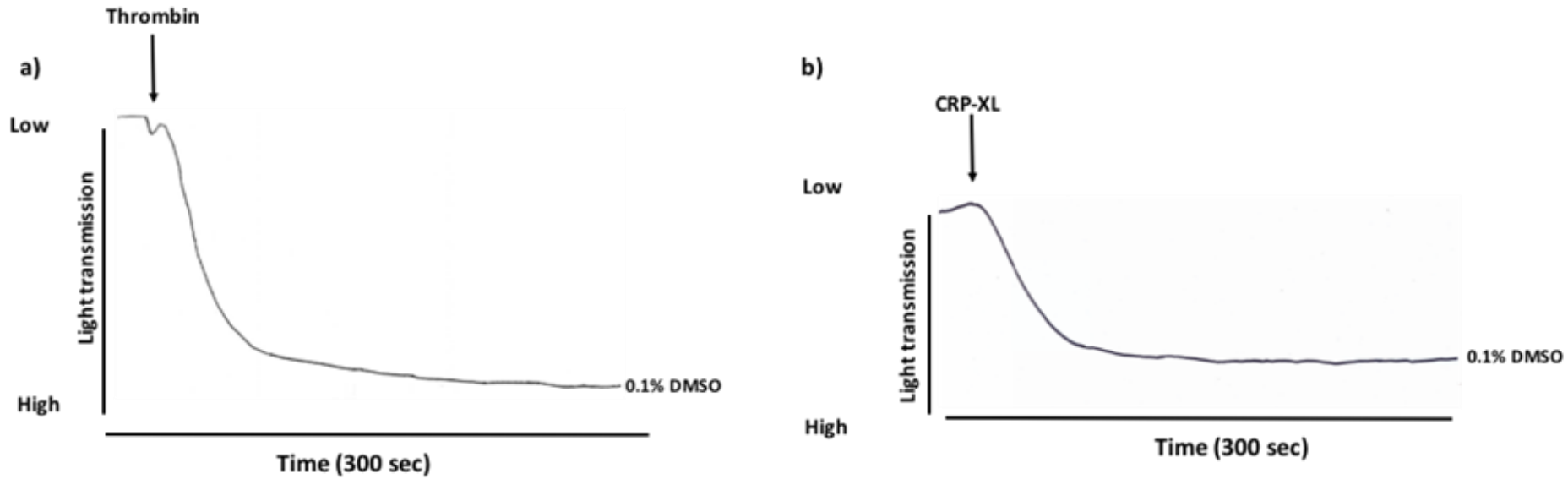

Figure 4.8 Human platelet aggregation in response to 300 seconds stimulation with thrombin and CRP-XL.

Human platelets were incubated with vehicle (containing DMSO, 0.1 % v/v) prior to their stimulation with thrombin (1 U/ml) and CRP-XL (3 μg/ml). Aggregation was measured as a change in light transmission and monitored for 300 seconds at 37 ^{o}C under constant stirring (1,200 rpm). Representative aggregation traces of platelets stimulated with **a)** Thrombin and **b)** CRP-XL.

4.4 Quantifying the rate of fibrinogen binding by flow cytometric real time assay in response to thrombin or CRP-XL

Previous reports have indicated that fibrinogen binding to integrin $\alpha_{IIb}\beta_3$ on activated platelets causes β_3 clustering (Shattil and Newman, 2004; Goggs and Poole, 2012). Here, real-time flow cytometric analysis of fibrinogen binding was studied in order to further confirm whether β_3 clustering is dependent of fibrinogen binding overtime **(section 4.4)**.

Fibrinogen binding to human platelets was measured by diluting PRP in HEPES, followed by FITC labelled anti-fibrinogen antibody. Samples were transferred to a 96-well plate, analysed by an Accuri C6 flow cytometry at 37 °C. During data acquisition, platelets were stimulated by similar concentrations of thrombin (1 U/ml) in the presence of (GPRP 25 mg/ml) and CRP-XL (3 μg/ml) that were used in STORM imaging were applied here. Agonists were added for 300 seconds.

Real-time flow cytometric analysis of the rates of fibrinogen binding confirmed in response to the GPVI-specific agonist CRP-XL and thrombin over 300 seconds of stimulation in vehicle treated samples. Fibrinogen binding to β_3 rate increases smoothly upon activation **(Figure 4.9)**. Surprisingly, the level of fibrinogen binding did not correspond with β_3 clustering pattern. The patterns of fibrinogen binding and β_3 clustering in response to CRP-XL and thrombin are not match. Therefore, integrin β_3 clustering is in part independent of fibrinogen binding.

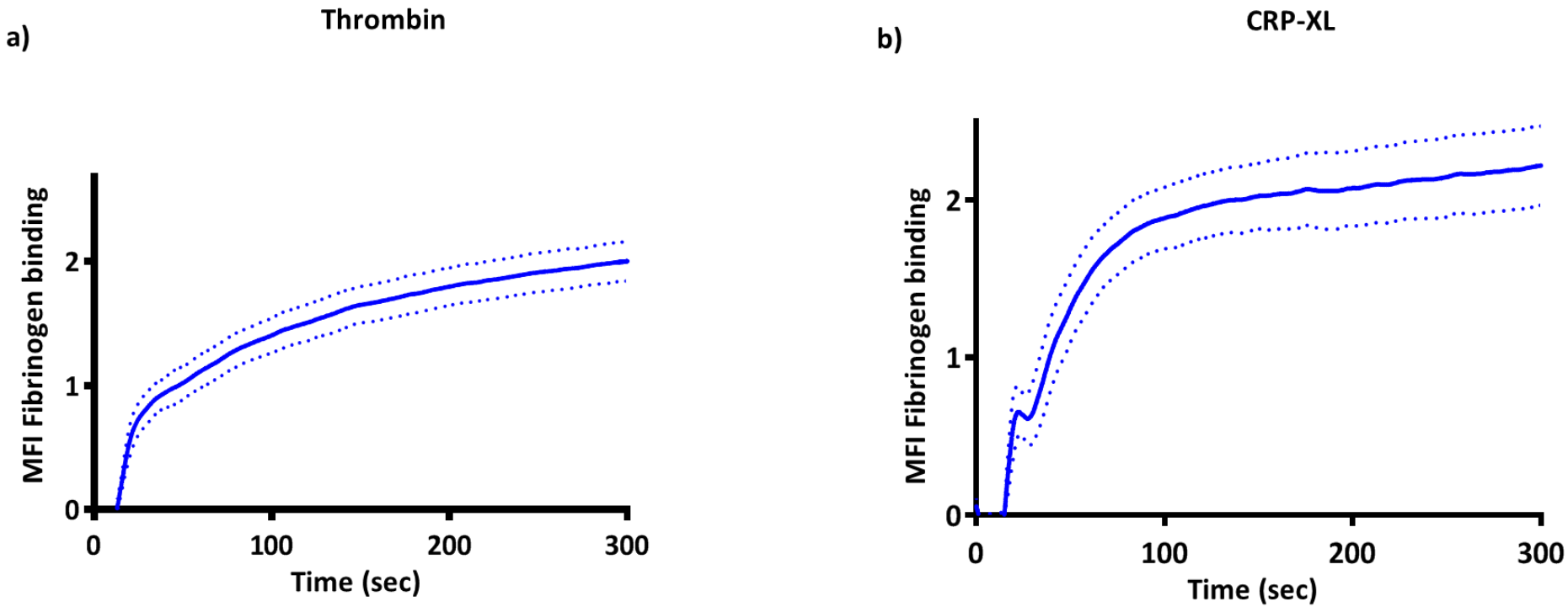

Figure 4.9 Real time flow cytometry of fibrinogen binding induced by thrombin or CRP-XL.

PRP were pre-treated with (0.1 %) DMSO and FITC labelled anti fibrinogen antibody. Platelets were stimulated with (1 U/ml) thrombin (in the presence of GPRP 25 mg/ml) or CRP-XL (3 μg/ml) during data acquisition. Samples were analysed using Accuri C6 flow cytometry.

4.5 β_3, Src and Syk phosphorylation in thrombin and CRP-XL aggregated platelets

Earlier studies reported that signalling downstream of β_3 is a consequence of integrin β_3 clustering (Postel et al., 2013). To test this, we will investigate whether β_3 downstream signalling followed the same biphasic pattern in β_3 clustering.

SFKs play a vital role to initiate and propagate signals from integrin $\alpha_{IIb}\beta_3$ and exist in an association with the β_3 domain. In resting platelets, SFKs are maintained in an inactive state by Csk, which form a complex with Src and β_3. Src undergoes auto-phosphorylation at pY418, which subsequently phosphorylates the β_3 subunit. The phosphorylated form of β_3 provides a docking site for adaptor proteins, cytoskeleton proteins (actinin), tyrosine kinases (Syk and FAK), lipid kinases (PI3K) and guanine nucleotide exchange factors. Each of these molecules ultimately participates in the initiation of outside-in signalling that facilitates spreading, secretion, stable adhesion and clot retraction (Shattil et al., 1998; Li et al., 2010; Senis et al., 2014).

Washed platelets ($4x10^8$ cell/ml) under aggregation conditions were stimulated with thrombin (1 U/ml) or CRP-XL (3 μg/ml) for 0, 30, 60, 90, 150, 300 seconds. For the sake of consistency the same concentrations of thrombin and CRP-XL used in STORM imaging of stimulated platelets were applied in the present signalling studies.

Levels of β_3, Src and Syk phosphorylation was elevated with increase in stimulation time. Following 30 - 60 seconds stimulation, it was observed early jump in the phosphorylation β_3, Src and Syk in response to thrombin and CRP-XL overtime **(Figure 4.10 and Figure 4.11)**.

Significant increase was seen in β_3 phosphorylation (Y773) at 150- and 300-seconds thrombin stimulated platelets when compared to 0 second. Remarkably, this finding is comparable with the observed β_3 clustering level in second phase time points, but not early time points **(Figure 4.2)**. Similar time dependent phosphorylation was also observed in Auto-phosphorylation of Src at Tyr418 and Syk (525/526). However, significant increase in the phosphorylation levels of both proteins were achieved at 30, 60, 90, 150, 300 seconds **(Figure 4.10)**.

Likewise, stimulation with 3 μg/ml of CRP-XL caused time dependent phosphorylation of β_3 at Y773. No significant differences in phosphorylation levels were observed at 0, 30, 60, 90 seconds compared to 0 second. However, Substantial increase was observed at 150- and 300 seconds in response to CRP-XL in comparison with 0 second **(Figure 4.11)**. CRP-XL-mediated tyrosine phosphorylation of Src at Tyr418 and Syk at 525/526 had a significant increase at 30, 60, 90, 150 and 300 seconds. We conclude that downstream signalling of β_3 is in part independent of β_3 clustering. Therefore, the current dogma is at least partially an over simplification of the physiological reality.

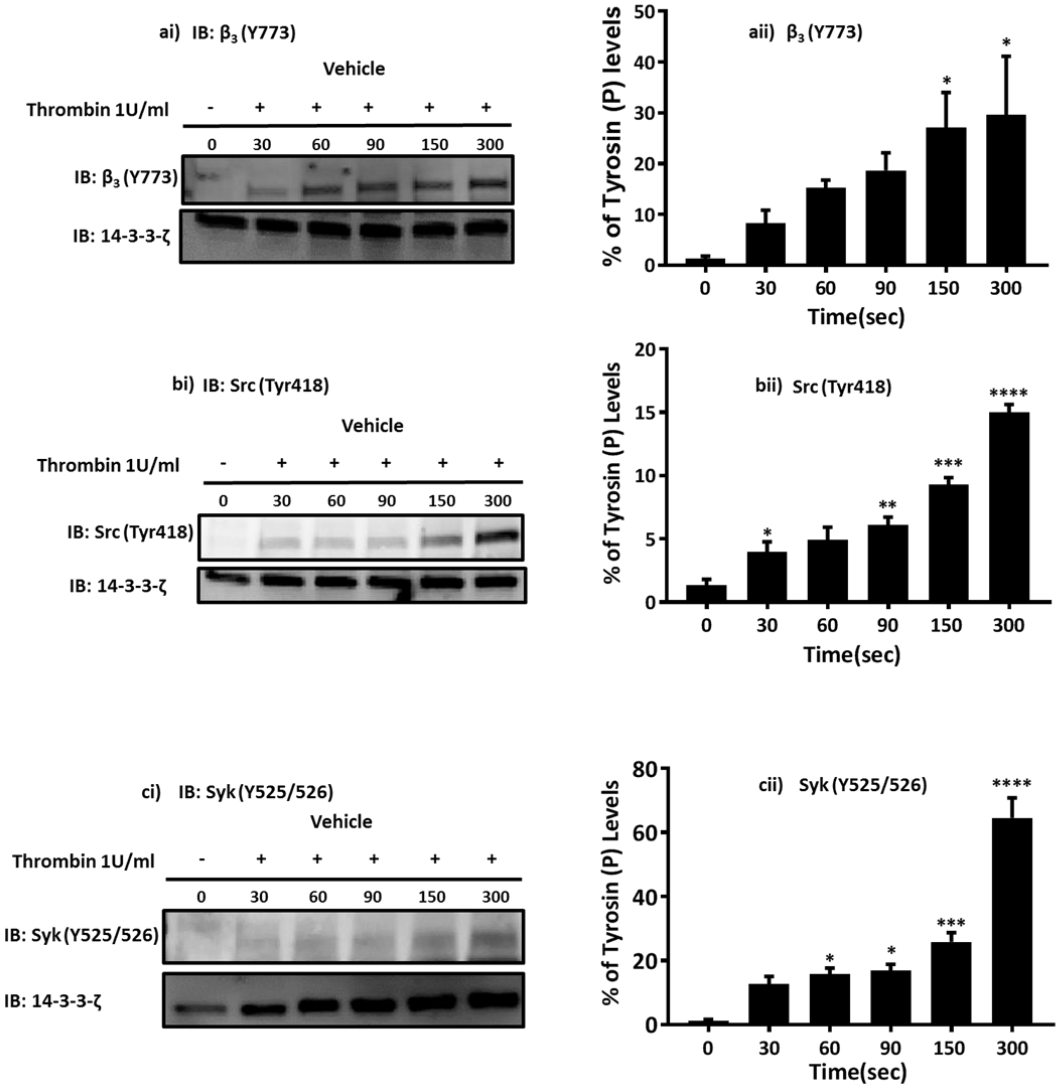

Figure 4.10 Phosphorylation patterns of β_3, Src and Syk in thrombin aggregated platelets.

Washed and vehicle control treated platelets were stimulated with thrombin (1 U/mL), the stimulation times for thrombin were 30, 60, 90, 150 and 300 seconds. Reactions were stopped by adding the Laemmli buffer and then lysates were analysed for tyrosine phosphorylation by western blotting using monoclonal anti-phospho β_3, Src and Syk. Equal loading of samples was confirmed by probing the samples with 14-3-3-ζ as a loading control. Bars represent β_3, Src and Syk phosphorylation levels normalised to loading control. Results are mean ± SEM (n = 3), *P ≤ 0.05, **P ≤ 0.01, ***P ≤ 0.001 and ****P ≤ 0.0001 was calculated by one-way ANOVA.

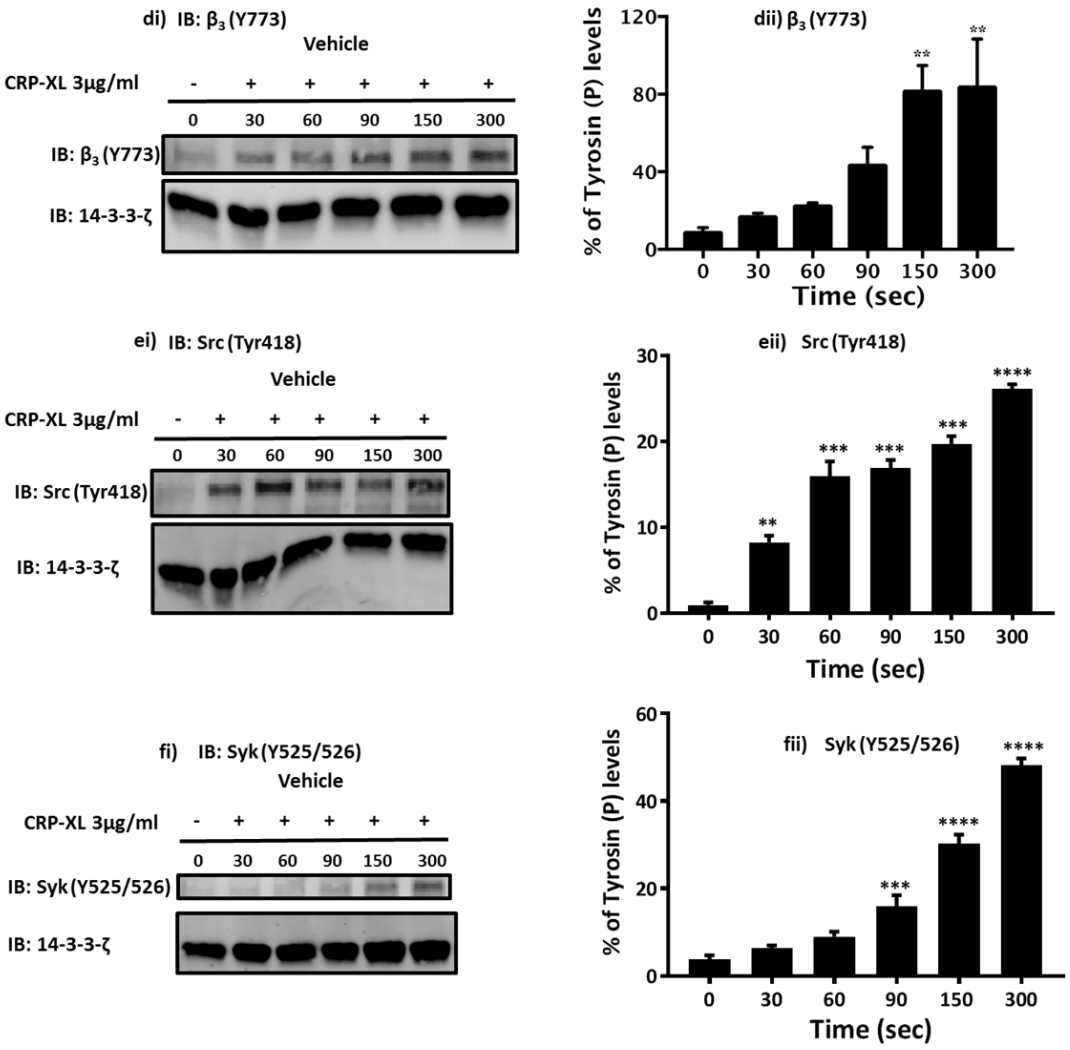

Figure 4.11 Phosphorylation patterns of β_3, Src and Syk in CRP-XL aggregated platelets.

(3 µg/ml) CRP-XL was used to stimulate vehicle control treated platelets at 30, 60, 90, 150 and 300 seconds. Laemmli buffer was used to stop and lyse the samples. Lysates were then separated on SDS-PAGE and immunoblotted for phospho β_3, Src and Syk. To control for protein loading, blots were re-probed with 14-3-3-ζ as a loading control. Bars represent β_3, Src and Syk phosphorylation levels normalised to loading control. Results are mean ± SEM (n = 3), *P ≤ 0.05, **P ≤ 0.01, ***P ≤ 0.001 and ****P ≤ 0.0001 was calculated by one-way ANOVA.

4.6 Discussion

Platelets undergo adhesion and aggregation to the vessels wall and hence the affinity of their surface expressed adhesive integrins to extracellular and matrix ligands should be closely monitored and controlled to appropriate sites of injury (Miranti and Brugge, 2002). Platelet and leukocyte integrins are the most explored and characterised pathways when it comes to integrin activation. However, integrin activation is widely spread process in many cell types playing pivotal roles in cellular migration, tissue formation and matrix remodelling (Calderwood, 2004).

In the vasculature platelets circulate freely in resting state and upon injury they must undergo sequential activation in well controlled and coordinated mechanisms. In fact, any disturbance in such control can lead to pathological conditions such as bleeding or thrombotic disorders and possibly blockage of blood supply to affected organs. Among controlled processes is the conversion of integrin $\alpha_{IIb}\beta_3$ from low to high affinity binding state and thereby allowing its ligand interaction and subsequent platelet aggregation in an activation process referred to as inside-out signalling. Several agonists are capable of generating such signals. A number of platelet receptors, such as the thrombin receptors, are able to generate inside-out signalling. Conversely, several of the mechanisms triggered by the integrin engagement, known as outside-in signalling, are now well studied and characterised. Following fibrinogen integrin binding, a complex cascade of intracellular signalling is evoked in a coordinated manner (Brass et al., 1997; Harburger and Calderwood, 2009; Bledzka et al., 2013). Exploring and investigating the nature of the outside-in signalling mediated by $\alpha_{IIb}\beta_3$ have provided significant understandings into integrin signalling and a better insight into mechanisms underlying the irreversible phase of platelet aggregation.

The pattern of integrin β_3 clustering was opposite to kindlin-3 - β_3 level in the first 30 seconds in thrombin and CRP-XL stimulated platelets in presence of vehicle. This pattern was evident in all individuals although the timing of the peaks and troughs did vary between individuals. Following 30 seconds agonist stimulation, integrin β_3 clustering and kindlin-3 - β_3 co-clustering changed overtime and shares a biphasic pattern. It is interesting to note that kindlin-3 associated with β_3 in unstimulated platelets, a situation not compatible with previous findings Malinin et al. (2010). However, such finding was not concluded with STORM microscopy, as employed approach in our project. Although our finding was not anticipated in resting platelets, we suggest that there is a basal level of interaction between Kindlin-3 and β_3 in the resting state, possibly to keep this protein in close proximity and available for recruiting and binding other effector proteins and kinases when the platelet is stimulated.

In response to thrombin or CRP-XL, platelets aggregated normally and smoothly. This finding indicates that platelets aggregation over 5 minutes was not attributable to β_3 clustering pattern.

Real-time fibrinogen binding also steadily increased over the time of stimulation with CRP-XL and thrombin. Although the literature states that β_3-β_3 clustering is driven by fibrinogen binding (Shattil et al., 2010; Fong et al., 2016). This cannot be the whole story because the pattern of fibrinogen binding steadily increased and was not comparable with the biphasic pattern of β_3 clustering.

Levels of tyrosine phosphorylation of β_3 along with Src and Syk over different time points mediated by thrombin and CRP-XL were also investigated. Early increase was noted in β_3, Src and Syk phosphorylation. Significant level of β_3, Src and Syk phosphorylation were observed at last stage of agonist stimulation. This indicate that β_3

signalling occur at late time of agonists stimulation. Also, a clear correlation between β_3 clustering and signalling was not observed.

In summary, our data provides compelling evidence that platelet aggregation along with fibrinogen binding are not affected by β_3-β_3 clustering. Moreover, levels of β_3, Src and Syk was increased significantly at late stages of stimulation and may correspond with second peak of β_3 clustering, although changes in signalling did not follow the same biphasic pattern as clustering and kindlin engagement.

In the next chapter, platelet functions were examined by targeting ILK activitiy and function in the presence of ILK inhibitor (Cpd-22) and studying the consequent effects on β_3 clustering and its association with kindlin-3 along with activatory events downstream of activated integrin β_3.

5 Screening the optimal condition of Cpd-22 and its effect on platelet function

5.1 Introduction

The primary role of platelets is their ability to aggregate at the injured vessel, preventing blood loss by forming a fibrin clot. Platelet function also play a pivotal role in haemostasis and thrombosis (Gibbins, 2004; Bledzka et al., 2013). Following vascular injury, platelets are exposed to sub endothelial matrix protein especially collagen through GPIb-V-XI and VWF. This association with collagen is mediated by its receptor integrin $\alpha_2\beta_1$ and GPVI resulting in tyrosine phosphorylation of the FcRγ-chain and promotes intracellular signalling pathways, forming PLCγ2 phosphorylation and calcium mobilization (Watson et al., 2005).

Moreover, at the site of injury, platelets exposed to thrombin which is generated from coagulation pathway, stimulates platelet signalling via the protease-activated receptors (PAR4 and PAR1 in human) (PAR3 in mouse) (Kahn et al., 1999; Nieswandt and Watson, 2003; Gibbins, 2004). During the next stage of platelet activation, platelets rely on integrin $\alpha_{IIb}\beta_3$ which represents the critical step of platelet aggregation via interaction between the adjacent platelets by several mediators, resulting in platelet aggregation (Offermanns, 2006). Integrin $\alpha_{IIb}\beta_3$ normally exist in a quiescent state (low affinity). Upon platelet activation of integrin $\alpha_{IIb}\beta_3$, it transforms to a high affinity state resulting in fibrinogen binding (inside-out signalling). Following this, β_3 clustering is initiated, subsequently, $\alpha_{IIb}\beta_3$ enables sustained thrombus growth via downstream signalling of kinases in a pathway known as outside-in signalling (Giancotti and Ruoslahti, 1999; Hantgan et al., 2003; Rivera et al., 2009; Bledzka et al., 2013)

Integrin $\alpha_{IIb}\beta_3$ activation occur via different agonists such as collagen, thromboxane A_2, thrombin and ADP. They act by binding to their receptors and introduce intracellular signalling leading to increase calcium mobilisation, platelet aggregation and ultimately

thrombus formation (Offermanns, 2006). Moreover, researchers have demonstrated that Integrin $\alpha_{IIb}\beta_3$ activation is triggered by intracellular proteins known as kindlin and talin. Kindlin is a major factor that play an essential role in supporting integrin $\alpha_{IIb}\beta_3$ via interaction with cytoplasmic tail of β_3 (Malinin et al., 2010; Ye et al., 2011). However, the mechanism of action is unclear (Xu et al., 2014). Lack of kindlin-3 leads to impaired integrin activation causing type III leukocyte adhesion deficiency (LAD-III) (Mory et al., 2008; Svensson et al., 2009; Rognoni et al., 2016).

ILK molecule was identified as scaffold protein. Reports suggest that binding of ILK molecule with kindlin recruits and activates kindlin, mediating integrin activation (Honda et al., 2013). Several studies on C. elegans confirmed that the ILK- kindlin interaction enables a conformational change of kindlin that leads to binding to the cytoplasmic tail of integrin β_3 (Qadota et al., 2012). Also, Structural and biochemical studies revealed that the association of ILK with kindlin is crucial for integrin activation (Kadry et al., 2018). This opens up the possibility of using an ILK inhibitor to modulate the binding of kindlin to β_3.

ILK exists in variety of tissues such as heart, kidney, liver and platelets. ILK has been shown to act as an effector molecule that interact with cytoplasmic tail of β_3 subunit (Hannigan et al., 1996; Stevens et al., 2004). ILK is composed of three distinct protein domains: ankyrin-repeats located in the N-terminus, a putative kinase domain at C-terminus and central PH-like domain, which facilitates binding to PIP3. ILK forms a ternary complex of other proteins such as pinch and parvin. The ankyrin-repeat of ILK can bind to Pinch-1 and Pinch-2 (particularly interesting new cysteine–histidine protein). The kinase domain binds to parvin (Widmaier et al., 2012).

Lack of ILK in mice platelets showed impaired cell adhesion, spreading and proliferation, indicating that ILK plays a pivotal role in outside-in signalling (Sakai et al., 2003; Grashoff et al., 2003). Furthermore, ablation of ILK in platelets leads to impaired platelet functions such as fibrinogen binding to Integrin $\alpha_{IIb}\beta_3$, aggregation and degranulation (Tucker et al., 2008; Honda et al., 2013).

(N-Methyl-3-(1-(4-(piperazin-1-yl) phenyl)-5-(4′-(trifluoromethyl) [1, 1′-biphenyl]-4-yl)-1H-pyrazol-3-yl) propanamide (22) (Cpd-22) is a recently identified ILK inhibitor in various cell lines, yet has not been studied in platelets. This inhibitor has been reported and established as a novel and selective inhibitor of ILK activity during library screening of several compounds that positively yielded Cpd-22 with an (IC50, 0.6 μM). However, higher levels of IC50 was reported in breast cancer cell lines (1-2.5 μM) (Lee et al., 2011).

Cpd-22 was chosen in the present thesis as an approach to study the impact of ILK inhibition on the association of kindlin-3 with β_3, the effect of this on the kinetics of β_3 clustering and the effect of ILK inhibition on various platelet functional and signalling studies. The aim of this chapter is to set up the optimal experimental conditions of Cpd-22 treatment in platelets using various platelet assays.

5.2 Defining the optimal concentration and incubation time for which platelets need to be treated with Cpd-22 in fibrinogen binding and alpha granules secretion tests

Given the lack of reports on the use of Cpd-22 in platelets, we first sought to test it in regard of incubation time and optimal concentration needed to attain its inhibitory effect on ILK in platelets.

To find an appropriate incubation time of Cpd-22 treated platelets, platelet fibrinogen binding was assessed in samples treated with vehicle (0.1 % DMSO) or Cpd-22 in a range of incubation periods (5, 10, 15, 30 and 60 minutes). Anti-human fibrinogen antibody (FITC labelled) was used to detect fibrinogen bound to platelets. The platelets were stimulated for 20 minutes with CRP-XL (1 μg/ml), then fixed with 0.2 % (v/v) formyl saline. Median fluorescence of 10,000 platelets was analysed.

Substantial inhibition was observed (approximately 93 to 95 %) at 30 and 60 minutes, respectively compared to vehicle control (0.1 % DMSO). On the other hand, 5- and 10-minutes incubation of Cpd-22 were not enough to achieve an inhibitory effect on ILK as no reduction was seen in their respective fibrinogen binding levels **(Figure 5.1)**. We therefore decided to choose 30 minutes to incubate Cpd-22 with platelets for further experiments.

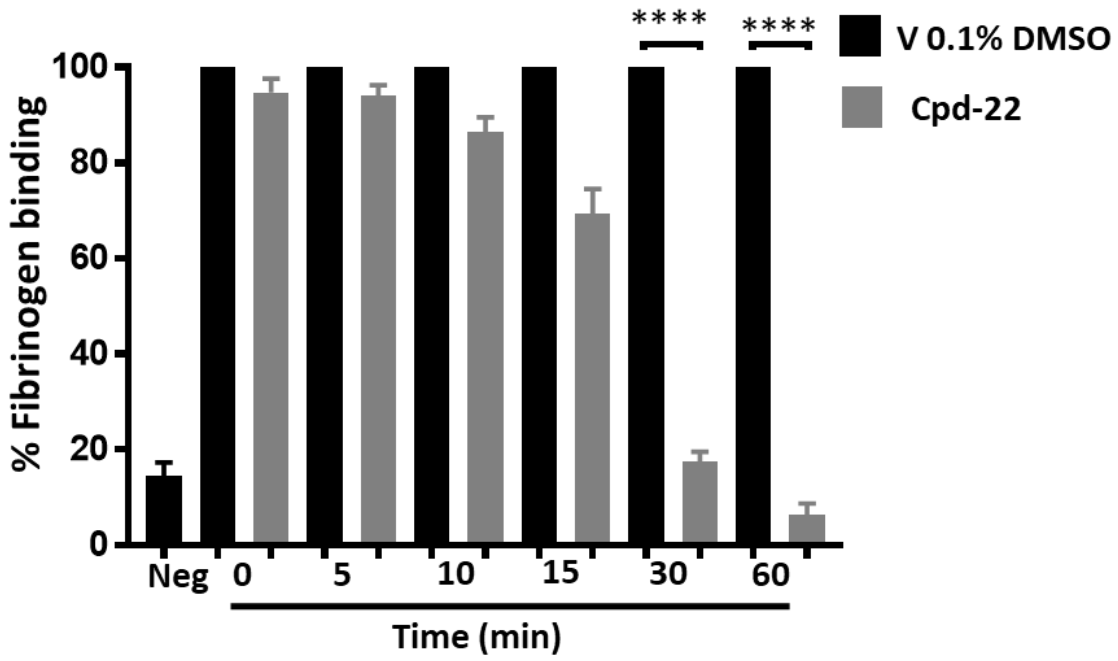

Figure 5.1 Fibrinogen binding mediated by CRP-XL is inhibited by Cpd-22.

Human PRP was treated with 10 μM Cpd-22 at 37 °C for 0, 5, 10, 15, 30 and 60 minutes, followed by stimulation with CRP-XL (1 μg/ml) for 20 minutes. Reactions were stopped after 20 minutes by 0.2 % formyl saline and analysed by flow cytometry. Fibrinogen binding to activated $\alpha_{IIb}\beta_3$ on platelets from human PRP was measured by anti-human fibrinogen antibody to the platelets. Resting platelets incubated with FITC labelled anti-human fibrinogen antibody used as negative control. The level of fibrinogen binding was set as 100 %. Results were recorded as the Mean ± SEM of the median fluorescence intensities (MFI) ($n \geq 3$). Data were analysed by t-test ****$P \leq 0.0001$.

Moreover, after determining the incubation time in which platelets can be inhibited, a set of serial concentration of Cpd-22 was studied to determine the concentration of Cpd-22 that maximally inhibit ILK activity in platelets in fibrinogen binding assay. Platelets treated with (0.01, 0.03, 0.1, 0.3, 1, 3 and 10 μM) Cpd-22 at 37 °C for 30 minutes. The range of concentrations was selected based on the previous studies in prostate and breast cancer cell lines (Lee et al., 2011). Anti-human fibrinogen antibody (FITC labelled) was used to detect fibrinogen bound platelets. Samples were then stimulated with (0.01, 0.03, 0.1, 0.3 and 1 μg/ml) CRP-XL in a dose response curve or (0.03, 0.1, 0.3, 1 and 3 U/ml) thrombin. The reaction was stopped with 0.2 % formal saline. The levels of fibrinogen binding were measured.

Treatment with 3 and 10 μM Cpd-22 inhibited the level of fibrinogen binding by 80 % and 90 % after stimulation with CRP-XL and thrombin, respectively in comparison with (0.1 % DMSO) vehicle control **(Figure 5.2 and Figure 5.3)**.

The data presented in **Figure 5.2 and Figure 5.3** display significant reduction in fibrinogen binding by both 0.3, 1, 3 and 10 μM concentrations of Cpd-22. These inhibitions were observed at all concentration of platelet agonist. The IC50 values were calculated for the inhibition of fibrinogen binding by Cpd-22 in response to thrombin and CRP-XL **(Figure 5.2 and Figure 5.3)**. The IC50 value was (0.8-2 μM) corresponding with previous studies in breast cancer cell lines (Lee et al., 2011).

ai)

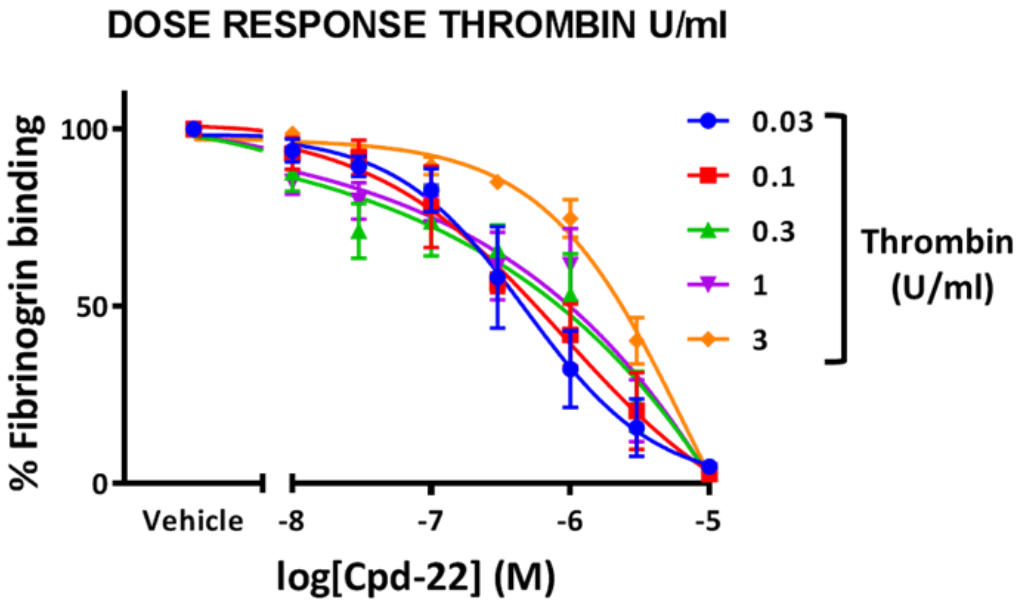

aii)

Thrombin (U/ml)	Cpd-22(µM)							
		0.01	0.03	0.1	0.3	1	3	10
	0.03					*	**	***
	0.1				*	**	***	****
	0.3					*	***	****
	1						***	****
	3				*	*	****	****

aiii)

Thrombin (U/ml)	IC50 (M)
0.03	$6.3x10^{-7}$
0.1	$1x10^{-6}$
0.3	$6.3x10^{-6}$
1	$3.9x10^{-6}$
3	$2.5x10^{-6}$

Figure 5.2 Cpd-22 inhibits fibrinogen binding induced by thrombin.

Vehicle containing controls or Cpd-22(0.01, 0.03, 0.1, 0.3, 1, 3 and 10 μM) pre-treated PRP was stimulated for 20 minutes with sets of concentration of **ai)** thrombin (3, 1, 0.3, 0.1 and 0.03 U/ml) in presence of anti-human fibrinogen antibody (FITC labelled) or isotype control. 0.2 % formyl saline was then used to stop the reactions and flow cytometry was used to analyse the samples. **aii)** Significant inhibition points. **aiii)** Four parameter nonlinear regression curves were utilised to calculate the IC50 of Cpd-22 in the inhibition of fibrinogen binding The level of fibrinogen binding was set as 100 % in the presence of vehicle control (DMSO 0.1 % v/v). The results represent the mean of ± SEM median fluorescence intensities (n = 5) and analysed by one-way ANOVA *P ≤ 0.05, **P ≤ 0.01, ***P ≤ 0.001 and ****P ≤ 0.0001.

ai)

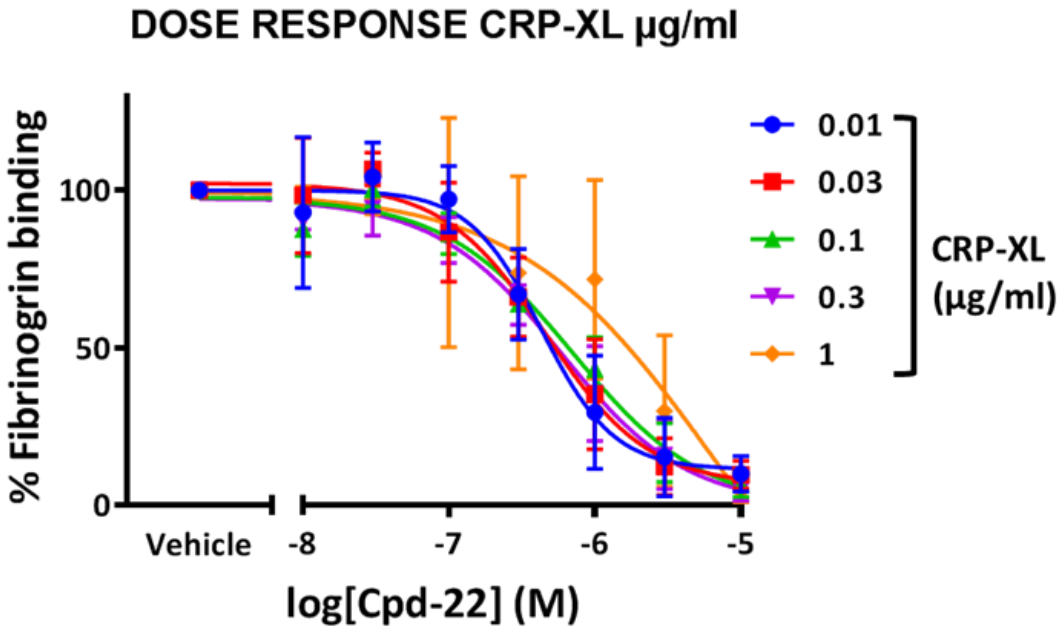

aii)

CRP-XL (µg/ml)	Cpd-22(µM)							
		0.01	0.03	0.1	0.3	1	3	10
	0.01					*	**	**
	0.03					**	***	***
	0.1				**	***	****	****
	0.3				*	***	****	****
	1						*	*

aiii)

CRP-XL (µg/ml)	IC50 (M)
0.01	$5x10^{-7}$
0.03	$5x10^{-7}$
0.1	$6.3x10^{-7}$
0.3	$6.3x10^{-7}$
1	$6.3x10^{-6}$

Figure 5.3 Cpd-22 inhibits fibrinogen binding in response to CRP-XL.

Platelets treated with (0.01, 0.03, 0.1, 0.3, 1, 3 and 10 μM) Cpd-22 or vehicle DMSO (0.1 % v/v) at 37 °C for 30 minutes. Anti-human fibrinogen antibody (FITC labelled) was used to detect fibrinogen bound platelets. Samples were then stimulated with **ai)** CRP-XL (0.01, 0.03, 0.1, 0.3 and 1 μg/ml) in a dose response curve. Reaction was stopped with 0.2 % formyl saline. **aii)** Significant inhibition points. **aiii)** significant inhibition points. Four parameter nonlinear regression curves were used to calculate the IC50 of Cpd-22 in the inhibition of fibrinogen binding. The level of fibrinogen binding was set as 100 % in the presence of vehicle control (DMSO 0.1 % v/v). The results represent the mean of ± SEM median fluorescence intensities (n = 5). Result was analysed by one-way ANOVA *P ≤ 0.05, **P ≤ 0.01, ***P ≤ 0.001 and ****P ≤ 0.0001.

A similar experimental setup was performed using a different platelet assay. P-selectin is present inside alpha-granules in resting platelets. After activation of platelets with agonists, P-selectin translocates from alpha granules to the cell surface of platelets (McEver, 2007). Previous studies have confirmed that P-selectin stabilises platelet aggregation causing large aggregation of platelets (Merten et al., 2000). Levels of P-selectin exposure were measured using a range of Cpd-22 concentrations (0.01, 0.03, 0.1, 0.3, 1, 3 and 10 μM) in addition to vehicle containing control samples.

Treatment of PRP with different concentrations of Cpd-22 or vehicle DMSO (0.1 % v/v) at 37 °C for 30 minutes were measured by diluting PRP in HEPES buffer containing PE-CY^{TM5}-labeled mouse anti-human CD62P antibody. Platelets were stimulated with (CRP- XL; 1, 0.3, 0.1, 0.03 and 0.01 μg/ml) or thrombin (3, 1, 0.3, 0.1, and 0.03 U/ml in the presence of GPRP 25 mg/ml) for 10 minutes. Reactions were then stopped by 0.2 % formyl saline and analysed by flow cytometry. The median fluorescence intensity was obtained to detect P-selectin exposure and the level of alpha granules secretion.

Alpha granules release was tested against the same concentrations of Cpd-22 stimulated with thrombin and CRP-XL. There was only significant inhibition seen in samples treated with Cpd-22 at 3 and 10 μM. Incubation of PRP with 3 and 10 μM of Cpd-22 resulted in 80 % inhibition of P-selectin exposure mediated by thrombin compared to (0.1 % DMSO) vehicle control **(Figure 5.4)**.

Samples treated with Cpd-22 (3 μM and 10 μM) inhibited significantly CRP-XL-mediated P-selectin exposure by approximately 55 % in comparison with (0.1 % DMSO) **(Figure 5.5)**.

As shown **Figure 5.4 and Figure 5.5**, our findings show significant reduction in P-selectin exposure by high (3 and 10 μM) concentrations of Cpd-22. These reductions

were observed at (0.03, 0.1 and 1 U/ml thrombin stimulation) or (0.01, 0.03, 0.1 and 0.3 μg/ml CRP-XL), but not the highest concentration of either agonist. The IC50 were measured for the reduction of P-selectin exposure by Cpd-22 in response to thrombin and CRP-XL. It was observed less potent in comparison with the IC50 data of fibrinogen binding.

Collectively, these data were not comparable to the reduction in fibrinogen binding in thrombin or CRP-XL stimulated samples in the presence of Cpd-22. Inhibition of fibrinogen binding by Cpd-22 in response to thrombin or CRP-XL **(Figure 5.2 and Figure 5.3)** was more potent in comparison with the inhibition of alpha-granule secretion.

ai)

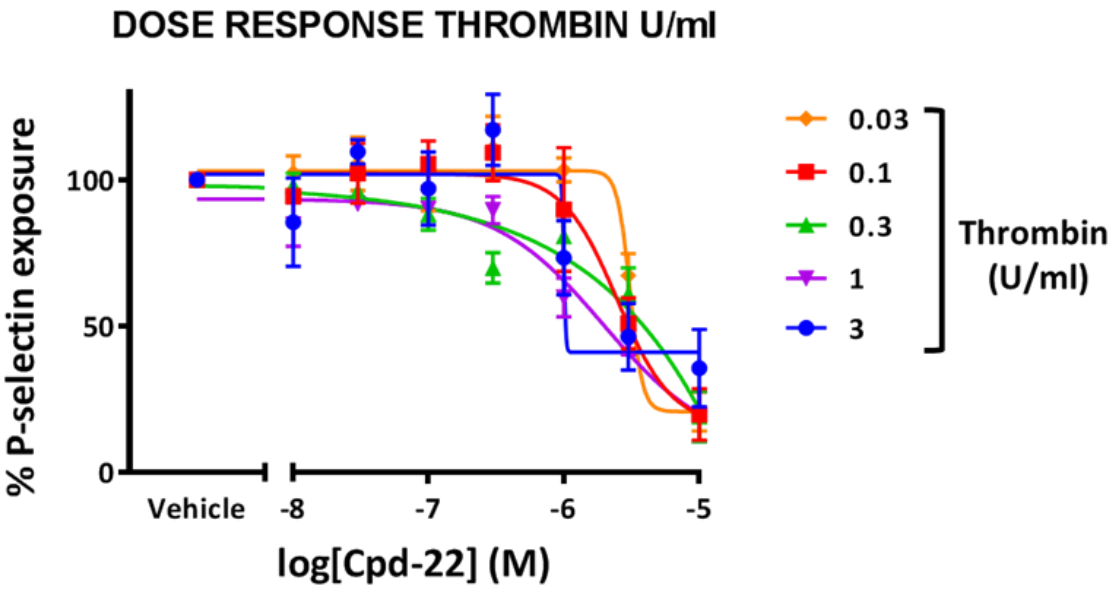

aii)

Thrombin (U/ml)	Cpd-22(µM)							
		0.01	0.03	0.1	0.3	1	3	10
	0.03						*	**
	0.1						*	***
	0.3							**
	1						*	****
	3							

aiii)

Thrombin (U/ml)	IC50 (M)
0.03	$1.2x10^{-6}$
0.1	$2.5x10^{-6}$
0.3	$6.3x10^{-6}$
1	$1.9x10^{-6}$
3	$3.1x10^{-6}$

Figure 5.4 Cpd-22 down regulates P-selectin exposure in response to thrombin.

P-selectin level from human PRP in the presence of Cpd-22 (0.01, 0.03, 0.1, 0.3, 1, 3 and 10 μM) was measured, incubated at at 37 °C for 30 minutes. Platelets were stimulated with **ai)** thrombin (3, 1, 0.3, 0.1 and 0.03 U/mL). Reactions were then stopped after 20 minutes by 0.2 % formyl saline and analysed by flow cytometry. **aii)** Significant inhibition points. **aiii)** Four parameter nonlinear regression curves were used to calculate the IC50 of Cpd-22 in the inhibition of P-selectin exposure. 100 % of P-selectin exposure was defined in the presence of 0.1 % DMSO vehicle control. The results represent the mean of ± SEM median fluorescence intensities (n = 5) and analysed by one-way ANOVA, *P ≤ 0.05, **P ≤ 0.01, ***P ≤ 0.001 and ****P ≤ 0.0001.

ai)

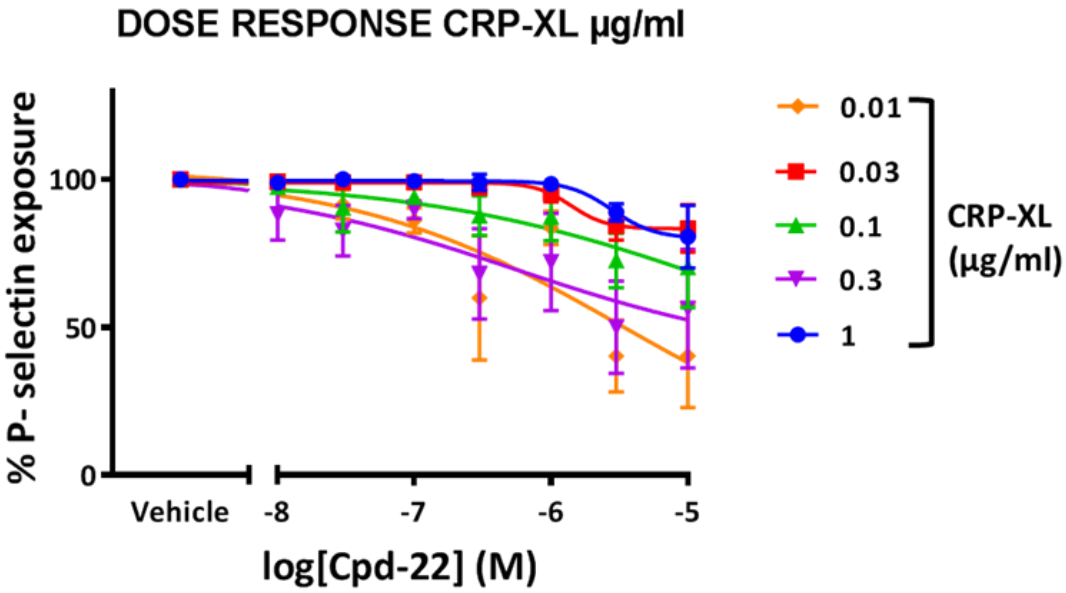

aii)

CRP-XL (µg/ml)	Cpd-22(µM)							
		0.01	0.03	0.1	0.3	1	3	10
	0.01						***	****
	0.03						*	*
	0.1						*	**
	0.3						*	*
	1							

aiii)

CRP-XL (µg/ml)	IC50 (M)
0.01	3.1×10^{-6}
0.03	1.5×10^{-6}
0.1	7.9×10^{-6}
0.3	1.9×10^{-6}
1	7.9×10^{-7}

Figure 5.5 Cpd-22 inhibits P-selectin exposure evoked by CRP-XL.

PRP was pre-treated with different concentration of Cpd-22 or vehicle DMSO (0.1 % v/v) at 37 °C for 30 minutes. Samples were measured by diluting PRP in HEPES buffer containing PE-CY^{TM}5-labeled mouse anti-human CD62P antibody. Platelets were stimulated with **ai)** (CRP- XL; 1, 0.3, 0.1, 0.03 and 0.01 μg/ml) for 20 minutes. Reactions were then stopped by 0.2 % formal saline and analysed by flow cytometry. **aii)** Significant inhibition points. **aiii)** Four parameter nonlinear regression curves were used to calculate the IC50 of Cpd-22 in the inhibition of P-selectin exposure. 100 % of P-selectin exposure was defined in the presence of 0.1 % DMSO vehicle control. The results represent the mean of ± SEM median fluorescence intensities (n = 5) and analysed by one-way ANOVA *P ≤ 0.05, **P ≤ 0.01, ***P ≤ 0.001 and ****P ≤ 0.0001.

5.3 Role of Cpd-22 in platelet aggregation

To further confirm the inhibitory effect of Cpd-22, platelet aggregation in the presence of Cpd-22 was measured. The impact of Cpd-22 was assessed using a variety of agonists that target different pathway of platelets activation; cross-linked collagen related peptide (CRP-XL), a selective agonist for glycoprotein VI (GPVI) (Gibbins et al., 1997) and thrombin as GPCR receptor agonist (Li et al., 2010).

5.3.1 Cpd-22 inhibits Platelet Aggregation induced by thrombin

The aim was to investigate the impact of ILK inhibition on platelet aggregation in response to thrombin using Cpd-22. Platelets rich plasma (PRP) was treated with Cpd-22 (1, 3 and 10 μM) or DMSO (0.1 % v/v) at 37 °C for 30 minutes and then stimulated with 1U/ml of thrombin in the presence (25 mg/ml of GPRP to prevent fibrin polymerization) for 5 minutes. Aggregation was performed using turbidimetric aggregometry at 37°C under stirring conditions (1,200 rpm). The concentration of the agonist was based on the concentration of agonist used in the STORM experiments**.** Platelet aggregation stimulated with thrombin was indicated by observing the difference in light transmission over 5 minutes.

Incubation of human PRP with Cpd-22, negatively regulated platelet aggregation induced by thrombin by approximately 80 % and 90 % at 3 and 10 μM, respectively, in comparison to 0.1 % DMSO vehicle control **(Figure 5.6 a, b).** 1 μM of Cpd-22 failed to induce any inhibitory effect on platelet aggregation when compared to vehicle control. This indicates that Cpd-22 has the ability to hinder platelet aggregation following thrombin stimulation and confirms our flow cytometry finding.

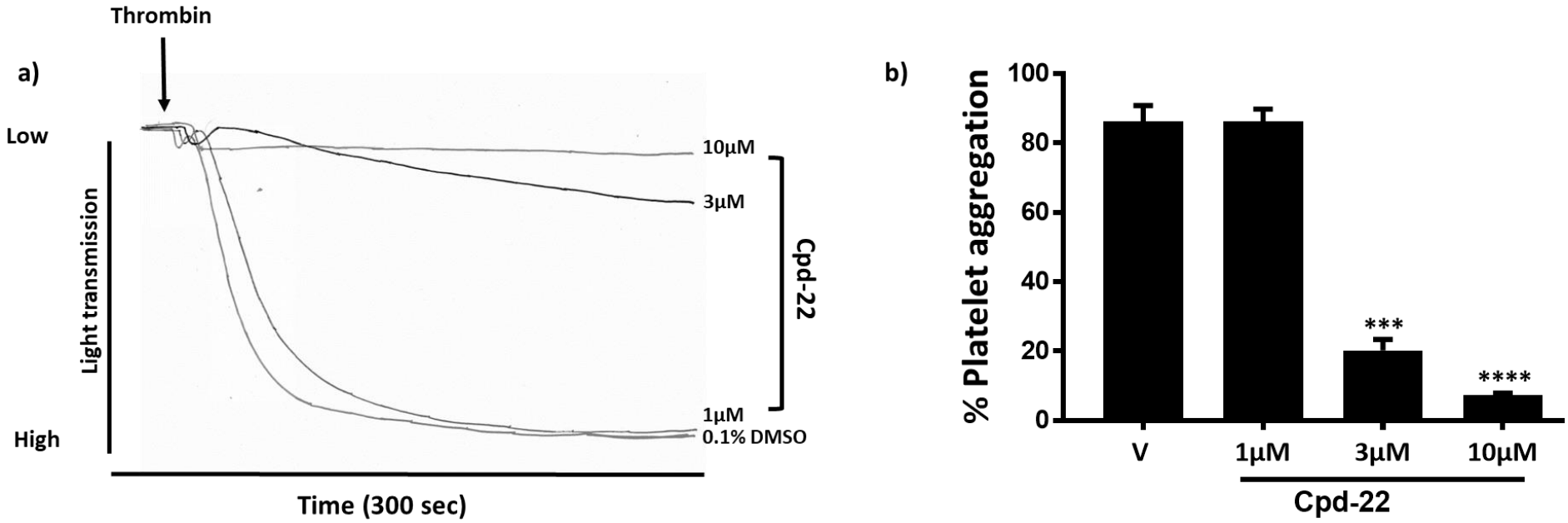

Figure 5.6 Cpd-22 inhibits Platelet Aggregation induced by thrombin

Human PRP was pre-incubated with Cpd-22 at 37 °C for 30 minutes (1, 3, 10 µM) or DMSO (0.1 % v/v) vehicle control, followed by stimulation with (1 U/ml) thrombin in the presence (25 mg/ml of GPRP). Changes in light transmission were recorded for 300 seconds. **a)** Representative aggregation traces. **b)** The percentage of aggregation was compared to DMSO (0.1 % v/v) vehicle control (V). Results demonstrate the mean (± SEM), (n = 3) and analysed by one-way ANOVA ***P ≤ 0.001 and ****P ≤ 0.0001.

5.3.2 Cpd-22 attenuates CRP-XL mediated aggregation

Having established the effect of Cpd-22 on platelet aggregation induced by thrombin (GPCR agonist). We studied the effect of Cpd-22 on the platelet aggregation induced by GPVI agonist Collagen-related peptide (CRP-XL). CRP-XL is a selective agonist for glycoprotein VI (GPVI) (Gibbins et al., 1997). We stimulated PRP with CRP-XL (3 μg/ml). The purpose of this work is to examine CRP-XL mediated platelet aggregation in the presence of Cpd-22.

To study the effects of Cpd-22 on CRP-XL stimulated platelet aggregation, human PRP was pre-incubated with (1, 3, 10 μM) Cpd-22 or DMSO (0.1 % v/v) vehicle control at 37 °C for 30 minutes, then stimulated with (3 μg/ml) CRP-XL for 5 minutes. Aggregation responses were recorded using turbidometric aggregometry at 37 °C under stirring conditions (1,200 rpm).

Treatment with (3 and 10 μM) Cpd-22 inhibited platelet aggregation by approximately 50 % and 40 % respectively, induced with CRP-XL in comparison to DMSO (0.1 % v/v) vehicle control **(Figure 5.7 a, b)**. Similar to thrombin mediated aggregation observed with 1 μM Cpd-22 treated platelets, no significant reduction was observed in CRP-XL mediated platelet aggregation following 1 μM Cpd-22 treatment.

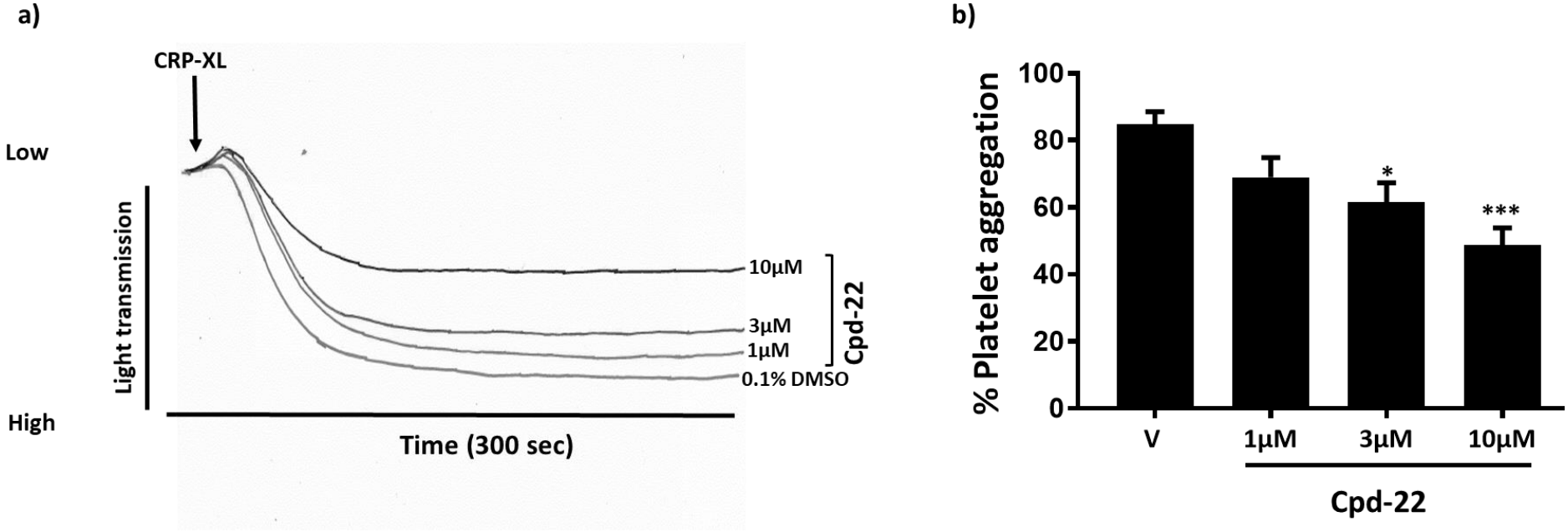

Figure 5.7 Cpd-22 attenuates CRP-XL mediated aggregation

Human PRP was pre-incubated at 37 °C for 30 minutes with (1, 3, 10 µM) Cpd-22 or 0.1 % DMSO vehicle control, then stimulated with CRP-XL. Changes in light transmission were recorded for 300 seconds. **a)** Representative aggregation traces. **b)** The percentage of aggregation was compared to 0.1 % DMSO vehicle control (V). Results demonstrate the mean (± SEM), (n = 3) and analysed by one-way ANOVA *P ≤ 0.01 and ***P ≤ 0.0001.

Taken together, the results underpin that role of ILK in the regulation of platelets aggregation induced either with thrombin (GPCR agonist) or CRP-XL (GPVI receptor agonist), agonists that follow different activatory pathways and the ability of Cpd-22 to inhibit platelet activation. Moreover, the reduction in platelet aggregation by Cpd-22 after thrombin **(Figure 5.6)** or CRP-XL activation **(Figure 5.7)** was due to upstream integrin $\alpha_{IIb}\beta_3$ activation that was down regulated by Cpd-22.

5.4 Cpd-22 does not affect different receptors

As previously mentioned, the chosen ILK inhibitor (Cpd-22) has never been employed in platelet studies. Moreover, we established negative impact of inhibition on various platelet functions. Therefore, levels of platelet receptors were evaluated as a marker of platelet function in presence or absence of Cpd-22. This evaluation will simultaneously ensure the lack of impact of Cpd-22 treatment on basal levels of platelet receptors in resting and stimulated platelets, and to examine whether Cpd-22 affects different receptors.

The expression of different receptors integrin $\alpha_2\beta_1$ **(Figure 5.8a)**, GPIb **(Figure 5.8b)**, GPVI (**Figure 5.8c)** and integrin $\alpha_{IIb}\beta_3$ **(Figure 5.8d)** was assessed in vehicle containing control (DMSO 0.1 % v/v) and Cpd-22 treated samples using fluorophore-conjugated antibodies against aforementioned receptors in resting and (1 U/ml) thrombin (in the presence of GPRP 25 mg/ml) stimulated platelets. Samples were fixed with 0.2 % formyl saline and flow cytometry was used to detect antibody bound platelets.

As shown in **Figure 5.8**, levels of platelet receptors were unaffected in resting and activated platelets by Cpd-22 treatment when compared to vehicle controls. These findings suggest that Cpd-22 neither influence receptor number or translocation upon platelet activation.

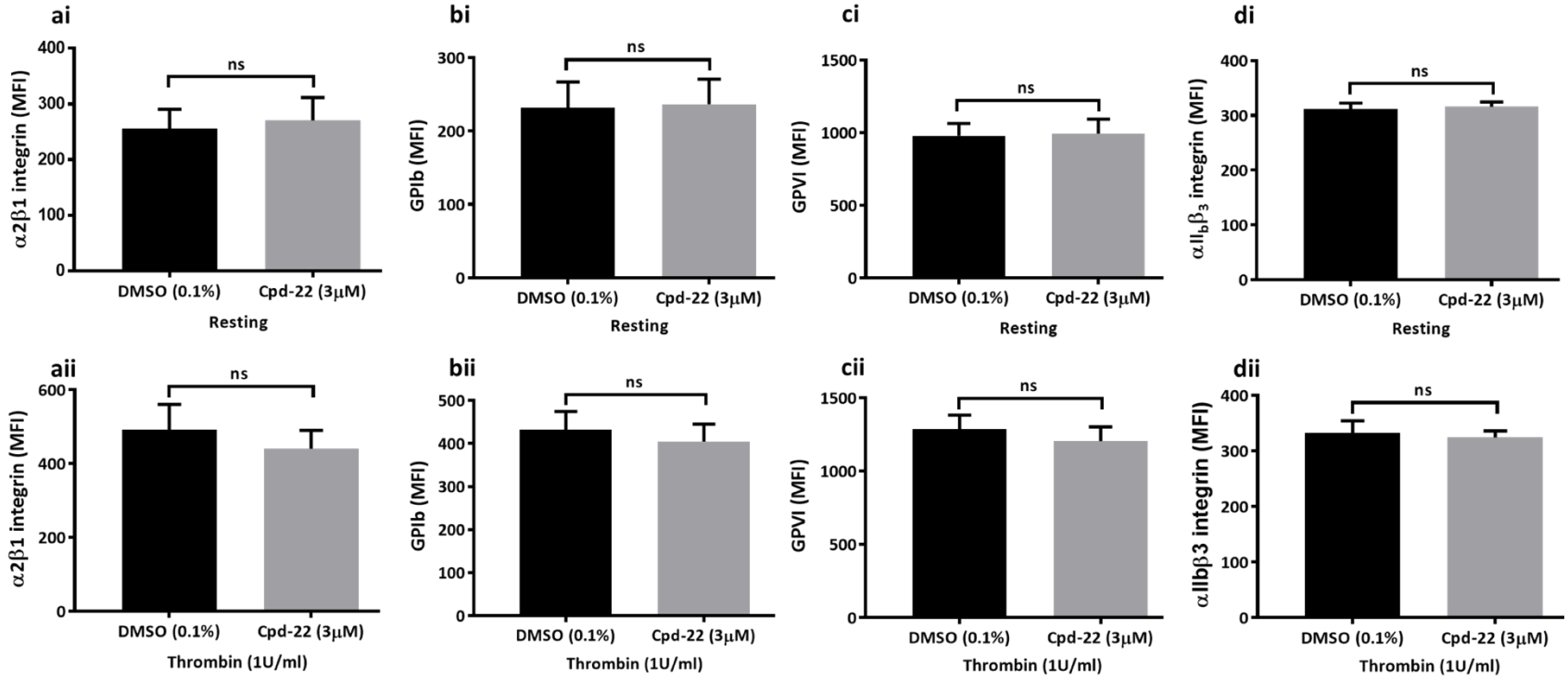

Figure 5.8 Cpd-22 does not impair receptor levels in human platelets.

The expression level of integrin $\alpha_2\beta_1$, GPIb, GPVI and integrin $\alpha_{IIb}\beta_3$ was examined on resting and activated (1 U/ml) thrombin. PRP was pre-treated with Cpd-22 (3 μM) or DMSO (0.1% v/v) at 37 °C for 30 minutes. Then, samples incubated with antibodies against antibodies **(ai)** integrin $\alpha_2\beta_1$ (FITC- labelled), **(bi)** GPIb (Cy5-labelled), **(ci)** GPVI (Cy5-labelled) and **(di)** integrin $\alpha_{IIb}\beta_3$ (FITC-labelled) for 20 minutes, followed by stimulation with (1 U/ml) thrombin (in the presence of GPRP 25 mg/ml). Cells were fixed with 0.2 % formyl saline. Results represent the mean ± SEM (n=5) of the median fluorescence intensities and analysed by t-test, *$P \leq 0.01$.

5.5 Cpd-22 selectively reduces the function of ILK

Although Cpd-22 was established as selective ILK inhibitor, these reports were conducted in different cell lines (Lee et al., 2011; Pan et al., 2014; de la Puente et al., 2015) and hence, off-target effects cannot be excluded when used in platelets. Accordingly, and prior of using the inhibitor in the following experiments, it was prudent to confirm Cpd-22 selectivity in platelets. For this purpose, a multiple inhibitors approach was employed as a method to confirm Cpd-22 selectivity. QLT0267, has been reported and established as a selective ILK inhibitor in platelets in which it down regulates platelet activity in a comparable way to the effect of Cpd-22 shown here (Jones et al., 2014). Hence, the inhibition of (1 U/ml) thrombin mediated fibrinogen binding was assessed following the treatment with vehicle control DMSO (0.1 % v/v), Cpd-22, QLT0267 and combination of them.

PRP was obtained from healthy donors and incubated with FITC-labelled anti- human Fibrinogen antibody followed by treatment with QLT0267 (1 μM) or Cpd-22 (3 μM) or and combined them at 37 °C for 30 minutes, then the PRP was also stimulated with (1 U/ml) thrombin for 20 minutes with gentle mixing in presence of 25 mg/ml GPRP. Samples were fixed with 0.2 % formyl saline and analysed by flow cytometry (10,000 events).

Incubation of platelets with Cpd-22 or QLT0267, inhibited thrombin stimulated fibrinogen binding by approximately 75 % compared with DMSO (0.1 % v/v) vehicle control. Interestingly, no further inhibition was observed in the presence of the combination of Cpd-22 or QLT0267 **(Figure 5.9)**. These data indicate Cpd-22 is a selective inhibitor for ILK activity in platelets.

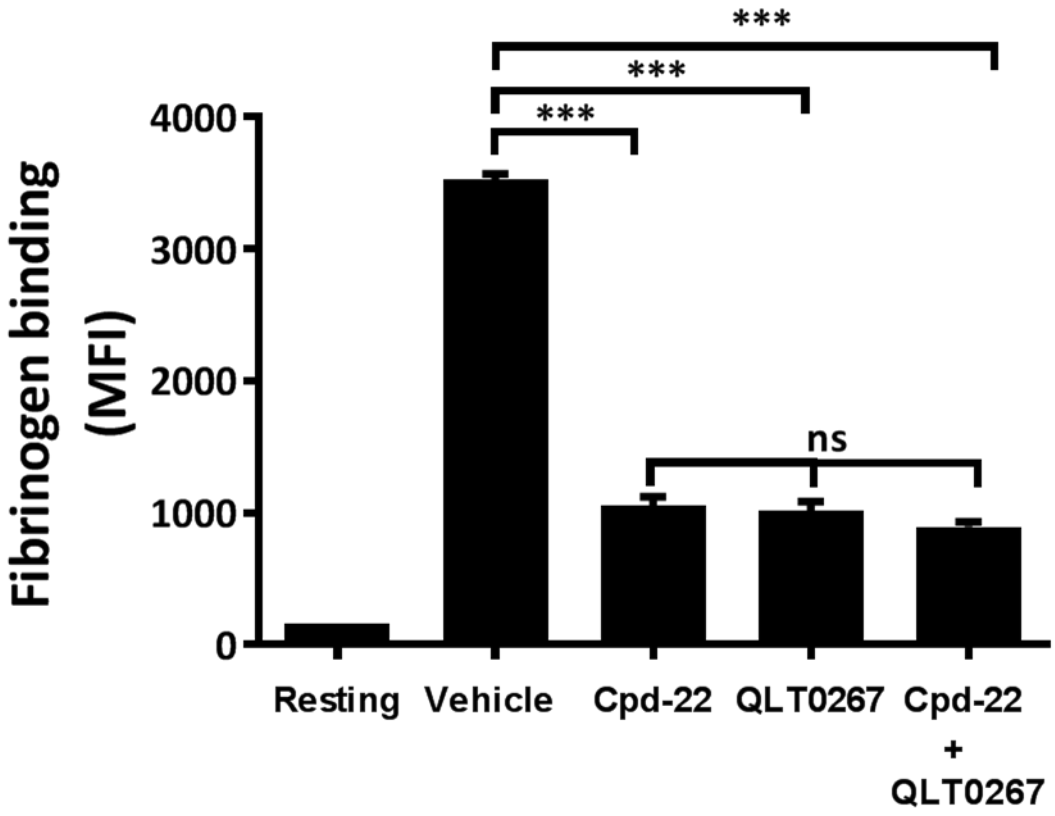

Figure 5.9 Cpd-22 selectively reduces the function of ILK.

PRP from human was pre-incubated with vehicle control DMSO (0.1 % v/v), Cpd-22 (3 μM), QLT0267 (1 μM) or combined them at 37 °C for 30 minutes for 30 minutes. Then, the samples were then treated with FITC-labelled rabbit anti-fibrinogen antibody and then stimulated with (1 U/ml) thrombin (in the presence of GPRP 25 mg/ml) for 20 minutes. The cells were fixed in 0.2 % formyl saline. The samples were examined by flow cytometry. The data were analysed with one-way ANOVA and displayed as the mean ± SEM (n = 5). ***P ≤ 0.001.

5.6 Discussion

Binding of ILK with kindlin has been shown to play a role in the regulation of platelet function and integrin activation by interacting with β_3 (Calderwood et al., 2013; Fukuda et al., 2014). ILK has been shown to act as an effector molecule and confirmed to be important for the function of platelet. Furthermore, ILK inhibition has been shown to be implicated in the reduction of platelet function including aggregation, fibrinogen binding and granule secretion (Jones et al., 2014). Most recent studies have been supported by Guan et al. (2018) who reported that kindlin-2 associates with the ILK-putative kinase domain (PKD). Impaired binding of kindlin-2 to ILK-pKD causes defects in cell spreading and signalling downstream of integrins (Kadry et al., 2018).

5.6.1 Effect of Cpd-22 on platelet functions

To examine the role of Cpd-22 in the regulation of platelet function, platelet response to CRP-XL or thrombin in the presence of Cpd-22 in a concentration-dependent manner was assessed. It was observed that (3 μM and 10 μM) of Cpd-22 following (30 minutes incubation) in response to CRP-XL or thrombin inhibits platelet function.

Firstly, it was observed that platelet aggregation was reduced by Cpd-22, suggesting that the reduction in platelet aggregation may indicate that ILK play a pivotal role in inhibiting platelet aggregation. These findings confirms previous work demonstrating ILK knockout mice and ILK deficient platelets, which showed a reduction in platelet aggregation (Tucker et al., 2008).

Since Cpd-22 affects platelet aggregation, the fibrinogen binding to integrin $\alpha_{IIb}\beta_3$ is one such early event leading to platelet aggregation. The level of fibrinogen binding to activated $\alpha_{IIb}\beta_3$ in CRP-XL or thrombin stimulated platelets was examined to investigate

the role of ILK in integrin $\alpha_{IIb}\beta_3$ activation. Cpd-22 suppresses the activation of $\alpha_{IIb}\beta_3$ to a higher affinity binding state for fibrinogen. These findings indicate that ILK modulation can cause reduction in the $\alpha_{IIb}\beta_3$ affinity. This is in agreement with previous studies reported ILK deficient mice displayed reduced abilities of fibrinogen binding (Tucker et al., 2008; Jones et al., 2014)**.** In conclusion, flow cytometric data confirms ILK has a significant role in $\alpha_{IIb}\beta_3$ activation.

P-selectin is measured as a marker of alpha granule secretion. Degranulation of platelets upon activation is an important positive feedback mechanism that ensures activation of nearby platelets in circulation and further strengthens the platelet plug formation at the site of injury. Consistent with previous studies on other ILK inhibitors (Jones et al., 2014). Incubation of platelets with Cpd-22 in response to thrombin or CRP-XL, reduced the level of P-selectin exposure on surface of platelet.

However, the inhibition of platelet alpha granules secretion by Cpd-22 was less potent compared to its inhibitory effect on the level of the reduction of fibrinogen binding, indicating that ILK is a key regulator of integrin $\alpha_{IIb}\beta_3$ activation but less important in degranulation. These data are again in agreement with earlier reports in the ILK–ablated mouse which showed reduced alpha granules secretion. This data suggests that Cpd-22 inhibition of ILK has the same effect as previously reported with other ILK inhibitors or in ILK knockout mice (Tucker et al., 2008; Jones et al., 2014).

5.6.2 Cpd-22 does not affect human platelet receptor levels and selectively inhibits ILK platelets

Several inhibitors have been reported in the literature that selectively inhibit ILK activity (Li et al., 2009; Lee et al., 2011; Jones et al., 2014). However, all of these reports were studied in different breast cancer cell lines except of the latter study that targeted ILK

function in human platelets using the small molecule inhibitor QLT0267. Due to the lack of reports on targeting platelet ILK activity with Cpd-22, it was then important to confirm such selectivity. With the aid of QLT0267, whose selectivity toward ILK was established in platelets (Jones et al., 2014), addition of Cpd-22 did not exert any further inhibition when testing the levels of fibrinogen binding to integrin $\alpha_{IIb}\beta_3$ in response to platelet stimulation and therefore confirming its ILK selectivity and excluding potential off-target effects. Additionally, pre-treatment with Cpd-22 did not affect levels of several platelet receptors in resting and stimulated platelets compared to 0.1 % DMSO control. Altogether, these findings demonstrate the selective actions of the ILK inhibitor Cpd-22 in treated platelets. This finding fits with previous studies in breast cancer cell lines, which demonstrated that Cpd-22 has ability to selectively inhibit ILK kinase activity (Lee et al., 2011). Cpd-22 selectivity can be confirmed by investigating any platelet function assay in ILK wild type and knockout mice in the presence of Cpd-22. We would expect to see inhibition in wild type not knockout, this would confirm Cpd-22 selectivity.

Briefly, the results in this chapter support a negative regulatory role for the ILK inhibitor (Cpd-22) in human platelet function. Platelet aggregation induced by a range of agonists was suppressed by Cpd-22. Cpd-22 attenuated CRP-XL- or thrombin- stimulated fibrinogen binding and P-selectin exposure.

Collectively, data in this chapter demonstrate that ILK acts as an effector molecule which activate platelets and trigger signal pathway. The effect of Cpd-22 on human platelets was selective and targeting ILK protein, as no further inhibition was observed using QLT0267 (ILK inhibitor) (Jones et al., 2014). Having characterised Cpd-22, the next chapter will examine the effect of ILK inhibition on kindlin-3 - β_3 association and how this may alter β_3-β_3 clustering and the subsequent function of integrin $\alpha_{IIb}\beta_3$.

6 Evaluation of ILK and its effect on β_3-β_3 and kindlin-3 - β_3 co clustering in human platelets

6.1 Introduction

ILK has been implicated as an important adaptor molecule that has ability to bind the β_3 integrin cytoplasmic tail. However, the exact interaction of ILK with β_3 still not clear whether it is direct or indirect (Legate et al., 2006). Studies have established that platelets deficient in ILK display a reduced ability of fibrinogen to bind activated $\alpha_{IIb}\beta_3$, impaired platelet aggregation and reduced alpha granule secretion (Hannigan et al., 1996; Friedrich et al., 2004; Tucker et al., 2008; Jones et al., 2014). It is also known that ILK binds to kindlin which promotes a conformational change of kindlin, thereby promoting its association to the cytoplasmic integrin tail and enhancing integrin clustering (Qadota et al., 2012; Ye et al., 2013).

In this chapter, to test the importance of kindlin-3 - β_3 co-clustering and whether this can be disrupted and the consequence of this disruption on β_3 clustering, we looked into action of Cpd-22 on kindlin-3 to β_3. To do this, we tested the ILK inhibitor characterised in **chapter 5,** which according to the literature should inhibit the binding of kindlin-3 with β_3 cytoplasmic tail. Therefore, this chapter will answer the following questions;

1) Does ILK inhibition reduce the association of kindlin-3 with β_3?

2) Does ILK inhibition reduce β_3 β_3 clustering?

3) Does β_3 clustering inhibition suppress fibrinogen binding?

4) What is the implication of β_3 β_3 clustering on integrin β_3 downstream signalling?

6.2 Cpd-22 downregulated thrombin or CRP-XL induced kindlin-3 - β_3 co-clustering

It has been demonstrated that ILK is a critical molecule in platelet function. However, the literature lacks any reports on how this affects integrin clustering and co-clustering with kindlin-3 at nanoscales. Using the novel method developed in chapter 3 and 4, we will use STORM microscopy to observe of β_3 clustering and its association with kindlin-3. The role of ILK in such distribution was further examined using novel cluster analysis R based method.

PRP was pre-treated with Cpd-22 at 37 °C for 30 minutes or 0.1 % DMSO vehicle control. Samples were then activated for 30, 60, 90, 150, 300 seconds with 1 U/ml of thrombin (in the presence of 25 μg/ml GPRP) or 3 μg/ml of CRP-XL. Platelets were fixed in 2 % (v/v) formyl saline then permeabilised with BD Phos Flow Perm Buffer III. Anti-kindlin-3 and anti-integrin β_3 were added and labelled with and Alexa Fluor® 647 and Alexa Fluor® 555 labelled secondary antibodies, respectively. Labelled platelets were washed and then adhered on poly-L-lysine coated ibidi slides overnight at 4 °C. Platelets were examined under x100 oil immersion using STORM microscopy.

Integrin β_3 molecules were observed scattered on the surface of platelet whereas kindlin-3 localised in close proximity to platelet membrane inside the platelet. A discoid and uniform morphological appearance was seen in resting platelets as shown in **Figure 6.1 and Figure 6.2**. Following activation with thrombin (1 U/ml) **(Figure 6.1)** or CRP-XL (3 μg/ml) **(Figure 6.2),** platelets underwent shape change, extended pseudopodia **(as detailed in chapter 4)**. A noticeable change in kindlin-3 - β_3 co-clustering was observed in Cpd-22 pre-treated platelets and a reduction of β_3 β_3 clustering at later time points (**Figure 6.1 and Figure 6.2**).

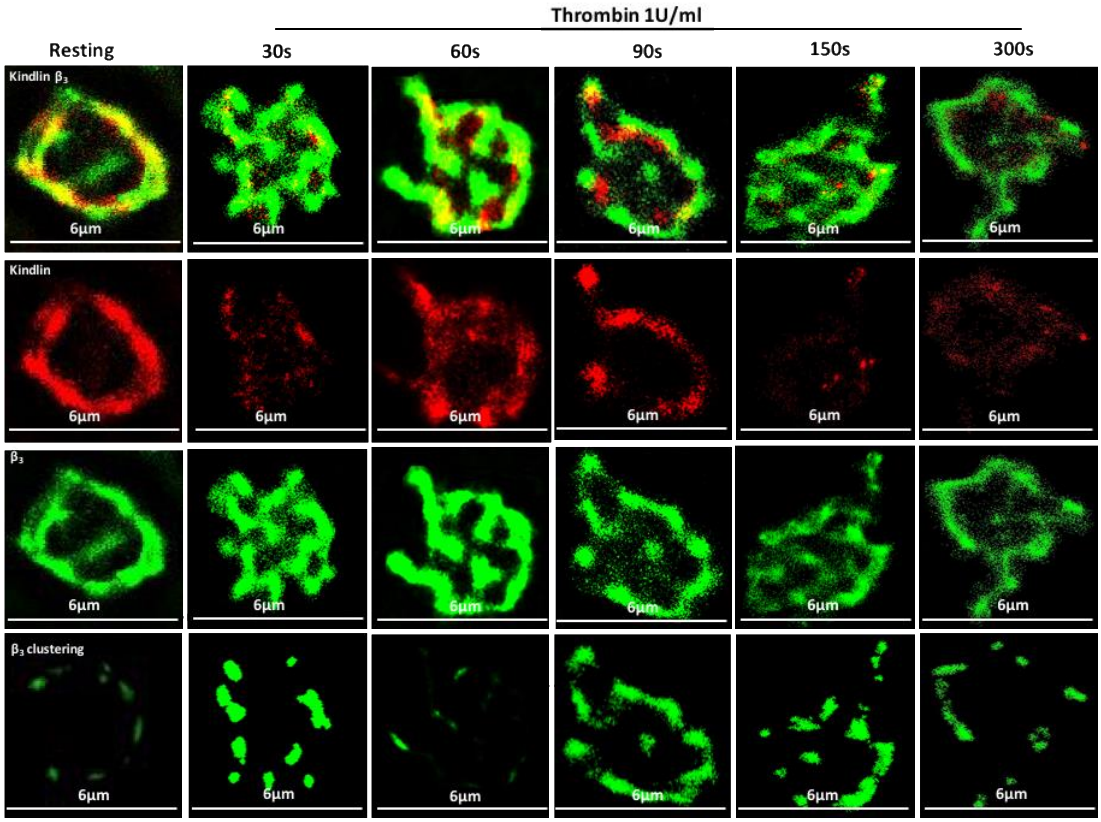
Thrombin 1U/ml
Resting
30s
60s
90s
150s
300s
Kindlin β3
Kindlin
β3
β3 clustering
6μm

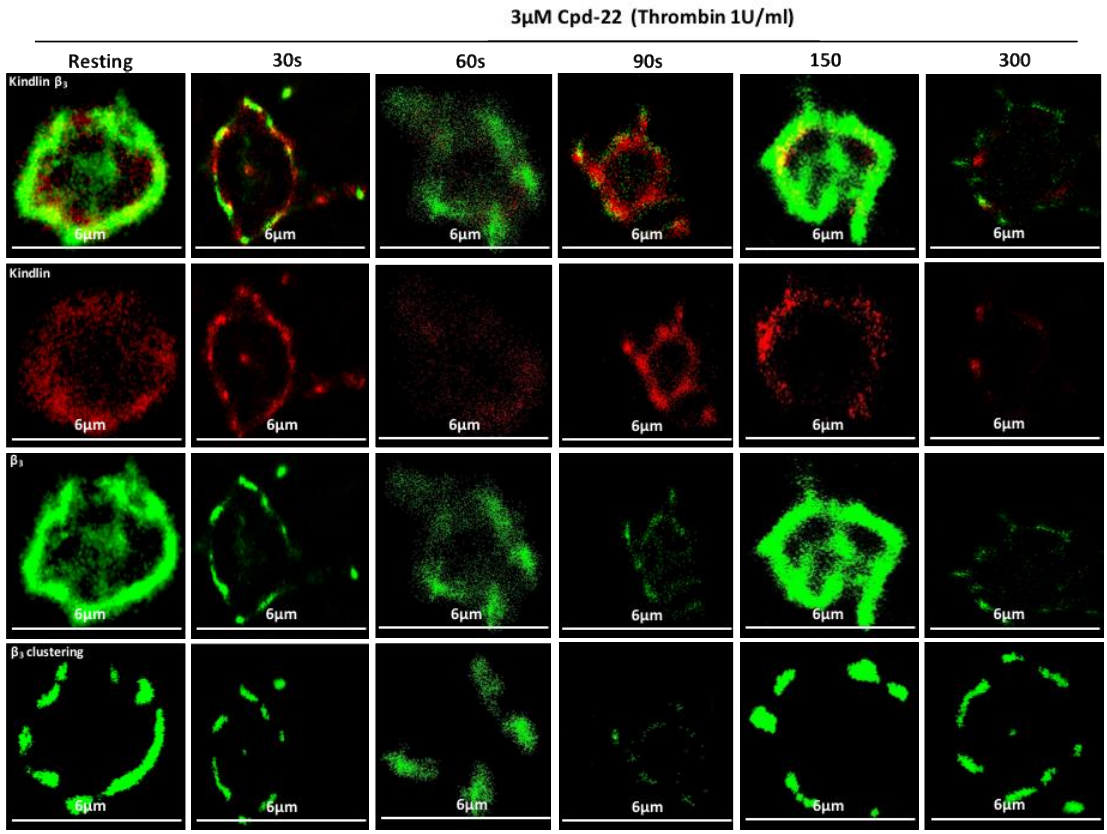
3μM Cpd-22 (Thrombin 1U/ml)
Resting
30s
60s
90s
150
300
Kindlin β3
Kindlin
β3
β3 clustering
6μm

Figure 6.1 Cpd-22 reduces integrin β_3 clustering and co-localisation with kindlin in response to thrombin

Platelet-rich-plasma (PRP) was incubated with Cpd-22 (3 μM) or vehicle, and then activated with thrombin (1 U/ml) in the presence of GPRP (25 mg/ml) for 30, 60, 90, 150 and 300 seconds, platelets were fixed with 2 % (v/v) formyl saline and permeablised with BD Phos Flow Perm Buffer III. Kindlin and integrin β_3 were identified with primary and Alexa Fluor 647 and 555 labelled secondary antibodies, respectively. Labelled platelets were washed then adhered overnight to poly-D-lysine coated ibidi slides before 3D STORM imaging. Images were reconstructed using Nikon-NIS-Elements. The results are representative of $\geq$3 individual experiments.

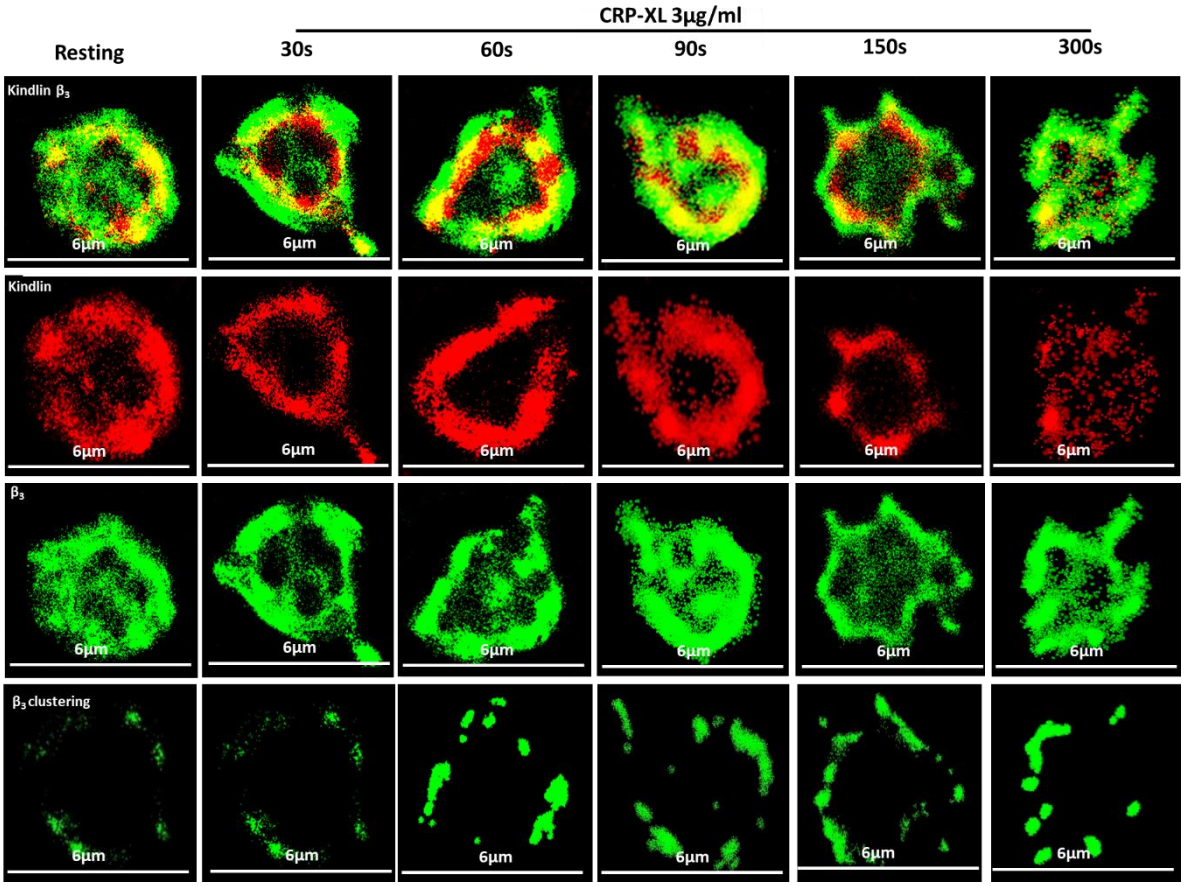
CRP-XL 3µg/ml
Resting
30s
60s
90s
150s
300s
Kindlin β3
Kindlin
β3
β3 clustering
6µm

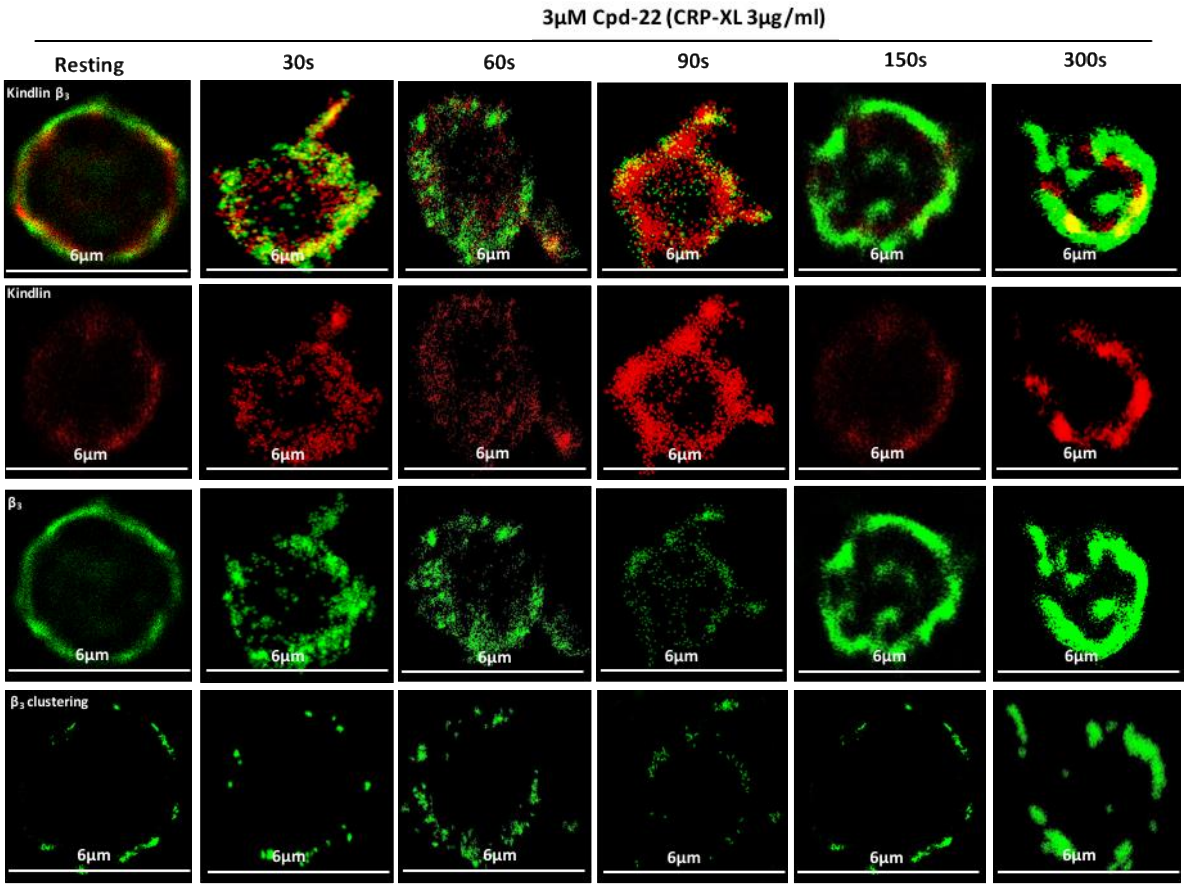
3µM Cpd-22 (CRP-XL 3µg/ml)
Resting
30s
60s
90s
150s
300s
Kindlin β3
Kindlin
β3
β3 clustering
6µm

Figure 6.2 Cpd-22 inhibits integrin β_3 clustering and co-localisation with kindlin evoked by CRP-XL.

Platelet-rich-plasma (PRP) was incubated with Cpd-22 (3 μM) or vehicle, resting and activated platelets with CRP-XL (3 μg/ml) for 30, 60, 90, 150 and 300 seconds were fixed with 2 % (v/v) formyl saline and permeablised with BD Phos Flow Perm Buffer III. Kindlin and integrin β3 were identified with primary and Alexa Fluor 647 and 555 labelled secondary antibodies, respectively. Labelled platelets were washed then adhered overnight to poly-D-lysine coated ibidi slides before 3D dSTORM imaging. Images were reconstructed using Nikon-NIS-Elements. Data are representative of ≥ 3 individual experiments.

As stated previously, kindlin-3 showed a relatively high association with integrin β_3 in resting platelets. This was reduced in Cpd-22 treated platelets **(Figure 6.3)**. Following stimulation with thrombin or CRP-XL the percentage of kindlin-3 - β_3 co-clusters initially fell showing the opposite trend to β_3-β_3 clusters, before increasing at later time points. Interestingly, a significant reduction in the kindlin-3 - β_3 co-clustering was displayed at resting state (first peak), 30 and 90 seconds (second peak) following thrombin stimulation in comparison with vehicle control **(Figure 6.3)**.

It was observed in samples treated with Cpd-22 inhibited significantly CRP-XL mediated kindlin-3 -β_3 co-clustering at 60 and 90 seconds (second peak) compared to vehicle control **(Figure 6.3).** Therefore, inhibition of ILK by Cpd-22 clearly disrupts the association of kindlin-3 - β_3 in resting and stimulated platelets using the new STORM technique. We have confirmed the role of ILK in mediating the interaction of kindlin-3 with β_3 as reported by Legate et al. (2006); (Fukuda et al., 2014).

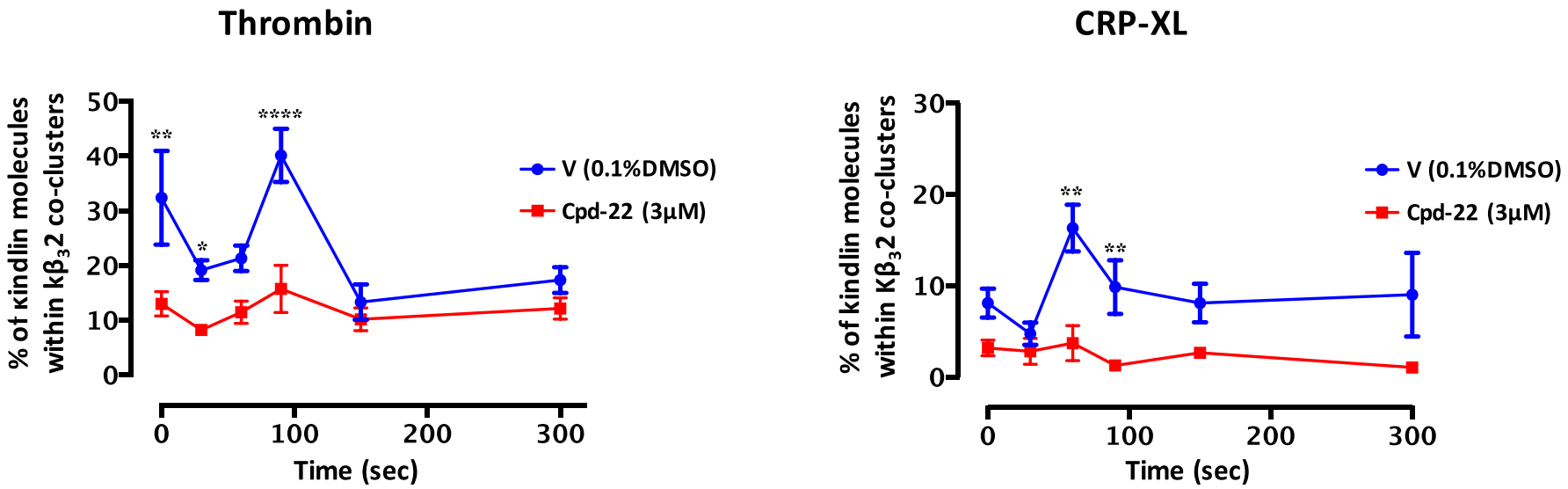

Figure 6.3 Kindlin-β_3 association is inhibited by Cpd-22 in response to thrombin or CRP-XL.

The association of kindlin-3 - β_3 co-clusters were analysed. The mean number of β_3 molecules within 50 nm of each kindlin molecule in 0, 30, 60, 90, 150 and 300 seconds were analysed. This mean value gave us the "average density" of β_3 molecules surrounded each kindlin. We define co-clusters as having 2 times ($k\beta_32$) the average density of β_3. The statistical differences in the mean ± SEM ($n \geq 3$) were assessed by two-way ANOVA, *$P < 0.05$, **$P \leq 0.01$, ***$P \leq 0.001$ and ****$P \leq 0.0001$.

6.3 Cpd-22 downregulated thrombin or CRP-XL induced β_3 - β_3 clustering

As stated previously in section 6.2, ILK inhibition reduced the association of kindlin-3 with β_3. Here, we tested whether the ILK inhibition also inhibits β_3-β_3 clustering over time.

PRP resting or stimulated with (1 U/ml) of thrombin (in the presence of 25 mg/ml GPRP) or (3 μg/ml) of CRP-XL for 30, 60, 90, 150, 300 seconds, were fixed in 2 % (v/v) formyl saline and permeabilised with BD Phos Flow Perm Buffer III. Primary antibodies anti-Kindlin-3 and anti-integrin β_3 were added, then labelled with Alexa Fluor® 647 and Alexa Fluor® 555 secondary antibodies, respectively. Labelled platelets were then washed and adhered overnight to poly-D-lysine coated ibidi slides.

In **Figure 6.4**, it was observed that upon stimulation with thrombin the percentage of β_3 molecules within β_3-β_3 clusters increased, peaking at approximately 60 seconds before falling at 90 seconds and then increasing at 150 seconds and falling again at 300 seconds. Following stimulation of platelets with CRP-XL the percentage of β_3 molecules within β_3 clustering started from low in resting platelets and followed the biphasic pattern up to 300 seconds.

Cpd-22 treated platelets displayed no significant effect on the percentage of β_3 clustering within β_3-β_3 clustering in resting platelets. Pre-treatment of platelets with Cpd-22 caused a significant reduction in the percentage of integrin β_3 clustering stimulated with thrombin at 30, 90, 150, 300 seconds inhibiting both phases of clustering in comparison with treatment with 0.1 % DMSO vehicle control **(Figure 6.4)**. The effect of the treatment of platelets with Cpd-22 for 30 minutes prior to stimulation with CRP-XL are

shown in **Figure 6.4**, a substantial reduction in the percentage of $\beta_3\beta_3$ within β_3 clustering at 60 and 90 seconds in comparison to vehicle. Therefore, only inhibition the second phase of clustering. To conclude, inhibition of ILK with Cpd-22 led to an inhibition of β_3 clustering particularly the second phase of clustering.

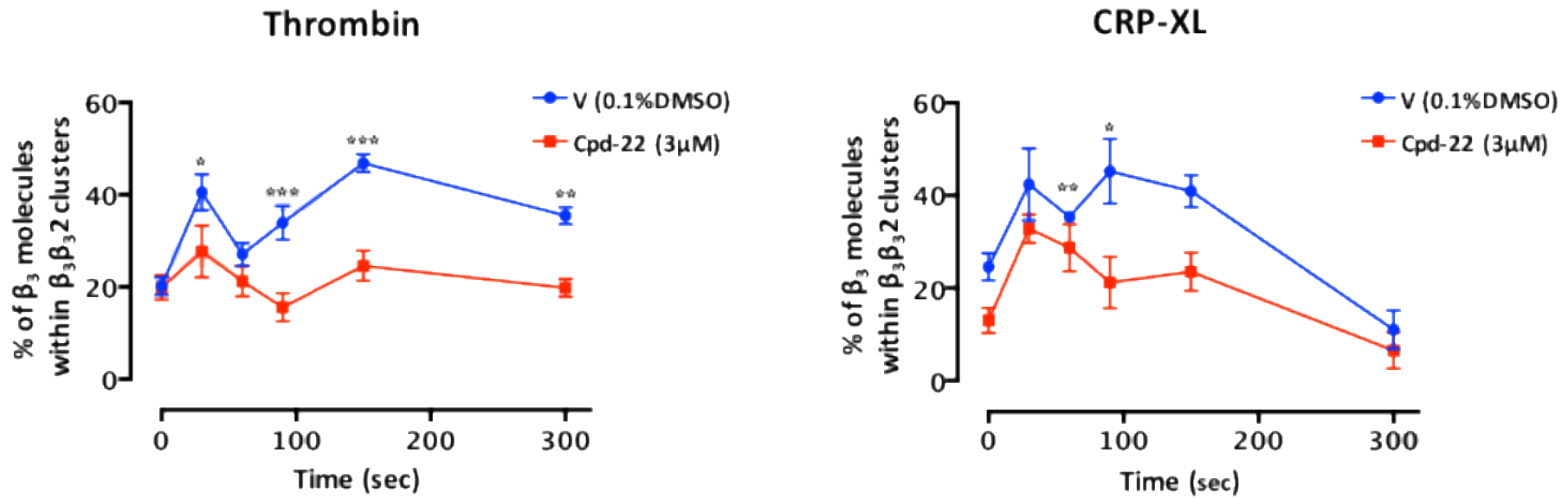

Figure 6.4 Cpd-22 down regulates thrombin or CRP-XL induced β_3-β_3.

The mean number of β_3 molecules within 50 nm of each β_3 molecule in 0, 30, 60, 90, 150 and 300 seconds were analysed. This mean value was the "average density of β_3 molecules surrounding each β_3 molecules using ThunderSTORM and cluster analysis in R. The statistical differences in the mean ± SEM ($n \geq 3$) were assessed by one-way ANOVA, *$P < 0.05$, **$P \leq 0.01$, ***$P \leq 0.001$ and ****$P \leq 0.0001$.

6.4 Cpd-22 inhibits fibrinogen binding to integrin in real time flow cytometry

As previously mentioned in section 6.3, inhibition of ILK with Cpd-22 caused inhibition of β_3 clustering. The purpose of this experiment was to investigate whether β_3 clustering inhibition lead to inhibit fibrinogen binding to integrin $\alpha_{IIb}\beta_3$ over the time scale of altered β_3 clustering via real-time flow cytometric analysis.

Fibrinogen binding to vehicle control (0.1 %) DMSO or (3 μM) Cpd-22 platelets from human platelets was measured by diluting PRP in HEPES, followed by FITC labelled anti-fibrinogen antibody. Samples were transferred to a 96-well plate and analysed by an Accuri C6 flow cytometry at 37 °C. During data acquisition, (1 U/ml) thrombin (in the presence of GPRP 25 mg/ml) and CRP-XL (3 μg/ml) were used to stimulate platelets. Platelet activation was measured over 300 seconds.

In presence of Cpd-22, thrombin and CRP-XL stimulated platelets showed a reduction in the rate of fibrinogen binding over 300 seconds of stimulation when compared to vehicle treated platelets **(Figure 6.5)**.

Previous research stated that fibrinogen binding to integrin $\alpha_{IIb}\beta_3$ leads to $\alpha_{IIb}\beta_3$ clustering (Shattil and Newman, 2004). In this experiment, fibrinogen binding was reduced but still present. This finding confirms that reduction of fibrinogen binding (**Figure 6.4)** is independent of integrin β_3 clustering inhibition **(Figure 6.5).**

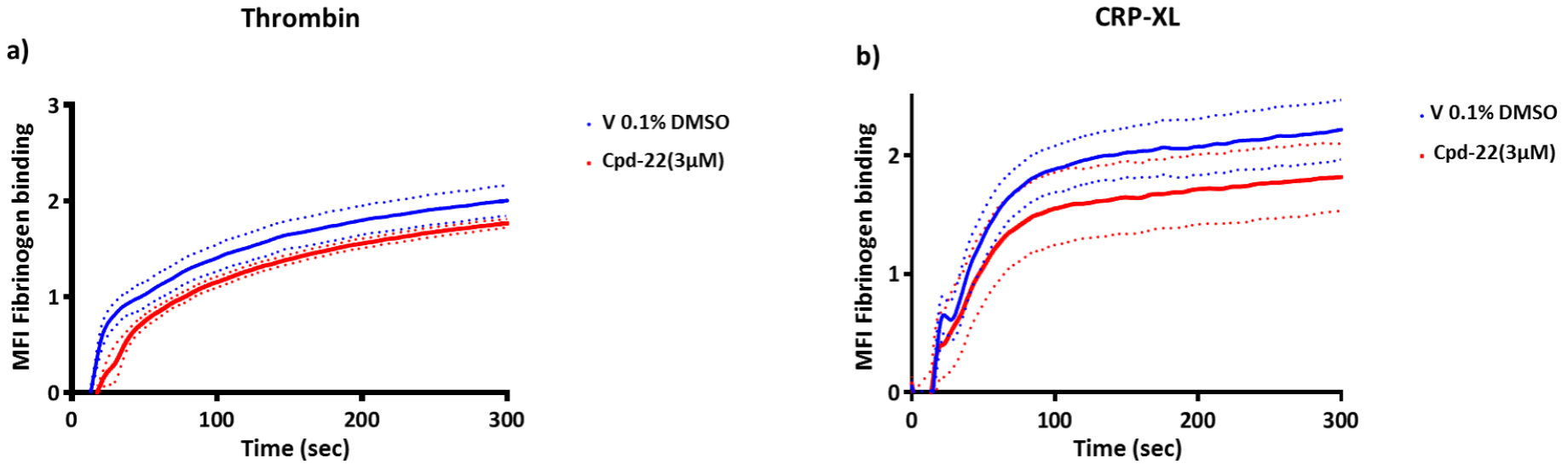

Figure 6.5 Cpd-22 inhibits real time fibrinogen binding in response to thrombin or CRP-XL.

PRP were pre-treated with (0.1 %) DMSO or (3 µM) Cpd-22 and FITC labelled anti fibrinogen antibody. Platelets were stimulated with (1 U/ml) thrombin (in the presence of GPRP 25 mg/ml) or CRP-XL (3 µg/ml) during data acquisition. Samples were analysed using Accuri C6 flow cytometry. Data are shown as mean ± SEM (n = 3), analysed by Student's t-test, ****P ≤ 0.0001.

6.5 Cpd-22 negatively impacted β_3, Src and Syk phosphorylation in thrombin and CRP-XL aggregated platelets

Integrin $\alpha_{IIb}\beta_3$ clustering is thought to be an important step in the outside-in pathway and consequently contributes significantly to arterial thrombus formation and normal haemostasis (Li et al., 2010).

Cpd-22 impacted on the pattern of kindlin-3 - β_3 association and β_3 clustering in response to CRP-XL and thrombin. Therefore, in this section, we examined the potential consequences of such impact on downstream signalling events of β_3 (outside-in signalling).

Washed platelets (4×10^8 cells/ml) pre-treated with (3 μM) Cpd-22 or (0.1 %) DMSO at 37 °C for 30 minutes were then stimulated with HEPES (resting), (1 U/ml) thrombin and (3 μg/ml) CRP-XL in aggregating conditions for 30, 60, 90, 150 and 300 seconds. Reactions were then stopped with Laemmli buffer prior to separation by SDS-PAGE. Tyrosine phosphorylation was assessed by immunoblotting.

In vehicle treated platelets a considerable rise in the phosphorylation of integrin β_3, Src, and Syk in response to thrombin or CRP-XL stimulation over different time points **(as discussed in chapter 4) (Figure 6.6)**.

Treatment with Cpd-22 resulted in a substantial decrease in the level of thrombin-induced tyrosine phosphorylation of β_3, Src, and Syk over different time courses. It was observed that a substantial reduction in the phosphorylation of β_3 at 60, 90 and 150 seconds compared to vehicle control. A significant reduction was observed in the level of Src and

Syk phosphorylation at 150 and 300 seconds in comparison with the vehicle control **(Figure 6.6).**

Likewise, pre-treatment of human washed platelets with Cpd-22 in response to CRP-XL displayed a significant reduction in the level of phosphorylation of β_3 at 60, 90, 150 seconds in comparison with vehicle control. Src and Syk was significantly reduced at (60, 90, 150 and 300 seconds) compared to vehicle control **(Figure 6.7)**.

This suggested that early time points of signalling are unaffected by Cpd-22. Also, outside-in signalling is inhibited by ILK inhibition and reduction in β_3 clustering, this inhibition was mostly seen in a late time points, corresponding with the second peak of β_3 β_3 clustering.

ai) IB: β_3 (Y773)

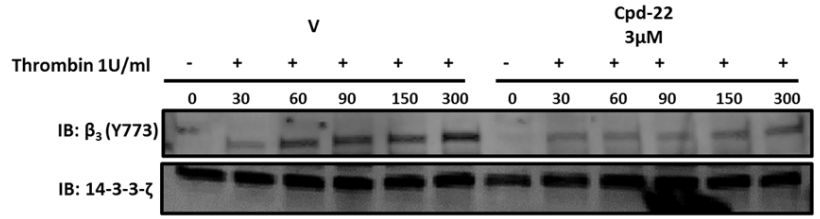

aii) β_3 (Y773)

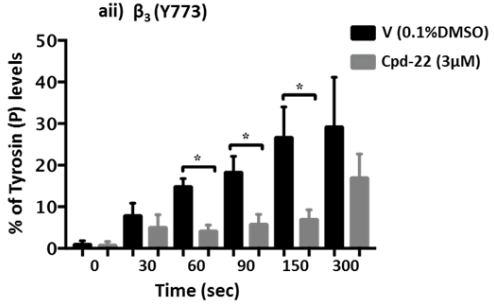

aiii) β_3 (Y773)

Time points thrombin stimulation (U/ml)	30	60	90	150	300
Vehicle(β_3) compared to 0sec				*	*
Cpd-22(β_3)compared to 0sec					**

bi) IB: Src (Y418)

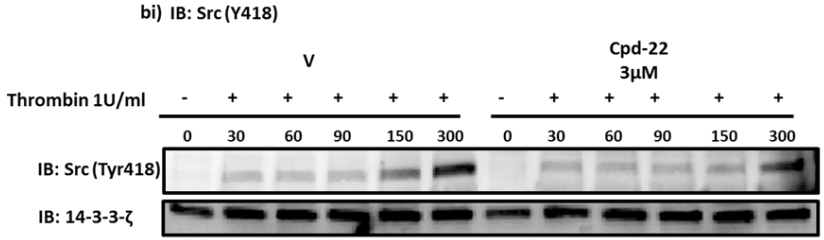

bii) Src (Tyr418)

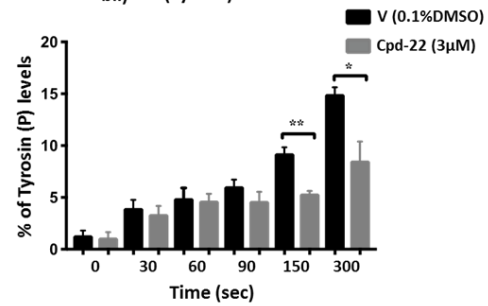

biii) Src (Tyr418)

Time points thrombin stimulation (U/ml)	30	60	90	150	300
Vehicle(Src) compared to 0sec		*	**	***	****
Cpd-22(Src)compared to 0sec				*	***

ci) IB: Syk (Y525/526)

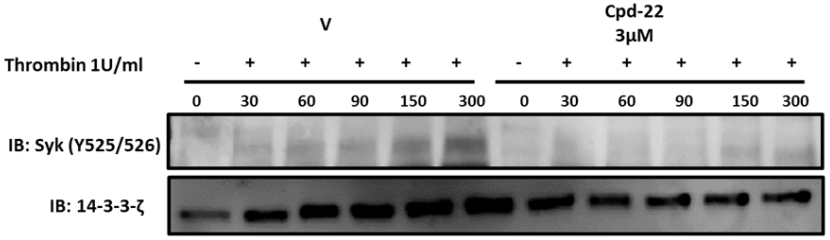

cii) Syk (Y525/526)

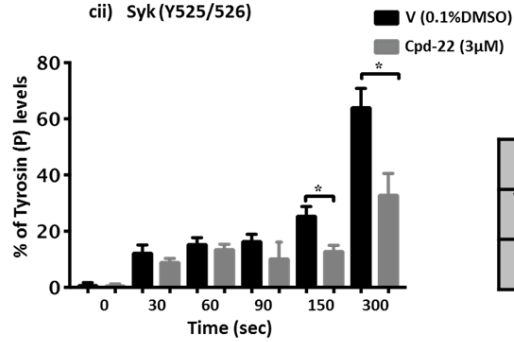

ciii) Syk (Y525/526)

Time points thrombin stimulation (U/ml)	30	60	90	150	300
Vehicle(Syk) compared to 0sec		*	*	***	****
Cpd-22(Syk)compared to 0sec	*	*	*	*	***

Figure 6.6 The impact of ILK inhibition of signal downstream of β_3 in response to thrombin

Human washed platelets were pre-treated with Cpd-22(3 μM) or 0.1 % vehicle control, and stimulated with thrombin (1 U/ml) for 30, 60, 90,150 and 300 seconds. Samples were lysed in Laemmli sample buffer, separated on SDS-PAGE and transferred to PVDF membranes. Blots were immunoblotted for tyrosine phosphorylation of β_3 (Y773), Src (Tyr418) and Syk (Y525/526). To control for protein loading, blots were probed with 14-3-3-ζ. Bars represent β_3, Src and Syk phosphorylation levels normalised to loading control. Western blot shown is representative of 3 donors. Results are mean ± SEM (n = 3), *P ≤ 0.05, **P ≤ 0.01, ***P ≤ 0.001 and ****P ≤ 0.0001 was calculated by Student's t-test.

ai) IB: β_3 (Y773)

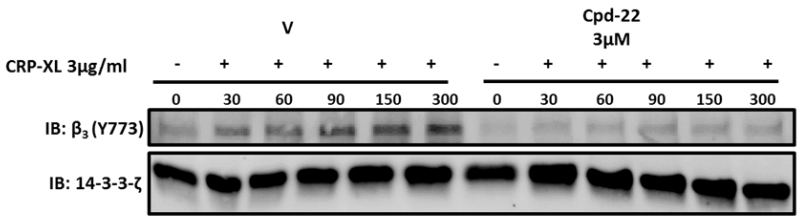

aii) β_3 (Y773)

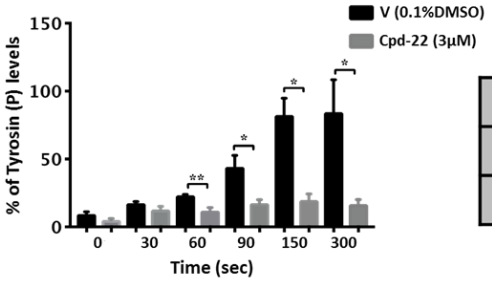

aiii) β_3 (Y773)

Time points CRP-XL stimulation(3µg/ml)	30	60	90	150	300
Vehicle(β_3) compared to 0sec				**	**
Cpd-22(β_3)compared to 0sec			*	*	

bi) IB: Src (Y418)

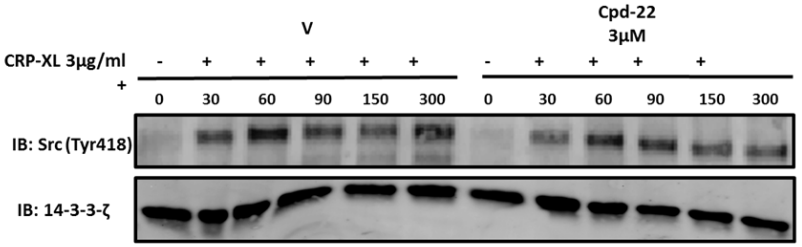

bii) Src (Tyr418)

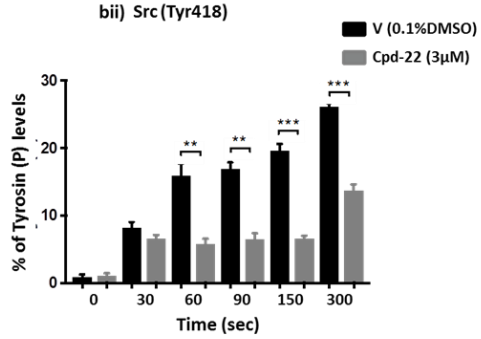

biii) Src (Tyr418)

Time points CRP-XL stimulation(3µg/ml)	30	60	90	150	300
Vehicle(Src) compared to 0sec	**	****	****	****	****
Cpd-22(Src)compared to 0sec	***	***	***	***	****

ci) IB: Syk (Y525/526)

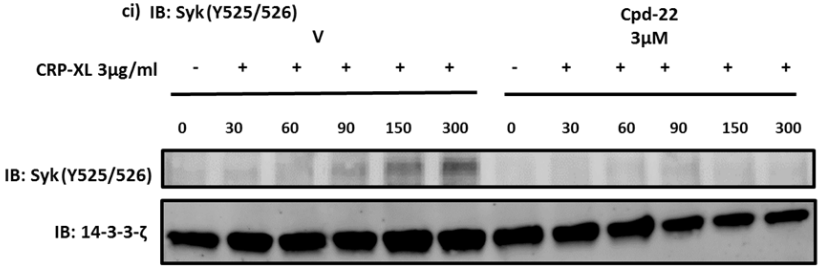

cii) Syk (Y525/526)

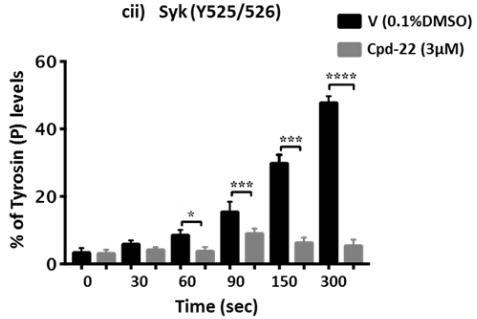

ciii) Syk (Y525/526)

Time points CRP-XL stimulation(3µg/ml)	30	60	90	150	300
Vehicle(Syk) compared to 0sec			***	****	****
Cpd-22(Syk)compared to 0sec			**		

Figure 6.7 Effect of Cpd-22 on tyrosine phosphorylation of β_3 and downstream signalling induced by CRP-XL.

Washed and Cpd-22-treated platelets were stimulated with CRP-XL (3 µg/ml), the stimulation times for CRP-XL were 30, 60, 90, 150 and 300 seconds, respectively. Reaction was stopped by adding the Laemmlli buffer and then lysates were analysed for tyrosin phosphorylation by western blotting using monoclonal anti-phospho β_3, Src and Syk. 14-3-3-ζ was detected by immunoblotting as a loading control. Western blot shown is representative of 3 donors. Results are mean ± SEM, *P ≤ 0.05, **P ≤ 0.01, ***P ≤ 0.001 and ****P ≤ 0.0001 was calculated by Student's t-test.

6.6 Discussion

Attenuated platelet reactivity can precipitate bleeding events. Although effective in preventing thrombotic diseases, available antiplatelet therapies have their limitations and side effects such as bleeding (Angiolillo et al., 2010). Also, some patients develop resistance to these medications. Moreover, the use of these agents is highly contradicted in patients with haemorrhagic stroke (Stolla et al., 2011; Shahpouri et al., 2012). Hence, elucidating the molecular basis underlying platelet activation adds an important value to the clinical implications.

Src family kinases (SFKs) have been investigated to be a central point in the primary activation of platelets (Shattil and Newman, 2004; Senis et al., 2014). SFKs in platelets namely Src, Lyn, and Fyn. They transform numerous activatory signlas from receptors such as integrin $\alpha_{IIb}\beta_3$, the immunoreceptor tyrosine–based activation motif–containing the collagen receptor complex GPVI-FcRγ-chain, and the von Willebrand factor receptor complex GPIb-IX-V (Ozaki et al., 2005; Watson et al., 2005). Researches has implicated that Src is highly expressed in human platelets. Moreover, it is necessary in coordinating signals from integrin $\alpha_{IIb}\beta_3$. Studies have confirmed that mouse platelets deficient in Src exhibit reduction in tyrosine phosphorylation (Golden et al., 1986; Shattil et al., 2010)

6.6.1 Down regulation of kindlin-β_3 co-clustering and β_3-β_3 by Cpd-22

Previous studies confirmed that ILK plays an important role in regulating the rate of platelet activation, and thrombus formation. Studies have confirmed that platelets from mice lacking ILK platelets exhibit reduced aggregation, fibrinogen binding and alpha granule secretion (Honda et al., 2009). We showed Cpd-22 treatment caused a reduction of kindlin-3 - β_3 in resting platelets and following agonist stimulation. ILK inhibition by

Cpd-22 exerted an impact on β_3 β_3 clustering and kindlin-3- β_3 clustering. This is consistent with Qadota et al. (2012) who reported a possible role of ILK in the localisation of kindlin to focal adhesion sites and the integrin cytoplasmic tail. Given the inhibitory effect of Cpd-22 on ILK activity, this could explain the reduced aforementioned co-clustering in ILK inhibited platelets. Collectively, it is clear that changes in the dynamic process of ILK mediated kindlin-3 - β_3 co-clustering can have effects on some aspects of β_3 clustering.

6.6.2 Cpd-22 inhibits thrombin or CRP-XL mediated rate of fibrinogen binding

Fibrinogen binding was measured using real time flow cytometry, and was moderately inhibited by the presence of Cpd-22. It seems unlikely this is linked to kindlin-3 - β_3 and $\beta_3\beta_3$ clustering biphasic patterns. This result reflected that fibrinogen binding is not fully dependent on $\beta_3\beta_3$ clustering.

6.6.3 Cpd-22 negatively impacted β_3, Src and Syk phosphorylation in thrombin and CRP-XL aggregated platelets

β_3 phosphorylation is necessary for downstream signalling of β_3 (Obergfell et al., 2002). Here, we observed that the inhibition of β_3 with Cpd-22 inhibits downstream signalling, following stimulation with CRP-XL or thrombin.

Thus, Src and Syk phosphorylation has been shown to have an activatory effect in of downstream signalling of β_3 (Boylan et al., 2008; Fong et al., 2016). Therefore, pretreatment of platelets with Cpd-22 was examined and Src and Syk phosphorylation levels found to be diminished particularly at late time points of stimulation. These findings explain that outside-in signals is disrupted by ILK inhibition and change in clustering. This mostly occurred at late time points.

Our findings confirm that inhibition of outside-in signalling events were linked to the inhibition of the second peak of β_3 clustering but crucially not the first. In conclusion, the data in this study indicate that ILK is important for platelet activation and downstream of fibrinogen binding. Furthermore, Inhibition of ILK reduced the association between kindlin-3 - β_3. The change in kindlin-3 - β_3 led to inhibition of β_3 β_3 clustering, and inhibition of β_3 downstream signalling in late time points, corresponds with the second peak of β_3 clustering.

7 General Discussion

7.1 Introduction

Integrins are surface receptors that mediate interactions between cells and between cell and ECM (Hynes, 2002). Open conformations are facilitated upon stimulation enabling ligand binding and integrin functioning (Nieswandt et al., 2009). With growing computational resources and tools becoming available to biologists, variety of computational models are employed to analyse the images that are generated by microscopes. These models are likely to help researchers to understand the biological process. Imaging studies of platelets have been studied by electron microscopy (EM) and immunofluorescence confocal microscopy (Kanemaru et al., 2009).

EM is a technique which can capture images with high resolution. However, before taking images, samples must undergo extensive preparation and several staining steps. Also, imaging molecules with high density is challenging due to the low labelling of antibodies. EM does not provide Multicolour imaging Capability in different cells (Thompson et al., 2016; Webster et al., 2008). Fluorescence microscopy is versatile, highly sensitive, 3D images can be captured with little perturbation. This allows researchers to examine dynamic process of cells. However, diameter of platelet is between 2 to 4 μm with even smaller subcellular structural dimensions. Hence, the fluorescence microscopy resolution which is about 250 nm, hampers the visualisation of nanoscale structures such as single β_3 molecules within platelets (Lichtman and Conchello, 2005; Huang et al., 2008)

To overcome the limitations of fluorescence and electron microscope, we used super-resolution microscopy (STORM). This powerful optical system enables examination of integrins behaviour and interaction with other proteins in human platelets. Nanoscale measurement has been studied with the aid of such microscopy as it can achieve a

resolution of 20 nm (Rust et al., 2006a; Huang et al., 2008; Bates et al., 2013). Study of proteins at subcellular molecular levels provide knowledge on the distribution of these proteins and on the positions the clusters in which the molecules accumulate. Analysing this information would give a feasible way to understand the kinetics of integrin activation and clustering in platelets. Moreover, development of applications and novel methods are now known as a particularly important target in quantifying the dynamic and temporal changes of integrins.

In this work, we designed a Stochastic Optical Reconstruction Microscopy (STORM) method for measuring molecular clustering in platelets and investigate the time course of integrin β_3 clustering and its association with kindlin-3. Moreover, this study examined how integrin β_3 clusters and interacts with kindlin-3 in human platelets at resting, and upon activation by thrombin and by CRP-XL. This study also investigated whether β_3 clustering was affected by fibrinogen binding and platelet aggregation (inside-out pathway) and ultimately identifies the regulatory role for integrin β_3 clustering in the regulation of β_3 downstream signalling (outside-in pathway). It is therefore critical to understand how platelets function, integrin β_3 clustering and kindlin-3 - β_3 co-clustering affected by targeting ILK activities using ILK inhibitor (Cpd-22). Thereby, the influence of aforementioned inhibitor on kindlin-3 - integrin β_3 association and integrin β_3 clustering may also result in affected integrin β_3 downstream signalling.

7.1.1 Role of ILK in integrin β_3 clustering and co-localisation with kindlin in human platelets using a novel super resolution STORM microscopy method

Molecular aspects of integrin β_3 clustering and activation in human platelets, a less scrutinised phenomenon, was investigated using a new STORM technique to visualise

the time course of integrin β_3 clustering and kindlin-3 - β_3 co-clustering and their behaviour following platelet stimulation with thrombin (GPCR receptor) or CRP-XL (GPVI agonist). In resting platelet, integrin β_3 was observed on the membrane whereas kindlin-3 was looked inside platelet close to membrane.

To better understand the visual findings of integrin β_3 clustering and its association with kindlin-3, analysis of these images was pertinent. Most previous methods rely on analysing images mathematically in which hindered the analysis such as SR-Tesseler. Although this method is robust, it is complicated for result interpretation (Levet et al., 2015). Additionally, DBSCAN has also been used extensively but the definition and quantification of clusters is complicated. This method also cannot defines clusters with different densities of molecules (Nan et al., 2013).

For this purpose, we decided to develop new method for measuring integrin β_3 clustering and its association with kindlin-3 using R, ImageJ plugin ThunderSTORM. A novel STORM microscopy analysis method was developed to quantify the temporal changes in the clustering of integrin β_3 clustering and the co-clustering of kindlin-3 in human platelets following thrombin stimulation. Our method is suitable for data cluster with variation in molecules densities. It is a computationally faster method of cluster analysis which allow to define and quantify clustering. It is also a biological method for analysing integrin β_3 clustering and its association with kindlin-3.

Our findings showed a biphasic pattern with β_3 clustering going through two peaks starting early within 30 seconds during platelet stimulation with thrombin. Paszek et al. (2009) observed drops and peaks of β_3 clustering pattern could be attributed to dynamic process of integrin clustering that is known to undergo repeated bondage and breakage during the process of clustering. Similar behaviour of integrin clustering triggered within

tens of seconds of stimulation as shown by Paszek et al. (2009). This method was validated by confirming obtained findings with those generated from flow cytometric FRET method that yielded similar findings.

Kindlin-3 - β_3 revealed opposite trend of Integrin β_3 clustering co-clustering at first 30 seconds and followed the same biphasic pattern as the β_3-β_3 clusters. Although the timing of the peaks did vary between donors, a pattern was evident in all individuals. Interestingly, kindlin-3 was found to form co-clusters with integrin β_3 in quiescent platelets. In spite of our finding not become anticipated in resting platelets, we suggest that there is basal level of association between kindlin-3 and β_3 in resting state, possibly to keep this protein in close proximity and available for recruiting and binding other effector proteins and kinases when the platelet is stimulated. Such co-cluster formation confirms kindlin-3 - integrin β_3 association and suggests the pivotal role of this protein in integrin β_3 clustering. However, the mechanism underlying the kinetic of integrin β_3 and kindlin-3 - β_3 is still not fully understood. Collectively, in both cases changing the density of molecules used to define a cluster altered the percentage of molecules within the cluster but had no effect on the temporal pattern of the change of these clusters.

Also, real time of fibrinogen binding was investigated. Real time flow cytometric data confirm that fibrinogen bound to $\alpha_{IIb}\beta_3$ over time points was moderately inhibited. This suggest that rate of fibrinogen binding was not linked to kindlin-3 - β_3 and $\beta_3\beta_3$ clustering biphasic patterns. This result reflected that $\beta_3\beta_3$ clustering is not fully dependent fibrinogen binding.

Having established this novel R based method, work was carried out to investigate the role of ILK in integrin β_3 clustering and its interaction with kindlin-3 protein. Therefore, disruption of ILK negatively impacted integrin β_3 clustering and co-clustering of kindlin-

3 with β_3 over different time points of platelet stimulation. Kindlin-3 showed a relatively high association with integrin β_3 in resting platelets. This was reduced in Cpd-22 treated platelets. Cpd-22 impaired thrombin mediated kindlin-3 - β_3 co-clustering over time (in resting and after stimulation). Thus, disruption of ILK by Cpd-22 clearly inhibited the interaction of kindlin-3 - β_3 in resting and stimulated platelets using the new STORM technique. This suggested the role of ILK in mediating the interaction of kindlin-3 with β_3 as reported by Legate et al. (2006) and Fukuda et al. (2014).

Cpd-22 treated platelets showed no significant effect on the percentage of β_3 clustering within β_3-β_3 clustering in resting platelet. A significant reduction in the percentage of integrin β_3 clustering was observed in thrombin stimulated platelets at 30, 90, 150, 300 seconds inhibiting both phases of clustering. To conclude, inhibition of ILK with Cpd-22 led to an inhibition of β_3 clustering particularly the second phase of clustering.

7.1.2 Effect of Cpd-22 in platelet function

ILK has been reported to downregulate various aspects of platelet activation in ILK inhibited platelets and in ILK depleted transgenic mice (Stevens et al., 2004; Jones et al., 2014). However, Cpd-22, presently used ILK inhibitor has not been studied in platelets. Hence, the impact of this inhibitor on range of platelets functional aspects was scrutinised. Similar to other ILK inhibitors (QLT0267) which was studied by Jones et al. (2014) and confirmed to inhibit platelet function in a similar way to the effect of Cpd-22 shown in this study. Here, Cpd-22 downregulated platelet aggregation in response to CRP-XL and thrombin stimulation. This indicates that ILK disruption leads to inhibit platelets aggregation. This is agreement with previous studies on ILK knockout mice (Tucker et al., 2008) . The level of fibrinogen binding to activated $\alpha_{IIb}\beta_3$ in CRP-XL or thrombin stimulated platelets was examined to investigate the role of ILK in integrin

$\alpha_{IIb}\beta_3$ activation. Therefore, Inside-out signalling was impacted as reflected on the levels of fibrinogen binding to integrin $\alpha_{IIb}\beta_3$ in stimulated platelets. P-selectin exposure, classical marker of alpha granule secretion and platelet activation was also diminished. This data suggest that Cpd-22 influences the level of P-selectin exposure. These findings are in agreement with previous studies reported in ILK deficient mice which exhibited decreased abilities of fibrinogen binding and alpha granules secretion (Tucker et al., 2008; Jones et al., 2014).

Collectively, these findings further confirm the implication and vital role of ILK in the regulation of fibrinogen binding but less potent in degranulation.

7.1.3 Impact of ILK inhibition on β_3 downstream signalling events

Having investigated ILK inhibition that impacted inside-out signalling levels in response to platelet stimulation. Such impact was further investigated by looking into the levels of activatory signals generated following the engagement of integrin β_3 with ligand in stimulated platelets. Thrombin and CRP-XL stimulated platelets causes a significant increase in β_3 phosphorylation (Y773) at 150- and 300-seconds thrombin stimulated platelets when compared to 0 seconds. This is consistent with the second phase of β_3 clustering. A significant increase in the phosphorylation levels of both Src and Syk were achieved at 30, 60, 90, 150, 300 seconds.

On the other hand, aforementioned levels of phosphorylation were downregulated in Cpd-22 pre-treated platelets. However, the effect of Cpd-22 on the phosphorylation of integrin β_3, Src and Syk phosphorylation occurred particularly at late time points of stimulation, corresponding with the second peak of β_3 clustering.

Together, our data confirm that ILK is essential in platelet function and activatory signalling events when platelets are exposed to agonist stimulation at late time points.

These data underpin the inhibition of ILK reduces the interaction between kindlin-3 and β_3. The change in the interaction of kindlin-3 - β_3 led to inhibit $\beta_3\beta_3$ clustering and ultimately inhibits β_3 downstream signalling in late time points, corresponding with second peak of β_3 clustering.

7.1.4 Conclusion and future work

The present study highlights the molecular aspects underlying integrin β_3 activation in human platelets with the aid of Stochastic Optical Reconstruction Microscopy (STORM) method for measuring molecular clustering in non-adherent platelets and investigate the time course of integrin β_3 clustering and its association with kindlin. With this method, we found that changing the density of molecules used to define a cluster did not affect the pattern of movement of molecules into or out of clusters over time. This indicates that clusters can be defined as a continuum of densities rather than a fixed threshold density. Moreover, integrin β_3 molecules exhibited a biphasic clustering pattern over different time points of platelet stimulation with various agonists. ILK inhibition negatively affected platelet function, inside-out signalling and activatory signalling events upon platelet stimulation.

Although the present findings unravelled the behaviour of integrin β_3 at a molecular level in response to platelet stimulation, however, the mechanisms underlying integrin β_3 is still not fully elucidated. Moreover, ILK inhibition attenuated kindlin-3 β_3 co-clustering, another phenomenon that needs further examination and study. In addition to kindlin, talin is another important cytosolic protein required for integrin β_3 clustering, it is also important in both inside-out and outside-in signalling (Anthis and Campbell, 2011). In spite of presence a large experimental studies on the role of talin in mediating integrin activation, the mechanism of action underlying this activation remains poorly

understood. It would be interesting to scrutinise the role of this protein on integrin β_3 clustering using the same presently employed STORM and R-based novel analytical method. Moreover, to investigate the time course of integrin β_3 clustering and its association with talin. This would provide insight into the association between talin and β_3 and how this interaction affects β_3 clustering, platelet functions and β_3 downstream signalling (out-side in signalling). Protein kinase C α, Rap-1A and RIAM have been implicated to play important roles to recruit talin in mediating integrin activation (Han et al., 2006; Das et al., 2014). However, the mechanism of these molecules is not clearly understood. It will be important to explore the role of these molecules in the regulation of talin. Also, identify how talin is regulated by these molecules, its influence on platelet function and downstream signalling of β_3. This will contribute to develop novel anti-thrombotic drug targeting thrombosis.

7.1.5 Concluding remarks

- A novel STORM microscopy method has been developed and used to quantify the temporal changes in the clustering of integrin β3and co-clustering of kindlin with integrin β_3 in human platelets following thrombin or CRP-XL stimulation.
- The clustering of integrin β_3 molecules and kidlin-3 - β_3 was biphasic.
- Cpd-22 is a selective inhibitor of ILK.
- Cpd-22 inhibits platelet functions in response to thrombin or CRP-XL.
- Integrin β_3 clustering and kidlin-3 - β_3 co-clustering were inhibited by Cpd-22.
- The inhibition of ILK reduces the interaction between kindlin-3 and β_3. The change in the interaction of kindlin-3 - β_3 cause inhibition of β_3 β_3 clustering and β_3 downstream signalling in late time points.

8 References

Akbar, H., Kim, J., Funk, K., Cancelas, J. A., Shang, X., Chen, L., Johnson, J. F., Williams, D. A. & Zheng, Y. (2007). Genetic and pharmacologic evidence that Rac1 GTPase is involved in regulation of platelet secretion and aggregation. *J Thromb Haemost*, **5**, 1747-55.

Al Ghumlas, A. K. (2013). The blood platelet: An intriguing cell. *Journal of Applied Hematology*, **4**, 1.

Albelda, S. M., Muller, W. A., Buck, C. A. & Newman, P. J. (1991). Molecular and cellular properties of PECAM-1 (endoCAM/CD31): a novel vascular cell-cell adhesion molecule. *J Cell Biol*, **114**, 1059-68.

Angiolillo, D. J., Ueno, M. & Goto, S. (2010). Basic principles of platelet biology and clinical implications. *Circ J*, **74**, 597-607.

Anthis, N. J. & Campbell, I. D. (2011). The tail of integrin activation. *Trends Biochem Sci*, **36**, 191-8.

Anthis, N. J., Wegener, K. L., Critchley, D. R. & Campbell, I. D. (2010). Structural diversity in integrin/talin interactions. *Structure*, **18**, 1654-66.

Arias-Salgado, E. G., Haj, F., Dubois, C., Moran, B., Kasirer-Friede, A., Furie, B. C., Furie, B., Neel, B. G. & Shattil, S. J. (2005). PTP-1B is an essential positive regulator of platelet integrin signaling. *The Journal of cell biology*, **170**, 837-845.

Arthur, J. F., Gardiner, E. E., Matzaris, M., Taylor, S. G., Wijeyewickrema, L., Ozaki, Y., Kahn, M. L., Andrews, R. K. & Berndt, M. C. (2005). Glycoprotein VI is associated with GPIb-IX-V on the membrane of resting and activated platelets. *Thromb Haemost*, **93**, 716-23.

Asselin, J., Gibbins, J. M., Achison, M., Lee, Y. H., Morton, L. F., Farndale, R. W., Barnes, M. J. & Watson, S. P. (1997). A collagen-like peptide stimulates tyrosine phosphorylation of syk and phospholipase C gamma2 in platelets independent of the integrin alpha2beta1. *Blood*, **89**, 1235-42.

Banno, A. & Ginsberg, M. H. (2008). Integrin activation. *Biochem Soc Trans*, **36**, 229-34.

Bates, M., Jones, S. A. & Zhuang, X. (2013). Stochastic optical reconstruction microscopy (STORM): a method for superresolution fluorescence imaging. *Cold Spring Harbor Protocols*, **2013**, pdb. top075143.

Behnke, O. (1970). The morphology of blood platelet membrane systems. *Ser Haematol,* **3**, 3-16.

Beningo, K. A., Dembo, M., Kaverina, I., Small, J. V. & Wang, Y. L. (2001). Nascent focal adhesions are responsible for the generation of strong propulsive forces in migrating fibroblasts. *J Cell Biol,* **153**, 881-8.

Bennett, J. & Vilaire, G. (1979). Exposure of platelet fibrinogen receptors by ADP and epinephrine. *Journal of Clinical Investigation,* **64**, 1393.

Bennett, J. S. (2005). Structure and function of the platelet integrin α IIb β 3. *The Journal of clinical investigation,* **115**, 3363-3369.

Bergmeier, W., Rabie, T., Strehl, A., Piffath, C. L., Prostredna, M., Wagner, D. D. & Nieswandt, B. (2004). GPVI down-regulation in murine platelets through metalloproteinase-dependent shedding. *Thromb Haemost,* **91**, 951-8.

Berndt, M. C., Shen, Y., Dopheide, S. M., Gardiner, E. E. & Andrews, R. K. (2001). The vascular biology of the glycoprotein Ib-IX-V complex. *THROMBOSIS AND HAEMOSTASIS-STUTTGART-*, **86**, 178-188.

Berridge, M. J., Bootman, M. D. & Roderick, H. L. (2003). Calcium signalling: dynamics, homeostasis and remodelling. *Nat Rev Mol Cell Biol,* **4**, 517-29.

Berrier, A. L. & Yamada, K. M. (2007). Cell-matrix adhesion. *J Cell Physiol,* **213**, 565-73.

Bertagnolli, M. E. & Beckerle, M. C. (1993). Evidence for the selective association of a subpopulation of GPIIb-IIIa with the actin cytoskeletons of thrombin-activated platelets. *J Cell Biol,* **121**, 1329-42.

Best, D., Senis, Y. A., Jarvis, G. E., Eagleton, H. J., Roberts, D. J., Saito, T., Jung, S. M., Moroi, M., Harrison, P., Green, F. R. & Watson, S. P. (2003). GPVI levels in platelets: relationship to platelet function at high shear. *Blood,* **102**, 2811-8.

Blair, P. & Flaumenhaft, R. (2009). Platelet alpha-granules: basic biology and clinical correlates. *Blood Rev,* **23**, 177-89.

Bledzka, K., Smyth, S. S. & Plow, E. F. (2013). Integrin alphaIIbbeta3: from discovery to efficacious therapeutic target. *Circ Res,* **112**, 1189-200.

Bottcher, R. T., Lange, A. & Fassler, R. (2009). How ILK and kindlins cooperate to orchestrate integrin signaling. *Curr Opin Cell Biol,* **21**, 670-5.

Boylan, B., Gao, C., Rathore, V., Gill, J. C., Newman, D. K. & Newman, P. J. (2008). Identification of FcgammaRIIa as the ITAM-bearing receptor mediating

alphaIIbbeta3 outside-in integrin signaling in human platelets. *Blood,* **112**, 2780-6.

Brass, L. F., Manning, D. R., Cichowski, K. & Abrams, C. S. (1997). Signaling through G proteins in platelets: to the integrins and beyond. *Thromb Haemost,* **78**, 581-9.

Brass, L. F., Wannemacher, K. M., Ma, P. & Stalker, T. J. (2011). Regulating thrombus growth and stability to achieve an optimal response to injury. *Journal of Thrombosis and Haemostasis,* **9**, 66-75.

Braun, A., Bordoy, R., Stanchi, F., Moser, M., Kostka, G. G., Ehler, E., Brandau, O. & Fassler, R. (2003). PINCH2 is a new five LIM domain protein, homologous to PINCHand localized to focal adhesions. *Exp Cell Res,* **284**, 239-50.

Briddell, R. A., Brandt, J. E., Straneva, J. E., Srour, E. F. & Hoffman, R. (1989). Characterization of the human burst-forming unit-megakaryocyte. *Blood,* **74**, 145-151.

Briddon, S. J. & Watson, S. P. (1999). Evidence for the involvement of p59fyn and p53/56lyn in collagen receptor signalling in human platelets. *Biochem J,* **338 (Pt 1)**, 203-9.

Calderwood, D. A. (2004). Integrin activation. *J Cell Sci,* **117**, 657-66.

Calderwood, D. A., Campbell, I. D. & Critchley, D. R. (2013). Talins and kindlins: partners in integrin-mediated adhesion. *Nat Rev Mol Cell Biol,* **14**, 503-17.

Calderwood, D. A., Yan, B., de Pereda, J. M., Alvarez, B. G., Fujioka, Y., Liddington, R. C. & Ginsberg, M. H. (2002). The phosphotyrosine binding-like domain of talin activates integrins. *J Biol Chem,* **277**, 21749-58.

Campbell, I. D. & Humphries, M. J. (2011). Integrin structure, activation, and interactions. *Cold Spring Harbor perspectives in biology,* **3**, a004994.

Chiswell, B. P., Zhang, R., Murphy, J. W., Boggon, T. J. & Calderwood, D. A. (2008). The structural basis of integrin-linked kinase-PINCH interactions. *Proc Natl Acad Sci U S A,* **105**, 20677-82.

Chrzanowska-Wodnicka, M., Smyth, S. S., Schoenwaelder, S. M., Fischer, T. H. & White, G. C., 2nd (2005). Rap1b is required for normal platelet function and hemostasis in mice. *J Clin Invest,* **115**, 680-7.

Chu, H., Thievessen, I., Sixt, M., Lammermann, T., Waisman, A., Braun, A., Noegel, A. A. & Fassler, R. (2006). gamma-Parvin is dispensable for hematopoiesis, leukocyte trafficking, and T-cell-dependent antibody response. *Mol Cell Biol,* **26**, 1817-25.

Cicmil, M., Thomas, J. M., Leduc, M., Bon, C. & Gibbins, J. M. (2002). Platelet endothelial cell adhesion molecule-1 signaling inhibits the activation of human platelets. *Blood,* **99**, 137-44.

Cifuni, S. M., Wagner, D. D. & Bergmeier, W. (2008). CalDAG-GEFI and protein kinase C represent alternative pathways leading to activation of integrin alphaIIbbeta3 in platelets. *Blood,* **112**, 1696-703.

Cimmino, G. & Golino, P. (2013). Platelet Biology and Receptor Pathways. *Journal of Cardiovascular Translational Research,* **6**, 299-309.

Clemetson, J. M., Polgar, J., Magnenat, E., Wells, T. N. & Clemetson, K. J. (1999). The platelet collagen receptor glycoprotein VI is a member of the immunoglobulin superfamily closely related to FcalphaR and the natural killer receptors. *J Biol Chem,* **274**, 29019-24.

Clemetson, K. J. & Clemetson, J. M. (2001). Platelet collagen receptors. *Thromb Haemost,* **86**, 189-97.

Coller, B. S. (2012). A brief history of ideas about platelets in health and disease. *Platelets. Academic, New York, pp xix–liv*.

Coller, B. S., Scudder, L. E., Beer, J., Gold, H. K., Folts, J. D., Cavagnaro, J., Jordan, R., Wagner, C., Iuliucci, J., Knight, D. & et al. (1991). Monoclonal antibodies to platelet glycoprotein IIb/IIIa as antithrombotic agents. *Ann N Y Acad Sci,* **614**, 193-213.

Coller, B. S. & Shattil, S. J. (2008). The GPIIb/IIIa (integrin alphaIIbbeta3) odyssey: a technology-driven saga of a receptor with twists, turns, and even a bend. *Blood,* **112**, 3011-25.

Coughlin, S. R. (1998). Sol Sherry lecture in thrombosis: how thrombin 'talks' to cells: molecular mechanisms and roles in vivo. *Arterioscler Thromb Vasc Biol,* **18**, 514-8.

Coughlin, S. R. (2000). Thrombin signalling and protease-activated receptors. *Nature,* **407**, 258-264.

Crittenden, J. R., Bergmeier, W., Zhang, Y., Piffath, C. L., Liang, Y., Wagner, D. D., Housman, D. E. & Graybiel, A. M. (2004). CalDAG-GEFI integrates signaling for platelet aggregation and thrombus formation. *Nat Med,* **10**, 982-6.

D'Silva, N. J., Jacobson, K. L., Ott, S. M. & Watson, E. L. (1998). Beta-adrenergic-induced cytosolic redistribution of Rap1 in rat parotid acini: role in secretion. *Am J Physiol,* **274**, C1667-73.

Das, M., Ithychanda, S., Qin, J. & Plow, E. F. (2014). Mechanisms of talin-dependent integrin signaling and crosstalk. *Biochim Biophys Acta*, **1838**, 579-88.

Davi, G. & Patrono, C. (2007). Platelet activation and atherothrombosis. *N Engl J Med*, **357**, 2482-94.

Dawood, B. B., Lowe, G. C., Lordkipanidze, M., Bem, D., Daly, M. E., Makris, M., Mumford, A., Wilde, J. T. & Watson, S. P. (2012). Evaluation of participants with suspected heritable platelet function disorders including recommendation and validation of a streamlined agonist panel. *Blood*, **120**, 5041-9.

de la Puente, P., Weisberg, E., Muz, B., Nonami, A., Luderer, M., Stone, R. M., Melo, J. V., Griffin, J. D. & Azab, A. K. (2015). Identification of ILK as a novel therapeutic target for acute and chronic myeloid leukemia. *Leuk Res*.

Delcommenne, M., Tan, C., Gray, V., Rue, L., Woodgett, J. & Dedhar, S. (1998). Phosphoinositide-3-OH kinase-dependent regulation of glycogen synthase kinase 3 and protein kinase B/AKT by the integrin-linked kinase. *Proceedings of the National Academy of Sciences*, **95**, 11211-11216.

Dhanjal, T. S., Ross, E. A., Auger, J. M., Mccarty, O. J., Hughes, C. E., Senis, Y. A. & Watson, S. P. (2007). Minimal regulation of platelet activity by PECAM-1. *Platelets*, **18**, 56-67.

Djellas, Y., Manganello, J. M., Antonakis, K. & Le Breton, G. C. (1999). Identification of Gα13 as one of the G-proteins that couple to human platelet thromboxane A2 receptors. *Journal of Biological Chemistry*, **274**, 14325-14330.

Dorris, S. L. & Peebles, R. S., Jr. (2012). PGI2 as a regulator of inflammatory diseases. *Mediators Inflamm*, **2012**, 926968.

El-Haroun, H., Clarke, D. L., Deacon, K., Bradbury, D., Clayton, A., Sutcliffe, A. & Knox, A. J. (2008). IL-1beta, BK, and TGF-beta1 attenuate PGI2-mediated cAMP formation in human pulmonary artery smooth muscle cells by multiple mechanisms involving p38 MAP kinase and PKA. *Am J Physiol Lung Cell Mol Physiol*, **294**, L553-62.

Emambokus, N. R. & Frampton, J. (2003). The glycoprotein IIb molecule is expressed on early murine hematopoietic progenitors and regulates their numbers in sites of hematopoiesis. *Immunity*, **19**, 33-45.

Eyre, L. & Gamlin, F. (2010). Haemostasis, blood platelets and coagulation. *Anaesthesia & Intensive Care Medicine*, **11**, 244-246.

Ezumi, Y., Shindoh, K., Tsuji, M. & Takayama, H. (1998). Physical and functional association of the Src family kinases Fyn and Lyn with the collagen receptor glycoprotein VI-Fc receptor gamma chain complex on human platelets. *J Exp Med,* **188**, 267-76.

Fagerholm, S. C., Lek, H. S. & Morrison, V. L. (2014). Kindlin-3 in the immune system. *Am J Clin Exp Immunol,* **3**, 37-42.

Falati, S., Patil, S., Gross, P. L., Stapleton, M., Merrill-Skoloff, G., Barrett, N. E., Pixton, K. L., Weiler, H., Cooley, B. & Newman, D. K. (2006). Platelet PECAM-1 inhibits thrombus formation in vivo. *Blood,* **107**, 535-541.

FitzGerald, G. A. (1991). Mechanisms of platelet activation: thromboxane A2 as an amplifying signal for other agonists. *Am J Cardiol,* **68**, 11b-15b.

Fong, K. P., Zhu, H., Span, L. M., Moore, D. T., Yoon, K., Tamura, R., Yin, H., DeGrado, W. F. & Bennett, J. S. (2016). Directly Activating the Integrin alphaIIbbeta3 Initiates Outside-In Signaling by Causing alphaIIbbeta3 Clustering. *J Biol Chem,* **291**, 11706-16.

Frenette, P. S., Denis, C. V., Weiss, L., Jurk, K., Subbarao, S., Kehrel, B., Hartwig, J. H., Vestweber, D. & Wagner, D. D. (2000). P-Selectin glycoprotein ligand 1 (PSGL-1) is expressed on platelets and can mediate platelet-endothelial interactions in vivo. *The Journal of experimental medicine,* **191**, 1413-1422.

Friedrich, E. B., Liu, E., Sinha, S., Cook, S., Milstone, D. S., MacRae, C. A., Mariotti, M., Kuhlencordt, P. J., Force, T., Rosenzweig, A., St-Arnaud, R., Dedhar, S. & Gerszten, R. E. (2004). Integrin-linked kinase regulates endothelial cell survival and vascular development. *Mol Cell Biol,* **24**, 8134-44.

Frische, E. W. & Zwartkruis, F. J. (2010). Rap1, a mercenary among the Ras-like GTPases. *Dev Biol,* **340**, 1-9.

Fukuda, K., Bledzka, K., Yang, J., Perera, H. D., Plow, E. F. & Qin, J. (2014). Molecular basis of kindlin-2 binding to integrin-linked kinase pseudokinase for regulating cell adhesion. *J Biol Chem,* **289**, 28363-75.

Gachet, C., Leon, C. & Hechler, B. (2006). The platelet P2 receptors in arterial thrombosis. *Blood Cells Mol Dis,* **36**, 223-7.

Gao, J., Zoller, K. E., Ginsberg, M. H., Brugge, J. S. & Shattil, S. J. (1997). Regulation of the pp72syk protein tyrosine kinase by platelet integrin alpha IIb beta 3. *Embo j,* **16**, 6414-25.

Gardiner, E. E., Karunakaran, D., Shen, Y., Arthur, J. F., Andrews, R. K. & Berndt, M. C. (2007). Controlled shedding of platelet glycoprotein (GP)VI and GPIb-IX-V by ADAM family metalloproteinases. *J Thromb Haemost,* **5**, 1530-7.

Gerrard, J. M., White, J. G. & Peterson, D. A. (1978). The platelet dense tubular system: its relationship to prostaglandin synthesis and calcium flux. *Thromb Haemost,* **40**, 224-31.

Ghosh, D. K. & Salerno, J. C. (2003). Nitric oxide synthases: domain structure and alignment in enzyme function and control. *Front Biosci,* **8**, d193-209.

Giancotti, F. G. & Ruoslahti, E. (1999). Integrin signaling. *Science,* **285**, 1028-32.

Gibbins, J., Asselin, J., Farndale, R., Barnes, M., Law, C.-L. & Watson, S. P. (1996). Tyrosine phosphorylation of the Fc receptor γ-chain in collagen-stimulated platelets. *Journal of Biological Chemistry,* **271**, 18095-18099.

Gibbins, J. M. (2004). Platelet adhesion signalling and the regulation of thrombus formation. *J Cell Sci,* **117**, 3415-25.

Gibbins, J. M., Okuma, M., Farndale, R., Barnes, M. & Watson, S. P. (1997). Glycoprotein VI is the collagen receptor in platelets which underlies tyrosine phosphorylation of the Fc receptor γ-chain. *FEBS letters,* **413**, 255-259.

Gingras, A. R., Ziegler, W. H., Bobkov, A. A., Joyce, M. G., Fasci, D., Himmel, M., Rothemund, S., Ritter, A., Grossmann, J. G., Patel, B., Bate, N., Goult, B. T., Emsley, J., Barsukov, I. L., Roberts, G. C., Liddington, R. C., Ginsberg, M. H. & Critchley, D. R. (2009). Structural determinants of integrin binding to the talin rod. *J Biol Chem,* **284**, 8866-76.

Goggs, R. & Poole, A. W. (2012). Platelet signaling-a primer. *J Vet Emerg Crit Care (San Antonio),* **22**, 5-29.

Goksoy, E., Ma, Y.-Q., Wang, X., Kong, X., Perera, D., Plow, E. F. & Qin, J. (2008). Structural basis for the autoinhibition of talin in regulating integrin activation. *Molecular cell,* **31**, 124-133.

Golden, A., Brugge, J. S. & Shattil, S. J. (1990). Role of platelet membrane glycoprotein IIb-IIIa in agonist-induced tyrosine phosphorylation of platelet proteins. *J Cell Biol,* **111**, 3117-27.

Golden, A., Nemeth, S. P. & Brugge, J. S. (1986). Blood platelets express high levels of the pp60c-src-specific tyrosine kinase activity. *Proc Natl Acad Sci U S A,* **83**, 852-6.

Golebiewska, E. M. & Poole, A. W. (2015). Platelet secretion: From haemostasis to wound healing and beyond. *Blood Rev,* **29**, 153-62.

Grashoff, C., Aszodi, A., Sakai, T., Hunziker, E. B. & Fassler, R. (2003). Integrin-linked kinase regulates chondrocyte shape and proliferation. *EMBO Rep,* **4**, 432-8.

Grosse, J., Braun, A., Varga-Szabo, D., Beyersdorf, N., Schneider, B., Zeitlmann, L., Hanke, P., Schropp, P., Mühlstedt, S. & Zorn, C. (2007). An EF hand mutation in Stim1 causes premature platelet activation and bleeding in mice. *The Journal of clinical investigation,* **117**, 3540-3550.

Grüner, S., Prostredna, M., Schulte, V., Krieg, T., Eckes, B., Brakebusch, C. & Nieswandt, B. (2003). Multiple integrin-ligand interactions synergize in shear-resistant platelet adhesion at sites of arterial injury in vivo. *Blood,* **102**, 4021-4027.

Guan, S. Y., Chng, C. P., Ong, L. T., Tan, H. F., Alex Law, S. K. & Tan, S. M. (2018). The binding interface of kindlin-2 and ILK involves Asp344/Asp352/Thr356 in kindlin-2 and Arg243/Arg334 in ILK. *FEBS Lett,* **592**, 112-121.

Guidetti, G. F. & Torti, M. (2012). The Small GTPase Rap1b: A Bidirectional Regulator of Platelet Adhesion Receptors. *J Signal Transduct,* **2012**, 412089.

Han, J., Lim, C. J., Watanabe, N., Soriani, A., Ratnikov, B., Calderwood, D. A., Puzon-McLaughlin, W., Lafuente, E. M., Boussiotis, V. A., Shattil, S. J. & Ginsberg, M. H. (2006). Reconstructing and deconstructing agonist-induced activation of integrin alphaIIbbeta3. *Curr Biol,* **16**, 1796-806.

Hanafy, K. A., Krumenacker, J. S. & Murad, F. (2001). NO, nitrotyrosine, and cyclic GMP in signal transduction. *Med Sci Monit,* **7**, 801-19.

Hannigan, G. E., Leung-Hagesteijn, C., Fitz-Gibbon, L., Coppolino, M. G., Radeva, G., Filmus, J., Bell, J. C. & Dedhar, S. (1996). Regulation of cell adhesion and anchorage-dependent growth by a new beta 1-integrin-linked protein kinase. *Nature,* **379**, 91-6.

Hantgan, R. R., Lyles, D. S., Mallett, T. C., Rocco, M., Nagaswami, C. & Weisel, J. W. (2003). Ligand binding promotes the entropy-driven oligomerization of integrin alpha IIb beta 3. *J Biol Chem,* **278**, 3417-26.

Harburger, D. S., Bouaouina, M. & Calderwood, D. A. (2009). Kindlin-1 and -2 directly bind the C-terminal region of beta integrin cytoplasmic tails and exert integrin-specific activation effects. *J Biol Chem,* **284**, 11485-97.

Harburger, D. S. & Calderwood, D. A. (2009). Integrin signalling at a glance. *J Cell Sci,* **122**, 159-63.

Hartwig, J. H. & DeSisto, M. (1991). The cytoskeleton of the resting human blood platelet: structure of the membrane skeleton and its attachment to actin filaments. *J Cell Biol,* **112**, 407-25.

Hathaway, D. R. & Adelstein, R. S. (1979). Human platelet myosin light chain kinase requires the calcium-binding protein calmodulin for activity. *Proc Natl Acad Sci U S A,* **76**, 1653-7.

Hechler, B., Leon, C., Vial, C., Vigne, P., Frelin, C., Cazenave, J. P. & Gachet, C. (1998). The P2Y1 receptor is necessary for adenosine 5'-diphosphate-induced platelet aggregation. *Blood,* **92**, 152-9.

Heemskerk, J. W., Bevers, E. M. & Lindhout, T. (2002). Platelet activation and blood coagulation. *Thromb Haemost,* **88**, 186-93.

Heilemann, M., van de Linde, S., Schuttpelz, M., Kasper, R., Seefeldt, B., Mukherjee, A., Tinnefeld, P. & Sauer, M. (2008). Subdiffraction-resolution fluorescence imaging with conventional fluorescent probes. *Angew Chem Int Ed Engl,* **47**, 6172-6.

Henriques, R., Lelek, M., Fornasiero, E. F., Valtorta, F., Zimmer, C. & Mhlanga, M. M. (2010). QuickPALM: 3D real-time photoactivation nanoscopy image processing in ImageJ. *Nat Methods*, **7**, 339-40.

Hodivala-Dilke, K. M., McHugh, K. P., Tsakiris, D. A., Rayburn, H., Crowley, D., Ullman-Culleré, M., Ross, F. P., Coller, B. S., Teitelbaum, S. & Hynes, R. O. (1999). β3-integrin–deficient mice are a model for Glanzmann thrombasthenia showing placental defects and reduced survival. *The Journal of clinical investigation*, **103**, 229-238.

Holtkotter, O., Nieswandt, B., Smyth, N., Muller, W., Hafner, M., Schulte, V., Krieg, T. & Eckes, B. (2002). Integrin alpha 2-deficient mice develop normally, are fertile, but display partially defective platelet interaction with collagen. *J Biol Chem,* **277**, 10789-94.

Honda, S., Shirotani-Ikejima, H., Tadokoro, S., Maeda, Y., Kinoshita, T., Tomiyama, Y. & Miyata, T. (2009). Integrin-linked kinase associated with integrin activation. *Blood,* **113**, 5304-13.

Honda, S., Shirotani-Ikejima, H., Tadokoro, S., Tomiyama, Y. & Miyata, T. (2013). The integrin-linked kinase-PINCH-parvin complex supports integrin alphaIIbbeta3 activation. *PLoS One,* **8**, e85498.

Huang, B., Wang, W., Bates, M. & Zhuang, X. (2008). Three-dimensional super-resolution imaging by stochastic optical reconstruction microscopy. *Science,* **319**, 810-3.

Huang, J., Li, X., Shi, X., Zhu, M., Wang, J., Huang, S., Huang, X., Wang, H., Li, L., Deng, H., Zhou, Y., Mao, J., Long, Z., Ma, Z., Ye, W., Pan, J., Xi, X. & Jin, J. (2019). Platelet integrin alphaIIbbeta3: signal transduction, regulation, and its therapeutic targeting. *J Hematol Oncol,* **12**, 26.

Huang, J. S., Dong, L., Kozasa, T. & Le Breton, G. C. (2007). Signaling through G(alpha)13 switch region I is essential for protease-activated receptor 1-mediated human platelet shape change, aggregation, and secretion. *J Biol Chem,* **282**, 10210-22.

Huang, J. S., Ramamurthy, S. K., Lin, X. & Le Breton, G. C. (2004). Cell signalling through thromboxane A2 receptors. *Cell Signal,* **16**, 521-33.

Huang, M. M., Lipfert, L., Cunningham, M., Brugge, J. S., Ginsberg, M. H. & Shattil, S. J. (1993). Adhesive ligand binding to integrin alpha IIb beta 3 stimulates tyrosine phosphorylation of novel protein substrates before phosphorylation of pp125FAK. *J Cell Biol,* **122**, 473-83.

Huet-Calderwood, C., Brahme, N. N., Kumar, N., Stiegler, A. L., Raghavan, S., Boggon, T. J. & Calderwood, D. A. (2014). Differences in binding to the ILK complex determines kindlin isoform adhesion localization and integrin activation. *J Cell Sci,* **127**, 4308-21.

Hynes, R. O. (1987). Integrins: a family of cell surface receptors. *Cell,* **48**, 549-54.

Hynes, R. O. (2002). Integrins: bidirectional, allosteric signaling machines. *Cell,* **110**, 673-87.

Inoue, O., Suzuki-Inoue, K., Dean, W. L., Frampton, J. & Watson, S. P. (2003). Integrin alpha2beta1 mediates outside-in regulation of platelet spreading on collagen through activation of Src kinases and PLCgamma2. *J Cell Biol,* **160**, 769-80.

Inoue, O., Suzuki-Inoue, K., McCarty, O. J., Moroi, M., Ruggeri, Z. M., Kunicki, T. J., Ozaki, Y. & Watson, S. P. (2006). Laminin stimulates spreading of platelets through integrin alpha6beta1-dependent activation of GPVI. *Blood,* **107**, 1405-12.

Jackson, S. P., Schoenwaelder, S. M., Yuan, Y., Salem, H. H. & Cooray, P. (1996). Non-receptor protein tyrosine kinases and phosphatases in human platelets. *Thromb Haemost,* **76**, 640-50.

Jantzen, H. M., Milstone, D. S., Gousset, L., Conley, P. B. & Mortensen, R. M. (2001). Impaired activation of murine platelets lacking G alpha(i2). *J Clin Invest,* **108**, 477-83.

Jones, C. I., Garner, S. F., Moraes, L. A., Kaiser, W. J., Rankin, A., Ouwehand, W. H., Goodall, A. H. & Gibbins, J. M. (2009). PECAM-1 expression and activity negatively regulate multiple platelet signaling pathways. *FEBS Lett,* **583**, 3618-24.

Jones, C. I., Tucker, K. L., Sasikumar, P., Sage, T., Kaiser, W. J., Moore, C., Emerson, M. & Gibbins, J. M. (2014). Integrin-linked kinase regulates the rate of platelet activation and is essential for the formation of stable thrombi. *J Thromb Haemost,* **12**, 1342-52.

Jones, K. L., Hughan, S. C., Dopheide, S. M., Farndale, R. W., Jackson, S. P. & Jackson, D. E. (2001). Platelet endothelial cell adhesion molecule-1 is a negative regulator of platelet-collagen interactions. *Blood,* **98**, 1456-63.

Joo, S. J. (2012). Mechanisms of Platelet Activation and Integrin alphaIIbeta3. *Korean Circ J,* **42**, 295-301.

Jung, S. M. & Moroi, M. (2000). Activation of the platelet collagen receptor integrin alpha(2)beta(1): its mechanism and participation in the physiological functions of platelets. *Trends Cardiovasc Med,* **10**, 285-92.

Jurk, K. & Kehrel, B. E. (2005). Platelets: physiology and biochemistry. *Semin Thromb Hemost,* **31**, 381-92.

Kadry, Y. A., Huet-Calderwood, C., Simon, B. & Calderwood, D. A. (2018). Kindlin-2 interacts with a highly conserved surface of ILK to regulate focal adhesion localization and cell spreading. *Journal of Cell Science,* **131**, jcs221184.

Kahn, M. L., Nakanishi-Matsui, M., Shapiro, M. J., Ishihara, H. & Coughlin, S. R. (1999). Protease-activated receptors 1 and 4 mediate activation of human platelets by thrombin. *Journal of Clinical Investigation,* **103**, 879.

Kanaji, S., Kanaji, T., Furihata, K., Kato, K., Ware, J. L. & Kunicki, T. J. (2003). Convulxin binds to native, human glycoprotein Ib alpha. *J Biol Chem,* **278**, 39452-60.

Kanemaru, T., Hirata, K., Takasu, S., Isobe, S., Mizuki, K., Mataka, S. & Nakamura, K. (2009). A fluorescence scanning electron microscope. *Ultramicroscopy,* **109**, 344-9.

Karakose, E., Schiller, H. B. & Fassler, R. (2010). The kindlins at a glance. *J Cell Sci,* **123**, 2353-6.

Kaushansky, K. (1995). Thrombopoietin: the primary regulator of megakaryocyte and platelet production. *Thrombosis and haemostasis,* **74**, 521-525.

Kaushansky, K. (2009). Determinants of platelet number and regulation of thrombopoiesis. *Hematology Am Soc Hematol Educ Program,* 147-52.

Klinz, F. J., Seifert, R., Schwaner, I., Gausepohl, H., Frank, R. & Schultz, G. (1992). Generation of specific antibodies against the rap1A, rap1B and rap2 small GTP-binding proteins. Analysis of rap and ras proteins in membranes from mammalian cells. *Eur J Biochem,* **207**, 207-13.

Kloeker, S., Major, M. B., Calderwood, D. A., Ginsberg, M. H., Jones, D. A. & Beckerle, M. C. (2004). The Kindler syndrome protein is regulated by transforming growth factor-beta and involved in integrin-mediated adhesion. *J Biol Chem,* **279**, 6824-33.

Konishi, H., Katoh, Y., Takaya, N., Kashiwakura, Y., Itoh, S., Ra, C. & Daida, H. (2002). Platelets activated by collagen through immunoreceptor tyrosine-based activation motif play pivotal role in initiation and generation of neointimal hyperplasia after vascular injury. *Circulation,* **105**, 912-6.

Konopatskaya, O., Gilio, K., Harper, M. T., Zhao, Y., Cosemans, J. M., Karim, Z. A., Whiteheart, S. W., Molkentin, J. D., Verkade, P., Watson, S. P., Heemskerk, J. W. & Poole, A. W. (2009). PKCalpha regulates platelet granule secretion and thrombus formation in mice. *J Clin Invest,* **119**, 399-407.

Kulkarni, S., Dopheide, S. M., Yap, C. L., Ravanat, C., Freund, M., Mangin, P., Heel, K. A., Street, A., Harper, I. S., Lanza, F. & Jackson, S. P. (2000). A revised model of platelet aggregation. *J Clin Invest,* **105**, 783-91.

Kumar, R. A., Dong, J. F., Thaggard, J. A., Cruz, M. A., Lopez, J. A. & McIntire, L. V. (2003). Kinetics of GPIbalpha-vWF-A1 tether bond under flow: effect of GPIbalpha mutations on the association and dissociation rates. *Biophys J,* **85**, 4099-109.

Lagarrigue, F., Kim, C. & Ginsberg, M. H. (2016). The Rap1-RIAM-talin axis of integrin activation and blood cell function. *Blood,* **128**, 479-87.

Lai-Cheong, J., Ussar, S., Arita, K., Hart, I. & McGrath, J. (2008). Colocalization of kindlin-1, kindlin-2, and migfilin at keratinocyte focal adhesion and relevance to the pathophysiology of Kindler syndrome. *Journal of Investigative Dermatology,* **128**, 2156-2165.

Lam, W. A., Chaudhuri, O., Crow, A., Webster, K. D., Li, T. D., Kita, A., Huang, J. & Fletcher, D. A. (2011). Mechanics and contraction dynamics of single platelets and implications for clot stiffening. *Nat Mater,* **10**, 61-6.

Larjava, H., Plow, E. F. & Wu, C. (2008). Kindlins: essential regulators of integrin signalling and cell-matrix adhesion. *EMBO Rep,* **9**, 1203-8.

Lecut, C., Schoolmeester, A., Kuijpers, M. J., Broers, J. L., van Zandvoort, M. A., Vanhoorelbeke, K., Deckmyn, H., Jandrot-Perrus, M. & Heemskerk, J. W. (2004). Principal role of glycoprotein VI in alpha2beta1 and alphaIIbbeta3 activation during collagen-induced thrombus formation. *Arterioscler Thromb Vasc Biol,* **24**, 1727-33.

Lee, H.-S., Lim, C. J., Puzon-McLaughlin, W., Shattil, S. J. & Ginsberg, M. H. (2009). RIAM activates integrins by linking talin to ras GTPase membrane-targeting sequences. *Journal of Biological Chemistry,* **284**, 5119-5127.

Lee, S. L., Hsu, E. C., Chou, C. C., Chuang, H. C., Bai, L. Y., Kulp, S. K. & Chen, C. S. (2011). Identification and characterization of a novel integrin-linked kinase inhibitor. *J Med Chem,* **54**, 6364-74.

Legate, K. R., Montag, D., Bottcher, R. T., Takahashi, S. & Fassler, R. (2012). Comparative phenotypic analysis of the two major splice isoforms of phosphatidylinositol phosphate kinase type Igamma in vivo. *J Cell Sci,* **125**, 5636-46.

Legate, K. R., Montañez, E., Kudlacek, O. & Füssler, R. (2006). ILK, PINCH and parvin: the tIPP of integrin signalling. *Nature reviews Molecular cell biology,* **7**, 20-31.

Lemmon, M. A. (2004). Pleckstrin homology domains: not just for phosphoinositides. *Biochem Soc Trans,* **32**, 707-11.

Leung, B. O. & Chou, K. C. (2011). Review of super-resolution fluorescence microscopy for biology. *Appl Spectrosc,* **65**, 967-80.

Levet, F., Hosy, E., Kechkar, A., Butler, C., Beghin, A., Choquet, D. & Sibarita, J. B. (2015). SR-Tesseler: a method to segment and quantify localization-based super-resolution microscopy data. *Nat Methods,* **12**, 1065-71.

Li, Y., Tan, X., Dai, C., Stolz, D. B., Wang, D. & Liu, Y. (2009). Inhibition of integrin-linked kinase attenuates renal interstitial fibrosis. *J Am Soc Nephrol,* **20**, 1907-18.

Li, Z., Delaney, M. K., O'Brien, K. A. & Du, X. (2010). Signaling during platelet adhesion and activation. *Arterioscler Thromb Vasc Biol,* **30**, 2341-9.

Lichtman, J. W. & Conchello, J. A. (2005). Fluorescence microscopy. *Nat Methods,* **2**, 910-9.

Lieberman, E. H., O'Neill, S. & Mendelsohn, M. E. (1991). S-nitrosocysteine inhibition of human platelet secretion is correlated with increases in platelet cGMP levels. *Circ Res,* **68**, 1722-8.

Liou, J., Kim, M. L., Heo, W. D., Jones, J. T., Myers, J. W., Ferrell, J. E., Jr. & Meyer, T. (2005). STIM is a Ca2+ sensor essential for Ca2+-store-depletion-triggered Ca2+ influx. *Curr Biol,* **15**, 1235-41.

Lockyer, S., Okuyama, K., Begum, S., Le, S., Sun, B., Watanabe, T., Matsumoto, Y., Yoshitake, M., Kambayashi, J. & Tandon, N. N. (2006). GPVI-deficient mice lack collagen responses and are protected against experimentally induced pulmonary thromboembolism. *Thromb Res,* **118**, 371-80.

Lopez, J. A., Andrews, R. K., Afshar-Kharghan, V. & Berndt, M. C. (1998). Bernard-Soulier syndrome. *Blood,* **91**, 4397-418.

Lova, P., Paganini, S., Hirsch, E., Barberis, L., Wymann, M., Sinigaglia, F., Balduini, C. & Torti, M. (2003). A selective role for phosphatidylinositol 3, 4, 5-trisphosphate in the Gi-dependent activation of platelet Rap1B. *Journal of Biological Chemistry,* **278**, 131-138.

Luo, S. Z., Mo, X., Afshar-Kharghan, V., Srinivasan, S., Lopez, J. A. & Li, R. (2007). Glycoprotein Ibalpha forms disulfide bonds with 2 glycoprotein Ibbeta subunits in the resting platelet. *Blood,* **109**, 603-9.

Ma, Y. Q., Qin, J., Wu, C. & Plow, E. F. (2008). Kindlin-2 (Mig-2): a co-activator of beta3 integrins. *J Cell Biol,* **181**, 439-46.

Makris, M., O'Shaughnessy, D., & Lillicrap, D. (2009). Practical hemostasis and thrombosis. *Wiley-Blackwell.*, 1-6.

Malinin, N. L., Plow, E. F. & Byzova, T. V. (2010). Kindlins in FERM adhesion. *Blood,* **115**, 4011-7.

Malkusch, S., Endesfelder, U., Mondry, J., Gelleri, M., Verveer, P. J. & Heilemann, M. (2012). Coordinate-based colocalization analysis of single-molecule localization microscopy data. *Histochem Cell Biol,* **137**, 1-10.

Massberg, S., Gawaz, M., Gruner, S., Schulte, V., Konrad, I., Zohlnhofer, D., Heinzmann, U. & Nieswandt, B. (2003). A crucial role of glycoprotein VI for platelet recruitment to the injured arterial wall in vivo. *J Exp Med,* **197**, 41-9.

Maynard, D. M., Heijnen, H. F., Horne, M. K., White, J. G. & Gahl, W. A. (2007). Proteomic analysis of platelet alpha-granules using mass spectrometry. *J Thromb Haemost,* **5**, 1945-55.

McEver, R. (2007). P-Selectin/PSGL-1 and other interactions between platelets, leukocytes, and endothelium. *In:* Michelson, A. (ed.) *Platelets.* 2nd ed. San Diego (CA): Elsevier/Academic Press.

Merten, M., Chow, T., Hellums, J. D. & Thiagarajan, P. (2000). A new role for P-selectin in shear-induced platelet aggregation. *Circulation,* **102**, 2045-50.

Meves, A., Stremmel, C., Gottschalk, K. & Fassler, R. (2009). The Kindlin protein family: new members to the club of focal adhesion proteins. *Trends Cell Biol,* **19**, 504-13.

Michelson, A. D. (1992). Thrombin-induced down-regulation of the platelet membrane glycoprotein Ib-IX complex. *Semin Thromb Hemost,* **18**, 18-27.

Miranti, C. K. & Brugge, J. S. (2002). Sensing the environment: a historical perspective on integrin signal transduction. *Nat Cell Biol,* **4**, E83-90.

Mitchell, J. A., Ali, F., Bailey, L., Moreno, L. & Harrington, L. S. (2008). Role of nitric oxide and prostacyclin as vasoactive hormones released by the endothelium. *Exp Physiol*, **93**, 141-7.

Moerner, W. E. (2012). Microscopy beyond the diffraction limit using actively controlled single molecules. *J Microsc,* **246**, 213-20.

Mohite, A., Chillar, A., So, S. P., Cervantes, V. & Ruan, K. H. (2011). Novel mechanism of the vascular protector prostacyclin: regulating microRNA expression. *Biochemistry,* **50**, 1691-9.

Moncada, S. & Higgs, E. A. (2006). The discovery of nitric oxide and its role in vascular biology. *Br J Pharmacol,* **147 Suppl 1**, S193-201.

Morton, L. F., Hargreaves, P. G., Farndale, R. W., Young, R. D. & Barnes, M. J. (1995). Integrin alpha 2 beta 1-independent activation of platelets by simple collagen-like peptides: collagen tertiary (triple-helical) and quaternary (polymeric) structures

are sufficient alone for alpha 2 beta 1-independent platelet reactivity. *Biochem J,* **306 (Pt 2)**, 337-44.

Mory, A., Feigelson, S. W., Yarali, N., Kilic, S. S., Bayhan, G. I., Gershoni-Baruch, R., Etzioni, A. & Alon, R. (2008). Kindlin-3: a new gene involved in the pathogenesis of LAD-III. *Blood,* **112**, 2591-2591.

Moser, M., Bauer, M., Schmid, S., Ruppert, R., Schmidt, S., Sixt, M., Wang, H. V., Sperandio, M. & Fassler, R. (2009). Kindlin-3 is required for beta2 integrin-mediated leukocyte adhesion to endothelial cells. *Nat Med,* **15**, 300-5.

Moser, M., Nieswandt, B., Ussar, S., Pozgajova, M. & Fässler, R. (2008). Kindlin-3 is essential for integrin activation and platelet aggregation. *Nature medicine,* **14**, 325-330.

Mumford, A. D., Dawood, B. B., Daly, M. E., Murden, S. L., Williams, M. D., Protty, M. B., Spalton, J. C., Wheatley, M., Mundell, S. J. & Watson, S. P. (2010). A novel thromboxane A2 receptor D304N variant that abrogates ligand binding in a patient with a bleeding diathesis. *Blood,* **115**, 363-9.

Murugappa, S. & Kunapuli, S. P. (2006). The role of ADP receptors in platelet function. *Front Biosci,* **11**, 1977-86.

Nakeff, A. & Maat, B. (1974). Separation of Megakaryocytes From Mouse Bone Marrow by Velocity Sedimentation. *Blood,* **43**, 591-595.

Nan, X., Collisson, E. A., Lewis, S., Huang, J., Tamguney, T. M., Liphardt, J. T., McCormick, F., Gray, J. W. & Chu, S. (2013). Single-molecule superresolution imaging allows quantitative analysis of RAF multimer formation and signaling. *Proc Natl Acad Sci U S A,* **110**, 18519-24.

Newman, P. J. & Newman, D. K. (2003). Signal transduction pathways mediated by PECAM-1: new roles for an old molecule in platelet and vascular cell biology. *Arterioscler Thromb Vasc Biol,* **23**, 953-64.

Ni, H., Denis, C. V., Subbarao, S., Degen, J. L., Sato, T. N., Hynes, R. O. & Wagner, D. D. (2000). Persistence of platelet thrombus formation in arterioles of mice lacking both von Willebrand factor and fibrinogen. *J Clin Invest,* **106**, 385-92.

Niebuhr, K., Ebel, F., Frank, R., Reinhard, M., Domann, E., Carl, U. D., Walter, U., Gertler, F. B., Wehland, J. & Chakraborty, T. (1997). A novel proline-rich motif present in ActA of Listeria monocytogenes and cytoskeletal proteins is the ligand for the EVH1 domain, a protein module present in the Ena/VASP family. *Embo j,* **16**, 5433-44.

Nieswandt, B., Moser, M., Pleines, I., Varga-Szabo, D., Monkley, S., Critchley, D. & Fässler, R. (2007). Loss of talin1 in platelets abrogates integrin activation, platelet aggregation, and thrombus formation in vitro and in vivo. *Journal of Experimental Medicine,* **204**, 3113-3118.

Nieswandt, B., Varga-Szabo, D. & Elvers, M. (2009). Integrins in platelet activation. *J Thromb Haemost,* **7 Suppl 1**, 206-9.

Nieswandt, B. & Watson, S. P. (2003). Platelet-collagen interaction: is GPVI the central receptor? *Blood,* **102**, 449-61.

Nikolopoulos, S. N. & Turner, C. E. (2001). Integrin-linked kinase (ILK) binding to paxillin LD1 motif regulates ILK localization to focal adhesions. *J Biol Chem,* **276**, 23499-505.

Nurden, A. T. (2006). Glanzmann thrombasthenia. *Orphanet J Rare Dis,* **1**, b1.

Nurden, A. T. & Caen, J. P. (1975). Specific roles for platelet surface glycoproteins in platelet function. *Nature,* **255**, 720-2.

Obergfell, A., Eto, K., Mocsai, A., Buensuceso, C., Moores, S. L., Brugge, J. S., Lowell, C. A. & Shattil, S. J. (2002). Coordinate interactions of Csk, Src, and Syk kinases with [alpha]IIb[beta]3 initiate integrin signaling to the cytoskeleton. *J Cell Biol,* **157**, 265-75.

Offermanns, S. (2006). Activation of platelet function through G protein–coupled receptors. *Circulation research,* **99**, 1293-1304.

Ofosu, F. A. (2003). Protease activated receptors 1 and 4 govern the responses of human platelets to thrombin. *Transfusion and apheresis science,* **28**, 265-268.

Opal, S. M., Kessler, C. M., Roemisch, J. & Knaub, S. (2002). Antithrombin, heparin, and heparan sulfate. *Crit Care Med,* **30**, S325-31.

Ossovskaya, V. S. & Bunnett, N. W. (2004). Protease-activated receptors: contribution to physiology and disease. *Physiol Rev,* **84**, 579-621.

Owen, D. M., Rentero, C., Rossy, J., Magenau, A., Williamson, D., Rodriguez, M. & Gaus, K. (2010). PALM imaging and cluster analysis of protein heterogeneity at the cell surface. *J Biophotonics,* **3**, 446-54.

Ozaki, Y., Asazuma, N., Suzuki-Inoue, K. & Berndt, M. C. (2005). Platelet GPIb-IX-V-dependent signaling. *J Thromb Haemost,* **3**, 1745-51.

Pan, L., North, H. A., Sahni, V., Jeong, S. J., McGuire, T. L., Berns, E. J., Stupp, S. I. & Kessler, J. A. (2014). beta1-Integrin and integrin linked kinase regulate astrocytic differentiation of neural stem cells. *PLoS One,* **9**, e104335.

Parekh, A. B. & Putney, J. W., Jr. (2005). Store-operated calcium channels. *Physiol Rev,* **85**, 757-810.

Parise, L. V. (1999). Integrin alpha(IIb)beta(3) signaling in platelet adhesion and aggregation. *Curr Opin Cell Biol,* **11**, 597-601.

Pasquali, C., Bertschy-Meier, D., Chabert, C., Curchod, M.-L., Arod, C., Booth, R., Mechtler, K., Vilbois, F., Xenarios, I., Ferguson, C. G., Prestwich, G. D., Camps, M. & Rommel, C. (2007). A Chemical Proteomics Approach to Phosphatidylinositol 3-Kinase Signaling in Macrophages. *Molecular & Cellular Proteomics,* **6**, 1829-1841.

Paszek, M. J., Boettiger, D., Weaver, V. M. & Hammer, D. A. (2009). Integrin clustering is driven by mechanical resistance from the glycocalyx and the substrate. *PLoS Comput Biol,* **5**, e1000604.

Patil, S., Newman, D. K. & Newman, P. J. (2001). Platelet endothelial cell adhesion molecule-1 serves as an inhibitory receptor that modulates platelet responses to collagen. *Blood,* **97**, 1727-32.

Patrono, C., Garcia Rodriguez, L. A., Landolfi, R. & Baigent, C. (2005). Low-dose aspirin for the prevention of atherothrombosis. *N Engl J Med,* **353**, 2373-83.

Petrich, B. G. (2009). Talin-dependent integrin signalling in vivo. *Thromb Haemost,* **101**, 1020-4.

Phillips, D. R., Nannizzi-Alaimo, L. & Prasad, K. S. (2001). Beta3 tyrosine phosphorylation in alphaIIbbeta3 (platelet membrane GP IIb-IIIa) outside-in integrin signaling. *Thromb Haemost,* **86**, 246-58.

Polgar, J., Chung, S. H. & Reed, G. L. (2002). Vesicle-associated membrane protein 3 (VAMP-3) and VAMP-8 are present in human platelets and are required for granule secretion. *Blood,* **100**, 1081-3.

Pollock, J. S., Förstermann, U., Mitchell, J. A., Warner, T. D., Schmidt, H. H., Nakane, M. & Murad, F. (1991). Purification and characterization of particulate endothelium-derived relaxing factor synthase from cultured and native bovine aortic endothelial cells. *Proceedings of the National Academy of Sciences of the United States of America,* **88**, 10480-10484.

Poole, A., Gibbins, J. M., Turner, M., van Vugt, M. J., van de Winkel, J. G., Saito, T., Tybulewicz, V. L. & Watson, S. P. (1997). The Fc receptor gamma-chain and the tyrosine kinase Syk are essential for activation of mouse platelets by collagen. *Embo j,* **16**, 2333-41.

Postel, R., Margadant, C., Fischer, B., Kreft, M., Janssen, H., Secades, P., Zambruno, G. & Sonnenberg, A. (2013). Kindlin-1 mutant zebrafish as an in vivo model system to study adhesion mechanisms in the epidermis. *J Invest Dermatol,* **133**, 2180-90.

Qadota, H., Moerman, D. G. & Benian, G. M. (2012). A molecular mechanism for the requirement of PAT-4 (integrin-linked kinase (ILK)) for the localization of UNC-112 (Kindlin) to integrin adhesion sites. *J Biol Chem,* **287**, 28537-51.

Quek, L. S., Pasquet, J.-M., Hers, I., Cornall, R., Knight, G., Barnes, M., Hibbs, M. L., Dunn, A. R., Lowell, C. A. & Watson, S. P. (2000). Fyn and Lyn phosphorylate the Fc receptor γ chain downstream of glycoprotein VI in murine platelets, and Lyn regulates a novel feedback pathway. *Blood,* **96**, 4246-4253.

Raaijmakers, J. H. & Bos, J. L. (2009). Specificity in Ras and Rap signaling. *J Biol Chem,* **284**, 10995-9.

Reed, G. L., Fitzgerald, M. L. & Polgar, J. (2000). Molecular mechanisms of platelet exocytosis: insights into the "secrete" life of thrombocytes. *Blood,* **96**, 3334-42.

Ren, Q., Wimmer, C., Chicka, M. C., Ye, S., Ren, Y., Hughson, F. M. & Whiteheart, S. W. (2010). Munc13-4 is a limiting factor in the pathway required for platelet granule release and hemostasis. *Blood,* **116**, 869-77.

Ren, Q., Ye, S. & Whiteheart, S. W. (2008). The platelet release reaction: just when you thought platelet secretion was simple. *Curr Opin Hematol,* **15**, 537-41.

Richardson, J. L., Shivdasani, R. A., Boers, C., Hartwig, J. H. & Italiano, J. E. (2005). Mechanisms of organelle transport and capture along proplatelets during platelet production. *Blood,* **106**, 4066-4075.

Ripley, B. D. (1977). Modelling Spatial Patterns. *Journal of the Royal Statistical Society. Series B (Methodological),* **39**, 172-212.

Rivera, J., Lozano, M. L., Navarro-Núñez, L. & Vicente, V. (2009). Platelet receptors and signaling in the dynamics of thrombus formation. *haematologica,* **94**, 700-711.

Roberts, D. E., McNicol, A. & Bose, R. (2004). Mechanism of collagen activation in human platelets. *J Biol Chem,* **279**, 19421-30.

Rognoni, E., Ruppert, R. & Fassler, R. (2016). The kindlin family: functions, signaling properties and implications for human disease. *J Cell Sci,* **129**, 17-27.

Rosado, J. A., Jenner, S. & Sage, S. O. (2000). A role for the actin cytoskeleton in the initiation and maintenance of store-mediated calcium entry in human platelets. Evidence for conformational coupling. *J Biol Chem,* **275**, 7527-33.

Rossy, J., Cohen, E., Gaus, K. & Owen, D. M. (2014). Method for co-cluster analysis in multichannel single-molecule localisation data. *Histochem Cell Biol,* **141**, 605-12.

Ruggeri, Z. M. (2002). Platelets in atherothrombosis. *Nat Med,* **8**, 1227-34.

Rust, M. J., Bates, M. & Zhuang, X. (2006a). Stochastic optical reconstruction microscopy (STORM) provides sub-diffraction-limit image resolution. *Nature methods,* **3**, 793.

Rust, M. J., Bates, M. & Zhuang, X. (2006b). Sub-diffraction-limit imaging by stochastic optical reconstruction microscopy (STORM). *Nat Methods,* **3**, 793-5.

Sakai, T., Li, S., Docheva, D., Grashoff, C., Sakai, K., Kostka, G., Braun, A., Pfeifer, A., Yurchenco, P. D. & Fassler, R. (2003). Integrin-linked kinase (ILK) is required for polarizing the epiblast, cell adhesion, and controlling actin accumulation. *Genes Dev,* **17**, 926-40.

Savage, B., Almus-Jacobs, F. & Ruggeri, Z. M. (1998). Specific synergy of multiple substrate-receptor interactions in platelet thrombus formation under flow. *Cell,* **94**, 657-66.

Savi, P., Beauverger, P., Labouret, C., Delfaud, M., Salel, V., Kaghad, M. & Herbert, J. M. (1998). Role of P2Y1 purinoceptor in ADP-induced platelet activation. *FEBS Lett,* **422**, 291-5.

Schafer, A., Alexander, R. & Handin, R. (1980). Inhibition of platelet function by organic nitrate vasodilators. *Blood,* **55**, 649-654.

Semple, J. W., Italiano, J. E., Jr. & Freedman, J. (2011). Platelets and the immune continuum. *Nat Rev Immunol,* **11**, 264-74.

Senis, Y. A., Mazharian, A. & Mori, J. (2014). Src family kinases: at the forefront of platelet activation. *Blood,* **124**, 2013-24.

Shahpouri, M. M., Mousavi, S., Khorvash, F., Mousavi, S. M. & Hoseini, T. (2012). Anticoagulant therapy for ischemic stroke: A review of literature. *J Res Med Sci,* **17**, 396-401.

Shattil, S. J. & Brass, L. F. (1987). Induction of the fibrinogen receptor on human platelets by intracellular mediators. *J Biol Chem,* **262**, 992-1000.

Shattil, S. J., Kashiwagi, H. & Pampori, N. (1998). Integrin signaling: the platelet paradigm. *Blood,* **91**, 2645-2657.

Shattil, S. J., Kim, C. & Ginsberg, M. H. (2010). The final steps of integrin activation: the end game. *Nat Rev Mol Cell Biol,* **11**, 288-300.

Shattil, S. J. & Newman, P. J. (2004). Integrins: dynamic scaffolds for adhesion and signaling in platelets. *Blood,* **104**, 1606-1615.

Shi, X. & Wu, C. (2008). A suppressive role of mitogen inducible gene-2 in mesenchymal cancer cell invasion. *Mol Cancer Res,* **6**, 715-24.

Shrimpton, C. N., Borthakur, G., Larrucea, S., Cruz, M. A., Dong, J. F. & Lopez, J. A. (2002). Localization of the adhesion receptor glycoprotein Ib-IX-V complex to lipid rafts is required for platelet adhesion and activation. *J Exp Med,* **196**, 1057-66.

Siegel, D. H., Ashton, G. H., Penagos, H. G., Lee, J. V., Feiler, H. S., Wilhelmsen, K. C., South, A. P., Smith, F. J., Prescott, A. R., Wessagowit, V., Oyama, N., Akiyama, M., Al Aboud, D., Al Aboud, K., Al Githami, A., Al Hawsawi, K., Al Ismaily, A., Al-Suwaid, R., Atherton, D. J., Caputo, R., Fine, J. D., Frieden, I. J., Fuchs, E., Haber, R. M., Harada, T., Kitajima, Y., Mallory, S. B., Ogawa, H., Sahin, S., Shimizu, H., Suga, Y., Tadini, G., Tsuchiya, K., Wiebe, C. B., Wojnarowska, F., Zaghloul, A. B., Hamada, T., Mallipeddi, R., Eady, R. A., McLean, W. H., McGrath, J. A. & Epstein, E. H. (2003). Loss of kindlin-1, a human homolog of the Caenorhabditis elegans actin-extracellular-matrix linker protein UNC-112, causes Kindler syndrome. *Am J Hum Genet,* **73**, 174-87.

Soberman, R. J. & Christmas, P. (2006). Revisiting prostacyclin: new directions in pulmonary fibrosis and inflammation. *Am J Physiol Lung Cell Mol Physiol,* **291**, L142-3.

Song, X., Yang, J., Hirbawi, J., Ye, S., Perera, H. D., Goksoy, E., Dwivedi, P., Plow, E. F., Zhang, R. & Qin, J. (2012). A novel membrane-dependent on/off switch mechanism of talin FERM domain at sites of cell adhesion. *Cell Res,* **22**, 1533-45.

Stefanini, L. & Bergmeier, W. (2018). Negative regulators of platelet activation and adhesion. *J Thromb Haemost,* **16**, 220-230.

Stefanini, L., Roden, R. C. & Bergmeier, W. (2009). CalDAG-GEFI is at the nexus of calcium-dependent platelet activation. *Blood,* **114**, 2506-14.

Stevens, J., Jordan, P., Sage, T. & Gibbins, J. (2004). The regulation of integrin-linked kinase in human platelets: evidence for involvement in the regulation of integrin α2β1. *Journal of Thrombosis and Haemostasis,* **2**, 1443-1452.

Stitham, J., Arehart, E. J., Gleim, S. R., Douville, K. L. & Hwa, J. (2007). Human prostacyclin receptor structure and function from naturally-occurring and synthetic mutations. *Prostaglandins Other Lipid Mediat,* **82**, 95-108.

Stolla, M., Stefanini, L., Roden, R. C., Chavez, M., Hirsch, J., Greene, T., Ouellette, T. D., Maloney, S. F., Diamond, S. L., Poncz, M., Woulfe, D. S. & Bergmeier, W. (2011). The kinetics of alphaIIbbeta3 activation determines the size and stability of thrombi in mice: implications for antiplatelet therapy. *Blood,* **117**, 1005-13.

Suzuki-Inoue, K., Tulasne, D., Shen, Y., Bori-Sanz, T., Inoue, O., Jung, S. M., Moroi, M., Andrews, R. K., Berndt, M. C. & Watson, S. P. (2002). Association of Fyn and Lyn with the proline-rich domain of glycoprotein VI regulates intracellular signaling. *J Biol Chem*, **277**, 21561-6.

Svensson, L., Howarth, K., McDowall, A., Patzak, I., Evans, R., Ussar, S., Moser, M., Metin, A., Fried, M., Tomlinson, I. & Hogg, N. (2009). Leukocyte adhesion deficiency-III is caused by mutations in KINDLIN3 affecting integrin activation. *Nat Med,* **15**, 306-12.

Szollosi, J., Damjanovich, S. & Matyus, L. (1998). Application of fluorescence resonance energy transfer in the clinical laboratory: routine and research. *Cytometry,* **34**, 159-79.

Szollosi, J., Nagy, P., Sebestyen, Z., Damjanovicha, S., Park, J. W. & Matyus, L. (2002). Applications of fluorescence resonance energy transfer for mapping biological membranes. *J Biotechnol,* **82**, 251-66.

Tadokoro, S., Shattil, S. J., Eto, K., Tai, V., Liddington, R. C., de Pereda, J. M., Ginsberg, M. H. & Calderwood, D. A. (2003). Talin binding to integrin beta tails: a final common step in integrin activation. *Science,* **302**, 103-6.

Tan, J. L., Tien, J., Pirone, D. M., Gray, D. S., Bhadriraju, K. & Chen, C. S. (2003). Cells lying on a bed of microneedles: an approach to isolate mechanical force. *Proc Natl Acad Sci U S A,* **100**, 1484-9.

Thomas, D. W., Mannon, R. B., Mannon, P. J., Latour, A., Oliver, J. A., Hoffman, M., Smithies, O., Koller, B. H. & Coffman, T. M. (1998). Coagulation defects and altered hemodynamic responses in mice lacking receptors for thromboxane A2. *Journal of Clinical Investigation,* **102**, 1994.

Thompson, R. F., Walker, M., Siebert, C. A., Muench, S. P. & Ranson, N. A. (2016). An introduction to sample preparation and imaging by cryo-electron microscopy for structural biology. *Methods (San Diego, Calif.),* **100**, 3-15.

Thon, J. & Italiano, J. (2012). *Platelets: Production, Morphology and Ultrastructure.*

Torti, M. & Lapetina, E. G. (1994). Structure and function of rap proteins in human platelets. *Thromb Haemost,* **71**, 533-43.

Tsuji, M., Ezumi, Y., Arai, M. & Takayama, H. (1997). A novel association of Fc receptor γ-chain with glycoprotein VI and their co-expression as a collagen receptor in human platelets. *Journal of Biological Chemistry,* **272**, 23528-23531.

Tu, Y., Huang, Y., Zhang, Y., Hua, Y. & Wu, C. (2001). A new focal adhesion protein that interacts with integrin-linked kinase and regulates cell adhesion and spreading. *The Journal of cell biology,* **153**, 585-598.

Tucker, K. L., Sage, T., Stevens, J. M., Jordan, P. A., Jones, S., Barrett, N. E., St-Arnaud, R., Frampton, J., Dedhar, S. & Gibbins, J. M. (2008). A dual role for integrin-linked kinase in platelets: regulating integrin function and α-granule secretion. *Blood,* **112**, 4523-4531.

Ussar, S., Wang, H.-V., Linder, S., Fässler, R. & Moser, M. (2006). The Kindlins: subcellular localization and expression during murine development. *Experimental cell research,* **312**, 3142-3151.

Vane, J. R. & Botting, R. M. (1995). Pharmacodynamic profile of prostacyclin. *Am J Cardiol,* **75**, 3a-10a.

Varga-Szabo, D., Braun, A. & Nieswandt, B. (2009). Calcium signaling in platelets. *J Thromb Haemost,* **7**, 1057-66.

Vemana, H. P., Karim, Z. A., Conlon, C. & Khasawneh, F. T. (2015). A critical role for the transient receptor potential channel type 6 in human platelet activation. *PLoS One,* **10**, e0125764.

Wagner, C. L., Mascelli, M. A., Neblock, D. S., Weisman, H. F., Coller, B. S. & Jordan, R. E. (1996). Analysis of GPIIb/IIIa receptor number by quantification of 7E3 binding to human platelets. *Blood,* **88**, 907-14.

Walter, U. & Gambaryan, S. (2009). cGMP and cGMP-dependent protein kinase in platelets and blood cells. *Handb Exp Pharmacol*, 533-48.

Wang, Y., Reheman, A., Spring, C. M., Kalantari, J., Marshall, A. H., Wolberg, A. S., Gross, P. L., Weitz, J. I., Rand, M. L., Mosher, D. F., Freedman, J. & Ni, H. (2014). Plasma fibronectin supports hemostasis and regulates thrombosis. *J Clin Invest,* **124**, 4281-93.

Watanabe, N., Bodin, L., Pandey, M., Krause, M., Coughlin, S., Boussiotis, V. A., Ginsberg, M. H. & Shattil, S. J. (2008). Mechanisms and consequences of

agonist-induced talin recruitment to platelet integrin αIIbβ3. *The Journal of cell biology*, **181**, 1211-1222.

Watson, S., Auger, J., McCarty, O. & Pearce, A. (2005). GPVI and integrin αIIbβ3 signaling in platelets. *Journal of Thrombosis and Haemostasis,* **3**, 1752-1762.

Watson, S. P. & Gibbins, J. (1998). Collagen receptor signalling in platelets: extending the role of the ITAM. *Immunol Today,* **19**, 260-4.

Watson, S. P. & Harrison, P. (2010). The vascular function of platelets. *Postgraduate Haematology, Sixth edition*, 772-792.

Webster, P., Schwarz, H. & Griffiths, G. (2008). Preparation of cells and tissues for immuno EM. *Methods Cell Biol,* **88**, 45-58.

Wei, A. H., Schoenwaelder, S. M., Andrews, R. K. & Jackson, S. P. (2009). New insights into the haemostatic function of platelets. *Br J Haematol,* **147**, 415-30.

Weisel, J. W. & Litvinov, R. I. (2017). Fibrin Formation, Structure and Properties. *Sub-cellular biochemistry,* **82**, 405-456.

White, J. G. (1972). Interaction of membrane systems in blood platelets. *Am J Pathol,* **66**, 295-312.

Wickstrom, S. A., Lange, A., Montanez, E. & Fassler, R. (2010). The ILK/PINCH/parvin complex: the kinase is dead, long live the pseudokinase! *Embo j,* **29**, 281-91.

Widmaier, M., Rognoni, E., Radovanac, K., Azimifar, S. B. & Fassler, R. (2012). Integrin-linked kinase at a glance. *J Cell Sci,* **125**, 1839-43.

Wilner, G. D., Nossel, H. L. & LeRoy, E. C. (1968). Aggregation of platelets by collagen. *J Clin Invest,* **47**, 2616-21.

Woodside, D. G., Obergfell, A., Leng, L., Wilsbacher, J. L., Miranti, C. K., Brugge, J. S., Shattil, S. J. & Ginsberg, M. H. (2001). Activation of Syk protein tyrosine kinase through interaction with integrin beta cytoplasmic domains. *Curr Biol,* **11**, 1799-804.

Wu, Y., Span, L. M., Nygren, P., Zhu, H., Moore, D. T., Cheng, H., Roder, H., DeGrado, W. F. & Bennett, J. S. (2015). The Tyrosine Kinase c-Src Specifically Binds to the Active Integrin alphaIIbbeta3 to Initiate Outside-in Signaling in Platelets. *J Biol Chem,* **290**, 15825-34.

Wu, Y., Suzuki-Inoue, K., Satoh, K., Asazuma, N., Yatomi, Y., Berndt, M. C. & Ozaki, Y. (2001). Role of Fc receptor gamma-chain in platelet glycoprotein Ib-mediated signaling. *Blood,* **97**, 3836-45.

Xu, Z., Chen, X., Zhi, H., Gao, J., Bialkowska, K., Byzova, T. V., Pluskota, E., White, G. C., 2nd, Liu, J., Plow, E. F. & Ma, Y.-Q. (2014). Direct interaction of kindlin-3 with integrin αIIbβ3 in platelets is required for supporting arterial thrombosis in mice. *Arteriosclerosis, thrombosis, and vascular biology,* **34**, 1961-1967.

Ye, F., Kim, C. & Ginsberg, M. H. (2011). Molecular mechanism of inside-out integrin regulation. *J Thromb Haemost,* **9 Suppl 1**, 20-5.

Ye, F., Kim, S. J. & Kim, C. (2014). Intermolecular transmembrane domain interactions activate integrin alphaIIbbeta3. *J Biol Chem,* **289**, 18507-13.

Ye, F., Petrich, B. G., Anekal, P., Lefort, C. T., Kasirer-Friede, A., Shattil, S. J., Ruppert, R., Moser, M., Fassler, R. & Ginsberg, M. H. (2013). The mechanism of kindlin-mediated activation of integrin alphaIIbbeta3. *Curr Biol,* **23**, 2288-95.

Yuan, H., Deng, N., Zhang, S., Cao, Y., Wang, Q., Liu, X. & Zhang, Q. (2012). The unfolded von Willebrand factor response in bloodstream: the self-association perspective. *Journal of hematology & oncology,* **5**, 1-10.

Zhang, Y., Chen, K., Guo, L. & Wu, C. (2002). Characterization of PINCH-2, a new focal adhesion protein that regulates the PINCH-1-ILK interaction, cell spreading, and migration. *J Biol Chem,* **277**, 38328-38.

Zucker-Franklin, D. (1997). Platelet Structure and Function. *In:* Kuter, D. J., Hunt, P., Sheridan, W. & Zucker-Franklin, D. (eds.) *Thrombopoiesis and Thrombopoietins: Molecular, Cellular, Preclinical, and Clinical Biology.* Totowa, NJ: Humana Press.

9 Appendix: Novel cluster analysis for β_3 clustering using R.

9.1 Appendix 1: Processing raw data for thunderstorm.

```
file<-"C:/Users/nn848637/Desktop/thrombin 1uml/raw/ml 0 sec list.txt"
raw<-read.table(file, header=TRUE, sep="\t")
names(raw)<-c("Channel",  "X",  "Y",  "x",  "y",  "Height",
              "Area", "Width",  "Phi",  "Ax", "BG", "I",  "Frame",
              "Length", "Link", "Valid",  "Z",  "z",  "Photons",
              "LateralLocalizationAccuracy",  "Xw", "Yw", "Xwc",  "Ywc")

p<-25

minx<-min(raw$x); x<-(raw$x-minx)/p
miny<-min(raw$y); y<-(raw$y-miny)/p
z<-raw$z/25

shrunk<-data.frame(raw$Channel,x,y,z)

#select tow colours
beta3<-subset(shrunk, raw.Channel=="Cy2/Alexa555")
kindlin<-subset(shrunk, raw.Channel=="Cy3/Alexa647")

kindlin$raw.Channel<-NULL
beta3$raw.Channel<-NULL

#output
write.table(kindlin,file="C:/Users/nn848637/Desktop/thrombin 1uml/cbc25k/1thr0.csv",
            row.names=FALSE,col.names=TRUE,sep=",",append=TRUE)
write.table(beta3,file="C:/Users/nn848637/Desktop/thrombin 1uml/cbc25b/1thr0.csv",
            row.names=FALSE,col.names=TRUE,sep=",",append=TRUE)

```

Read in the raw data

Shrink the data space of the raw data

Select data

Output

9.2 Appendix 2: Extracting data from thunderstorm.

```
file<-"C:/Users/nn848637/Desktop/thrombin 1uml/cbc25b/1thr0s.csv"
raw<-read.table(file,header=TRUE,sep=",")

cbcz<-recode(raw$cbc,"NaN=-1")

j<-c(1:1000)/1000
cbc<-quantile(cbcz, c(j), type=8)

j<-max(raw$neighbors_in_dist_1)
n1<-hist(raw$neighbors_in_dist_1, breaks=j)
count<-length(raw$neighbors_in_dist_1)
percn1<-(n1$counts/count)*100
n1z<-data.frame(n1$mids, percn1)
names(n1z)<-c("neighbours in 25nm",  file)

j<-max(raw$neighbors_in_dist_2)
n2<-hist(raw$neighbors_in_dist_2, breaks=j)
count<-length(raw$neighbors_in_dist_2)
percn2<-(n2$counts/count)*100
n2z<-data.frame(n2$mids, percn2)
names(n2z)<-c("neighbours in 50nm",  file)

j<-max(raw$neighbors_in_dist_3)
n3<-hist(raw$neighbors_in_dist_3, breaks=j)
count<-length(raw$neighbors_in_dist_3)
percn3<-(n3$counts/count)*100
n3z<-data.frame(n3$mids, percn3)
names(n3z)<-c("neighbours in 75nm",  file)

j<-max(raw$neighbors_in_dist_4)
n4<-hist(raw$neighbors_in_dist_4, breaks=j)
count<-length(raw$neighbors_in_dist_4)
percn4<-(n4$counts/count)*100
n4z<-data.frame(n4$mids, percn4)
names(n4z)<-c("neighbours in 100nm",  file)

j<-max(raw$neighbors_in_dist_5)
n5<-hist(raw$neighbors_in_dist_5, breaks=j)
count<-length(raw$neighbors_in_dist_5)
percn5<-(n5$counts/count)*100
n5z<-data.frame(n5$mids, percn5)
names(n5z)<-c("neighbours in 125nm",  file)

j<-max(raw$neighbors_in_dist_6)
n6<-hist(raw$neighbors_in_dist_6, breaks=j)
count<-length(raw$neighbors_in_dist_6)
percn6<-(n6$counts/count)*100
n6z<-data.frame(n6$mids, percn6)
names(n6z)<-c("neighbours in 150nm",  file)

j<-max(raw$neighbors_in_dist_7)
n7<-hist(raw$neighbors_in_dist_7, breaks=j)
count<-length(raw$neighbors_in_dist_7)
percn7<-(n7$counts/count)*100
n7z<-data.frame(n7$mids, percn7)
names(n7z)<-c("neighbours in 175nm",  file)

j<-max(raw$neighbors_in_dist_8)
n8<-hist(raw$neighbors_in_dist_8, breaks=j)
count<-length(raw$neighbors_in_dist_8)
percn8<-(n8$counts/count)*100
n8z<-data.frame(n8$mids, percn8)
names(n8z)<-c("neighbours in 200nm",  file)

j<-max(raw$neighbors_in_dist_9)
n9<-hist(raw$neighbors_in_dist_9, breaks=j)
count<-length(raw$neighbors_in_dist_9)
percn9<-(n9$counts/count)*100
n9z<-data.frame(n9$mids, percn9)
names(n9z)<-c("neighbours in 225nm",  file)

j<-max(raw$neighbors_in_dist_10)
n10<-hist(raw$neighbors_in_dist_10, breaks=j)
count<-length(raw$neighbors_in_dist_10)
percn10<-(n10$counts/count)*100
n10z<-data.frame(n10$mids, percn10)
names(n10z)<-c("neighbours in 250nm",  file)

dista<-raw$nn_dist..nm*25
j<-max(dista)
dist<-hist(dista, breaks=j)
count<-length(raw$nn_dist..nm)
percdist<-(dist$counts/count)*100
distz<-data.frame(dist$mids, percdist)
names(distz)<-c("nearest neighbour nm",  file)


write.table(t(n1z),
            file="C:/Users/nn848637/Desktop/thrombin 1uml/summary beta 3/n25.csv",
            row.names=TRUE,col.names=FALSE,sep=",",append=TRUE)
write.table(t(n2z),
            file="C:/Users/nn848637/Desktop/thrombin 1uml/summary beta 3/n50.csv",
            row.names=TRUE,col.names=FALSE,sep=",",append=TRUE)
write.table(t(n3z),
            file="C:/Users/nn848637/Desktop/thrombin 1uml/summary beta 3/n75.csv",
            row.names=TRUE,col.names=FALSE,sep=",",append=TRUE)
write.table(t(n4z),
            file="C:/Users/nn848637/Desktop/thrombin 1uml/summary beta 3/n100.csv",
            row.names=TRUE,col.names=FALSE,sep=",",append=TRUE)
write.table(t(n5z),
            file="C:/Users/nn848637/Desktop/thrombin 1uml/summary beta 3/n125.csv",
            row.names=TRUE,col.names=FALSE,sep=",",append=TRUE)
write.table(t(n6z),
            file="C:/Users/nn848637/Desktop/thrombin 1uml/summary beta 3/n150.csv",
            row.names=TRUE,col.names=FALSE,sep=",",append=TRUE)
write.table(t(n7z),
            file="C:/Users/nn848637/Desktop/thrombin 1uml/summary beta 3/n175.csv",
            row.names=TRUE,col.names=FALSE,sep=",",append=TRUE)
write.table(t(n8z),
            file="C:/Users/nn848637/Desktop/thrombin 1uml/summary beta 3/n200.csv",
            row.names=TRUE,col.names=FALSE,sep=",",append=TRUE)
write.table(t(n9z),
            file="C:/Users/nn848637/Desktop/thrombin 1uml/summary beta 3/n225.csv",
            row.names=TRUE,col.names=FALSE,sep=",",append=TRUE)
write.table(t(n10z),
            file="C:/Users/nn848637/Desktop/thrombin 1uml/summary beta 3/n250.csv",
            row.names=TRUE,col.names=FALSE,sep=",",append=TRUE)
write.table(t(distz),
            file="C:/Users/nn848637/Desktop/thrombin 1uml/summary beta 3/dist.csv",
            row.names=TRUE,col.names=FALSE,sep=",",append=TRUE)
```

Read in processed data

Neighbour β_3 molecules

Output

9.3 Appendix 3: Mean number of β_3 molecules surrounded each β_3 molecules in all individuals.

```
file1<-"C:/Users/nn848637/Desktop/thrombin 1Uml/cbc25b.csv"
raw1<-read.table(file1,header=TRUE,sep=",")

tmean<-mean(raw1$t)
umean<-mean(raw1$u)
vmean<-mean(raw1$v)
wmean<-mean(raw1$w)
xmean<-mean(raw1$x)
ymean<-mean(raw1$y)
zmean<-mean(raw1$z)

res1<-data.frame(tmean,umean,vmean,wmean,xmean,ymean,zmean)

#output
write.table(res1,file="C:/Users/nn848637/Desktop/thrombin 1Uml/cbc25b/mean res.csv",row.names=FALSE,col.names=TRUE,sep=",",append=TRUE)
```

Select data

Output

9.4 Appendix 4: Percentage of β_3 molecules within cluster.

```
#count

file<-"C:/Users/nn848637/Desktop/ thrombin 1uml/cbc25b/0 sec list.csv"
raw<-read.table(file,header=TRUE,sep=",")
tall<-length(raw$neighbors_in_dist_3)

t0<-(length(which(raw$neighbors_in_dist_1 == 1)) / tall)*100
t.5<-(length(which(raw$neighbors_in_dist_1 > (0.5*tmean))) / tall)*100
t0..0.5<-100-(t0+t.5)
t1<-(length(which(raw$neighbors_in_dist_1 > (1*tmean))) / tall)*100
t0.5..1<-t.5-t1
t1.5<-(length(which(raw$neighbors_in_dist_1 > (1.5*tmean))) / tall)*100
t1..1.5<-t1-t1.5
t2<-(length(which(raw$neighbors_in_dist_1 > (2*tmean))) / tall)*100
t1.5..2<-t1.5-t2
t2.5<-(length(which(raw$neighbors_in_dist_1 > (2.5*tmean))) / tall)*100
t2..2.5<-t2-t2.5
t3<-(length(which(raw$neighbors_in_dist_1 > (3*tmean))) / tall)*100
t2.5..3<-t2.5-t3
t4<-(length(which(raw$neighbors_in_dist_1 > (4*tmean))) / tall)*100
t3..4<-t3-t4
t5<-(length(which(raw$neighbors_in_dist_1 > (5*tmean))) / tall)*100
t4..5<-t4-t5
t6<-(length(which(raw$neighbors_in_dist_1 > (6*tmean))) / tall)*100
t5..6<-t5-t6
t7<-(length(which(raw$neighbors_in_dist_1 > (7*tmean))) / tall)*100
t6..7<-t6-t7
t8<-(length(which(raw$neighbors_in_dist_1 > (8*tmean))) / tall)*100
t7..8<-t7-t8
t9<-(length(which(raw$neighbors_in_dist_1 > (9*tmean))) / tall)*100
t8..9<-t8-t9
t10<-(length(which(raw$neighbors_in_dist_1 > (10*tmean))) / tall)*100
t9..10<-t9-t10

res2<-data.frame(file,t0,t.5,t1,t1.5,t2,t2.5,t3,t4,t5,t6,t7,t8,t9,t10,t0..0.5,t0.5..1,t1..1.5,t1.5..2,t2..2.5,t2.5..3,t3..4,t4..5,t5..6,t6..7,t7..8,t8..9,t9..10)

write.table(res2,file="C:/Users/nn848637/Desktop/ thrombin 1uml/per cluster res b3b3 t.csv",row.names=FALSE,col.names=FALSE,sep=",",append=TRUE)

t0<-(length(which(raw$neighbors_in_dist_2 == 1)) / tall)*100
t.5<-(length(which(raw$neighbors_in_dist_2 > (0.5*umean))) / tall)*100
t0..0.5<-100-(t0+t.5)
t1<-(length(which(raw$neighbors_in_dist_2 > (1*umean))) / tall)*100
t0.5..1<-t.5-t1
t1.5<-(length(which(raw$neighbors_in_dist_2 > (1.5*umean))) / tall)*100
t1..1.5<-t1-t1.5
t2<-(length(which(raw$neighbors_in_dist_2 > (2*umean))) / tall)*100
t1.5..2<-t1.5-t2
t2.5<-(length(which(raw$neighbors_in_dist_2 > (2.5*umean))) / tall)*100
t2..2.5<-t2-t2.5
t3<-(length(which(raw$neighbors_in_dist_2 > (3*umean))) / tall)*100
t2.5..3<-t2.5-t3
t4<-(length(which(raw$neighbors_in_dist_2 > (4*umean))) / tall)*100
t3..4<-t3-t4
t5<-(length(which(raw$neighbors_in_dist_2 > (5*umean))) / tall)*100
t4..5<-t4-t5
t6<-(length(which(raw$neighbors_in_dist_2 > (6*umean))) / tall)*100
```

Defining β_3 clusters

```
t5..6<-t5-t6
t7<-(length(which(raw$neighbors_in_dist_2 > (7*umean))) / tall)*100
t6..7<-t6-t7
t8<-(length(which(raw$neighbors_in_dist_2 > (8*umean))) / tall)*100
t7..8<-t7-t8
t9<-(length(which(raw$neighbors_in_dist_2 > (9*umean))) / tall)*100
t8..9<-t8-t9
t10<-(length(which(raw$neighbors_in_dist_2 > (10*umean))) / tall)*100
t9..10<-t9-t10

res2<-data.frame(file,t0,t.5,t1,t1.5,t2,t2.5,t3,t4,t5,t6,t7,t8,t9,t10,t0..0.5,t0.5..1,t1..1.5,t1.5..2,t2..2.5,t2.5..3,t3..4,t4..5,t5..6,t6..7,t7..8,t8..9,t9..10)

write.table(res2,file="C:/Users/nn848637/Desktop/ thrombin 1uml/per cluster res b3b3 u.csv",row.names=FALSE,col.names=FALSE,sep=",",append=TRUE)

t0<-(length(which(raw$neighbors_in_dist_3 == 1)) / tall)*100
t.5<-(length(which(raw$neighbors_in_dist_3 > (0.5*vmean))) / tall)*100
t0..0.5<-100-(t0+t.5)
t1<-(length(which(raw$neighbors_in_dist_3 > (1*vmean))) / tall)*100
t0.5..1<-t.5-t1
t1.5<-(length(which(raw$neighbors_in_dist_3 > (1.5*vmean))) / tall)*100
t1..1.5<-t1-t1.5
t2<-(length(which(raw$neighbors_in_dist_3 > (2*vmean))) / tall)*100
t1.5..2<-t1.5-t2
t2.5<-(length(which(raw$neighbors_in_dist_3 > (2.5*vmean))) / tall)*100
t2..2.5<-t2-t2.5
t3<-(length(which(raw$neighbors_in_dist_3 > (3*vmean))) / tall)*100
t2.5..3<-t2.5-t3
t4<-(length(which(raw$neighbors_in_dist_3 > (4*vmean))) / tall)*100
t3..4<-t3-t4
t5<-(length(which(raw$neighbors_in_dist_3 > (5*vmean))) / tall)*100
t4..5<-t4-t5
t6<-(length(which(raw$neighbors_in_dist_3 > (6*vmean))) / tall)*100
t5..6<-t5-t6
t7<-(length(which(raw$neighbors_in_dist_3 > (7*vmean))) / tall)*100
t6..7<-t6-t7
t8<-(length(which(raw$neighbors_in_dist_3 > (8*vmean))) / tall)*100
t7..8<-t7-t8
t9<-(length(which(raw$neighbors_in_dist_3 > (9*vmean))) / tall)*100
t8..9<-t8-t9
t10<-(length(which(raw$neighbors_in_dist_3 > (10*vmean))) / tall)*100
t9..10<-t9-t10

res2<-data.frame(file,t0,t.5,t1,t1.5,t2,t2.5,t3,t4,t5,t6,t7,t8,t9,t10,t0..0.5,t0.5..1,t1..1.5,t1.5..2,t2..2.5,t2.5..3,t3..4,t4..5,t5..6,t6..7,t7..8,t8..9,t9..10)

write.table(res2,file="C:/Users/nn848637/Desktop/ thrombin 1uml/per cluster res b3b3 v.csv",row.names=FALSE,col.names=FALSE,sep=",",append=TRUE)

t0<-(length(which(raw$neighbors_in_dist_4 == 1)) / tall)*100
t.5<-(length(which(raw$neighbors_in_dist_4 > (0.5*wmean))) / tall)*100
t0..0.5<-100-(t0+t.5)
t1<-(length(which(raw$neighbors_in_dist_4 > (1*wmean))) / tall)*100
t0.5..1<-t.5-t1
t1.5<-(length(which(raw$neighbors_in_dist_4 > (1.5*wmean))) / tall)*100
t1..1.5<-t1-t1.5
t2<-(length(which(raw$neighbors_in_dist_4 > (2*wmean))) / tall)*100
t1.5..2<-t1.5-t2
t2.5<-(length(which(raw$neighbors_in_dist_4 > (2.5*wmean))) / tall)*100
t2..2.5<-t2-t2.5
```

Defining β_3 clusters

```
t3<-(length(which(raw$neighbors_in_dist_4 > (3*wmean))) / tall)*100
t2.5..3<-t2.5-t3
t4<-(length(which(raw$neighbors_in_dist_4 > (4*wmean))) / tall)*100
t3..4<-t3-t4
t5<-(length(which(raw$neighbors_in_dist_4 > (5*wmean))) / tall)*100
t4..5<-t4-t5
t6<-(length(which(raw$neighbors_in_dist_4 > (6*wmean))) / tall)*100
t5..6<-t5-t6
t7<-(length(which(raw$neighbors_in_dist_4 > (7*wmean))) / tall)*100
t6..7<-t6-t7
t8<-(length(which(raw$neighbors_in_dist_4 > (8*wmean))) / tall)*100
t7..8<-t7-t8
t9<-(length(which(raw$neighbors_in_dist_4 > (9*wmean))) / tall)*100
t8..9<-t8-t9
t10<-(length(which(raw$neighbors_in_dist_4 > (10*wmean))) / tall)*100
t9..10<-t9-t10

res2<-data.frame(file,t0,t.5,t1,t1.5,t2,t2.5,t3,t4,t5,t6,t7,t8,t9,t10,t0..0.5,t0.5..1,t1..1.5,t1.5..2,t2..2.5,t2.5..3,t3..4,t4..5,t5..6,t6..7,t7..8,t8..9,t9..10)

write.table(res2,file="C:/Users/nn848637/Desktop/ thrombin 1uml/per cluster res b3b3 w.csv",row.names=FALSE,col.names=FALSE,sep=",",append=TRUE)

t0<-(length(which(raw$neighbors_in_dist_5 == 1)) / tall)*100
t.5<-(length(which(raw$neighbors_in_dist_5 > (0.5*xmean))) / tall)*100
t0..0.5<-100-(t0+t.5)
t1<-(length(which(raw$neighbors_in_dist_5 > (1*xmean))) / tall)*100
t0.5..1<-t.5-t1
t1.5<-(length(which(raw$neighbors_in_dist_5 > (1.5*xmean))) / tall)*100
t1..1.5<-t1-t1.5
t2<-(length(which(raw$neighbors_in_dist_5 > (2*xmean))) / tall)*100
t1.5..2<-t1.5-t2
t2.5<-(length(which(raw$neighbors_in_dist_5 > (2.5*xmean))) / tall)*100
t2..2.5<-t2-t2.5
t3<-(length(which(raw$neighbors_in_dist_5 > (3*xmean))) / tall)*100
t2.5..3<-t2.5-t3
t4<-(length(which(raw$neighbors_in_dist_5 > (4*xmean))) / tall)*100
t3..4<-t3-t4
t5<-(length(which(raw$neighbors_in_dist_5 > (5*xmean))) / tall)*100
t4..5<-t4-t5
t6<-(length(which(raw$neighbors_in_dist_5 > (6*xmean))) / tall)*100
t5..6<-t5-t6
t7<-(length(which(raw$neighbors_in_dist_5 > (7*xmean))) / tall)*100
t6..7<-t6-t7
t8<-(length(which(raw$neighbors_in_dist_5 > (8*xmean))) / tall)*100
t7..8<-t7-t8
t9<-(length(which(raw$neighbors_in_dist_5 > (9*xmean))) / tall)*100
t8..9<-t8-t9
t10<-(length(which(raw$neighbors_in_dist_5 > (10*xmean))) / tall)*100
t9..10<-t9-t10

res2<-data.frame(file,t0,t.5,t1,t1.5,t2,t2.5,t3,t4,t5,t6,t7,t8,t9,t10,t0..0.5,t0.5..1,t1..1.5,t1.5..2,t2..2.5,t2.5..3,t3..4,t4..5,t5..6,t6..7,t7..8,t8..9,t9..10)

write.table(res2,file="C:/Users/nn848637/Desktop/ thrombin 1uml/per cluster res b3b3 x.csv",row.names=FALSE,col.names=FALSE,sep=",",append=TRUE)
```

Defining β_3 clusters

```
t0<-(length(which(raw$neighbors_in_dist_6 == 1)) / tall)*100
t.5<-(length(which(raw$neighbors_in_dist_6 > (0.5*ymean))) / tall)*100
t0..0.5<-100-(t0+t.5)
t1<-(length(which(raw$neighbors_in_dist_6 > (1*ymean))) / tall)*100
t0.5..1<-t.5-t1
t1.5<-(length(which(raw$neighbors_in_dist_6 > (1.5*ymean))) / tall)*100
t1..1.5<-t1-t1.5
t2<-(length(which(raw$neighbors_in_dist_6 > (2*ymean))) / tall)*100
t1.5..2<-t1.5-t2
t2.5<-(length(which(raw$neighbors_in_dist_6 > (2.5*ymean))) / tall)*100
t2..2.5<-t2-t2.5
t3<-(length(which(raw$neighbors_in_dist_6 > (3*ymean))) / tall)*100
t2.5..3<-t2.5-t3
t4<-(length(which(raw$neighbors_in_dist_6 > (4*ymean))) / tall)*100
t3..4<-t3-t4
t5<-(length(which(raw$neighbors_in_dist_6 > (5*ymean))) / tall)*100
t4..5<-t4-t5
t6<-(length(which(raw$neighbors_in_dist_6 > (6*ymean))) / tall)*100
t5..6<-t5-t6
t7<-(length(which(raw$neighbors_in_dist_6 > (7*ymean))) / tall)*100
t6..7<-t6-t7
t8<-(length(which(raw$neighbors_in_dist_6 > (8*ymean))) / tall)*100
t7..8<-t7-t8
t9<-(length(which(raw$neighbors_in_dist_6 > (9*ymean))) / tall)*100
t8..9<-t8-t9
t10<-(length(which(raw$neighbors_in_dist_6 > (10*ymean))) / tall)*100
t9..10<-t9-t10

res2<-data.frame(file,t0,t.5,t1,t1.5,t2,t2.5,t3,t4,t5,t6,t7,t8,t9,t10,t0..0.5,t0.5..1,t1..1.5,t1.5..2,t2..2.5,t2.5..3,t3..4,t4..5,t5..6,t6..7,t7..8,t8..9,t9..10)

write.table(res2,file="C:/Users/nn848637/Desktop/ thrombin 1uml/per cluster res b3b3 y.csv",row.names=FALSE,col.names=FALSE,sep=",",append=TRUE)

t0<-(length(which(raw$neighbors_in_dist_7 == 1)) / tall)*100
t.5<-(length(which(raw$neighbors_in_dist_7 > (0.5*zmean))) / tall)*100
t0..0.5<-100-(t0+t.5)
t1<-(length(which(raw$neighbors_in_dist_7 > (1*zmean))) / tall)*100
t0.5..1<-t.5-t1
t1.5<-(length(which(raw$neighbors_in_dist_7 > (1.5*zmean))) / tall)*100
t1..1.5<-t1-t1.5
t2<-(length(which(raw$neighbors_in_dist_7 > (2*zmean))) / tall)*100
t1.5..2<-t1.5-t2
t2.5<-(length(which(raw$neighbors_in_dist_7 > (2.5*zmean))) / tall)*100
t2..2.5<-t2-t2.5
t3<-(length(which(raw$neighbors_in_dist_7 > (3*zmean))) / tall)*100
t2.5..3<-t2.5-t3
t4<-(length(which(raw$neighbors_in_dist_7 > (4*zmean))) / tall)*100
t3..4<-t3-t4
t5<-(length(which(raw$neighbors_in_dist_7 > (5*zmean))) / tall)*100
t4..5<-t4-t5
t6<-(length(which(raw$neighbors_in_dist_7 > (6*zmean))) / tall)*100
t5..6<-t5-t6
t7<-(length(which(raw$neighbors_in_dist_7 > (7*zmean))) / tall)*100
t6..7<-t6-t7
t8<-(length(which(raw$neighbors_in_dist_7 > (8*zmean))) / tall)*100
t7..8<-t7-t8
t9<-(length(which(raw$neighbors_in_dist_7 > (9*zmean))) / tall)*100
t8..9<-t8-t9
t10<-(length(which(raw$neighbors_in_dist_7 > (10*zmean))) / tall)*100
t9..10<-t9-t10

res2<-data.frame(file,t0,t.5,t1,t1.5,t2,t2.5,t3,t4,t5,t6,t7,t8,t9,t10,t0..0.5,t0.5..1,t1..1.5,t1.5..2,t2..2.5,t2.5..3,t3..4,t4..5,t5..6,t6..7,t7..8,t8..9,t9..10)

write.table(res2,file="C:/Users/nn848637/Desktop/ thrombin 1uml/per cluster res b3b3 z.csv",row.names=FALSE,col.names=FALSE,sep=",",append=TRUE)
```

Defining β_3 clusters